UNIVERSIDAD AUTÓNOMA DE MADRID

Departamento de Química Orgánica

Post-functionalized Hybrid Materials as Multi-site Catalysts

Directores:

Dra. Marta Iglesias Hernández

Prof. Dr. Félix Sánchez Alonso

Memoria para optar al grado de

DOCTOR EN CIENCIAS QUÍMICAS

Antonia María Rasero Almansa

Madrid, 2016

Table of contents

Chapter 2. ***Post-functionalization in the linker of Zr-MOFs***

Chapter 3. ***Mixed-metal MOFs***

Abbreviations

The following terms have been used in this manuscript:

a. u.	Arbitrary units
Ar	Argon
BTC	1,4-bencenedicarboxylate
BPDC	(1,1'-biphenyl)-4,4'-dicarboxylate
ca.	Approximately
CT	Charge transfer
DMF	*N,N*-Dimethylformamide
DMSO	Dimethylsulfoxyde
ESI-MS	Electrospray ionization mass-spectrometry
FTIR	Fourier transform infrared
HKUST	Hong Kong University of Science and Technology
HT	High-throughput
ICP-OES	Inductively coupled plasma-optical emission spectrometry
IRMOF	Isoreticular metal-organic framework
IUPAC	International Union of Pure and Applied Chemistry
λ	Wavelength
MIL	Matérial Institut Lavoisier
MOF	Metal-Organic Framework
MS	Mass spectrometry
MW	Molecular weight
NDC	2,6-naphthalenedicarboxylate
NMR	Nuclear magnetic resonance
p-	para-
PCP	Porous coordination polymer
PSE	Postsynthetic exchange
PSM	Postsynthetic modification
r.p.m.	Revolution per minute
rt	Room temperature
SBU	Secondary Building Unit
SEM	Scanning electron microscopy
T	Temperature
t-Bu	tert-Butyl-
TEA	Triethylamine
TEM	Transmission electron microscopy
TFA	Trifluoroacetic acid
TGA	Thermogravimetric analysis

TLC	Thin-layer chromatography
TOF	Turnover frequency
TON	Turnover number
UiO	Universitet i Oslo
UV	Ultraviolet
V	Voltage
V	Volt
vis	Visible
XPS	X-ray photoelectron spectroscopy
PXRD	Powder X-ray diffraction
ZIF	Zeolitic imidazolate framework

Summary

Post-functionalized Hybrid Materials as Multi-site Catalysts

Catalysis is one of the fundamental pillars of green chemistry, this concept was described as design of chemical products and processes that reduce or eliminate the use and generation of hazardous substances. The design and application of new catalysts and catalytic systems lead to the dual goals of environmental protection and economic benefit.[3]

Heterogeneous catalysts are the most used in industry because they present several advantages such as easy post reaction separation, high stability and reusability. Another great advantage of the solid catalysts is the possibility to immobilize different functional groups on the same support preventing catalyst deactivation as they are isolated from each other. For that reason, heterogeneous catalysts are promising candidates to act as multifunctional catalysts.[4a]

Metal-organic frameworks (MOFs) are crystalline and porous materials which possess advantageous properties to be used in catalysis, such as high specific surface areas and tunable porosity, the ability to fine tune the structure of the active site and its environment and thermal stability. In addition, these materials are good candidates to be multifunctional catalysts since they can present multiple active sites; therefore, multistep reactions can be carried out in the same vessel and under the same reaction conditions.

In this thesis, we performed the synthesis, functionalization and characterization of different zirconium-based MOFs (UiO-type MOFs) and then, they have been used as catalysts in different catalytic reactions. The work has been divided in three chapters, depending on the functionalization of the MOF.

Chapter 1: Zirconium Metal-Organic Frameworks.

The Zr-MOF structures are formed by clusters of zirconium [$Zr_6O_4(OH)_4$] coordinated with linear ligands to give coordination polymers. The organic

linker is assembled from six Zr(IV) ions each with a square antiprismatic coordination geometry comprised of eight oxygen atoms. Each inorganic Secondary Building Unit (SBU) is bound by twelve carboxylate groups from twelve different 1,4-bencenedicarboxylate (BDC) ligands. Besides, if amino-functionalized linkers are used in the synthesis, we obtain materials with the same topology[91a] and it is also possible to obtain isoreticular structures by mixing different organic linkers in the same material.

In the first chapter, the synthesis of mixed linker Zr-MOFs without any post-functionalization is described; we performed the synthesis with different mixtures of linkers: BDC/2-aminobenzene-1,4-dicarboxylic acid (BDC/BDC-NH_2), 2,6-naphthalenedicarboxylic acid/4-amino-2,6-naphthalenedicarboxylic acid (NDC/NDC-NH_2) or 1,1'-biphenyl)-4,4'-dicarboxylic acid/2-amino-(1,1'-biphenyl)-4,4'-dicarboxylic acid (BPDC/BPDC-NH_2) (Scheme S1). We decided to synthesize the NDC-MOF searching a more stable material than those with BPDC as linker and with larger pore size than BDC-MOFs.

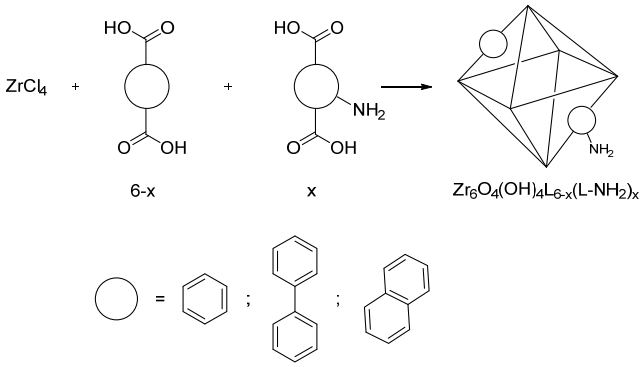

Scheme S1. Preparation of mixed linker Zr-MOFs.

Once synthesized and characterized, these materials were tested as catalysts in the one pot synthesis of 1,1-dicyanomethylenebutadiene derivatives (Scheme S2) where two condensation reactions take place.

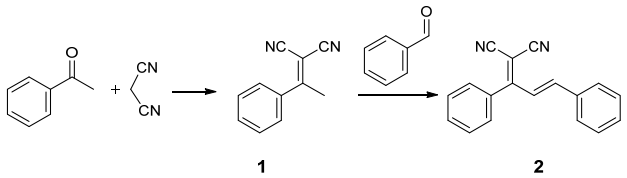

Scheme S2. One-pot synthesis of 1,1-dicyanomethylenebutadiene derivatives.

Chapter 2: Post-functionalization in the linker of Zr-MOFs.

The heterogenization of transition-metal complexes over a solid matrix leads to the formation of solid recyclable molecular catalysts with well-defined active centers. MOFs can be easily modified by post-synthesis treatments with the aim of introducing functional groups that can act or be transformed into catalytic active sites.[117]

We describe the heterogenization of metal complexes in Zr-MOFs by post-functionalization of the amino linker to incorporate pincer-type ligands in the structure and subsequent anchoring of a transition metal (Ir or Rh) as depicted in scheme S3. Following this procedure, we obtained multifunctional catalysts that can be used in different catalytic reactions.

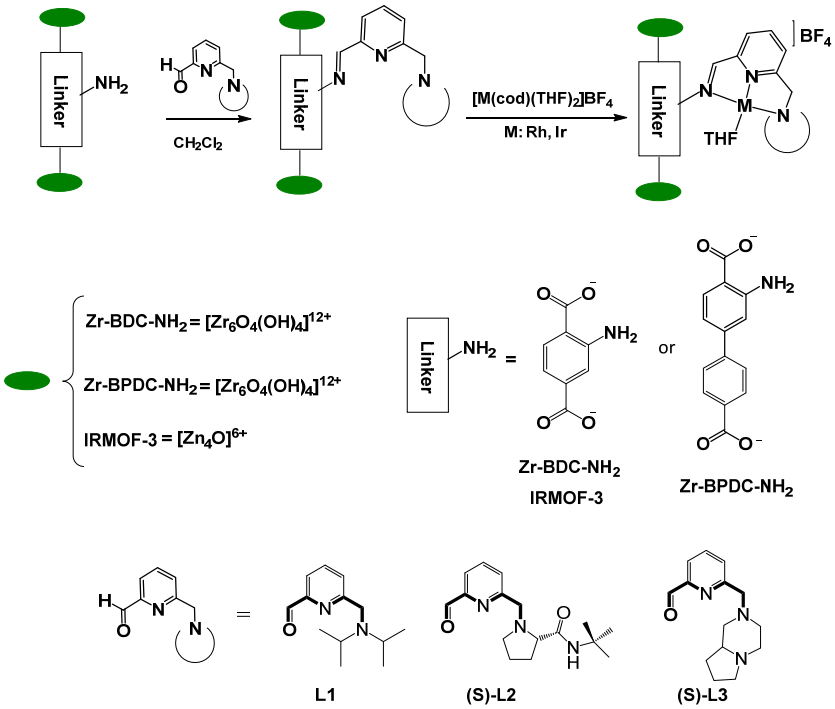

Scheme S3. Preparation of Post-functionalized MOFs.

In this chapter the catalytic activity is divided in two sub-sections for easy reading since four different reactions have been tested. In part A, we describe a one-step reaction (hydrogenation of aromatic compounds), scheme S4(a) and in part B, multistep reactions: *N*-alkylation of amines (scheme S4(b), synthesis of secondary amines (scheme S4(c)) and cascade olefination-hydrogenation reactions of aldehydes (scheme S4(d)).

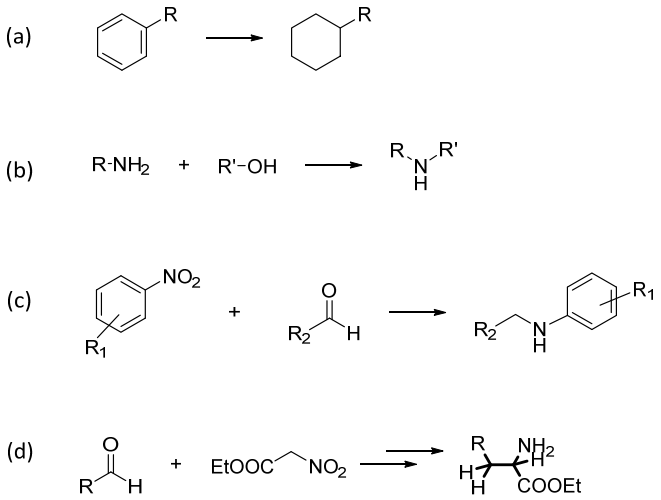

Scheme S4. Catalytic reactions in chapter 2: (a) Hydrogenation of aromatic compounds, (b) *N*-alkylation of amines, (c) Synthesis of secondary amines and (d) Condensation-hydrogenation reaction.

Chapter 3: Mixed metal MOFs.

Introduction of different metal cations in metal-organic frameworks provides an interesting strategy to tune the properties of porous materials towards practical applications. Mixed-metal MOFs may be synthesized by direct synthesis under solvothermal conditions, by post-synthesis metal exchange,[172] or by secondary building unit rational design.[173]

In this case, we describe the introduction of another metal in the structure of the material. We obtain mixed metal ZrTi-MOF by post-synthesis method as we can see in scheme S5(a) and ZrCe-MOFs by direct synthesis (scheme S5(b)) in order to tune the properties of the original Zr-MOF.

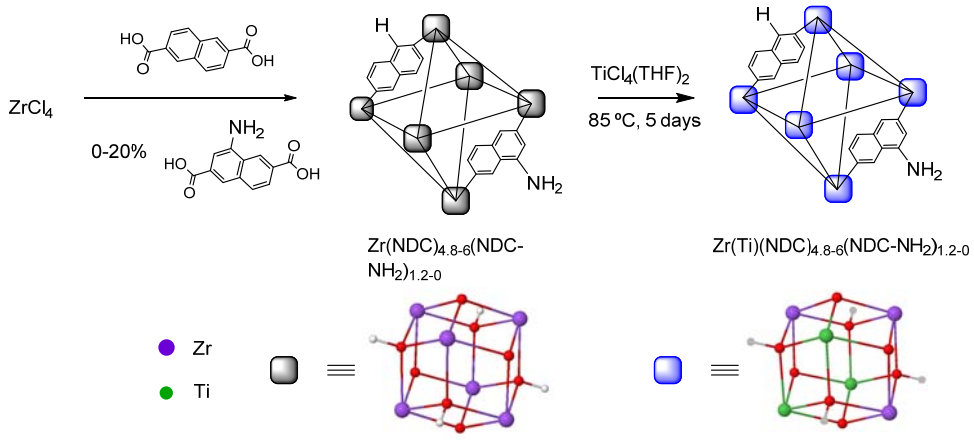

Scheme S5. Synthesis of mixed metal MOFs: (a) ZrTi-MOF by post-synthesis method and (b) ZrCe-MOF by direct synthesis.

ZrTi-MOFs have been used as catalyst in three different reactions as shown in Scheme S6. These materials presented higher Lewis acidity than Zr-MOFs and we decided to use them in cascade Meerwein-Ponndorf-Verley reduction-etherification, isomerization of α-pinene oxide and cyclization of citronellal, obtaining good conversions and selectivities.

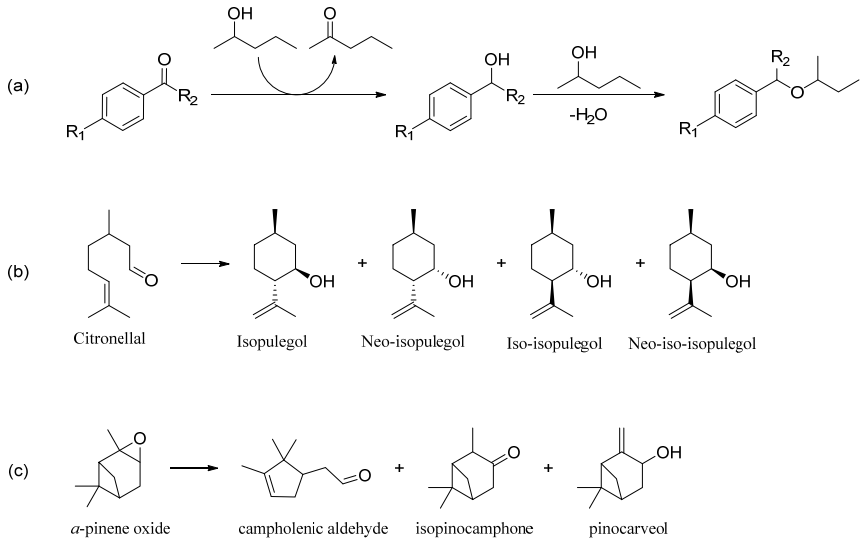

Scheme S6. ZrTi-MOF catalysed reactions: (a) Meerwein-Ponndorf-Verley reduction-etherification, (b) isomerization of α-pinene oxide, (c) cyclization of citronellal.

ZrCe-MOFs were applied as catalyst for the synthesis of imines from alcohols and amines.

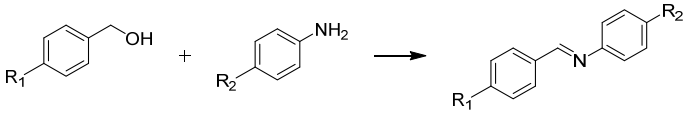

Scheme S7. Formation the imines from alcohols and amines.

After the catalytic experiments, the recyclability of the catalysts has been studied for all the reactions tested. We can conclude that the linker that gives the most robust MOFs is the BDC since with other linkers the activity decreases in each cycle.

We found that MOFs are good supports to heterogenize transition metal complexes as metal leaching is not observed when they are used in catalytic reactions. MOFs are versatile materials that allow us to introduce various functional groups in its structure and therefore they can catalyse different transformations with good conversions.

Resumen

Materiales Híbridos Post-funcionalizados como Catalizadores Multi-funcionales

La catálisis es un pilar fundamental de la química sostenible, este concepto fue descrito como el diseño de productos químicos y de los procesos que reducen o eliminan el uso y la generación de sustancias peligrosas. El diseño y el uso de nuevos catalizadores y sistemas catalíticos están logrando al mismo tiempo el doble objetivo de protección del medio ambiente y el beneficio económico.[3]

En la industria se utilizan mayoritariamente catalizadores heterogéneos ya que presentan ventajas tales como fácil separación del medio de reacción, alta estabilidad y que pueden ser reutilizados en varios ciclos. Otra gran ventaja que presentan los catalizadores sólidos es la posibilidad de inmovilizar diferentes grupos funcionales sobre el mismo soporte evitando la desactivación del catalizador ya que se encuentran aislados entre ellos. Por esta razón, los catalizadores heterogéneos son candidatos prometedores para actuar como catalizadores multifuncionales.[4a]

Las Redes Metal-Orgánicas (MOFs) son materiales cristalinos y porosos que poseen propiedades interesantes para ser usados en catálisis, tales como una alta superficie específica y porosidad, la posibilidad de ajustar con precisión la estructura del centro activo y su entorno, la presencia de múltiples centros activos y la estabilidad térmica que presentan. Además, estos materiales son buenos candidatos para ser catalizadores multifuncionales; por tanto, es posible llevar a cabo reacciones de varias etapas en un mismo recipiente y bajo las mismas condiciones de reacción.

En esta tesis, hemos llevado a cabo la síntesis, funcionalización y caracterización de diferentes MOFs de zirconio (MOFs tipo UiO) los cuales, han sido utilizados como catalizadores en diferentes reacciones catalíticas. El trabajo realizado se organiza en 3 capítulos, en función del tipo de funcionalización del MOF y sus aplicaciones.

Capítulo 1: Redes Metal-Orgánicas de Zirconio.

Los MOFs de zirconio están formados por clusters de zirconio [$Zr_6O_4(OH)_4$] coordinados con ligandos lineales que danlugar a polímeros de coordinación. El ligando orgánico está unido a seis iones de Zr(IV) con una geometría de coordinación antiprismática cuadrada compuesto por ocho átomos de oxígeno. Cada unidad secundaria de construcción (SBU) inorgánica está enlazada a doce grupos carboxilato de doce ligandos 1,4-bencenodicarboxylato (BDC) diferentes. Además, si se utilizan ligandos funcionalizados con un grupo amino en la síntesis, obtenemos materiales con la misma topología,[91a] también es posible obtener estructuras isoreticulares mezclando diferentes ligandos orgánicos en el mismo material.

En el primer capítulo, se describe la síntesis de Zr-MOFs con ligandos mixtos sin realizar ninguna post-funcionalización del material; hemos llevado a cabo la síntesis utilizando diferentes mezclas de ligandos: BDC/ácido 2-aminobenzeno-1,4-dicarboxílico (BDC/BDC-NH_2), ácido 2,6-naftalenodicarboxílico/ácido 4-amino-2,6-naftalenodicarboxílico (NDC/NDC-NH_2) o ácido (1,1'-bifenil)-4,4'-dicarboxílico/ácido 2-amino-(1,1'-bifenil)-4,4'-dicarboxílico (BPDC/BPDC-NH_2) (Esquema R1). Decidimos sintetizar el NDC-MOF buscando un matetial más estable que los que los que tienen BPDC como ligando y con mayor tamaño de poro que los BDC-MOFs.

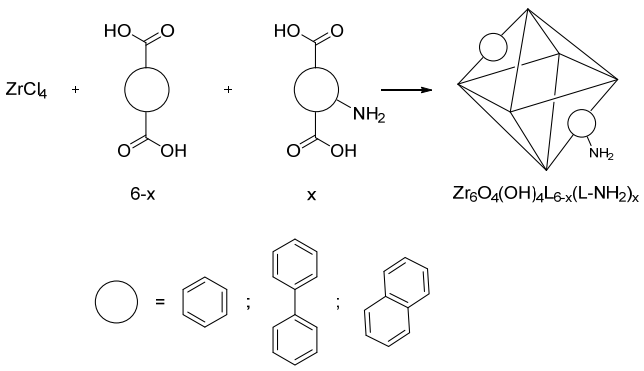

Esquema R1. Preparación de Zr-MOFs con mezcla de ligandos.

Una vez sintetizados y caracterizados, estos materiales fueron probados como catalizadores en la síntesis 'one-pot' de derivados del 1,1-dicianometilenbutadieno (Esquema R2), en la cual tienen lugar dos reacciones de condensación consecutivas.

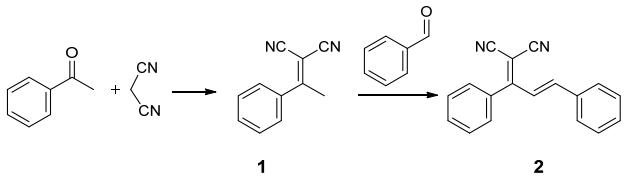

Esquema R2. Síntesis 'One-pot' de derivados del 1,1-dicianometilenbutadieno.

Capítulo 2: Zr-MOFs Post-funcionalizados en el ligando orgánico.

La heterogenización de complejos de metales de transición sobre matrices sólidas conduce a la formación de catalizadores moleculares sólidos reciclables con centros activos bien definidos. Los MOFs pueden ser fácilmente modificados mediante tratamientos post-síntesis con el objetivo de introducir grupos funcionales que pueden actuar o ser transformados en centros catalíticos activos.[117]

En este capñítulo se describe la heterogeneización de complejos metálicos en los Zr-MOFs mediante la post-funcionalización del ligando con un grupo amino para incorporar ligandos tipo pinza en la estructura del material y posteriormente, se coordina el segundo metal (Ir o Rh) como se representa en el esquema R3. Siguiendo este procedimiento, se obtienen catalizadores multifuncionales que pueden ser utilizados en diferentes reacciones catalíticas.

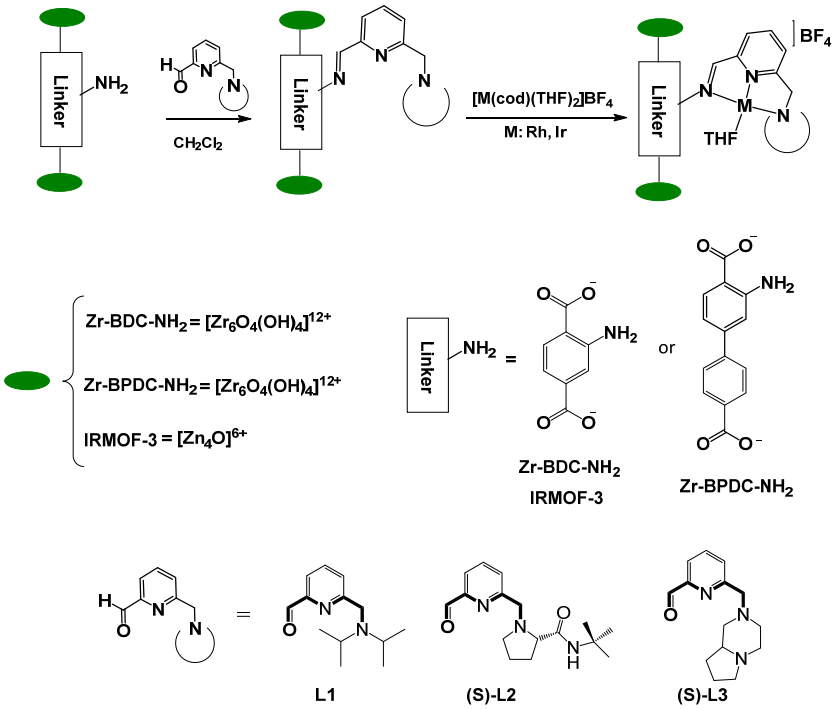

Esquema R3. Preparación de MOFs Post-funcionalizados.

En este capítulo la actividad catalítica es dividida en dos sub apartados para facilitar la lectura ya que se probaron cuatro reacciones diferentes. En la parte A, describimos una reacción en un solo paso (hidrogenación de compuestos aromáticos), Esquema R4(a) y en la parte B, se explican las reacciones multietapa como: *N*-alquilación de aminas (Esquema R4(b), síntesis de aminas secundarias (Esquema R4(c)) y reacciones de olefinación-hidrogenación de aldehídos en cascada (Esquema R4(d)).

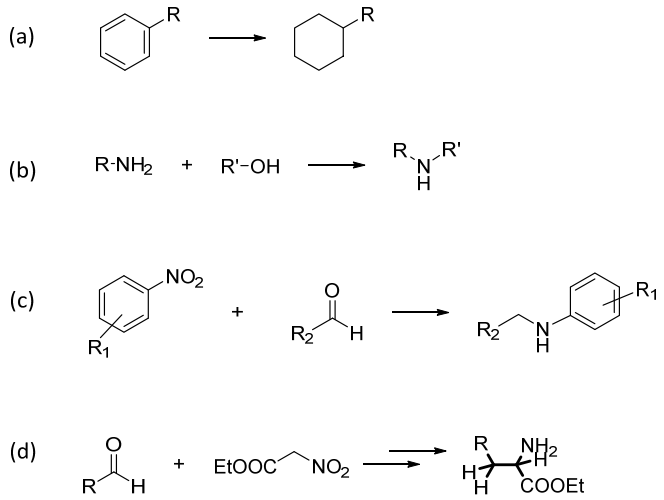

Esquema R4. Reacciones catalíticas del capítulo 2: (a) Hidrogenación de compuestos aromáticos, (b) *N*-alquilación de aminas, (c) Síntesis de aminas secundarias y (d) Reacción de Condensación-hidrogenación en cascada.

Capítulo 3: MOFs con mezcla de metales.

La introducción de varios cationes metálicos en las redes metal-orgánicas es una estrategia interesante para modular las propiedades de materiales porosos hacia aplicaciones prácticas. Los MOFs con mezcla de metales pueden ser sintetizados mediante síntesis directa bajo condiciones solvotermales, mediantes intercambio de metal post-síntesis[172] o por diseño racional de unidad de construcción secundaria.[173]

En este capítulo, describimos la formación de MOFs bimetálicos mediante la introducción de un nuevo metal en la estructura del Zr-MOF. Obtenemos ZrTi-MOF mediante un proceso post-sínteis como se puede ver en el Esquema R5(a) y ZrCe-MOFs mediante síntesis directa (Esquema R5(b)).

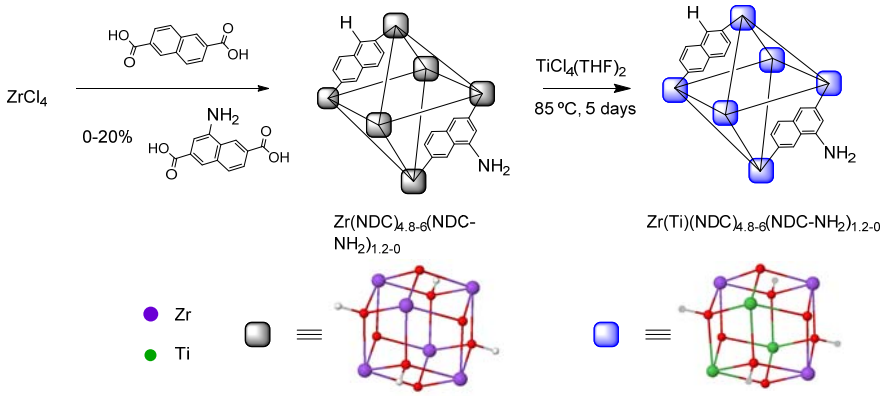

Esquema R5. Síntesis de MOFs con mezcla de metales: (a) ZrTi-MOF mediante intercambio catiónico y (b) ZrCe-MOF mediante síntesis directa.

Los ZrTi-MOFs obtenidos, han sido utilizados como catalizadores en tres reacciones diferentes como se muestra en el Esquema R6. Estos materiales presentan mayor acidez de Lewis que los Zr-MOFs y se estudió el efecto del Ti en la reacción en cascada reducción Meerwein-Ponndorf-Verley-eterificación, en la isomerización del óxido de α-pineno y en la ciclación del citronelal, obteniendo buenas conversiones y selectividades.

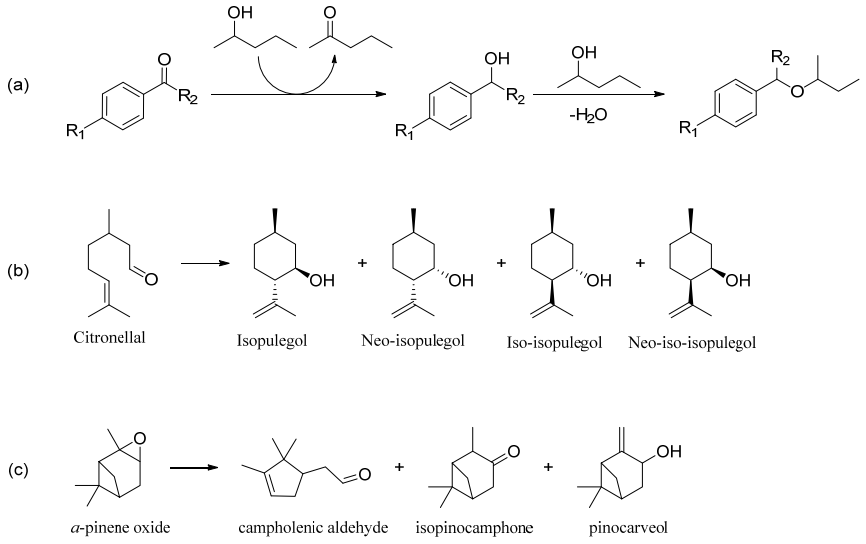

Esquema R6. Reacciones catalíticas utilizando ZrTi-MOF como catalizador: (a) Reducción Meerwein-Ponndorf-Verley-eterificación, (b) Isomerización del óxido de α-pineno, (c) Ciclación del citronelal.

Los ZrCe-MOFs se utilizaron como catalizadores para la síntesis de iminas a partir de alcoholes y aminas.

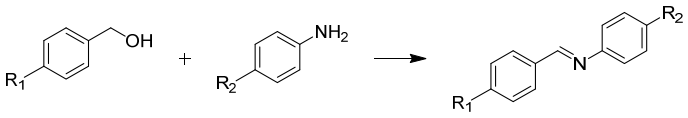

Esquema R7. Formación de iminas a partir de alcohols y aminas.

Después de los experimentos catalíticos, se ha estudiado la reciclabilidad de los catalizadores y podemos concluir que los MOFs formados con el ligando BDC son más robustos ya que cuando se utilizan otros ligandos, la actividad disminuye en cada ciclo.

Los MOFs son buenos materiales para heterogeneizar complejos metálicos ya que no hemos observado lixiviado de los centros activos en las reacciones catalíticas probadas. Son materiales muy vertátiles que nos permiten introducir varios grupos funcionales en su estructura y por lo tanto, pueden catalizar diferentes transformaciones catalíticas con buenas conversiones.

Introduction

1. Sustainable chemistry

Chemistry has contributed to highly increase our life expectancy since it has helped humanity by providing solutions to infectious diseases, agricultural pests or scarcity of food resources.[1] However, the production, use and management of synthetic chemicals and the waste generated cause problems in human health and in the environment. This fact, together with the social, political and judicial pressure, made at late last century arose a movement known as sustainable chemistry.[2] The term 'green chemistry' was described as design of chemical products and processes that reduce or eliminate the use and generation of hazardous substances, in order to improve the quality of life of the present population without compromising the needs of future generations.

Paul Anastas and John Warner developed 12 principles of green chemistry. These concepts include the environmentally safe uses of substances, energy efficient design processes and higher yields, etc. Following these principles, it is possible to design a synthetic route to obtain the desired molecule in the most efficient and respectful way with the environment and human health. To achieve these objectives, it is necessary to explore new chemical transformations that minimize the number of steps, using catalysts capable of carrying out the synthesis of the product of interest quickly and selectively. The applications of these discoveries will mean an advance in scientific knowledge and an improvement in process economics.

Catalysis is one of the fundamental pillars of green chemistry because the design and application of new catalysts and catalytic systems are simultaneously achieving the dual goals of environmental protection and economic benefit.[3] Catalysts can reduce energy expenditure, the number of reagents and separation stages since increase the selectivity.

[1] K. C. Nicolaou *Chem* **2016**, *1*, 331-334.
[2] P. T. Anastas and M. M. Kirchhoff *Acc. Chem. Res.* **2002**, *35*, 686-694.
[3] P. T. Anastas, M. M. Kirchhoff and T. C. Williamson *App. Catal., A* **2001**, *221*, 3-13.

2. Importance of catalysis for sustainable chemistry

In 1835, Berzelius used the term ‘catalysis’ to describe the increase in speed of same reactions when is added to the reaction vessel another substance that is not consumed during the reaction. Thus, when adding a substance in a reaction (in the same or different phase of reagents and solvent) and we obtain the reaction product and the regenerated substance added, this substance is a catalyst for this reaction.

The role of the catalyst is to provide to the reaction an alternative pathway, a faster route to reach the reaction products. Normally, the reaction catalyzed is faster because the alternative path has lower energy activation than no catalyzed reaction. In some cases the effect of the catalyst is only a slight acceleration of the reaction while in other cases the reaction does not take place in absence of the catalyst.

Catalytic reactions play a fundamental role in the development of chemical processes environmentally sustainable as they are involved in atomic economy, in spill prevention, in the improvement of energy efficiency, or in the reduction of derivatization-recovering processes. Catalysis is the key enabler to combine vast use of cars with good air quality. In the production of many healthcare, pharmaceutical and agrochemical products, catalysis is a core technology, thereby increasing our living standards. Catalysis is a key enabling technology for most of the seven societal challenges in Horizon 2020.

When the molecular complexity of the compound of interest increases, the number of stages of it synthesis increases as well, with subsequent separation and purification steps of intermediates. This increases the cost of the synthetic route, decreases the efficiency of the overall process and increases the volume of waste generated. Therefore, perform different reaction steps in the same vessel and under the same conditions is a great advantage from the point of view of sustainability. Efforts to perform these processes 'one pot' are focused on the development of highly selective catalysts and which simultaneously contain different types of catalytic sites necessary to perform each step.

However, the interaction of the different catalytic sites with each other or with other components of the reaction medium may lead to catalyst deactivation, especially when they are incompatible centers (as acids and bases), so that it is necessary to immobilize these centers on a support in order to isolate them

from each other. The active centers can act cooperatively in the transition state or sequentially, where each active site catalyzes a different step resulting in cascade processes (Figure I.1).

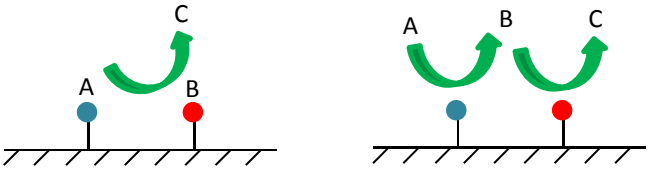

Figure I.1. Example of two isolated active centers and selective to compounds A and B. (a) The active sites act cooperatively in the transition state $[A\text{-}B]^{\neq}$. (b) Each center catalyzes a different step resulting in a cascade reaction.

For that reason, heterogeneous catalysts are promising candidates to be multifunctional catalysts for such synthetic processes.[4]

3. Heterogeneous catalysis

Over 90% of chemicals produced involve some form of catalyst.[5] We use every day many materials and chemicals produced by catalytic processes such as food, drugs, fuels and plastics.[1] Catalysts can be classified as homogeneous or heterogeneous catalysts. Homogeneous catalysts are in the same phase as the reactants, (normally in the liquid phase) whereas heterogeneous catalysts are in a different phase to the reactants (typically solid catalysts and liquid or gaseous reactants). Catalysts are found in nature in the form of enzymes and are responsible for many metabolic processes that sustain life.[6] Enzymes are being used more frequently in industry as biocatalysts for enantioselective

[4] M. J. Climent, A. Corma and S. Iborra *Chem. Rev.* **2011**, *111*, 1072-1133; M. J. Climent, A. Corma and S. Iborra *RSC. Adv.* **2012**, *2*, 16-58; M. J. Climent, A. Corma, S. Iborra and M. J. Sabater *ACS Catal.* **2014**, *4*, 870-891.
[5] J. M. Thomas and W. J. Thomas *Principles and practice of heterogeneous catalysis*, Vol.; VCH, **1997**.
[6] D. L. Nelson and M. M. Cox *Lehninger Principles of Biochemistry*, Vol.; W.H. Freeman, **2013**.

synthesis (and are often treated separately from classical homogeneous and heterogeneous catalysts).[7]

The search for new catalytic systems that are more selective, stable and efficient and that can operate at lower temperatures and pressures is important in academia and industry to minimize waste, save energy and reduce costs. Currently, the field of catalysis is moving from description to prediction. A more rational approach to the development of new catalytic materials for chemical processes is in demand. Important elements of such an approach are computational modelling of catalytic processes at various length- and time-scales and advanced synthetic approaches aimed at delivering materials with improved catalytic performance, preferably starting from cheap, earth-abundant and easily accessible raw building blocks. The catalysis by design approach mostly refers to model/ideal systems.

Although heterogeneous catalysis will likely still dominate future industrial uses of catalysis, it is evident that many of the new challenges facing catalysis, from the use of solar energy to the use of biomass, require integrating homogeneous, heterogeneous and bio-catalysis.

Nevertheless, most catalysts used in industry are solids. These are generally high surface area solids often containing finely dispersed metallic particles.[8] Zeolites are one of the most commercially important classes of catalysts.[9] They are used in oil refining, petrochemistry and organic synthesis. Their porosity and uniform pore channels lead to high catalytic reactivity and selectivity for gas phase reactions. However, zeolites in liquid phase catalysis encounter problems due to their limited pore sizes that restrict diffusion of reactants and products. This can lead to lower catalytic activity and deactivation of the catalyst by poisoning and pore blocking. It is also difficult to introduce organic functionalities into zeolites. Therefore, when Metal-Organic Frameworks (MOFs) emerged several decades ago they attracted attention as catalysts due to their similarity to zeolites, as well as several advantages such as higher surface areas, larger pore sizes and the capacity to be functionalized. But their greatest advantage over zeolites is that chiral MOFs[10] are unmatched by

[7] A. Schmid, J. S. Dordick, B. Hauer, A. Kiener, M. Wubbolts and B. Witholt *Nature* **2001**, *409*, 258-268.
[8] A. T. Bell *Science* **2003**, *299*, 1688-1691.
[9] A. Corma *Chem. Rev.* **1997**, *97*, 2373-2420.
[10] M. Yoon, R. Srirambalaji and K. Kim *Chem. Rev.* **2012**, *112*, 1196-1231.

inorganic solid catalysts in promoting asymmetric transformations. The well-defined structure of the MOFs materials can aid in determining mechanisms and asymmetric inductions pathways.[11]

4. Metal-organic frameworks

Coordination polymers are solid materials formed by an extended network of metal ions (or clusters) coordinated to multidentate organic molecules. A special group of this is Metal-Organic Frameworks which are porous and crystalline compounds involving coordination bonds between metal and organic units. Their most relevant properties are crystallinity, porosity and strong metal-linker interactions (coordination bonds are weaker than covalent bonds but they present higher directionality and are stronger than π-π stacking or hydrogen bonds); besides, they can have very high surface areas, large pore volumes and tunable pore dimensions. The number of potential structures is nearly unlimited due to the wide possible combinations between inorganic and organic building units. MOFs have attracted considerable interest for potential applications in gas adsorption,[12] separations,[13] catalysis,[14] gas storage,[15] sensors and other technologies[16], because of their high porosity, thermal stability, and chemical suitability.

[11] P. Garcia-Garcia, M. Muller and A. Corma *Chem. Sci.* **2014**, *5*, 2979-3007.
[12] L. J. Murray, M. Dinca and J. R. Long *Chem. Soc. Rev.* **2009**, *38*, 1294-1314.
[13] J.-R. Li, R. J. Kuppler and H.-C. Zhou *Chem. Soc. Rev.* **2009**, *38*, 1477-1504; C. Gücüyener, J. van den Bergh, J. Gascon and F. Kapteijn *J. Am. Chem. Soc.* **2010**, *132*, 17704-17706.
[14] O. M. Yaghi, M. O'Keeffe, N. W. Ockwig, H. K. Chae, M. Eddaoudi and J. Kim *Nature* **2003**, *423*, 705-714; O. M. Yaghi *Nat. Mater.* **2007**, *6*, 92-93; L. Ma, C. Abney and W. Lin *Chem. Soc. Rev.* **2009**, *38*, 1248-1256.
[15] J. R. Long and O. M. Yaghi *Chem. Soc. Rev.* **2009**, *38*, 1213-1214; D. J. Tranchemontagne, J. L. Mendoza-Cortes, M. O'Keeffe and O. M. Yaghi *Chem. Soc. Rev.* **2009**, *38*, 1257-1283; H.-L. Jiang and Q. Xu *Chem. Commun.* **2011**, *47*, 3351-3370; R. J. Kuppler, D. J. Timmons, Q.-R. Fang, J.-R. Li, T. A. Makal, M. D. Young, D. Yuan, D. Zhao, W. Zhuang and H.-C. Zhou *Coord. Chem. Rev.* **2009**, *253*, 3042-3066.
[16] A. C. McKinlay, R. E. Morris, P. Horcajada, G. Férey, R. Gref, P. Couvreur and C. Serre *Angew. Chem. Int. Ed.* **2010**, *49*, 6260-6266.

Chemists started to construct framework materials from metal and organic or inorganic units long ago. Prussian blue,[17] a pigment synthesized in 1704 in Berlin by the paint maker Heinrich Diesbach is the first example of coordination polymer. Trying to obtain a red pigment, he mixed iron sulfate with potassium hydroxide that was contaminated and obtained a dark blue dye. In this compound, metal ions are linked through cyanide bridges, is a mixture of ferrous and ferric cyanide, with formula $Fe_4[Fe(CN)_6]_3 \cdot xH_2O$ (Figure I.2). At that time, Diesbach unaware that his unexpected discovery would become one of the most important in the coordination chemistry and in industry because, due to its high dye-ability, Prussian blue has been very important in the textile industry and in the manufacture of paints and pigments.

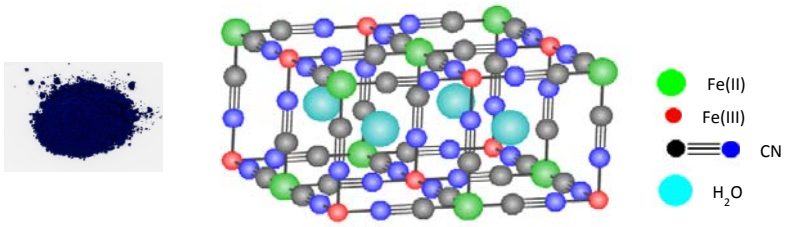

Figure I.2. Prussian blue sample and it crystal structure.

However, due to lack of proper technique required for structural elucidation, Prussian blue was marked 273 years later.[18] In fact, in 1897 the chemists Hofmann and Küspert began to delve into the structural conformation of coordination compounds using for the first time the network concept, related to the structural skeleton. Meanwhile, the term coordination polymer was introduced for the first time in a publication in 1916.[19] However, these emerging concepts could not be fully verified until obtaining the corresponding crystal structures, the structures of these materials were unknown until the advent of X-ray crystallography.[20] Following the International Union of Pure

[17] G. E. Stahl *Experimenta, Observationes, Animadversiones, CCC numero Chymicae et Physicae*, Vol.; Ambrosius Haude, Berlin, **1731**.
[18] H. J. Buser, D. Schwarzenbach, W. Petter and A. Ludi *Inorg. Chem.* **1977**, *16*, 2704-2710.
[19] Y. Shibata *J. Coll. Sci., Imp. Univ. Tokyo* **1916**, *37*, 1-17.
[20] W. L. Bragg *Proc. R. Soc. A* **1913**, *89*, 248-277; W. H. Bragg and W. L. Bragg *Proc. R. Soc. A* **1913**, *89*, 277-291.

and Applied Chemistry (IUPAC) definitions, we treat coordination polymers as 'coordination compounds with repeating coordination entities extending in 1, 2, or 3 dimensions' and MOFs 'coordination networks with organic ligands containing potential voids'.

The first example of a crystalline coordination polymer containing organic linkers (adiponitrile) was reported in 1959 (Figure I.3.a),[21] although the concept MOF was defined much later, in 1995 by Yaghi *et all*. in an article in the prestigious journal *Nature*.[22] In the nineties it was when this field of research was pushed by the groups of Yaghi,[23] Ferey[24] and Kitagawa[25] among others. The evidence of porosity in PCPs and MOFs was independently shown by Kitagawa in 1997[26] and Yaghi in 1998.[27] However, a major breakthrough in MOFs was MOF-5 in 1999[28] (Figure I.3.b), which has a Brunauer-Emmett-Teller (BET) surface of 2320 $m^2 \cdot g^{-1}$ and with proper handling, the surface area can be increased to 3800 $m^2 \cdot g^{-1}$.[29]

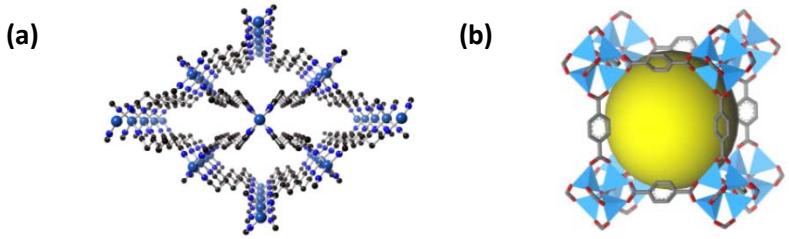

Figure I.3. (a) [Cu(adiponitrile)$_2$] and (b) MOF-5.

[21] Y. Kinoshita, I. Matsubara, T. Higuchi and Y. Saito *Bull. Chem. Soc. Jpn.* **1959**, *32*, 1221-1226.
[22] O. M. Yaghi, G. Li and H. Li *Nature* **1995**, *378*, 703-706.
[23] O. M. Yaghi and H. Li *J. Am. Chem. Soc.* **1995**, *117*, 10401-10402.
[24] D. Riou and G. Ferey *J. Mater. Chem.* **1998**, *8*, 2733-2735.
[25] S. Kitagawa, S. Matsuyama, M. Munakata and T. Emori *J. Chem.Soc., Dalton Trans.* **1991**, 2869-2874; S. Kitagawa, S. Kawata, Y. Nozaka and M. Munakata *J. Chem. Soc., Dalton Trans.* **1993**, 1399-1404.
[26] M. Kondo, T. Yoshitomi, H. Matsuzaka, S. Kitagawa and K. Seki *Angew. Chem. Int. Ed.* **1997**, *36*, 1725-1727.
[27] H. Li, M. Eddaoudi, T. L. Groy and O. M. Yaghi *J. Am. Chem. Soc.* **1998**, *120*, 8571-8572.
[28] H. Li, M. Eddaoudi, M. O'Keeffe and O. M. Yaghi *Nature* **1999**, *402*, 276-279.
[29] S. S. Kaye, A. Dailly, O. M. Yaghi and J. R. Long *J. Am. Chem. Soc.* **2007**, *129*, 14176-14177.

MOF synthesis is dominated by solution-based routes[30] using a pure solvent or a suitable mixture of solvents (the synthesis of MOF-74 uses DMF, ethanol and water).[31] The most used method is the solvothermal crystallization, this method involves the combination of organic ligand and metal precursor in a coordinating solvent (water, dimethylformamide 'DMF', tetrahydrofuran 'THF', …) at a given temperature for a certain time. Under these conditions the MOF crystallization occurs by self-assembly processes of organic and metal units through coordination bonds. There are alternative synthesis techniques such as microwave-assisted, mechano-, electro-, and sonochemical methods introducing energy into the reaction through microwave irradiation,[32] mechanical force (mechanochemistry)[33], electric potential (electrochemistry)[34] and mecanical vibration (sonochemistry)[35] respectively. These methods can have several advantages compared to conventional electric heating, for example shorter reaction times, smaller particle sizes, lower amounts of solvents and safer conditions.

In the synthesis of MOFs are generally used additives, such as modulators. Modulators have been often assumed to play two important roles in the modulated synthesis of MOFs: (1) to facilitate the formation of metal clusters and thus the growth of crystals; (2) to slow down the crystal growth rate avoiding fast precipitation of amorphous products.[36] Thus, the porosity is increased and the crystallinity of these materials is improved.[37] The modulators for carboxylate-MOFs are typically monocarboxylic acids such as benzoic acid (BA) or trifluoroacetic acid (TFA). The proposed role of the modulator is that acts as capping agent, coordinating to the metal ions or

[30] N. Stock and S. Biswas *Chem. Rev.* **2012**, *112*, 933-969.
[31] T. Grant Glover, G. W. Peterson, B. J. Schindler, D. Britt and O. Yaghi *Chem. Eng. Sci.* **2011**, *66*, 163-170.
[32] J. Klinowski, F. A. Almeida Paz, P. Silva and J. Rocha *Dalton Trans.* **2011**, *40*, 321-330.
[33] D. Prochowicz, K. Sokolowski, I. Justyniak, A. Kornowicz, D. Fairen-Jimenez, T. Friscic and J. Lewinski *Chem. Commun.* **2015**, *51*, 4032-4035.
[34] H. Al-Kutubi, J. Gascon, E. J. R. Sudhölter and L. Rassaei *ChemElectroChem* **2015**, *2*, 462-474.
[35] A. A. Tehrani, V. Safarifard, A. Morsali, G. Bruno and H. A. Rudbari *Inorg. Chem. Commun.* **2015**, *59*, 41-45.
[36] Z. Hu, I. Castano, S. Wang, Y. Wang, Y. Peng, Y. Qian, C. Chi, X. Wang and D. Zhao *Cryst. Growth Des.* **2016**, *16*, 2295-2301.
[37] S. Diring, S. Furukawa, Y. Takashima, T. Tsuruoka and S. Kitagawa *Chem. Mater.* **2010**, *22*, 4531-4538; D. Zacher, R. Nayuk, R. Schweins, R. A. Fischer and K. Huber *Cryst. Growth Des.* **2014**, *14*, 4859-4863.

clusters during MOF synthesis, slowing the crystal growth and the nucleation rate. When basic modulators are using in MOF synthesis, smaller particles sizes are obtained (e. g. sodium acetate). The rate of crystal growth was significantly accelerated by the sodium acetate. The enhancing effect is related to the basicity of the sodium acetate which, due to the increase in the pH of the reaction medium, can greatly prompt the deprotonation rate of the organic linkers and hence the nucleation rate.[38] The synthesis parameters (temperature, pH, molar ratio of reactants, addition order, solvent and reaction time) play an essential role in MOF crystallization. High-throughput (HT) methods are a useful approach for investigating synthesis parameters. These methods consist in carry out many reactions simultaneously using parallel reactors in small-scale.[39]

5. Building units and structures of MOFs

A metal organic framework is a compound built out of organic ligands as linkers and metal centers as connectors. The structure is formed through coordination bonds between the organic ligand and the metal ion. Therefore, a metallic aggregate with particular coordination geometry is formed (Secondary Building Unit, SBU). Examples of SBUs are shown in Figure I.4. For the synthesis of MOFs have been successfully employed a variety of metal atoms in their most stable oxidation states (i.e., alkaline, alkaline-earth, transition metals, main group metals and rare-earth metals). The organic linkers are multidentate organic ligands, which are usually carboxylates, azoles, nitriles, etc. As organic spacers, rigid molecules are preferred over flexible molecules because they favor the generation of crystalline, stable and porous MOFs. The properties of the metal centers and the linker, generally determine the function of the material, such as porosity, pore size, pore surface, and other physical properties.[40]

[38] H. Guo, Y. Zhu, S. Wang, S. Su, L. Zhou and H. Zhang *Chem. Mater.* **2012**, *24*, 444-450.
[39] S. Han, Y. Huang, T. Watanabe, Y. Dai, K. S. Walton, S. Nair, D. S. Sholl and J. C. Meredith *ACS Comb. Sci.* **2012**, *14*, 263-267; C. McKinstry, E. J. Cussen, A. J. Fletcher, S. V. Patwardhan and J. Sefcik *Cryst. Growth Des.* **2013**, *13*, 5481-5486.
[40] S. Qiu and G. Zhu *Coord. Chem. Rev.* **2009**, *253*, 2891-2911.

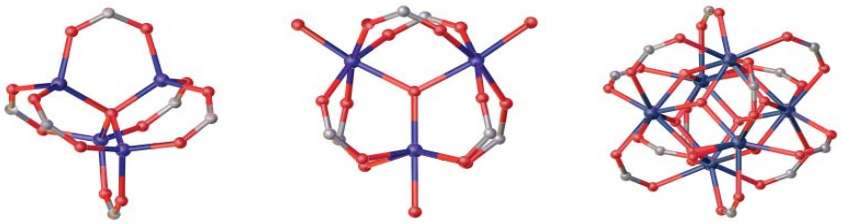

Figure I.4. Examples of SBU: The $Zn_4(\mu_4\text{-O})$ unit of MOF-5 (left), the $Cr_3(\mu_3\text{-O})$ SBU of MIL-101 (in the middle) and the Zr_6O_8 'brick' of UiO-66 (right).[41]

A given metal-linker combination can generate different structures of MOFs with subtle changes in the parameters of the material synthesis, such as the temperature, the nature of solvents or the presence of guest molecules. Thus, the same SBU and linker are used, but they present different connectivity between them.[42] This phenomenon is known as polymorphism and is the ability of a material to adopt more than one crystal structure. Polymorphism occurs in most types of crystals such as metals, inorganic solids, organic molecules and metal-organic materials. For example, Tin shifts from a ductile β-form to a brittle α-form when cooled;[43] Silica has many polymorphs, quartz, cristobalite, coesite, etc;[44] in chocolate making, polymorphism is also important since cocoa butter crystallizes in six different polymorphs being the β-phase the preferred one.[45] An example of polymorphism in MOFs can be found in the low density phase MIL-101, which becomes the phase MIL-88B, and this, in the densest and more thermodynamically stable MIL-47 at high temperatures as shown in figure I.5. The properties of MIL-88B and MIL-101 are much different, while the MIL-88B has a flexible structure and is sensitive to the type of solvent; the MIL-101 is rigid, contains mesoporous cavities and has a high specific surface area.[46]

[41] M. Bosch, M. Zhang and H.-C. Zhou *Adv. Chem.* **2014**, *2014*, 8.
[42] J.-P. Zhang, X.-C. Huang and X.-M. Chen *Chem. Soc. Rev.* **2009**, *38*, 2385-2396.
[43] S. Kean *The Disappearing Spoon: And Other True Tales of Madness, Love, and the History of the World from the Periodic Table of the Elements*, Vol.; Little, Brown, **2010**.
[44] J. V. Smith and C. S. Blackwell *Nature* **1983**, *303*, 223-225.
[45] H. Schenk and R. Peschar *Radiat. Phys. Chem.* **2004**, *71*, 829-835.
[46] F. Carson, J. Su, A. E. Platero-Prats, W. Wan, Y. Yun, L. Samain and X. Zou *Cryst. Growth Des.* **2013**, *13*, 5036-5044.

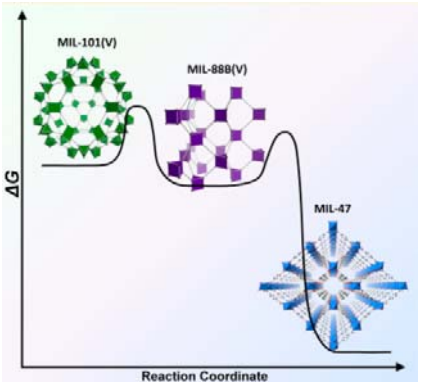

Figure I.5. Depending on the temperature, time and pH of the synthesis, different families of MOFs are obtained for the same combination of metal and organic ligand. Reprinted with permission from reference 46, Copyright (2013) American Chemical Society.

Among all families of MOFs, we can stand out the family called MOF-n (n = 2, 3, 4, 5, ...) synthesized with ligands such as 1,4-bencenedicarboxylate (BDC) or 1,3,5-bencenetricarboxylate (BTC), among others, and developed by Yaghi et al.,[28,47] as well as the compounds known as MIL-n (Matérial Institut Lavoisier) and HKUST-1 (Hong Kong University of Science and Technology), which contain the ligand BTC with different metal centers, developed by groups Ferey[48] and Williams,[49] respectively. Another important family is that of the UiO-MOFs (Universitet i Oslo), which are formed by cluster zirconium with different organic ligands described by Lillerud et al.[50] (Figure I.6).

[47] M. Eddaoudi, H. Li and O. M. Yaghi *J. Am. Chem. Soc.* **2000**, *122*, 1391-1397; J. Kim, B. Chen, T. M. Reineke, H. Li, M. Eddaoudi, D. B. Moler, M. O'Keeffe and O. M. Yaghi *J. Am. Chem. Soc.* **2001**, *123*, 8239-8247.

[48] F. Millange, C. Serre and G. Ferey *Chem. Commun.* **2002**, 822-823; C. Serre, F. Millange, C. Thouvenot, N. Gardant, F. Pelle and G. Ferey *J. Mater. Chem.* **2004**, *14*, 1540-1543.

[49] S. S.-Y. Chui, S. M.-F. Lo, J. P. H. Charmant, A. G. Orpen and I. D. Williams *Science* **1999**, *283*, 1148-1150.

[50] J. H. Cavka, S. Jakobsen, U. Olsbye, N. Guillou, C. Lamberti, S. Bordiga and K. P. Lillerud *J. Am. Chem. Soc.* **2008**, *130*, 13850-13851.

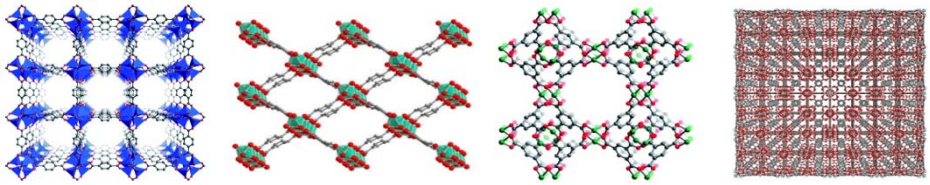

Figure I.6. From left to right: Crystalline structures of MOF-5, MIL-53, HKUST-1 and UiO-66.

6. Stability of MOFs

Most MOFs show chemical stability towards organic solvents and present reasonably high thermal stability (thermal decomposition usually occurs around 300-500 °C). However, MOFs are sensitive to water and tend to decompose in acidic and basic aqueous media. The design and development of moisturestable porous materials are crucial for industrial applications such as gas storage and separation, sensing, catalysis, and proton conduction.[51]

The stability of MOF depends on different factors: charge and coordination of the metal, chemical functionality and connectivity of the organic linker, basicity, flexibility, degree of interpenetration, linker stiffness and length and framework dimensionality. MOF stability is related to both the thermodynamic stability (e.g. metal-ligand bond strength) and the kinetic stability (e.g. framework accessibility).[52]

The key structural property common to thermodynamically stable MOFs is an inert metal cluster that renders it unfavorable for an irreversible hydrolysis reaction to occur. The oxygen in water is a nucleophile whereas the metal coordination centers in MOFs are electrophilic. If this metal center is not sufficiently inert, water can coordinate with the metal cluster and distort or destroy the MOF's crystal lattice. Low and co-workers concluded that the metal-ligand strength is the most critical factor affecting MOF stability.[53] The strength of the metal-ligand bond is related to the ligand in terms of basicity of the coordinating atom, and the metal, in terms of oxidation state and ionic radius. More acidic metals that are highly oxophilic (those with higher

[51] J. Canivet, A. Fateeva, Y. Guo, B. Coasne and D. Farrusseng *Chem. Soc. Rev.* **2014**, *43*, 5594-5617.
[52] N. C. Burtch, H. Jasuja and K. S. Walton *Chem. Rev.* **2014**, *114*, 10575-10612.
[53] J. J. Low, A. I. Benin, P. Jakubczak, J. F. Abrahamian, S. A. Faheem and R. R. Willis *J. Am. Chem. Soc.* **2009**, *131*, 15834-15842.

oxidation states or smaller ionic radii) have stronger M-O bonds and therefore MOFs based on M^{III} and M^{IV} metals are normally more stable then M^{II}-based MOFs. The use of more basic linkers also results in stronger metal-ligand bonds. Due to the metal-linker pairing is essentially Lewis acid-base chemistry, the pK_a of the coordinating group on the linker correlates with the stability of the framework. Long *et al*. demonstrated that as the pK_a of the linker increases, the framework becomes more stable in MOFs.[54]

In addition to thermodynamic contributions, kinetic effects contribute to the water stability of MOFs. A hydrolysis reaction can only progress if two distinct events occur. First, the water molecule must come sufficiently close to the metal to allow interaction between the electron orbitals on the electrophilic metal and nucleophilic water. Second, the energetics of this interaction must be great enough to overcome the activation energy barrier of the reaction. The necessity of this first event underscores the important role framework hydrophobicity can play in improving MOF water stability. It has been widely reported that MOF stability under humid conditions can be improved by incorporating hydrophobic fluorinated and alkyl functional groups on the ligand.[55] Even if water molecules can come sufficiently close to the metal center, the presence of steric factors can reduce the reaction kinetics by providing a significant activation energy barrier to overcome. Despite the relatively low pK_a of carboxylate ligands, the high coordination number of the metal in the well-known Zr-based UiO-66 MOF helps make this structure highly stable even after adsorbing large amounts of water.[56]

[54] V. Colombo, S. Galli, H. J. Choi, G. D. Han, A. Maspero, G. Palmisano, N. Masciocchi and J. R. Long *Chem. Sci.* **2011**, *2*, 1311-1319.

[55] C. Serre *Angew. Chem. Int. Ed.* **2012**, *51*, 6048-6050; T.-H. Chen, I. Popov, O. Zenasni, O. Daugulis and O. S. Miljanic *Chem. Commun.* **2013**, *49*, 6846-6848; J. G. Nguyen and S. M. Cohen *J. Am. Chem. Soc.* **2010**, *132*, 4560-4561; T. Wu, L. Shen, M. Luebbers, C. Hu, Q. Chen, Z. Ni and R. I. Masel *Chem. Commun.* **2010**, *46*, 6120-6122.

[56] J. B. DeCoste, G. W. Peterson, B. J. Schindler, K. L. Killops, M. A. Browe and J. J. Mahle *J. Mater. Chem., A* **2013**, *1*, 11922-11932; F. Jeremias, V. Lozan, S. K. Henninger and C. Janiak *Dalton Trans.* **2013**, *42*, 15967-15973; W. Zhang, H. Huang, D. Liu, Q. Yang, Y. Xiao, Q. Ma and C. Zhong *Microporous Mesoporous Mater.* **2013**, *171*, 118-124.

7. Functionalization of MOFs

The functionalization of MOF materials is a powerful strategy to tune their properties to fit a specific application (i.e. the flexibility, the porosity and the functionalities). The interior pore surface of a MOF can be designed by chemically functionalizing the metal SBU,[49] the linker[57] or the pores.[58] There are three main routes to functionalize MOFs; the first route is direct synthesis in which the MOF is synthesized from pre-functionalized components. The second route is post-synthetic functionalization (PSM), wherein the MOF is modified after it has been synthesized. PSM can be classified in four different types of modification: (a) covalent PSM if a covalent bond is formed (usually on the linker) (b) dative PSM if a dative bond is formed, (c) post-synthetic deprotection (PSD) if a chemical bond is cleaved inside an intact MOF and (d) host-guest PSM if the cavities host metallic nanoparticles or molecules.[59] The third route is post-synthetic exchange (PSE) which involves the metathesis of linkers, metal ions or counter-ions in the MOF.[60] In figure I.7 are represented the three main routes for functionalization of these materials; in this case, the functionalization is shown in the linker although may be used the same three methods in the metal SBU.

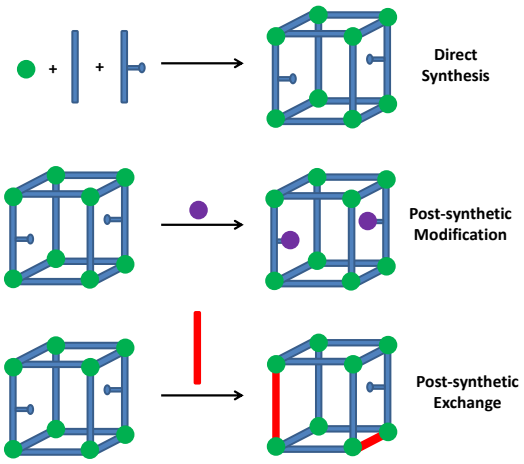

Figure I.7. Functionalization routes for MOFs.

[57] M. Eddaoudi, J. Kim, N. Rosi, D. Vodak, J. Wachter, M. O'Keeffe and O. M. Yaghi *Science* **2002**, *295*, 469-472.
[58] S. Hermes, M.-K. Schröter, R. Schmid, L. Khodeir, M. Muhler, A. Tissler, R. W. Fischer and R. A. Fischer *Angew. Chem. Int. Ed.* **2005**, *44*, 6237-6241.
[59] S. M. Cohen *Chem. Rev.* **2012**, *112*, 970-1000.
[60] M. Kim, J. F. Cahill, Y. Su, K. A. Prather and S. M. Cohen *Chem. Sci.* **2012**, *3*, 126-130.

Direct synthesis is the simplest route to synthesize functionalized MOFs. This method requires that the components do not interfere with the formation of the desired framework and they must be stable under the synthesis conditions. Simple organic functional groups, such as bromo or amino functionalized linkers, can be introduced directly into the MOF without affecting the structure of the material.[57] It may be advantageous to make the MOF with a mixture of linkers with an equivalent geometry, this allows to control the load of functionalization. These MOFs have been called as mixed-linker MOFs,[61] multivariate (MVT) MOFs,[62] doped-MOFs[63] or MOF copolymers.[64] Linkers containing metal complexes (metallolinkers) have been introduced in the structure of MOFs as well.[65] Mixed-metal MOFs may also be synthesized by using multiple metals in the MOF synthesis.[66]

The PSM is an attractive strategy for functionalizing MOFs as it avoids the limitations of the direct synthesis. In this route for functionalizing MOFs, the material is chemically modified after it has been formed. Classical organic chemistry reactions can be applied to modify MOFs containing functional groups (also called chemical handles or tags) with covalent PSM.[67] Dative Bonds can be formed by anchoring organic molecules onto open metal sites of the metal SBU or metal complexes onto the organic linker (known as post-synthetic metalation, PSMet).[68] Some metal SBUs in MOFs contain aqua ligands that can be removed and replaced with other coordinating molecules (e.g. amines).[69] PSMet treats the MOF as a ligand to obtain the metallation through the functional group on the linker. PSD is a useful strategy to introduce new functionalities into the MOF that are impossible to achieve by

[61] S. Yuan, J.-S. Qin, L. Zou, Y.-P. Chen, X. Wang, Q. Zhang and H.-C. Zhou *J. Am. Chem. Soc.* **2016**, *138*, 6636-6642.
[62] H. Deng, C. J. Doonan, H. Furukawa, R. B. Ferreira, J. Towne, C. B. Knobler, B. Wang and O. M. Yaghi *Science* **2010**, *327*, 846-850.
[63] C. Wang, Z. Xie, K. E. deKrafft and W. Lin *J. Am. Chem. Soc.* **2011**, *133*, 13445-13454.
[64] K. Koh, A. G. Wong-Foy and A. J. Matzger *Chem. Commun.* **2009**, 6162-6164.
[65] B. F. Abrahams, B. F. Hoskins, D. M. Michail and R. Robson *Nature* **1994**, *369*, 727-729; C. A. Kent, B. P. Mehl, L. Ma, J. M. Papanikolas, T. J. Meyer and W. Lin *J. Am. Chem. Soc.* **2010**, *132*, 12767-12769.
[66] G.-T. Vuong, M.-H. Pham and T.-O. Do *CrystEngComm* **2013**, *15*, 9694-9703.
[67] A. D. Burrows, C. G. Frost, M. F. Mahon and C. Richardson *Angew. Chem. Int. Ed.* **2008**, *47*, 8482-8486.
[68] J. D. Evans, C. J. Sumby and C. J. Doonan *Chem. Soc. Rev.* **2014**, *43*, 5933-5951.
[69] Y. K. Hwang, D.-Y. Hong, J.-S. Chang, S. H. Jhung, Y.-K. Seo, J. Kim, A. Vimont, M. Daturi, C. Serre and G. Férey *Angew. Chem. Int. Ed.* **2008**, *47*, 4144-4148.

other PSM methods. PSD allows ligands with protecting groups to be chemically, thermolytically or photochemically deprotected after the framework has been synthesized.[70] And host-guest PSM is used to encapsulate guests in the pores of the MOF.[58]

Analogous to PSM, the PSE route can be used to design materials that are not accessible by other methods. It may be exchange either the metal ions of the SBU (cation exchange), organic linkers (linker exchange) and counter-ions in the pores of the MOFs (exchange of the guests molecules is also performed).[60] The substitution of the metal in the SBU with the metal in solution can be achieved by soaking a MOF in a solution containing metal ions. The partial metal substitution leads to a mixed-metal MOF.[71] Similar to cation exchange, exposure of a MOF to either a solution containing free organic linkers or a mixture containing MOFs with different linkers results in substitution or mixing of the linkers.[72] The counter-ions in the pores of cationic or anionic MOFs may be exchanged as well and this strategy has been used to introduce cationic metal complexes into the pores of an anionic MOF.[73]

8. Catalysis with MOFs

As mentioned above, the MOFs have attracted much interest in the field of heterogeneous catalysis in recent years.[74] The crystalline nature of MOFs allows to accurately know the position of each atom within the crystalline network and therefore its coordination environment, bond distances, electronic properties of the metal ions, etc. It allows the application of computational methods to understand, or even predict the properties and

[70] T. Yamada and H. Kitagawa *J. Am. Chem. Soc.* **2009**, *131*, 6312-6313.
[71] M. Dincă and J. R. Long *J. Am. Chem. Soc.* **2007**, *129*, 11172-11176.
[72] B. J. Burnett, P. M. Barron, C. Hu and W. Choe *J. Am. Chem. Soc.* **2011**, *133*, 9984-9987; C. Y. Lee, O. K. Farha, B. J. Hong, A. A. Sarjeant, S. T. Nguyen and J. T. Hupp *J. Am. Chem. Soc.* **2011**, *133*, 15858-15861.
[73] D. T. Genna, A. G. Wong-Foy, A. J. Matzger and M. S. Sanford *J. Am. Chem. Soc.* **2013**, *135*, 10586-10589.
[74] D. Farrusseng, S. Aguado and C. Pinel *Angew. Chem. Int. Ed.* **2009**, *48*, 7502-7513; J. Lee, O. K. Farha, J. Roberts, K. A. Scheidt, S. T. Nguyen and J. T. Hupp *Chem. Soc. Rev.* **2009**, *38*, 1450-1459; J. Gascon, A. Corma, F. Kapteijn and F. X. Llabrés i Xamena *ACS Catal.* **2014**, *4*, 361-378; A. Corma, H. García and F. X. Llabrés i Xamena *Chem. Rev.* **2010**, *110*, 4606-4655.

reactivity of a real or hypothetical material and establish structure-activity relationships. Moreover, the excellent textural properties of some MOFs with high specific surface areas and pore volumes, facilitate the diffusion of reactants from the solution to the active centers and, in turn, allows depositing catalytically active species within the pores of the material.

The first example of catalysis with a coordination polymer was described in 1994 by a Cd-4,4'-bipy MOF for the cyanosilylation of aldehydes.[75] Since then, a wide variety of MOFs have been designed with various transition metals as well as different poly-topic ligands and screened in heterogeneous catalysis of organic transformations, including asymmetric transformations with homochiral MOFs.[76] Therefore, the use of MOFs in catalysis is extremely broad and increasing continuously (Figure I.8).[77]

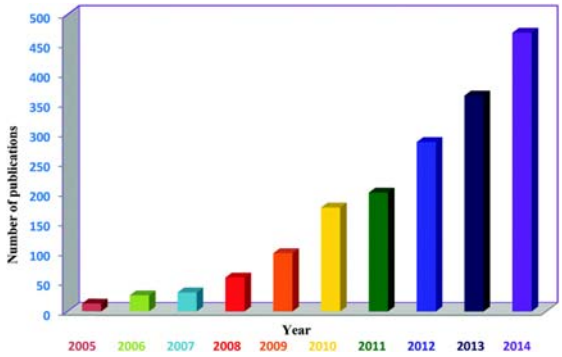

Figure I.8. Publications related to catalysis by MOFs since 2005.

The potential of MOFs as catalysts resides in the ability to adjust their chemical composition, dimensions of the pores and chemical environment within the

[75] M. Fujita, Y. J. Kwon, S. Washizu and K. Ogura *J. Am. Chem. Soc.* **1994**, *116*, 1151-1152.
[76] L. Ma and W. Lin, in *Functional Metal-Organic Frameworks: Gas Storage, Separation and Catalysis*, Vol.; Ed.Schröder), Springer Berlin Heidelberg **2010**, pp. 175-205; K. Mo, Y. Yang and Y. Cui *J. Am. Chem. Soc.* **2014**, *136*, 1746-1749; D. Dang, P. Wu, C. He, Z. Xie and C. Duan *J. Am. Chem. Soc.* **2010**, *132*, 14321-14323; Y. Liu, W. Xuan and Y. Cui *Adv. Mater. (Weinheim, Ger.)* **2010**, *22*, 4112-4135.
[77] A. H. Chughtai, N. Ahmad, H. A. Younus, A. Laypkov and F. Verpoort *Chem. Soc. Rev.* **2015**, *44*, 6804-6849.

pores, which is achieved by selecting the appropriate construction units or by post synthesis modifications (PSM) of the solid material. MOFs combine the benefits of heterogeneous catalysis like easy post reaction separation, catalyst reusability, high stability and homogeneous catalysis such as high efficiency, selectivity, controllability and mild reaction conditions. The possible organization of active centers like metallic nodes, organic linkers, and their chemical synthetic functionalization on the nanoscale shows potential to build up MOFs particularly modified for catalytic challenges.

In MOFs, the active catalytic centers can be in three different positions: (1) the metal SBU, as the case of metal ions with coordinative unsaturation.[49,78] In this case, the metal component of the MOF is weakly coordinated to ligand or solvent molecules that after thermally removed, they leave free positions for interaction with reagents. This provides the MOFs Lewis acid and/or redox properties and gives them the subsequent catalytic activity. In addition, these cations with coordinative unsaturation may be used as anchor points for the introduction of additional functional groups.[79] (2) The linker may contain active functional groups[80] or be design for anchoring active metal centers.[81] The possibility to design MOFs containing catalytic chiral centers by employing chiral organic ligands during synthesis of MOF gives rise to a high number of new heterogeneous asymmetric catalysts.[10, 82] or (3) Besides, it is possible to introduce an encapsulated guest in the pores. The high surface area and the porous structure forming three dimensional interconnected cavities, makes them the ideal media where disperse catalytically active species.[83] Due to the high price of noble metals with catalytic activity, it is very important to have a

[78] F. Vermoortele, P. Valvekens and D. De Vos, in *Metal Organic Frameworks as Heterogeneous Catalysts*, Vol., The Royal Society of Chemistry **2013**, pp. 268-288.
[79] M. Banerjee, S. Das, M. Yoon, H. J. Choi, M. H. Hyun, S. M. Park, G. Seo and K. Kim *J. Am. Chem. Soc.* **2009**, *131*, 7524-7525.
[80] S. Hasegawa, S. Horike, R. Matsuda, S. Furukawa, K. Mochizuki, Y. Kinoshita and S. Kitagawa *J. Am. Chem. Soc.* **2007**, *129*, 2607-2614; J. E. Mondloch, O. K. Farha and J. T. Hupp, in *Metal Organic Frameworks as Heterogeneous Catalysts*, Vol., The Royal Society of Chemistry **2013**, pp. 289-309.
[81] X. Zhang, F. X. Llabrés i Xamena and A. Corma *J. Catal.* **2009**, *265*, 155-160; S.-H. Cho, B. Ma, S. T. Nguyen, J. T. Hupp and T. E. Albrecht-Schmitt *Chem. Commun.* **2006**, 2563-2565.
[82] J. M. Falkowski, S. Liu and W. Lin, in *Metal Organic Frameworks as Heterogeneous Catalysts*, Vol., The Royal Society of Chemistry **2013**, pp. 344-364.
[83] D. Esken, S. Turner, O. I. Lebedev, G. Van Tendeloo and R. A. Fischer *Chem. Mater.* **2010**, *22*, 6393-6401; C. Rosler and R. A. Fischer *CrystEngComm* **2015**, *17*, 199-217.

porous medium which adequately disperse the metal to maximize their interaction with reaction substrates and prevent aggregation and inactivation of nanoparticles. Thus, the MOF can act as a simple support to disperse the catalytic species or may also be involved in the reaction, stabilizing transition states or providing additional active centers. Accordingly, MOFs offer us the possibility to design multifunctional catalysts which allow carrying out processes 'one-pot' involving multiple stages using a single catalyst and reaction vessel, avoiding separation and purification steps of the intermediates. Therefore, in bifunctional or cascade catalysis, several catalytic functionalities in the MOF are involved.

However, when considering the possible application of MOFs as heterogeneous catalysts, it should be noted that an important limitation is their low chemical stability under certain conditions (acids, bases or even some organic functional groups) that can cause leaching of the organic or metallic component from the solid to the reaction medium. This fact compromises the crystal structure of the material and promotes progressive loss of catalytic activity. Although MOFs have lower stability than aluminosilicates or zeolites since they cannot be used in reactions at high temperatures and/or pressures, there are MOFs stable enough to be used in reactions below 200 °C, typical of most fine chemicals processes.

Another important aspect that seems to limit the stability of MOFs is their mechanical strength when to compress or model in different shapes and sizes is required to place them in a reactor.[84] It is therefore necessary to check that the material remains intact in the reaction conditions, which is usually determined by comparing the pattern of X-ray diffraction, the chemical composition and the textural properties of the freshly prepared MOF with measurements of the recovered solid after the reaction.

[84] B. Van de Voorde, I. Stassen, B. Bueken, F. Vermoortele, D. De Vos, R. Ameloot, J.-C. Tan and T. D. Bennett *J. Mater. Chem., A* **2015**, *3*, 1737-1742.

Objectives

The main objective of this thesis is to study the catalytic properties of some MOFs of zirconium. Therefore, we have performed the synthesis and characterization of different metal-organic materials. The work has been divided into three chapters, depending on the type of functionalization of MOFs. The objectives in this thesis are.

- Synthesis of Zr-MOFs using different organic linkers and mixtures of linkers within the same material (Chapter 1).

- Heterogenization of transition metal complexes by post-functionalization of the amino linker in Zr-MOFs (Chapter 2).

- Synthesis of bimetallic MOFs obtaining mixed-metals ZrTi-MOFs and ZrCe-MOFs (Chapter 3).

- Characterization by usual techniques in materials.

- Catalytic activity of the resulting materials:

  - C-C coupling reactions in Chapter 1.

  - Hydrogenation of aromatic compounds, *n*-alkylation of amines, synthesis of secondary amines and cascade olefination-hydrogenation reaction of aldehydes in chapter 2.

  - Cascade Meerwein-Ponndorf-Verley (MPV) reduction and etherification, cyclization of citronellal, isomerization of α-pinene oxide and direct synthesis of imines from alcohols and amines (chapter 3).

- Study of the recyclability of the different MOFs in several cycles.

Chapter 1

Zirconium Metal-Organic Frameworks

1.1. Introduction

Among the large family of metal-organic frameworks, Zr-based MOFs, which exhibit rich structure types, outstanding stability, intriguing properties and functions, are foreseen as one of the most promising MOF materials for practical applications.[85]

Zirconium is one of the common transition metals on earth, and is mainly obtained from the mineral zircon. Like other group 4 elements, zirconium is highly resistant to corrosion and has high affinity for hard oxygen donor ligands.[86] $Zr_6O_4(OH)_4(CO_2)_{12}$, as a new 12 connected inorganic brick, was first reported in 2008 and has been the highest coordination cluster reported for a MOF to date.[50] It was a decisive step towards improving the stability of MOFs, this structure exhibits unprecedented hydrothermal stability beyond most reported MOFs.

The inorganic brick is the key to the exceptional stability possessed by these structures. It consists of an inner $Zr_6O_4(OH)_4$ core in which the triangular faces of the Zr_6-octahedron are alternatively capped by μ_3-O and μ_3-OH groups (Figure 1.1a). The same inner Zr_6-cluster core has been reported by Puchberger *et al*.[87] but only as isolated clusters. All the polyhedron edges are bridged by carboxylates ($-CO_2$) originating from the dicarboxylic acids forming a $Zr_6O_4(OH)_4(CO_2)_{12}$ cluster (Figure 1.1b). Each zirconium atom is eight-coordinated forming a square-antiprismatic coordination consisting of eight oxygen atoms. One square face is formed by oxygen atoms supplied by carboxylates while the second square face is formed by oxygen atoms coming from the μ_3-O and μ_3-OH groups. This, results in a cluster shaped like a Maltese star (Figure 1.1c). The high symmetry and this famous graphical icon contribute to the exceptional beauty of these structures.[50]

Dehydroxylation of the cluster starts at 250 °C and is completed at 300 °C. Two of the 4 μ_3-OH groups leave together with the hydrogen from the remaining two μ_3-OH groups, resulting in a Zr_6O_6 inner cluster with seven-coordinated

[85] Y. Bai, Y. Dou, L.-H. Xie, W. Rutledge, J.-R. Li and H.-C. Zhou *Chem. Soc. Rev.* **2016**, *45*, 2327-2367.
[86] W. Lu, Z. Wei, Z.-Y. Gu, T.-F. Liu, J. Park, J. Park, J. Tian, M. Zhang, Q. Zhang, T. Gentle Iii, M. Bosch and H.-C. Zhou *Chem. Soc. Rev.* **2014**, *43*, 5561-5593.
[87] M. Puchberger, F. R. Kogler, M. Jupa, S. Gross, H. Fric, G. Kickelbick and U. Schubert *Eur. J. Inorg. Chem.* **2006**, *2006*, 3283-3293.

zirconium. The phenomenon is fully reversible. Figure 1.1d shows the new Zr_6O_6 inner cluster while Figure 1.1e shows the full $Zr_6O_6(CO_2)_{12}$ cluster. This rearrangement results in large changes in Zr-Zr distances within the cluster. However, the overall framework structure is virtually unchanged, as seen by powder X-Ray Diffraction (PXRD). This ability to maintain the network structure upon dehydroxylation and change in coordination around zirconium is the key to understanding the extension in structural stability.[50]

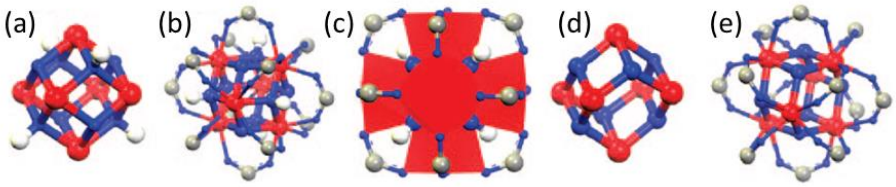

Figure 1.1. Structures (a) and (d) show the inner core Zr_6-cluster drawn alone for clarity, in hydroxylated and dehydroxylated form, and the symmetry change from T_d (-43 m) to D_{3d} (-3 m) when the two μ_3-OH groups are removed. (c) Cluster shaped like a Maltese star. Structures (b) and (e) show the full cluster to illustrate the change in zirconium coordination from 8 to 7 upon dehydration. Zirconium, oxygen, carbon and hydrogen atoms are red, blue, gray, and white, respectively.

The Zr-MOF structures are formed by clusters of zirconium coordinated with linear ligands to give coordination polymers (Figure 1.2). UiO-66 (UiO = University of Oslo, from now on it will be called Zr-BDC; BDC = 1,4-benzenedicarboxylate) was prepared under standard solvothermal conditions using $ZrCl_4$ as a metal precursor, BDC as the organic linker, and dimethylformamide (DMF) as the solvent. The organic linker is assembled from six Zr(IV) ions each with a square antiprismatic coordination geometry comprised of eight oxygen atoms. Each SBU is bound by twelve carboxylate groups from twelve different BDC ligands. Zr-BDC structure shows that it is composed of octahedral (diameter ~11 Å) and tetrahedral (diameter ~8 Å) cages in a 1 : 2 ratio and the cages are connected by triangular windows (diameter of ~6 Å).[88] The connectivity of Zr-BDC was determined by PXRD to be a cubic structure close packed with octahedral cage. It was demonstrated that this unique regular octahedral cage can be easily expanded with increasing

[88] Q. Yang, A. D. Wiersum, P. L. Llewellyn, V. Guillerm, C. Serre and G. Maurin *Chem. Commun.* **2011**, *47*, 9603-9605.

length of the linkers. For example, UiO-67 (It will be called Zr-BPDC in the rest of the thesis; BPDC = (1,1'-biphenyl)-4,4'-dicarboxylic acid) is a Zr-MOF with BPDC as linker, and is isoreticular structure to Zr-BDC with estimated windows size of the pores of 8 Å.[89]

Structural resistance toward solvents and mechanical pressure are critical for the application of MOFs. The resistance of Zr-BDC MOF toward solvents like water, DMF, benzene, and acetone was investigated by stirring the desolvated sample in the solvents for 24 h. The Zr-BDC material has been further exposed to high pressure up to 10.000 kg cm^{-2}. Evidently, the PXRD pattern remains virtually unaltered by the applied treatment.[86] Thermogravimetric analysis (TGA) indicates that Zr-BDC and Zr-BPDC show weight losses at temperatures as high as 540 °C. The Brunauer-Emmett-Teller (BET) surface area of Zr-BDC is 1144 $m^2 \cdot g^{-1}$; Meanwhile, extending the linkers to two rings increases the surface area of the material to 1575 $m^2 \cdot g^{-1}$.[90]

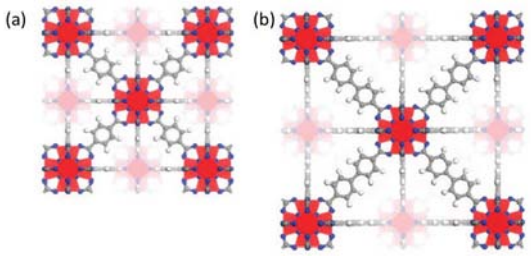

Figure 1.2. (a) Zr-MOF with 1,4-benzene-dicarboxylate (BDC) as linker, Zr-BDC, (b) Zr-MOF with 4,4'-biphenyl-dicarboxylate (BPDC) as linker, Zr-BPDC. Zirconium, oxygen, carbon, and hydrogen atoms are red, blue, gray, and white, respectively.

One issue that has impeded the wider scope of the application of many frameworks is their stability, Zr-NDC (NDC = 2,6-naphthalenedicarboxylate) was reported to be thermally stable up to 500 °C. Owing to the highly oxophilic nature of Zr^{IV}, the Zr_6-cluster SBU, makes these MOFs thermally stable and resistant towards various solvents and elevated pressures, and its structure remains unaltered in a wide range of aqueous solvents.[50,56c] Linker substitution

[89] M. Kim and S. M. Cohen *CrystEngComm* **2012**, *14*, 4096-4104; A. Schaate, P. Roy, A. Godt, J. Lippke, F. Waltz, M. Wiebcke and P. Behrens *Chem. Eur. J.* **2011**, *17*, 6643-6651.

[90] V. Guillerm, F. Ragon, M. Dan-Hardi, T. Devic, M. Vishnuvarthan, B. Campo, A. Vimont, G. Clet, Q. Yang, G. Maurin, G. Férey, A. Vittadini, S. Gross and C. Serre *Angew. Chem. Int. Ed.* **2012**, *51*, 9267-9271.

with BPDC, NDC, or terphenyl dicarboxylate leads to the formation of isoreticular MOFs. This series of MOFs are characterized by a high surface area and an unprecedented linker-independent stability.[50]

The amino-functionalized Zr-BDC-NH_2 and Zr-BPDC-NH_2 derivatives were found to have the same topology[91] and it is also possible to obtain isoreticular structures by mixing different organic linkers in the same material. There are several examples in literature, among different isoreticular MOFs: the IRMOF,[14a,92] the MIL-53,[93] or the Zr-BDC topologies.[50,89b,94] If a precursor solution containing 2-aminobenzene-1,4-dicarboxylate (BDC-NH_2) is used instead of the BDC linker, various MOFs with a NH_2 function in the linker can be obtained, such as Zn_4O(BDC-NH_2)[62] (IRMOF-3). The synthesis of functional MOFs from solutions composed of two or more different linkers is one of the latest developments in the field.[89a,95] Thus, MOFs isoreticular to MOF-5, which contains two to eight different linkers, have been synthesized using a self-assembly method under solvothermal conditions.[62] Although the authors demonstrated no change in the crystal composition at the millimeter scale, they did not exclude the presence of microscopic domains that exhibit a composition different from the average composition of the crystal.[96] A series of Al-MIL-53 materials with the general formula Al(OH)$(BDC)_{1-n}$(BDC-$NH_2)_n$ have been synthesized,[97] in which the terephthalate linker (BDC) is partially

[91] F. Vermoortele, R. Ameloot, A. Vimont, C. Serre and D. De Vos *Chem. Commun.* **2011**, *47*, 1521-1523; C. Gomes Silva, I. Luz, F. X. Llabrés i Xamena, A. Corma and H. García *Chem. Eur. J.* **2010**, *16*, 11133-11138.

[92] N. L. Rosi, J. Eckert, M. Eddaoudi, D. T. Vodak, J. Kim, M. O'Keeffe and O. M. Yaghi *Science* **2003**, *300*, 1127-1129.

[93] T. Devic, P. Horcajada, C. Serre, F. Salles, G. Maurin, B. Moulin, D. Heurtaux, G. Clet, A. Vimont, J.-M. Grenèche, B. L. Ouay, F. Moreau, E. Magnier, Y. Filinchuk, J. Marrot, J.-C. Lavalley, M. Daturi and G. Férey *J. Am. Chem. Soc.* **2010**, *132*, 1127-1136.

[94] S. Chavan, J. G. Vitillo, D. Gianolio, O. Zavorotynska, B. Civalleri, S. Jakobsen, M. H. Nilsen, L. Valenzano, C. Lamberti, K. P. Lillerud and S. Bordiga *Phys. Chem. Chem. Phys.* **2012**, *14*, 1614-1626.

[95] A. D. Burrows *CrystEngComm* **2011**, *13*, 3623-3642.

[96] T. Lescouet, E. Kockrick, G. Bergeret, M. Pera-Titus and D. Farrusseng *Dalton Trans.* **2011**, *40*, 11359-11361.

[97] S. Marx, W. Kleist, J. Huang, M. Maciejewski and A. Baiker *Dalton Trans.* **2010**, *39*, 3795-3798.

substituted by BDC-NH_2. In addition, a Zr-BPDC framework, which contains both urea-functionalized dicarboxylate and BPDC was reported recently.[98]

In this chapter we will show the possibility to synthesize new highly stable Zr-based MOFs by using mixtures of linkers: NDC and 4-amino-2,6-naphthalenedicarboxylic acid (NDC-NH_2) or BPDC and 2-amino-(1,1'-biphenyl)-4,4'-dicarboxylic acid (BPDC-NH_2) as organic linkers. As a result of their rigidity and/or larger pore sizes, these MOFs offer opportunities to enhance the catalytic behavior of Zr-BDC-NH_2 for cascade reactions.

[98] P. W. Siu, Z. J. Brown, O. K. Farha, J. T. Hupp and K. A. Scheidt *Chem. Commun.* **2013**, *49*, 10920-10922.

1.2. Objectives

- Synthesis of mixed linker Zr-MOF. Preparation of zirconium-based metal-organic frameworks from solutions composed of a mixed-ligand system BDC/BDC-NH_2, NDC/NDC-NH_2 or BPDC/BPDC-NH_2.

- Study of the stability of the resulting Zr-BDC-NH_2, Zr-NDC-NH_2 and Zr-BPDC-NH_2 MOFs attending to time, degree of functionalization and length of the linker.

- Catalytic activity of mixed Zr-MOFs in C-C coupling reactions: Knoevenagel-type condensation and subsequent condensation of the product with benzaldehyde to prepare 1,1-dicyanomethylenebutadiene derivatives.

- Recycling of Zr-mixed-linker catalysts.

1.3. Results and Discussion

1.3.1. Mixed Zr-BDC-NH_2, Zr-NDC-NH_2 and Zr-BPDC-NH_2 MOFs

As we have previously mentioned,the Zr-MOFs consist of a Zr(IV)-carboxylate cluster $Zr_6(\mu_3\text{-}O)_4(\mu_3\text{-}OH)_4(CO_2)_{12}$, which works as the inorganic secondary building unit for the framework. Cohen and Lillerud independently discovered that the Zr-BDC motif was very tolerant to functionalized ligands, allowing the synthesis of Zr-BDC MOFs and the amino-functionalized Zr-BDC-NH_2 MOFs derivatives with unchanged topology.[99]

We started with the synthesis of Zr-NH_2-MOFs loaded with 20% of amino ligand. Zr-MOFs-NH_2 were prepared by mixing $ZrCl_4$ with different molar ratios of the ligands (BDC/BDC-NH_2; BPDC/BPDC-NH_2 or NDC/NDC-NH_2) in DMF (Scheme 1.1), crystallization at 120 °C for 12-24 h, and activation by DMF exchange with tetrahydrofuran (THF) followed by drying under vacuum. The percentage of amino ligand that has been used in the synthesis of the material will be indicated in parentheses.

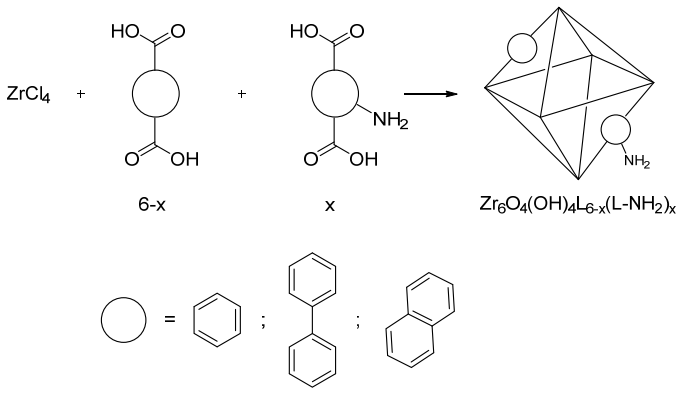

Scheme 1.1. Preparation of mixed Zr-MOFs.

PXRD patterns of Zr-BDC-NH_2(20), Zr-BPDC-NH_2(20) and Zr-NDC-NH_2(20) are shown in Figure 1.3. The diffraction patterns are in good agreement with

[99] S. J. Garibay and S. M. Cohen *Chem. Commun.* **2010**, *46*, 7700-7702; M. Kandiah, M. H. Nilsen, S. Usseglio, S. Jakobsen, U. Olsbye, M. Tilset, C. Larabi, E. A. Quadrelli, F. Bonino and K. P. Lillerud *Chem. Mater.* **2010**, *22*, 6632-6640.

previous reports, which indicates that MOF framework structures with micropores were successfully formed. Notably, the position of the diffraction peak at the lowest angle in the pattern of Zr-NDC (2θ = 6.5°), which is associated to the pore size, was between that of Zr-BPDC (2θ = 5.7°) and Zr-BDC (2θ = 7.4°).

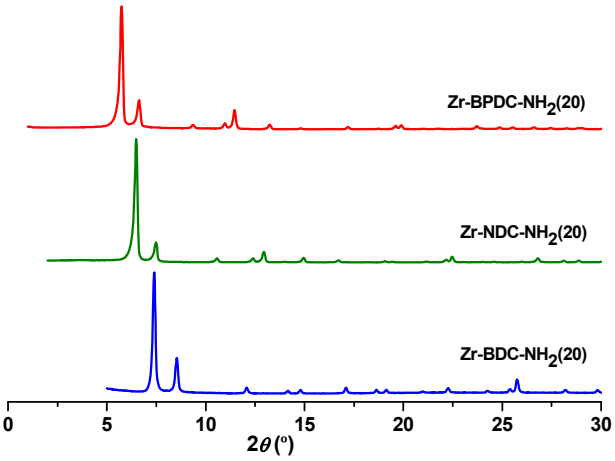

Figure 1.3. PXRD of mixed Zr-MOFs-NH_2(20).

The amino-functionalized Zr-BDC-NH_2(100) and Zr-BPDC-NH_2(100) derivatives presented the same topology[99a,91b] and BET surface areas (800 and 1800 m^2g^{-1}, respectively).

In order to develop a comprehensive study of the crystallinity of mixed Zr-NDC-NH_2 MOFs regarding the amount of NH_2-ligand, NDC and NDC-NH_2 were incorporated together into a single Zr-NDC framework.[100] To study the effect of the concentration of the amino ligand on the crystallinity and stability of the material, the synthesis of Zr-NDC-NH_2 MOFs was performed with different molar ratios of NDC/NDC-NH_2 (0, 5, 10, 20, 35, 50, and 100 %) as linkers obtaining powdered Zr-NDC, Zr-NDC-NH_2 (5), Zr-NDC-NH_2 (10), Zr-NDC-NH_2 (20), Zr-NDC-NH_2 (35), Zr-NDC-NH_2 (50), and Zr-NDC-NH_2 (100). The composition of MOFs with different loadings of substituted units was measured by elemental analysis.

[100] M. Kim, J. F. Cahill, K. A. Prather and S. M. Cohen *Chem. Commun.* **2011**, *47*, 7629-7631.

The PXRD patterns of Zr(NDC)(NDC-NH_2)(x) samples (x=0, 5, 10, 20, 50 and 100%) are given in Figure 1.4. The crystalline structure was maintained until 50% functionalization, and sample with 100% of NDC-NH_2 is essentially amorphous. Crystalline Zr-NDC-NH_2 samples with 20 and 35% of NDC-NH_2 were characterized and used as catalysts with a larger surface area and pore size than those of Zr(BDC-NH_2).

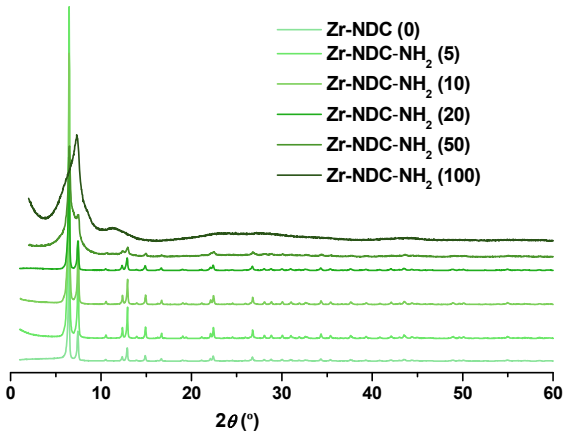

Figure 1.4. PXRD of Zr(NDC)/(NDC-NH_2) mixtures.

The experimental PXRD pattern shown in Fig. 1.3 indicates that the Zr-NDC material obtained is crystalline and topologically similar to the Zr-BDC[90,101]. Thus, the inorganic part $Zr_6O_4(OH)_4$ is bonded to twelve NDC ligands forming a 3D periodic structure, and each centric octahedral cage (≈ 13 Å) is connected by eight corner tetrahedral cages (≈ 10 Å) through windows of ≈ 7 Å. All samples exhibited octahedron-like morphology and the mixed $Zr_6O_4(OH)_4(NDC)_{6-x}(NDC\text{-}NH_2)_x$ samples are highly homogeneous in terms of crystal shape and size (≈ 0.4 μm) (Fig. 1.5).

[101] V. Guillerm, F. Ragon, M. Dan-Hardi, T. Devic, M. Vishnuvarthan, B. Campo, A. Vimont, G. Clet, Q. Yang, G. Maurin, G. Férey, A. Vittadini, S. Gross and C. Serre *Angew. Chem. Int. Ed.* **2012**, *124*, 9401-9405.

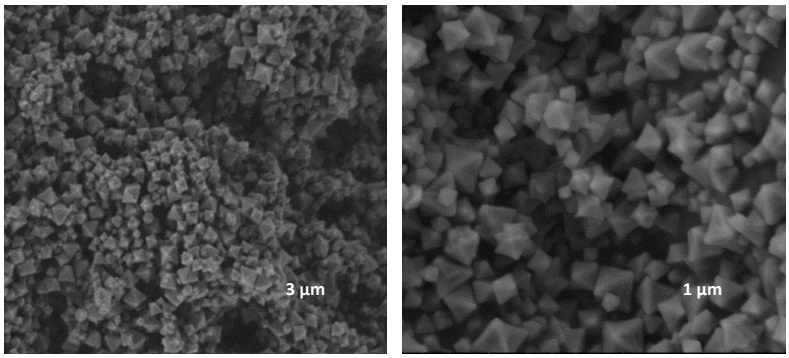

Figure 1.5. SEM micrographs of samples $Zr_6O_4(OH)_4(NDC)_{6-x}(NDC\text{-}NH_2)_x$ (20%).

The solids show a type-I isotherm for N_2 physisorption (Fig. 1.6). The BET surface area was 1053.6 and 1340.0 m^2g^{-1} for Zr-NDC-NH_2 and ZrNDC, respectively.

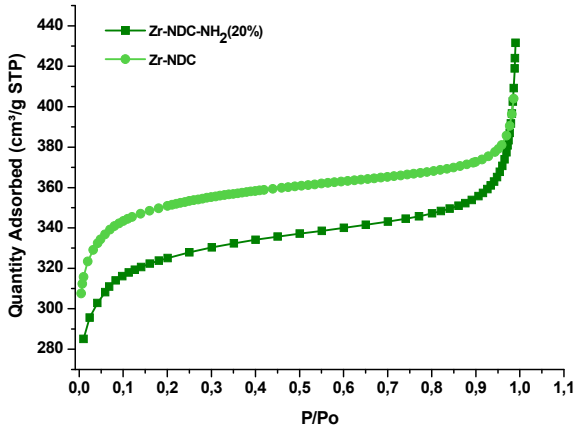

Fig. 1.6. Nitrogen adsorption/desorption isotherms for Zr-NDC and mixed Zr-NDC-NH_2 (20%).

^{13}C cross-polarization magic-angle (CP-MAS) NMR spectra of evacuated Zr-NDC-NH_2 samples showed resonances at δ = 171.6 (COO), 134.8 (CCOO), 132.8, 130.1, 127.4, and 125.5 ppm which are characteristic of the unique carbon atoms of NDC and NDC-NH_2 linkages, respectively. (Fig. 1.7). These spectra indicate the presence of these units in the MOF backbone.

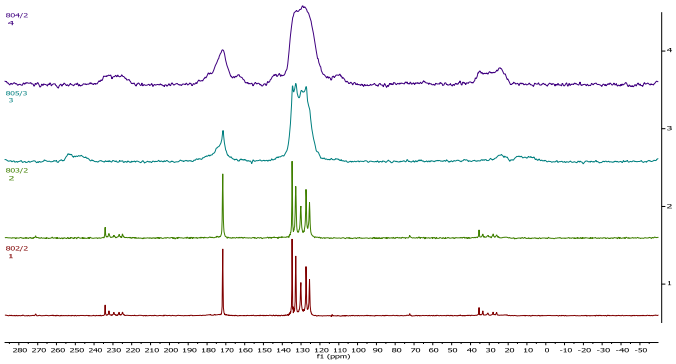

Figure 1.7. ^{13}C-NMR for Zr-NDC-NH_2 (100) top, Zr-NDC-NH_2 (50), Zr-NDC-NH_2 (20) and Zr-NDC (0) bottom.

To examine the thermal stability of the Zr-NDC-NH_2(20), thermal gravimetric analysis (TGA) was carried out, and the results are given in Fig. 1.8. The porous network releases its free molecules and solvent guests in the temperature range of 298-673 K to form the solvent-free phase, which is thermally stable up to 518 °C.

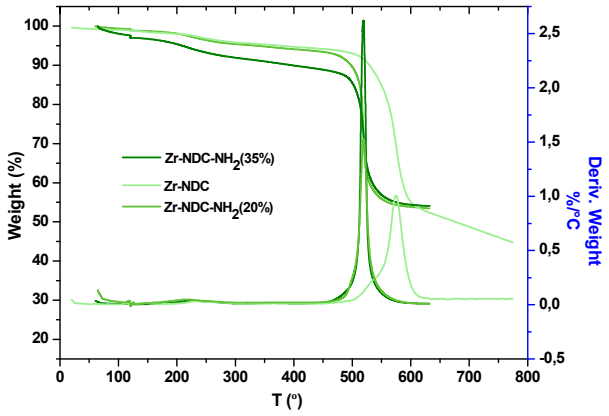

Figure 1.8. TGA curves for Zr-NDC-MOFs.

1.3.2. Stability studies

Zr-BDC, its terephthalate (BDC-NH_2) analogue and Zr-BPDC derivatives have been extensively studied. Thermogravimetric analysis (TGA) indicates that Zr-BDC and Zr-BPDC are stable towards thermal decomposition since they show weight losses only at temperatures as high as 540 °C. Zr-BDC shows high chemical and thermal stability and is stable in polar protic solvents including water and several alcohols. However, the extended isoreticular Zr-BPDC shows a lower chemical stability than Zr-BDC against water as evidenced by PXRD during dynamic light scattering (DLS) measurements.[89a]

Experiments confirmed that the ligand ratio used in the solvothermal preparation of the Zr-BPDC materials was generally preserved in the Zr-BPDC-NH_2 product, and PXRD analysis indicated that the ratio of the two ligands did not alter the quality of the lattice structure (Figure 1.9a). The stability with time was examined by PXRD, and we found that Zr-BPDC-NH_2 (100) was amorphous one month after synthesis, whereas Zr-BPDC-NH_2 (20) remains unaltered after one year (Figure 1.9b).

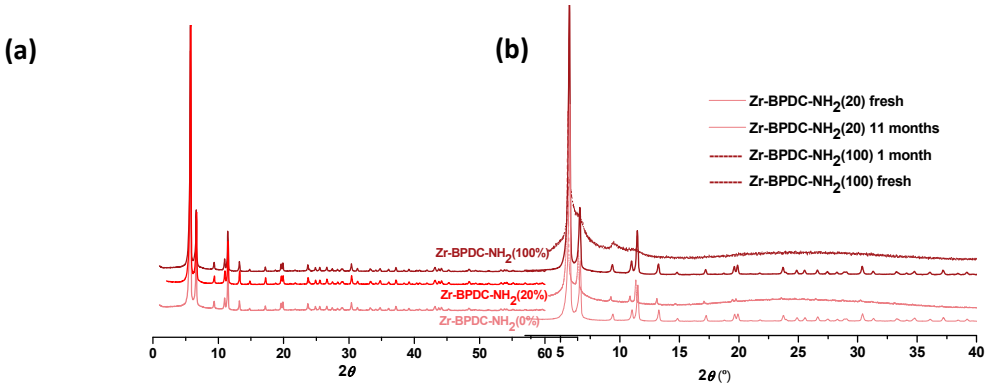

Figure 1.9. PXRD of Zr-BPDC-NH_2 series (a) as synthesized and (b) with time.

The structural degradation of the materials was also analyzed by N_2 adsorption measurements, and we found that the MOF integrity was lost with time for Zr-BPDC-NH_2(100), the BET specific surface area is 21.54 m^2g^{-1}.[102]

Similar results were found for the Zr-NDC-NH_2 series. The relative ratio of each functional group in the resulting Zr-NDC-NH_2 could be controlled by modulating the percentage of each ligand added to the reaction mixture. To obtain a wider pore size than that of Zr-BDC and better stability than Zr-BPDC, we have prepared a Zr-based MOF (Zr-NDC) with the rigid organic linker NDC. Zr-NDC-NH_2(20) remains stable after exposure to moisture at room temperature at least for three months (Figure 1.10).

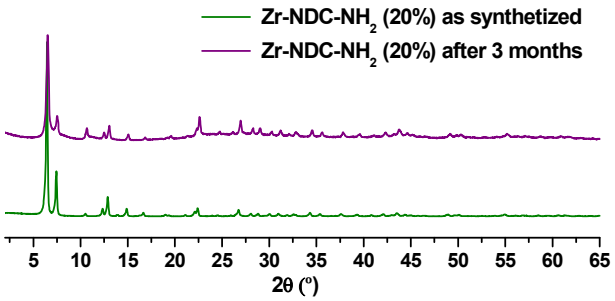

Figure 1.10. PXRD patterns of Zr-NH_2 (20) with time.

[102] P. M. Schoenecker, C. G. Carson, H. Jasuja, C. J. J. Flemming and K. S. Walton *Ind. Eng. Chem. Res.* **2012**, *51*, 6513-6519.

1.3.3. Catalytic applications

1.3.3.1. Synthesis of 1,1-dicyanomethylenebutadiene in a one pot process

In recent years, important efforts have been made to develop high-surface-area solid-base catalysts with different basic strengths able to catalyze a large variety of reactions, and extensive reviews on solid base catalysts and their catalytic applications have been published.[103] Among these materials, basic metal oxides, such as high-surface magnesium oxides,[104] layered magnesium aluminates[105] that bear strong Lewis basic sites, nitrated aluminum phosphates (ALPONs)[106] with medium basic strength sites, and alkali cation-exchanged zeolites[107] with weak basic strength sites have been widely utilized to promote base-catalyzed processes.

An example of Knoevenagel-type condensation using well-defined solid-base catalysts in a one-pot process is the preparation of 1,1-dicyanomethylenebutadiene derivatives, which are widely used as disperse dyes[108] and have interesting nonlinear optical properties.[109] These compounds can be successfully prepared in one pot using ALPONs as heterogeneous base catalysts by adjusting the basicity and the conditions[110] (scheme 1.2). In this work, our Zr-MOF catalysts, with different linkers and different amount of amino groups, have been tested for the preparation of dyes based on the 1,1-dicyanobutadiene structure.

---

[103] B. F. Sels, D. E. De Vos and P. A. Jacobs *Catalysis Reviews* **2001**, *43*, 443-488; D. Tichit, S. Iborra, A. Corma and D. Brunel, in *Catalysts for Fine Chemical Synthesis*, Vol., John Wiley & Sons, Ltd **2006**, pp. 171-205.

[104] A. Corma and S. Iborra, in *Adv. Catal.*, Vol. Volume 49; (Eds.Bruce and Helmut), Academic Press **2006**, pp. 239-302.

[105] F. Cavani, F. Trifirò and A. Vaccari *Catal. Today* **1991**, *11*, 173-301; A. Vaccari *Catal. Today* **1998**, *41*, 53-71.

[106] M. J. Climent, A. Corma, V. Fornés, A. Frau, R. Guil-López, S. Iborra and J. Primo *J. Catal.* **1996**, *163*, 392-398.

[107] A. Corma, V. Fornés, R. M. Martín-Aranda, H. García and J. Primo *Applied Catalysis* **1990**, *59*, 237-248.

[108] U. V. Gokhale and S. Seshadri *Dyes Pigm.* **1986**, *7*, 389-394.

[109] R. Dworczak, W. M. F. Fabian, B. N. Pawar and H. Junek *Dyes Pigm.* **1995**, *29*, 65-76; W. M. F. Fabian, R. Dworczak, H. Junek and B. N. Pawar *Journal of the Chemical Society, Perkin Transactions 2* **1995**, 903-906.

[110] M. J. Climent, A. Corma, R. Guil-Lopez and S. Iborra *Catal. Lett.* **2001**, *74*, 161-167.

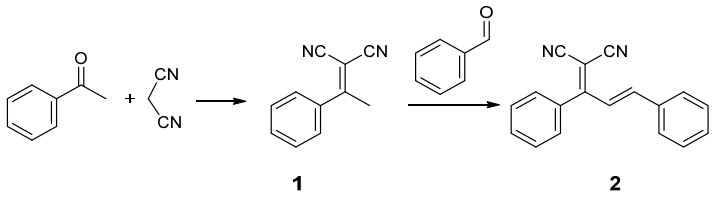

Scheme 1.2. One-pot synthesis of 1,1-dicyanomethylenebutadiene derivatives

In order to check the influence of the linker and amino functional group content of the Zr-MOFs on the catalytic activity for the one-pot reaction between acetophenone and malononitrile and subsequent reaction with benzaldehyde, we performed the reaction in the presence of different Zr-MOF catalysts. The results obtained with these catalysts are given in Table 1.1.

The reaction between acetophenone and malononitrile was performed at 393 K in presence of Zr-MOFs until the yield of α-methylbenzylidenemalononitrile (**1**) was ≈ 95 % (100 % selectivity). Then an appropiate amount of benzaldehyde was added (Experimental Section). After 8-13 h reaction time, a conversion >90% was obtained in all the cases. In the case of Zr-BPDC-NH_2(20), the final molar composition of the mixture (without considering the excess of benzaldehyde) was: 85 % of 1,1-dicyano-2,4-diphenylbutadiene and 15% of chalcone, and traces of condensation products from unreacted acetophenone and malononitrile from the first step or produced by retro-Knoevenagel condensation were detected.

From a preparative point of view, one has to take into account that there are not very significant differences between the final yields of the dye obtained on Zr-MOFs (table 1.1, figure 1.11). However the Zr-BPDC-NH_2 (20) catalyst is the most active and selective. For the preparative task, we have scaled up the reaction to three times the amounts of reagents and catalyst, and the final product was isolated with a yield of 85 % after 6 h.

Table 1.1. Zr-MOF-catalyzed cascade reaction between acetophenone and malononitrile-benzaldehyde.[a]

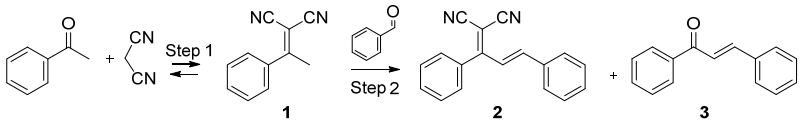

	Catalyst	Step 1				Step 2			
		Conv. (%)[b]	t(h)	Sel. (%)[c]	TOF[d]	Conv. (%)[e]	t(h)	Sel. (%)[f]	TOF
1	Zr-BPDC-NH_2(20)	99	5	100	480	98	12	85	360
2	Zr-NDC-NH_2(20)	99	4	100	600	99	13	75	300
3	Zr-NDC	99	7	100	150	97	13	72	120
4	Zr-BDC-NH_2(20)	99	7	100	300	98	14	55	60

[a] Reaction conditions: glass reactor (2 mL), catalyst (5 mol%), acetophenone (2 mmol), malononitrile (2 mmol), benzaldehyde (4.5 mmol) at 393 K; [b] Based on acetophenone; [c] With respect to **1**; [d] TOF = Turn-over frequency in [$mmol_{substrate}$ $mmol_{catalyst}^{-1}min^{-1}$]; [e] Based on α-methylbenzylidenemalononitrile; [f] With respect to dye **2**.

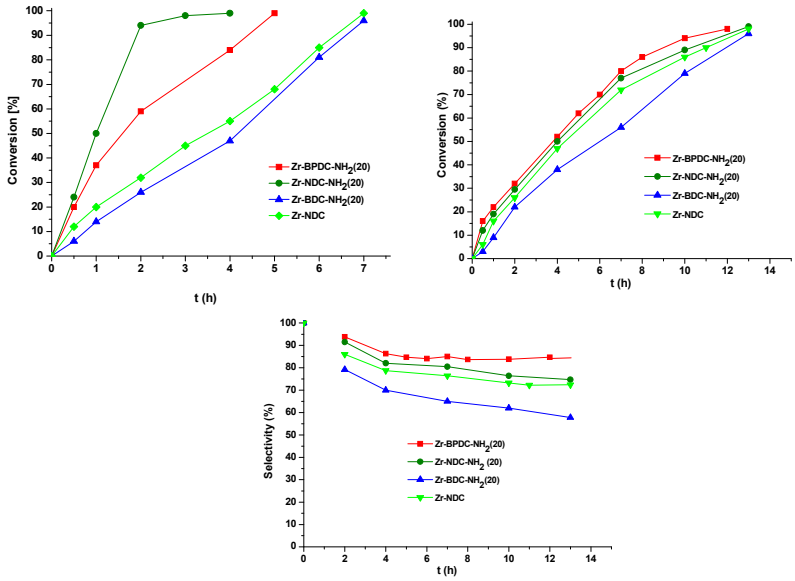

Figure 1.11. Kinetic profile for the one-pot reaction between acetophenone, malononitrile and benzaldehyde: a) Step 1, condensation acetophenone-malononitrile; b) Step 2, reaction of α-methylbenzylidenemalononitrile with benzaldehyde and c) Selectivity to 1,1-dicyano-2,4-diphenylbutadiene (**2**).

We also investigate the role of the pore size of our catalysts in the selectivity. Thus, the reaction was performed with more volume-demanding ketones and aldehydes (Table 1.2); if 1-indanone was used, the conversion to 2-(2,3-dihydro-1H-inden-1-ylidene)malononitrile decreased to 55% after 24 h. Furthermore, when benzaldehyde was added to the reaction mixture only the condensation product with the starting ketone (2-benzylidene-2,3-dihydro-1H-inden-1-one) was obtained (entry 5). Moreover, with large 1-(naphthalen-2-yl)ethan-1-one or 6-methoxy-3,4-dihydronaphthalen-1(2H)-one, conversions to condensation products of 5 and 22% were achieved (entries 6 and 7). Finally, α-methylbenzylidenemalononitrile reacts with 4-methoxybenzaldehyde to selectively afford 80% product after 30 h under the same conditions (entry 3), and a reaction with 6-methoxy-2-naphthaldehyde does not occur (entry 4). These results lead us to conclude that materials with a large pore size are essential for more bulky substrates in these reactions.

Table 1.2. Effect of pore size on the Zr-catalyzed condensation reactions.

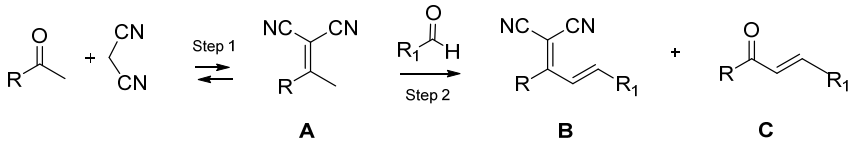

		Step 1		Step 2		
	Catalyst	**R**	**Conv. (%)[b] (h)**	**R_1**	**Conv. (%)[c] (h)**	**Product (%)**
1	Zr-BPDC	Ph	99 (5)	Ph	98 (12)	B (85)
2	Zr-NDC		99 (4)	Ph	99 (13)	B (75)
3	Zr-NDC		99 (5)	4-OMePh	80 (30)	B (100)
4	Zr-NDC/ Zr-BPDC		99	6-OMeN$_{ph}$	0	-
5	Zr-BPDC		55 (24)	Ph	60 (30)	C (100)
6	Zr-BPDC	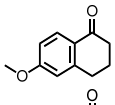	22 (24)	-	-	-
7	Zr-NDC/ Zr-BPDC	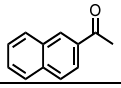	<5 (24)	-	-	-

[a] Reaction conditions: glass reactor (2 mL), catalyst (5 mol%), ketone (2 mmol), malononitrile (2 mmol), aldehyde (4.5 mmol) at 393 k; [b] Based on acetophenone; [c] Based on α-methylbenzylidenemalononitrile.

At this point, it is also important to compare the performance of Zr-based MOFs with other solid-base catalysts with different base strengths for the preparation of dyes or sensors based on the 1,1-dicyanobutadiene structure, and we studied the influence of the catalysts on the two-step synthesis as well as in the one-pot reaction. It has been reported that MgO was not a good catalyst for the second step of the reaction, and there are not very significant differences between the final yields on hydrotalcite (HT) and ALPON, of which ALPON was more selective to the dye. A comparison of the ALPON and Zr-based catalysts is given in Table 1.3. Zr-BPDC-NH_2 (Table 1.3, entry 3) shows a similar activity and selectivity to ALPON (Table 1.3, entry 1), although in our case only ≈ 3 wt% (5 mol %) of catalyst was used compared to 10 wt% ALPON. As described previously,[109] the results obtained with solid-base catalysts are much better than those achieved by using the homogeneous system (NH_4Ac / AcOH) as catalyst.

Table 1.3. One pot condensation reactions without solvent on different basic catalysts: acetophenone-malononitrile-benzaldehyde.[a]

Catalyst (wt%)	Step 1	One pot reaction
	Conv. (h)	Conv. (h) (Sel.)
ALPON (10)	90 (3)	100 (6) (76)[b]
Zr-BDC-NH_2 (2.1)	37 (3)	78 (10) (62)
Zr-BPDC-NH_2 (2.7)	98 (3)	94 (10) (85)
Zr-NDC-NH_2 (3.0)	73 (3)	89 (10) (76)

[a] T: 393 K; [b] Step 1 at 373 K and Step 2 at 423 K.

The possibility of recycling and reusing the catalyst was then examined. After completion of the reactions (GC-MS), CH_2Cl_2 was added, and the catalyst was collected by filtration and reused. We performed seven catalytic cycles to check the efficiency of the catalyst, observing no changes in the activity (Figure 1.12).

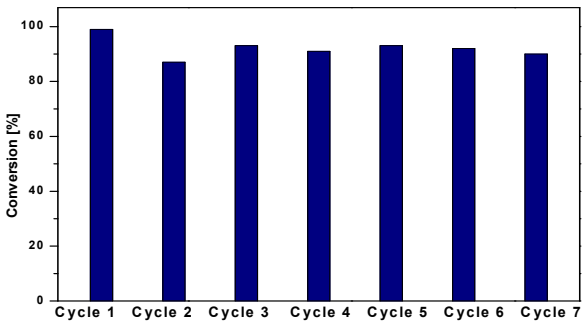

Figure 1.12. Recycling experiments for the Zr-BPDC-NH_2-catalyzed one-pot condensation.

The PXRD pattern of the recovered catalyst after seven catalytic cycles was the same as that of the as-synthesized catalyst, which suggests the high thermal and chemical stability of the framework. The morphology of the material is also conserved after the catalytic reaction that was probed by SEM images (Figure 1.13).

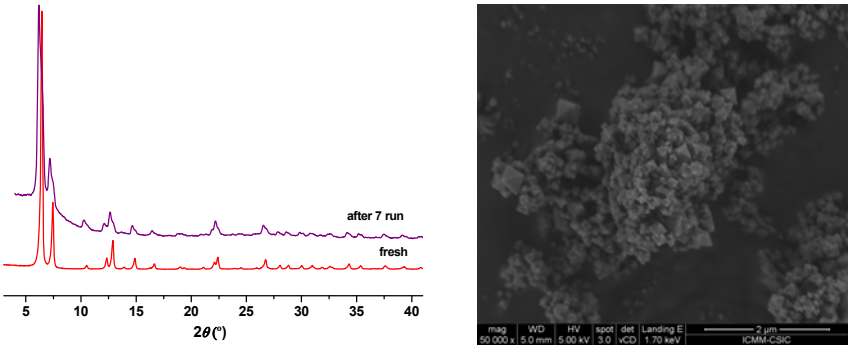

Figure 1.13. PXRD of Zr-BPDC-NH_2 as-synthetized and recovered from the recycling experiments and SEM for Zr-NDC-NH_2 (20%) recycled.

1.4. Conclusions

- We report the synthesis of three series of Zr-based MOFs with mixed dicarboxylate linkers. Materials synthesized with low loading of functionalized linkers exhibited long-term chemical and thermal stability.

- These materials and their corresponding organometallic derivatives had shown to be excellent catalysts in cascade reactions. Thus, we have carried out the one-pot synthesis of dicyanomethylene derivative dyes with good conversions and fair selectivity.

- The recycling experiments demonstrate an interesting prospect for the long-term reusability of these materials.

1.5. Experimental Section

1.5.1. Synthesis of 3-Aminonaphthalene-2,6-Dicarboxylic acid.

Naphthalene-2,6-dicarboxylic acid employed was commercially available and used as supplied without further purification. 4-amino-2,6-naphthalenedicarboxylic acid (NDC-NH_2) was prepared starting from dimethyl naphthalene-2,6-dicarboxylate as shown in Scheme 1.3.

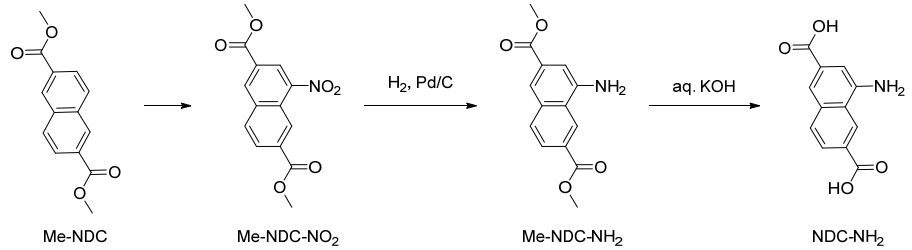

Scheme 1.3. Synthesis of 3-aminonaphthalene-2,6-dicarboxylic acid.

Characterization of Me-NDC-NO_2

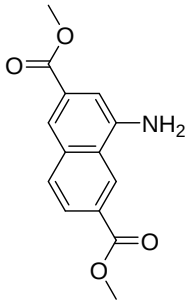

^{1}H NMR (300 MHz, $CDCl_3$, 25 °C, ppm): δ = 9.23 (s, 1H, -CH); 8.84 (s, 1H, -CH); 8.78 (s, 1H, -CH); 8.26 (d, 1H, -CH); 8.1 (d, 1H, -CH); 4.04 (s, 3H, $-CH_3$); 4.01 (s, 3H, $-CH_3$); 3.75.

^{13}C NMR (300 MHz, $CDCl_3$, 25 °C, ppm): δ = 165.9 (-CO-); 164.7 (-CO-); 147.5 (C-NO_2); 136.02 (-CH-); 135.4 (C-COOMe); 132.5 (C-COOMe); 130.3 (-CH-); 128.3 (CNf); 127.7 (-CH-); 126.1 (CNf); 125.7 (-CH-); 123.8 (-CH-); 52.9 (CH_3); 52.8 (CH_3).

ESI-MS (positive-mode): m/z 290 [NDMDC-NO_2]+H; m/z 242 [NDMDC]-NO_2; m/z 258 [NDMDC-NO_2]-OCH_3; m/z 312 [NDMDC-NO_2]+H+Na.

Characterization of Me-NDC-NH_2

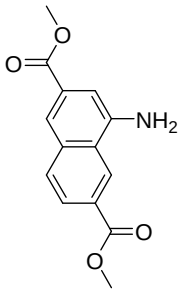

^{1}H NMR (300 MHz, $CDCl_3$, 25 °C, ppm): δ = 8.7 (s, 1H, -CH); 8.09 (d, 1H, -CH); 8.06 (d, 1H, -CH); 7.3 (d, 1H, -CH); 7.41 (s, 1H, -CH); 3.95 (s, 3H, $-CH_3$); 3.9 (s, 3H, $-CH_3$).

Elemental analysis, calc. $C_{14}H_{13}NO_4$ (259.26): C, 64.86; H, 5.05; N, 5.4. **Found:** C, 65.09; H, 5.44; N, 5.52.

EI: m/z 259 [NDMDC-NH_2]; m/z 243 [NDMDC]-NH_2; m/z 228 [NDMDC-NH_2]-OCH_3.

Characterization of NDC-NH_2

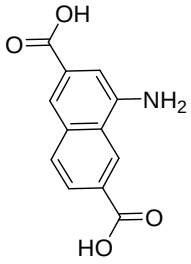

^{1}H NMR (300 MHz, DMSO, 25 °C, ppm): δ = 12.9 (s, 2H, -COOH); 8.8 (s, 1H, -CH); 7.9 (d, 1H, -CH); 7.8 (d, 1H, -CH); 7.75 (s, 1H, -CH); 7.25 (s, 1H, -CH); 6.3 (s, 2H, $-NH_2$).

ESI-MS (positive-mode): m/z 232 [NDC-NH_2]+H; m/z 214 [NDC-NH_2]-OH.

1.5.2. Materials Preparation

Zr-MOF was prepared according to the corresponding procedures reported in the original reference Zr-BDC-NH_2[89b] X-ray diffraction (Phillips X'Pert, Cu Kα radiation) was used to confirm the expected crystalline structure of the materials. Starting materials were purchased and used without further purification from commercial suppliers (Sigma-Aldrich and Alfa Aesar). Dried, distilled and deoxygenated solvents were used.

4.2.1. Synthesis of $Zr(BDC)_{6-x}(BDC\text{-}NH_2)_x$

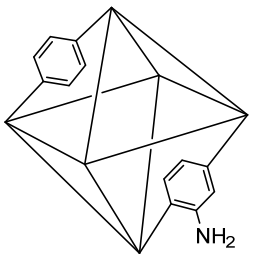

Synthesis of Zr-based metal-organic framework was performed in a 250 mL round bottom flask using a procedure similar to that previously described[89b]. $ZrCl_4$ (0.4 g, 1.7 mmol) in DMF (75 mL) was dispersed by ultrasound at 50-60 °C, acetic acid (2.85 mL, 850 mmol) was added. A DMF solution (25 mL) of the linkers (1,4-benzenedicarboxylic acid/2-amino-1,4-benzenedicarboxylic acid) in different molar ratios, was added to the clear solution in an equimolar ratio with regard to $ZrCl_4$; finally, water (0.125 mL, 0.007 mmol) was added to the solution. The tightly capped flask is sonicated at 60 °C and kept in a bath at 120 °C under static conditions for 24 h. After 24 h, the solutions were cooled to room temperature and the precipitate was isolated by centrifugation. The solid washed with DMF (10 mL). After standing at room temperature for 2 h, the suspension was centrifuged and the solvent was decanted off. The obtained particles were washed with ethanol several times in the same way as described for washing with DMF. Finally, the solid was dried under reduced pressure (80 °C, 3 h).

4.2.2. Synthesis of $Zr(BPDC)_{6-x}(BPDC\text{-}NH_2)_x$

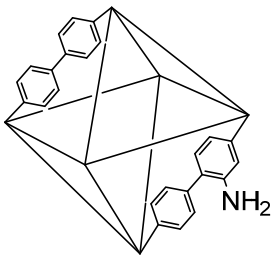

Synthesis of Zr-based metal-organic framework was performed in a 250 mL round bottom flask using a procedure similar to that previously described.[89b] $ZrCl_4$ (0.4 g, 1.7 mmol) in DMF (75 mL) was dispersed by ultrasound at 50-60 °C, acetic acid (2.85 mL, 850 mmol) was added. 1,1'-biphenyl-4,4'-dicarboxylic acid and 3-amino-[1,1'-biphenyl]-4,4'-dicarboxylic acid in different molar ratios (0, 20 and 100% as shown in table 1.4) in DMF solution (25 mL) was added to the clear solution; finally, water (0.125 mL, 0.007 mmol) was added to the solution. The tightly capped flask is sonicated at 60 °C and kept in a bath at 120 °C under static conditions for 24 h. After 24 h, the solutions were cooled to room temperature and the precipitate was isolated by centrifugation. The solid washed with DMF (10 mL). After standing at room temperature for 2 h, the suspension was centrifuged and the solvent was decanted off. The obtained particles were washed with ethanol several times in the same way as described for washing with DMF. Finally, the solid was dried

under reduced pressure (80 °C, 3 h). This standard washing procedure yielded the materials denoted with "as-synthesized". (Yield: 577 mg). $Zr_6O_4(OH)_4(BPDC\text{-}NH_2)_6$: Calculated: C, 45.39; H, 3.17; N, 3.78. Found: C, 43.62; H, 2.72; N, 3.70%. Zr-BPDC (20) : Calculated: C, 47.18; H, 2.51; N, 0.79. Found: C, 43.58; H, 2.72; N, 0.79%.

Table 1.4. Synthesis conditions of the mixed Zr-BPDC-NH_2 MOFs.

Zr-MOF	Ligand	mmol $ZrCl_4$	mmol NH_2 ligand	X-Ray
Zr-BPDC	BPDC	1.7	0	crystalline
Zr-BPDC-NH_2 (100)	BPDC-NH_2	1.7	1.7	crystalline
Zr-BPDC-NH_2 (20)	BPDC/BPDC-NH_2	1.7	0.34	crystalline

4.2.3. Synthesis of $Zr(NDC)_{6-x}(NDC\text{-}NH_2)_x$

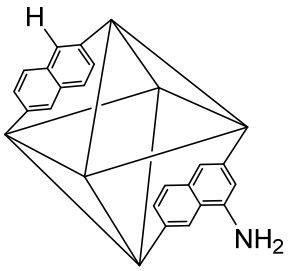

Five different samples (see table 1.5), including $Zr_6O_4(OH)_4(NDC)_6$, $Zr_6O_4(OH)_4(NDC\text{-}NH_2)_6$ and mixed $Zr_6O_4(OH)_4(NDC)_{6-x}(NDC\text{-}NH_2)_x$, were prepared and purified using the general synthesis.[89b] $ZrCl_4$ (0.4 g, 1.7 mmol) in dimethylformamide (DMF) (75 mL) was dispersed by ultrasound at 50-60 °C, acetic acid (2.85 mL, 850 mmol) was added. Naphthalene-2,6-dicarboxylic acid and 4-aminonaphthalene-2,6-dicarboxylic acid in different molar ratios (0, 20, 35, 50, and 100%) in DMF solution (25 mL) was added to the clear solution and finally, water (0.125 mL, 0.007 mmol) was added. The mixture was sonicated at 60 °C and kept in a bath at 120 °C under static conditions for 24 h. After this time, the solutions were cooled to room temperature and the precipitate was isolated by centrifugation and washed with DMF (10 mL) to remove the excess of unreacted NDC and then washed again with tetrahydrofurane several times in the same way as described for washing with DMF. Finally, the solid was dried under reduced pressure (100 °C, 3 h). (Yield: 80%).

Table 1.5. Synthesis conditions of the mixed Zr-NDC-NH_2 MOFs.

Zr-MOF	Ligand	mmol $ZrCl_4$	mmol NH_2 ligand	X-Ray
Zr-NDC	NDC	1.7	0	crystalline
Zr-NDC-NH_2 (100)	NDC-NH_2	1.7	1.7	amorphous
Zr-NDC-NH_2 (50)	NDC/NDC-NH_2	1.7	0.85	crystalline
Zr-NDC-NH_2 (35)	NDC/NDC-NH_2	1.7	0.595	crystalline
Zr-NDC-NH_2 (20)	NDC/NDC-NH_2	1.7	0.34	crystalline

The elemental analysis confirm that the amount of NH_2-linker incorporated into the structure is the percentage expected as is shown in table 1.6. The amount of zirconium in the sample was quantified by ICP.

Table 1.6. Contents of Zr, C and N analyzed in mixed Zr-MOFs.

	Zr_{exp} %	$Zr_{theor.}$ %	$C_{exp.}$ %	$C_{theor.}$ %	$N_{exp.}$ %	$N_{theor.}$.%
Zr-NDC	27.01	27.69	38.16	43.75	-	-
Zr-NDC-NH_2 (20)	26.87	27.44	39.2	43.36	0.81	0.84

4.3. Preparation of 1,1-dicyano-2,4-diphenyl-1,3-butadiene in a one-pot reaction

A solvent-free mixture of acetophenone (2 mmol) and malononitrile (2 mmol) was heated at 393 K with stirring. When the reaction temperature stabilized, the solid catalyst (5 mol%) was added.
When the yield was ≈90%, the temperature was increased to 423 K and benzaldehyde (4.5 mmol) was added. Isolation and purification of the products was performed by conventional column chromatography on silica gel (Merck 60; 0.063–0.200 mm) using dichloromethane as eluent.

^{1}H NMR (200 MHz, $CDCl_3$, 25 °C, ppm): δ = 7.78-7.35 (m, 11H, ArH, C-CH=CH); 6.84 (d, 1H, J = 15.8 Hz, CH=CH–Ph).

MS:256 (M+, 100).

Chapter 2

Post-functionalization in the linker of Zr-MOFs

2.1. Introduction

The heterogenization of transition-metal complexes over a solid matrix leads to the formation of solid recyclable molecular catalysts with well-defined active centers. Design and development of a suitable support to carry out the immobilization of homogeneous catalysts, while improving their characteristics by a cooperative effect between the metal complex and the support, has been an important challenge in recent years.[111]

The synthesis of hybrid organic-inorganic structured porous materials[112] and coordination polymers[74a,74b,74d,113] is another way to obtain heterogeneous catalysts. An important property of MOFs with respect to other crystalline porous solids is the possibility to introduce chiral groups and two or more active sites,[114] and to generate multifunctional solid catalysts (e.g., acid-base, metal-acid, metal-base or metal-metal catalysts)[115] to be used in domino reactions.[4a] Nevertheless, the preparation recovery and reusability of multifunctional MOF catalysts has been an active research area in the last years.[115,116]

MOFs can be easily modified by post-synthesis treatments with the aim of introducing functional groups that can act or be transformed into catalytic active sites.[117] Chelating groups, which can coordinate with a transition metal,

[111] A. Corma *Catalysis Reviews* **2004**, *46*, 369-417.
[112] C. Baleizão and H. Garcia *Chem. Rev.* **2006**, *106*, 3987-4043; A. Corma, U. Díaz, T. García, G. Sastre and A. Velty *J. Am. Chem. Soc.* **2010**, *132*, 15011-15021.
[113] G. Ferey *Chem. Soc. Rev.* **2008**, *37*, 191-214.
[114] C. Wang, M. Zheng and W. Lin *J. Phys. Chem. Lett.* **2011**, *2*, 1701-1709.
[115] A. Arnanz, M. Pintado-Sierra, A. Corma, M. Iglesias and F. Sánchez *Adv. Synth. Catal.* **2012**, *354*, 1347-1355; F. G. Cirujano, F. X. Llabres i Xamena and A. Corma *Dalton Trans.* **2012**, *41*, 4249-4254.
[116] F. G. Cirujano, A. Leyva-Pérez, A. Corma and F. X. Llabrés i Xamena *ChemCatChem* **2013**, *5*, 538-549; Y. Pan, B. Yuan, Y. Li and D. He *Chem. Commun.* **2010**, *46*, 2280-2282; P. Wu, J. Wang, Y. Li, C. He, Z. Xie and C. Duan *Adv. Funct. Mater.* **2011**, *21*, 2788-2794; F. X. Llabrés i Xamena, A. Abad, A. Corma and H. Garcia *J. Catal.* **2007**, *250*, 294-298; F. X. Llabrés i Xamena, O. Casanova, R. Galiasso Tailleur, H. Garcia and A. Corma *J. Catal.* **2008**, *255*, 220-227; F. Gándara, E. G. Puebla, M. Iglesias, D. M. Proserpio, N. Snejko and M. Á. Monge *Chem. Mater.* **2009**, *21*, 655-661; A. Monge, F. Gandara, E. Gutierrez-Puebla and N. Snejko *CrystEngComm* **2011**, *13*, 5031-5044; R. F. D'Vries, M. Iglesias, N. Snejko, S. Alvarez-Garcia, E. Gutierrez-Puebla and M. A. Monge *J. Mater. Chem.* **2012**, *22*, 1191-1198; Z. Wang, G. Chen and K. Ding *Chem. Rev.* **2009**, *109*, 322-359; Z. Wang and S. M. Cohen *Chem. Soc. Rev.* **2009**, *38*, 1315-1329.
[117] K. K. Tanabe and S. M. Cohen *Chem. Soc. Rev.* **2011**, *40*, 498-519.

can be easily introduced in MOFs.[118] For instance, IRMOF-3 reacts with salicylaldehyde to form the iminophenol ligand which reacts with Au(III) and V(V) complexes to give active catalysts in the hydrogenation of butadiene and in the oxidation of cyclohexene.[81a119] Zr-BDC-NH_2 has also been modified by reaction with salicylaldehyde (vapor-phase post-synthetic modification),[120] and with anhydrides[121] (see Figure 2.1), acting as an acid-base type catalyst for cross-aldol condensation reactions.[122] Here, we present the importance of properly selecting the starting MOF material to be used as support for the preparation of heterogenized catalysts.

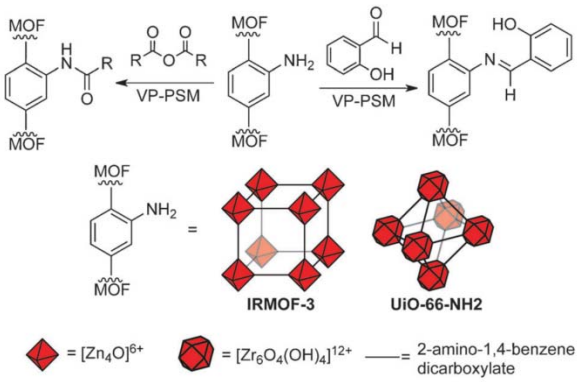

Figure 2.1. Post-synthetic modification of MOFs.

As previously mentioned, Zr-based metal-organic frameworks have a large specific surface area and pore size, which result in desirable properties for catalytic applications. These new, highly stable materials, after the adequate post-synthetic modification, can act as heterogeneous catalysts that combine the properties of soluble organometallic complexes with those of the MOF as a

[118] K. K. Tanabe and S. M. Cohen *Angew. Chem. Int. Ed.* **2009**, *48*, 7424-7427; C. J. Doonan, W. Morris, H. Furukawa and O. M. Yaghi *J. Am. Chem. Soc.* **2009**, *131*, 9492-9493.
[119] M. J. Ingleson, J. Perez Barrio, J.-B. Guilbaud, Y. Z. Khimyak and M. J. Rosseinsky *Chem. Commun.* **2008**, 2680-2682.
[120] M. Servalli, M. Ranocchiari and J. A. Van Bokhoven *Chem. Commun.* **2012**, *48*, 1904-1906.
[121] M. Kandiah, S. Usseglio, S. Svelle, U. Olsbye, K. P. Lillerud and M. Tilset *J. Mater. Chem.* **2010**, *20*, 9848-9851.

support, the preparation of ligands as, for instance, pincer-type ligands can be incorporated to the linker MOFs for transition-metal complexes, providing appropriate stereochemical and electronic environments around active metal centers, which induces additional active sites to the existing intrinsic active sites of MOFs.[122]

In this chapter we explain the post-functionalization of Zr-MOFs with metal complexes supported on their structure and then their use as heterogeneous catalyst. We describe the functionalization of the linker to obtain heterogenized transition metal (Ir, Rh) Zr-MOFs. These materials can act as multifunctional catalysts[123] containing metallic centers (Rh, Ir) along with Zr^{IV} sites with Lewis acid properties and base groups as ligands; these catalysts can be used as heterogeneous catalysts in several reactions. The catalytic activity of these materials is divided in two parts. In Part A, we will explain the catalytic activity of our post-functionalized Zr-MOFs in single step reactions, in particular, in the hydrogenation of aromatics; and in Part B, the catalytic activity in several multistep reactions: *N*-alkylation of amines with alcohols, synthesis of secondary amines by reductive amination of aldehydes with nitrobenzene and cascade olefination-hydrogenation reactions of aldehydes.
One-pot type reactions, in which several steps are performed in the same reaction vessel, are of much interest to achieve more sustainable process[4a,124] by avoiding intermediate separation and purifications steps and minimizing

[122] B. Rybtchinski and D. Milstein *Angew. Chem. Int. Ed.* **1999**, *38*, 870-883; M. Kanzelberger, B. Singh, M. Czerw, K. Krogh-Jespersen and A. S. Goldman *J. Am. Chem. Soc.* **2000**, *122*, 11017-11018; J. Zhao, A. S. Goldman and J. F. Hartwig *Science* **2005**, *307*, 1080-1082; D. G. Gusev, F.-G. Fontaine, A. J. Lough and D. Zargarian *Angew. Chem. Int. Ed.* **2003**, *42*, 216-219; T. Agapie and J. E. Bercaw *Organometallics* **2007**, *26*, 2957-2959; M. Ingleson, H. Fan, M. Pink, J. Tomaszewski and K. G. Caulton *J. Am. Chem. Soc.* **2006**, *128*, 1804-1805; M. J. Ingleson, M. Pink and K. G. Caulton *J. Am. Chem. Soc.* **2006**, *128*, 4248-4249; M. Gozin, M. Aizenberg, S.-Y. Liou, A. Weisman, Y. Ben-David and D. Milstein *Nature* **1994**, *370*, 42-44; D. M. Grove, G. Van Koten, P. Mul, A. A. H. Van der Zeijden, J. Terheijden, M. C. Zoutberg and C. H. Stam *Organometallics* **1986**, *5*, 322-326; D. G. Gusev, T. Maxwell, F. M. Dolgushin, M. Lyssenko and A. J. Lough *Organometallics* **2002**, *21*, 1095-1100; D. G. Gusev, M. Madott, F. M. Dolgushin, K. A. Lyssenko and M. Y. Antipin *Organometallics* **2000**, *19*, 1734-1739.
[123] W. Morris, C. J. Doonan and O. M. Yaghi *Inorg. Chem.* **2011**, *50*, 6853-6855.
[124] S. J. Broadwater, S. L. Roth, K. E. Price, M. Kobaslija and D. T. McQuade *Org. Biomol. Chem.* **2005**, *3*, 2899-2906; L. F. Tietze *Chem. Rev.* **1996**, *96*, 115-136; L. F. Tietze and U. Beifuss *Angew. Chem., Int. Ed.* **1993**, *32*, 131-163.

energy consumption.[125] These transformations known as tandem, domino, or cascade reactions[126] have become an important area of research in organic chemistry.[4a,4b,127]

[125] A. Ajamian and J. L. Gleason *Angew. Chem. Int. Ed.* **2004**, *43*, 3754-3760; J. M. Lee, Y. Na, H. Han and S. Chang *Chem. Soc. Rev.* **2004**, *33*, 302-312.

[126] D. E. Fogg and E. N. dos Santos *Coord. Chem. Rev.* **2004**, *248*, 2365-2379; G. Poli and G. Giambastiani *J. Org. Chem.* **2002**, *67*, 9456-9459.

[127] G. Balme, E. Bossharth and N. Monteiro *Eur. J. Org. Chem.* **2003**, *2003*, 4101-4111; M. Malacria *Chem. Rev.* **1996**, *96*, 289-306; P. J. Parsons, C. S. Penkett and A. J. Shell *Chem. Rev.* **1996**, *96*, 195-206; J.-C. Wasilke, S. J. Obrey, R. T. Baker and G. C. Bazan *Chem. Rev.* **2005**, *105*, 1001-1020; G. Battistuzzi, S. Cacchi and G. Fabrizi *Eur. J. Org. Chem.* **2002**, *2002*, 2671-2681; E.-i. Negishi, C. Copéret, S. Ma, S.-Y. Liou and F. Liu *Chem. Rev.* **1996**, *96*, 365-394.

2.2. Objectives

- Heterogenization of metal complexes in Zr-MOFs following these steps (Scheme 2.1):
  - Post-functionalization of the amino linker in the Zr-MOF to incorporate the pincer-type ligand obtaining de (*NNN*)-Zr-MOF.
  - Anchor the metals in the structures to obtain multifunctional catalyst (*NNN*)-M-Zr-MOFs (M = Ir, Rh) by post-synthetic modification.
  - Characterization of the different heterogenized catalysts.

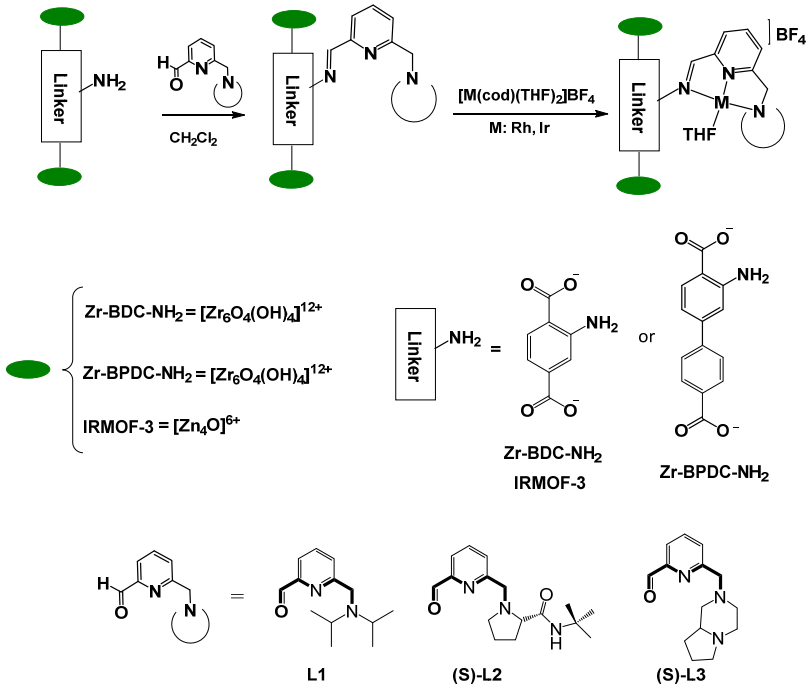

Scheme 2.1. Preparation of Post-functionalized MOFs.

Catalytic activity

-Part A: One step reactions

- Study of the catalytic activity of heterogenized Iridium MOF in hydrogenation of aromatics (Scheme 2.2).

Scheme 2.2. Hydrogenation of aromatic compounds.

- Recycling experiments.

-Part B: Multistep reactions

- Catalytic activity in *N*-alkylation of amines with alcohols (scheme 2.3.a), synthesis of secondary amines by reductive amination of aldehydes with nitrobenzene (scheme 2.3.b) and cascade olefination-hydrogenation reactions of aldehydes (scheme 2.3.c).

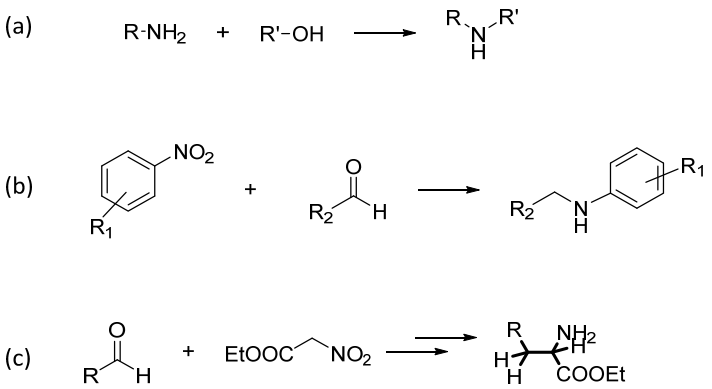

Scheme 2.3. (a) *N*-alkylation of amines, (b) Synthesis of secondary amines and (c) Condensation-hydrogenation reaction.

- Recycling of (*NNN*)-M-Zr-MOFs.

2.3. Results and Discussion

2.3.1. Synthesis of supported (*NNN*)-Zr-M-MOFs (M = Rh, Ir).

In this section we describe the synthesis of the catalysts used in this chapter. The characterization of Zr-BDC-[L1Ir]BF_4, Zr-BDC-[L2Ir]BF_4, Zr-BDC-[L3Rh]BF_4 and Zr-BPDC-[L3Rh]BF_4 will be explained since they are the most used catalysts in the catalytic reactions described in next section. The characterization data of the other catalysts are similar to those described in this section and can be found in annexes.

2.3.1.1. Zr-BDC-NH_2-[L1Ir].

The Zr-BDC-NH_2, Zr-BPDC-NH_2 and IRMOF MOFs may be functionalized because the presence of NH_2 in the linker enables the incorporation of ligands by conventional reactions. In this chapter, all starting MOFs contain 100% of amino linker, then that amount will not be specified in each case. Functionalized-MOFs can be prepared according to well established procedures: in the case of Zr-BDC-NH_2-[L1Ir]BF_4, the starting MOF was suspended in CH_2Cl_2 and treated with the aldehyde[120] (Scheme 2.4) at room temperature for 24 h to yield an imino pyridine amino ligand (N,N,N, pincer type ligand).

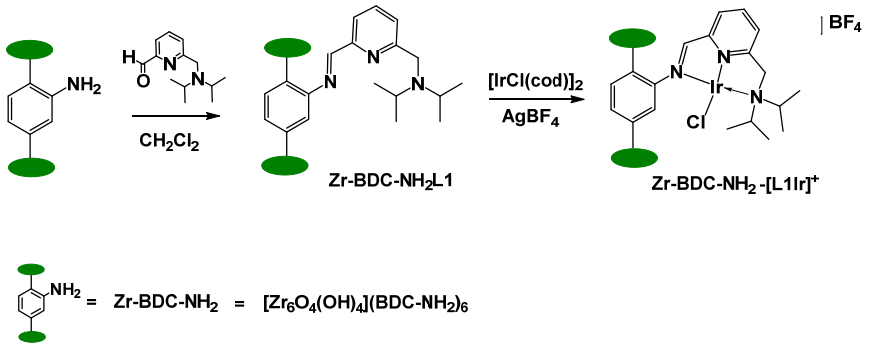

Scheme 2.4. Preparation of Zr-BDC-NH_2-[L1Ir]BF_4 MOF.

Addition of the adequate starting metal complex leads to the corresponding heterogenized (*NNN*)-M-Zr-MOF complex (M = Ir) (Scheme 2.4). All additional details for the preparation of this novel catalyst can be found in the experimental section. All steps occur without any apparent loss of the framework integrity, as depicted in Figure 2.2.

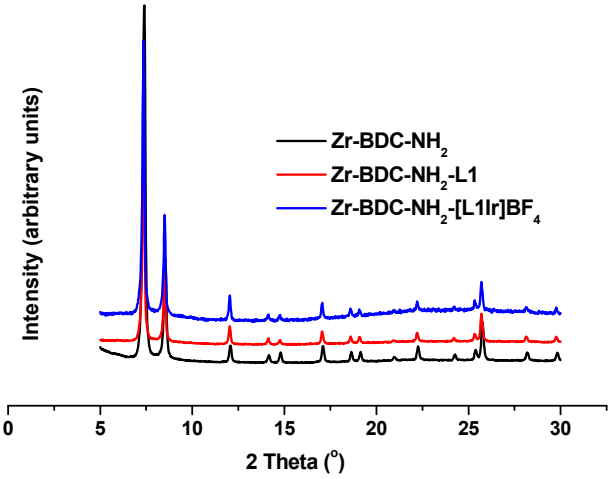

Figure 2.2. X-ray diffraction patterns of Zr-BDC-NH_2, Zr-BDC-NH_2L1, Zr-BDC-NH_2-[L1Ir]BF_4.

The ^{13}C NMR (see Figure A.2.1 in annexes) and FTIR (see Figure 2.3) spectra of the resulting samples are dominated by the bands assigned to the parent groups and by the skeletal modes of MOFs. The FTIR spectra demonstrate bands assigned to C-C aromatic vibrational modes, at 1600-1585 cm^{-1}, 1500-1430 cm^{-1} and 700 cm^{-1}. The carboxylate anion has two strongly coupled C-O bonds with bond strengths between C=O and C-O. Bands at 1650-1550 cm^{-1} (s) correspond to asymmetrical stretching for the carboxylates and band near 1400 cm^{-1} (w) corresponds to symmetrical stretching. The presence of functional groups from post-synthetic modification of the starting Zr-BDC-NH_2 can be observed in the full spectral range with intensity depending on the conversion percentage. Particularly, the band at 760 cm^{-1}, which is assigned to the C-C vibrational mode in aromatic compounds and which does not overlap with other vibrational modes, we can observe that the intensity of this band decreases when the material has been functionalized.

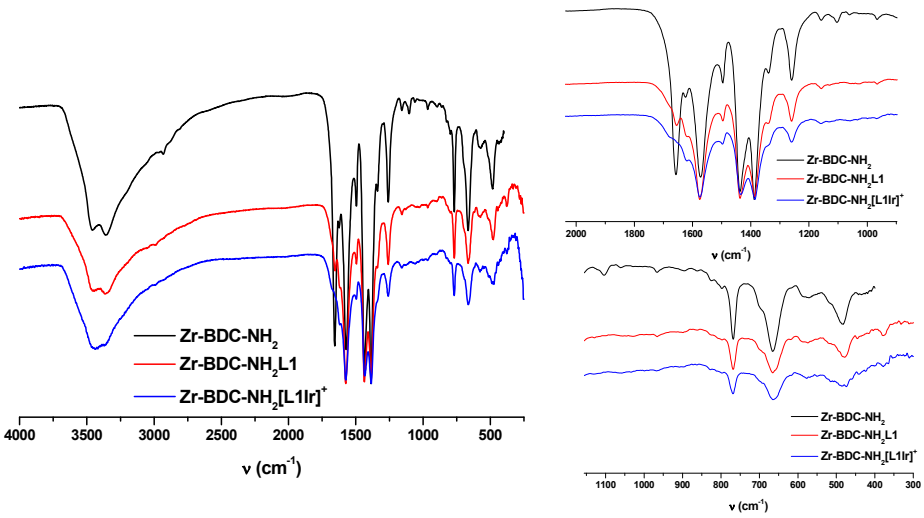

Figure 2.3. FT-IR (normalized) for Zr-BDC-NH_2, Zr-BDC-NH_2-L1, Zr-BDC-NH_2[L1Ir]$^+$ (left). MOF framework region and ν(C=O) region. (Note: for starting Zr-BDC-NH_2 peaks at 1657 cm^{-1} assigned to the C=O stretching vibration of residual DMF strongly adsorbed in the channels network) (right and up). Band at 760 cm^{-1} (right and down).

The stability of the modified Zr-BDC-NH_2 MOFs was examined by thermogravimetric analysis (Figure 2.4) which confirms that functionalized samples show thermal stabilities comparable to the starting Zr-BDC-NH_2 with decomposition temperatures near 350 °C in air.

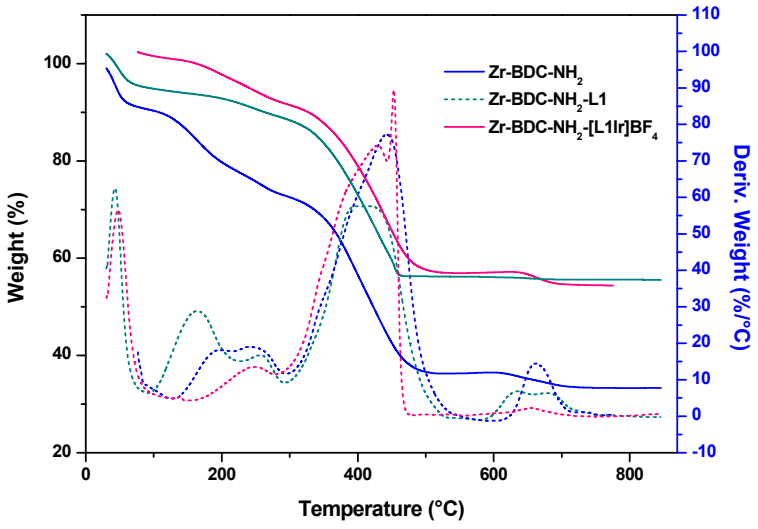

Figure 2.4. TGA patterns of Zr-BDC-NH_2, Zr-BDC-NH_2-L1, Zr-BDC-NH_2-[L1Ir]BF_4.

Experiments of N_2 adsorption-desorption isotherms obtained at 77 K on the functionalized Zr-BDC-NH_2 MOF result in type-I isotherms which further confirm the stability of the porous structure after the formation of the Ir complex attached to the framework (Figure 2.5). Moreover, they indicate that most of the porosity of the original material is retained after functionalization of the linker. Indeed BET surface area of 637 $m^2 \cdot g^{-1}$, total pore volume of 0.28 $cm^3 \cdot g^{-1}$, and pore diameter of 2.7 nm are obtained for Zr-BDC-L1, while for Zr-BDC-[L1Ir]BF_4 they are 568 $m^2 \cdot g^{-1}$, 0.25 $cm^3 \cdot g^{-1}$, and 2.71 nm respectively. The diminution in surface area can be related to the presence of a large ligand and the corresponding iridium complex.

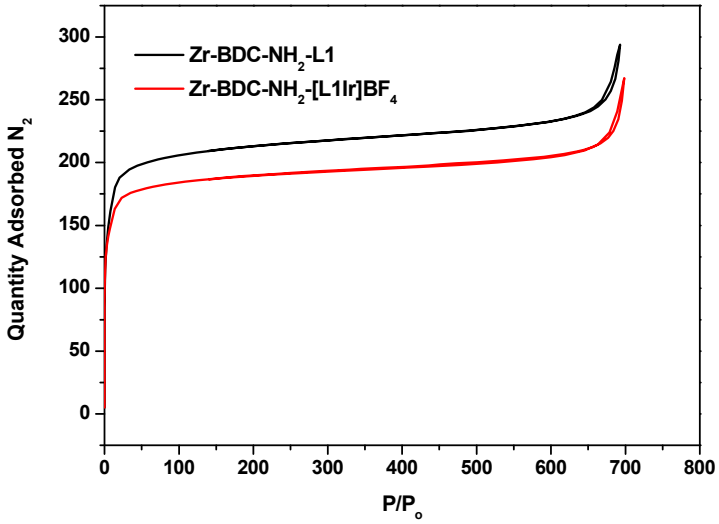

Figure 2.5. N_2 isotherms (77 K) of funcionalized Zr-BDC-NH_2: Zr-BDC-NH_2-L1, Zr-BDC-NH_2-[L1Ir]BF_4.

SEM images show that no textural changes in the materials occurred after the post-synthetic treatment. In any case, the observed Ir sites were homogeneously dispersed in the samples. TEM experiment does not confirm the presence of Ir nanoparticles (Figure 2.6).

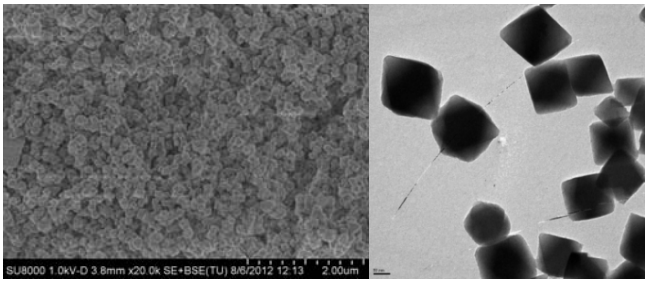

Figure 2.6. SEM (a) and TEM (b) images for Zr-BDC-NH_2-[L1Ir]BF_4.

X-ray photoelectron spectroscopy (XPS) analysis was performed on Zr-[L1Ir]-MOF. The sample was kept in vacuum overnight before XPS measurements. The spectrum was calibrated with respect to the C 1s peak. The survey scan XPS spectrum of the Zr-[L1Ir]-MOF sample (see Figure 2.7) confirms the presence of Ir atoms in addition to the Zr-BDC framework elements (Zr, C, N). The XPS spectrum shows N 1s (399.1 eV) and C 1s signals, and the latter comprises sp^2 carbon (284.6 eV) and sp^3 carbon neighboring oxygen (287.9 eV). The XPS core level for Ir (the Ir 4f region) shows peaks at 64.8 and 62.1 eV (assigned to Ir $4f_{7/2}$ and Ir $4f_{5/2}$), which indicates the $Ir^{\delta+}$ oxidation state in the samples.[128]

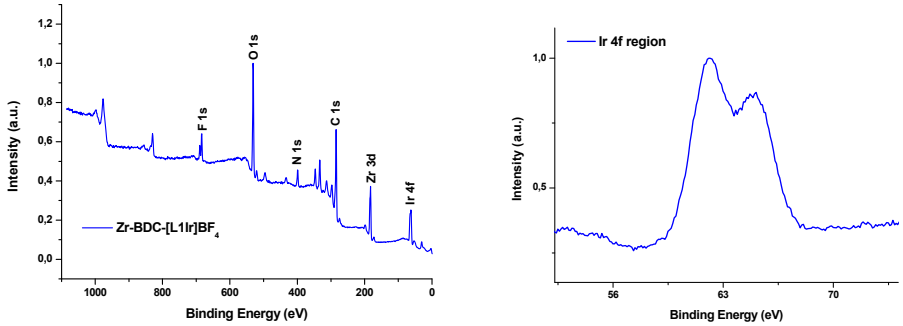

Figure 2.7. XPS survey scans and Ir(4f) region of Zr-BDC-[L1Ir]BF_4.

[128] W. M. R. C. D. Wanger, L. E. Davis, J. F. Moulder and G. E.Muilenberg *Handbook of X-ray Photoelectron Spectroscopy, Physical Electronics Division* **1981**, *3*; C. Campos, C. Torres, M. Oportus, M. A. Peña, J. L. G. Fierro and P. Reyes *Catal. Today* **2013**, *213*, 93-100; U. Hintermair, S. W. Sheehan, A. R. Parent, D. H. Ess, D. T. Richens, P. H. Vaccaro, G. W. Brudvig and R. H. Crabtree *J. Am. Chem. Soc.* **2013**, *135*, 10837-10851; M. Blanco, P. Álvarez, C. Blanco, M. V. Jiménez, J. Fernández-Tornos, J. J. Pérez-Torrente, L. A. Oro and R. Menéndez *ACS Catal.* **2013**, *3*, 1307-1317.

2.3.1.2. Synthesis of Zr-BDC-NH_2-[L2Ir]BF_4, Zr-BDC-NH_2-[L3Rh]BF_4 and Zr-BPDC-NH_2-[L3Rh]BF_4.

The synthetic procedure of these MOFs was developed as followed: a starting cream powder Zr-BDC-NH_2 was suspended in CH_2Cl_2 and treated with (S)-N-(*tert*-butyl)-1-((6-formylpyridin-2-yl)methyl)pyrrolidine-2-carboxamide ((S)-L2) or (S)-6-((hexahydropyrrolo[1,2-a]pyrazin-2(*1H*)-yl)methyl)picolinaldehyde ((S)-L3)[81a] (scheme 2.5) at room temperature for 24-48 h; this procedure causes a color change in the dispersion from cream to yellow. The reaction was then stopped by repeated washing of the solid material with CH_2Cl_2, and drying under vacuum. The elemental analysis indicates that a functionalization of about 17% (for L2) and 5% (for L3) of the total -NH_2 groups was produced without losing the integrity of the framework. The final step to prepare the Zr-BDC-NH_2-LM and Zr-BPDC-NH_2-LM catalysts (M = Rh, Ir), involved reacting a suitable precursor, [M(cod)$(THF)_2$]BF_4 (M= Rh, Ir; cod = cyclooctadiene), with the imine-modified material. The preparative procedure is summarized in scheme 2.5, and a detailed description, of both the synthesis and the characterization of the catalysts, is given in experimental section.

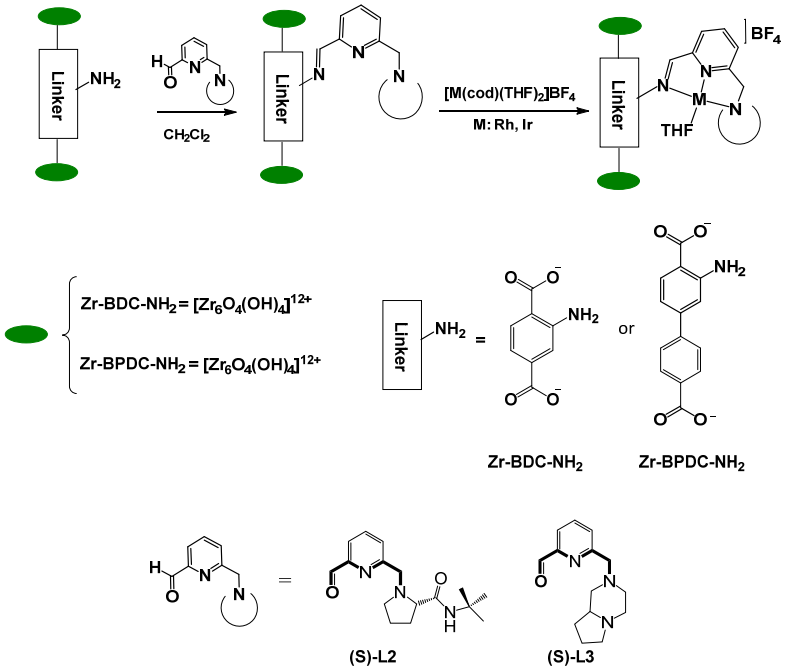

Scheme 2.5. Preparation of Zr-BDC-NH_2-[L2Ir]BF_4, Zr-BDC-NH_2-[L3Rh]BF_4 and Zr-BPDC-NH_2-[L3Rh]BF_4.

The resulting Zr-BDC-microcrystalline powders present the same structure as the parent Zr-BDC-NH_2 material, which was confirmed by power X-ray diffraction (Figure 2.8). The chemical stability of these Zr-BDC-NH_2-L derivatives was found to be similar to that of Zr-BDC, with good tolerance to polar solvents, such a water, methanol, ethanol, dichloromethane, and DMF. The materials also demonstrated thermal stability with decomposition temperatures near 350 °C in air, which are comparable to those of other Zr-BDC derivatives, as confirmed by TGA (Figure 2.9).

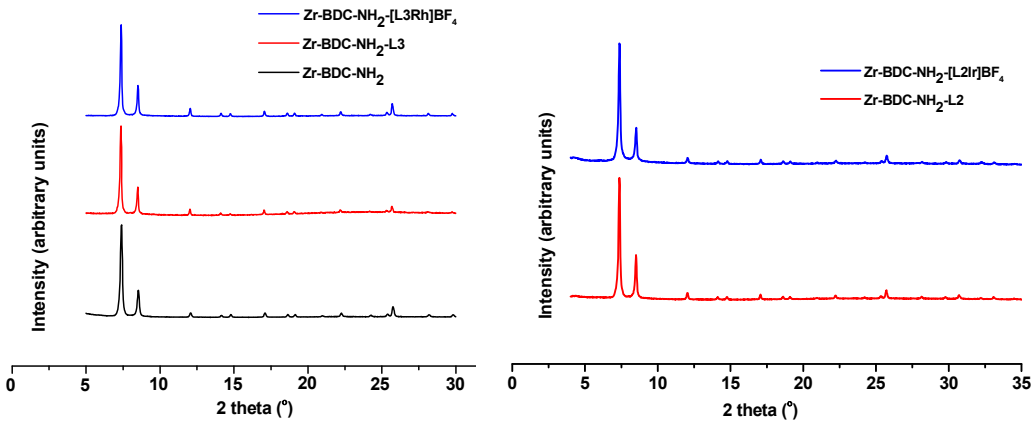

Figure 2.8. Powder X-ray diffraction patterns of a) Zr-BDC-NH_2, Zr-BDC-NH_2-L3 and Zr-BDC-[L3Rh]BF_4 b) Zr-BDC-NH_2-L2 and Zr-BDC-[L2Ir]BF_4.

The FTIR spectra show bands assigned to C-C aromatic vibrational modes and the percentage of functionalization can be determined by normalizing FTIR spectra to the band at 760 cm^{-1} assigned to the C-C vibrational mode in aromatic compounds (this band is relatively little affected by ring substituents),[99b] and no overlap from other vibrational modes is observed. Hereafter, these samples are referred to as Zr-BDC-NH_2-L. The full spectra are given in the annexes.

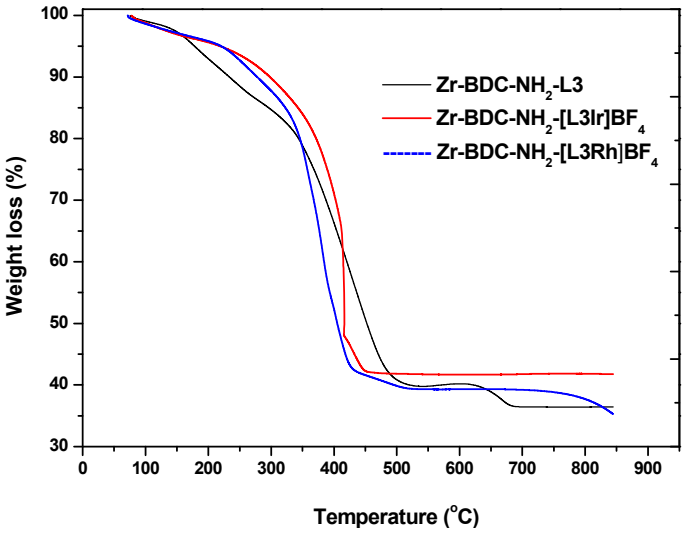

Figure 2.9. TGA patterns of Zr-BDC-NH_2-L3, Zr-BDC-NH_2-[L3Ir]BF_4, Zr-BDC-NH_2-[L3Rh]BF_4.

The analysis of the ^{1}H NMR spectra and electrospray ionization mass spectrometry (ESI-MS) spectra after the digestion of the MOFs under acidic conditions indicate that the ligands and iridium complexes remained in all PSM-materials (annexes). Hydrofluoric acid was employed to digest the materials. The inicial Zr-BDC-NH_2 was digested as reference, and the negative-mode mass spectra obtained showed a base peak at *m/z* 180 corresponding to H_2BDC-NH_2 ([H_2BDC-NH_2 + H]$^-$). The negative-mode mass spectra obtained for H_2BDC-NH_2L2 showed peaks at *m/z* 346 (H_2BDC-NH_2-L2-COOH) and 563 (ZrBDC-NH_2-L2+Na), which corresponded to the modified ligand. The spectra of H_2BDC-[L2Ir] showed a peak at *m/z* 512 ([L2Ir] + MeOH), 675 ({[H_2BDC-[L2Ir(MeOH)] + H}) and 841 (ZrBDC-NH_2[L2Ir]BF_4 + Na+ H). The ESI-MS for H_2BDC-NH_2L3 showed peaks at *m/z* 362 (H_2BDC-NH_2L3-COOH); a peak for H_2BDC-[L3Ir] was observed a peak at *m/z* 601 ({[H_2BDC-[L3Ir] + H}), and peaks for H_2BDC-[L3Rh] were observed at *m/z* 727 ({[H_2BDC-[L3Rh(cod)BF_4] + Na}), 639 ([H_2BDC-[L3Rh(cod)]) and 541 ([L3Rh(cod)BF_4]). Finally, HF cleaved the Zr cluster, and the fluoro complex [ZrF_5]$^-$ was discerned readily in the mass spectra, with a peak at *m/z* 185. The ^{1}H NMR spectra after the digestion of the MOFs under acic conditions indicate that the ligands remained in Zr-BDC-NH_2-L, Zr-BDC-NH_2-[LIr]BF_4 and Zr-BDC-NH_2-[LRh]BF_4 materials.

The N_2 adsorption-desorption isotherms of functionalized Zr-BDC-NH_2-MOF samples indicated that the materials demonstrate type-I isotherms (figure 2.10). All isotherms were found to retain porosity despite the functionalization of the linker. The BET surface areas were found to be 650 $m^2 \cdot g^{-1}$, total pore volume 0.25 $cm^3 \cdot g^{-1}$, and pore diameter 2.69 nm for Zr-BDC-L2, 500 $m^2 \cdot g^{-1}$, 0.20 $cm^3 \cdot g^{-1}$, and 2.51 nm for Zr-BDC-[L3Ir]BF_4 and 266 $m^2 \cdot g^{-1}$, 0.25 $cm^3 \cdot g^{-1}$, and 3.34 nm for Zr-BDC-[L3Rh]BF_4. The decrease in the BET surface area is mostly due to the increase in the mass of the material (attributed to the presence of large ligand and the corresponding rhodium or iridium complex) rather than a loss of porosity.

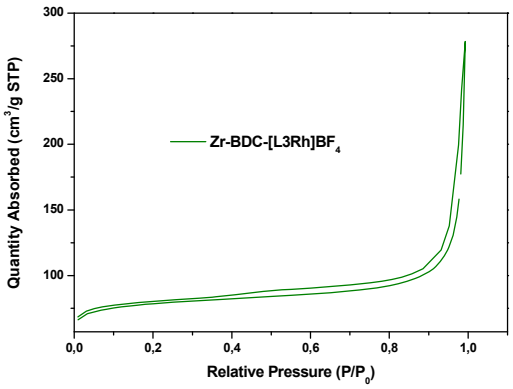

Figure 2.10. The N_2 isotherm (77K) of functionalized Zr-BDC-NH_2-[L3Rh]BF_4.

Finally, SEM experiments confirmed that the particle size remains unchanged during the ligand formation, because no significant increase or decrease in particle size was observed by using this technique (Figures 2.11a-c and in annexes).

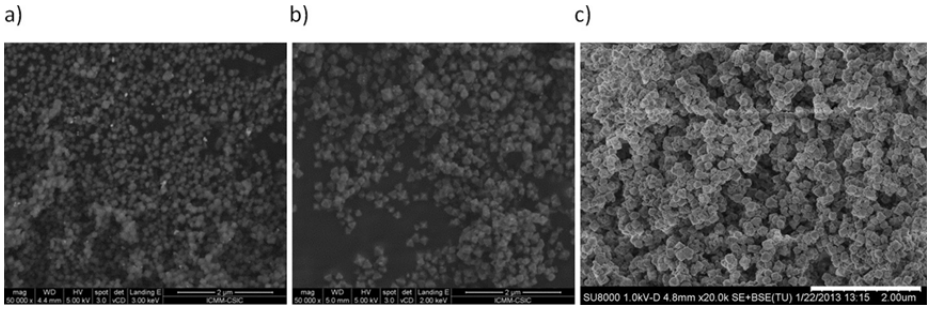

Figure 2.11. SEM image for a) Zr-BDC-NH_2-L2, b) Zr-BDC-NH_2-[L2Ir]BF_4, c) Zr-BDC-NH_2-[L3Rh]BF_4.

The post-synthetic modification of Zr-BPDC-NH_2 was performed following a similar method to that for Zr-BDC-NH_2; the diffraction peaks for the fresh Zr-BPDC-NH_2 materials are in agreement with those published in the literature.[50,94,63] Zr-BPDC derivatives lost their crystallinity after modification in both moist and dry conditions, although the collapse is most pronounced when water is present in the system; this is in agreement with the decreased porosity (Figure 2.12a). The materials demonstrated thermal stability with decomposition temperatures near 450 °C in air, which was confirmed by TGA (Figure 2.12b). Zr-BPDC-NH_2-L derivatives were characterized by using FTIR spectroscopy, ^{13}C NMR spectroscopy, SEM, and so on (spectra are given in the annexes) and the results are similar to those discussed previously for Zr-BDC-NH_2 materials. The ESI-MS spectra for digested samples showed peaks at *m/z* 507 for {H_2BPDC-NH_2-L3 + Na}, 639 for {H_2BPDC-NH_2-L3Rh + Na + MeOH}, and 750 for {H_2BPDC-NH_2-[L3Rh(cod)] + Na + MeOH}. The apparent modification of the morphology of the materials is observed in SEM images presented in Figure 2.12c, and in annexes. The octahedral shape of the crystals is observed. The material exhibits some surface roughness; however, the overall shape of the crystals is preserved.

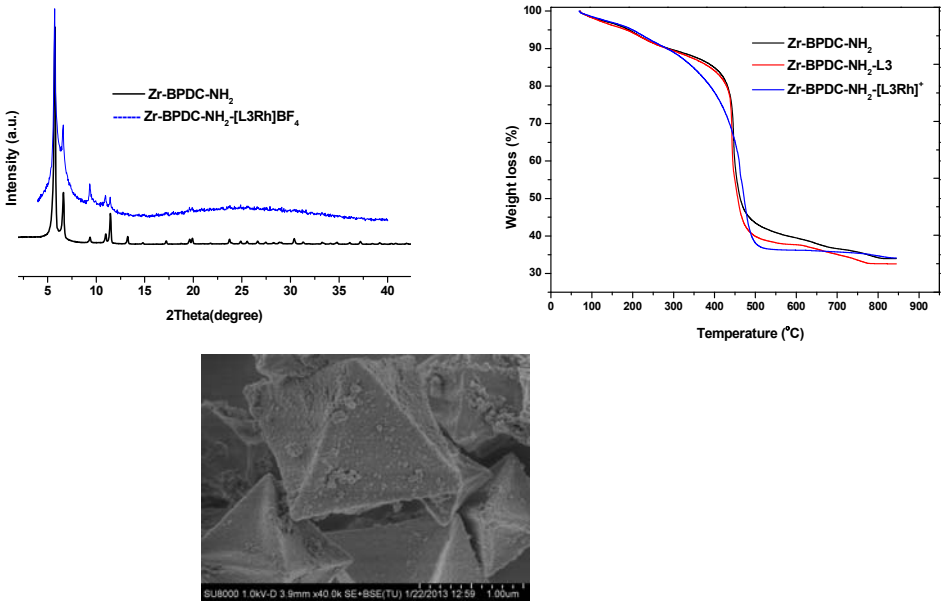

Figure 2.12. a) PXRD patterns of Zr-BPDC-NH_2-MOFs; b) TGA patterns of Zr-BPDC-NH_2, Zr-BPDC-NH_2-L3, Zr-BPDC-NH_2-[L3Rh]BF_4 and c) SEM image.

IRMOF-3[81a,57] will be used as reference material to compare its behavior with that from Zr-BDC-NH_2 due to they have the same linker. IRMOF-3 consists of a Zn_4O tetrahedron connected with six carboxylates to give a three-dimensional cubic porous material ($Zn_4O(BDC\text{-}NH_2)_3$); it has been prepared, in the last years, by different groups[57] with different textural properties. Rowsell et al., synthesized IRMOF-3 solvothermally with BDC-NH_2 and $Zn(NO_3)_2{\cdot}4H_2O$ in N,N-diethylformamide with a BET surface area of 2446 $m^2\ g^{-1}$.[129] Gascon et al. obtain a high BET surface area of 3130 $m^2\ g^{-1}$ in the N_2 protection.[130] When IRMOF-3 was synthesized by a "direct mixing" synthesis strategy at room temperature, samples with a BET surface area of 750 $m^2{\cdot}g^{-1}$ were obtained.[81a,131] This last strategy, using DMF as solvent, was employed in this work, also obtaining IRMOF-3 with 750 $m^2{\cdot}g^{-1}$ BET surface area and pores of ≈10 Å.[81a] Although the Zn(II)-based MOFs have many favorable aspects, their poor stability to moisture and protic solvents is likely to limit their applications. This prompted us to use here more stable, chemically resistant frameworks such as Zr(IV)-based MOFs.[50,81a]

[129] J. L. C. Rowsell and O. M. Yaghi *J. Am. Chem. Soc.* **2006**, *128*, 1304-1315.
[130] J. Gascon, U. Aktay, M. D. Hernandez-Alonso, G. P. M. van Klink and F. Kapteijn *J. Catal.* **2009**, *261*, 75-87.
[131] L. Huang, H. Wang, J. Chen, Z. Wang, J. Sun, D. Zhao and Y. Yan *Microporous Mesoporous Mater.* **2003**, *58*, 105-114.

2.3.2. Catalytic applications

Part A: One step reactions.

2.3.2.1. Zr-BDC-NH_2-[L1Ir]BF_4 for hydrogenation of aromatic compounds

The efficient synthesis of cyclohexane derivatives *via* the catalytic hydrogenation of aromatic compounds is of both scientific and industrial importance. However, the complete hydrogenation of aromatics still requires highly energetic (>100 °C) and dangerous reaction conditions (50 atm H_2) due to the lack of efficient catalysts. Recent publications suggest that palladium,[132] ruthenium,[133] rhodium,[134] iridium,[135] platinum[136] and nickel[137] may be used to achieve the hydrogenation of aromatic compounds under milder conditions.

On the other hand, it is well known that Lewis acids can activate aromatic compounds[138] resulting in a sequential process in which the hydrogenation by hydrogen atoms is activated by the metal as depicted in Scheme 2.6. These

[132] C. Zhao, Y. Kou, A. A. Lemonidou, X. Li and J. A. Lercher *Angew. Chem. Int. Ed.* **2009**, *48*, 3987-3990; J. Huang, Y. Jiang, N. van Vegten, M. Hunger and A. Baiker *J. Catal.* **2011**, *281*, 352-360; Y. Wang, J. Yao, H. Li, D. Su and M. Antonietti *J. Am. Chem. Soc.* **2011**, *133*, 2362-2365; P. Makowski, R. Demir Cakan, M. Antonietti, F. Goettmann and M.-M. Titirici *Chem. Commun.* **2008**, 999-1001.

[133] C. J. Boxwell, P. J. Dyson, D. J. Ellis and T. Welton *J. Am. Chem. Soc.* **2002**, *124*, 9334-9335; C. Hubert, A. Denicourt-Nowicki, A. Roucoux, D. Landy, B. Leger, G. Crowyn and E. Monflier *Chem. Commun.* **2009**, 1228-1230.

[134] E. Bayram, J. C. Linehan, J. L. Fulton, J. A. S. Roberts, N. K. Szymczak, T. D. Smurthwaite, S. Özkar, M. Balasubramanian and R. G. Finke *J. Am. Chem. Soc.* **2011**, *133*, 18889-18902; N. Yan, Y. Yuan, R. Dykeman, Y. Kou and P. J. Dyson *Angew. Chem. Int. Ed.* **2010**, *49*, 5549-5553; C. Hubert, A. Denicourt-Nowicki, P. Beaunier and A. Roucoux *Green Chem.* **2010**, *12*, 1167-1170; Y. Motoyama, M. Takasaki, S.-H. Yoon, I. Mochida and H. Nagashima *Org. Lett.* **2009**, *11*, 5042-5045; T. Maegawa, A. Akashi, K. Yaguchi, Y. Iwasaki, M. Shigetsura, Y. Monguchi and H. Sajiki *Chem. Eur. J.* **2009**, *15*, 6953-6963.

[135] E. Bayram, M. Zahmakıran, S. Özkar and R. G. Finke *Langmuir* **2010**, *26*, 12455-12464; M. Zieliński, M. Pietrowski and M. Wojciechowska *ChemCatChem* **2011**, *3*, 1653-1658.

[136] Z. Guo, L. Hu, H.-h. Yu, X. Cao and H. Gu *RSC. Adv.* **2012**, *2*, 3477-3480.

[137] S. Toppinen, T. K. Rantakylä, T. Salmi and J. Aittamaa *Ind. Eng. Chem. Res.* **1996**, *35*, 4424-4433; L. Lu, Z. Rong, W. Du, S. Ma and S. Hu *ChemCatChem* **2009**, *1*, 369-371.

[138] H. Liu, T. Jiang, B. Han, S. Liang and Y. Zhou *Science* **2009**, *326*, 1250-1252; R. R. Deshmukh, J. W. Lee, U. S. Shin, J. Y. Lee and C. E. Song *Angew. Chem. Int. Ed.* **2008**, *47*, 8615-8617; P. Tarakeshwar, J. Y. Lee and K. S. Kim *The Journal of Physical Chemistry A* **1998**, *102*, 2253-2255; H. Ahn, C. P. Nicholas and T. J. Marks *Organometallics* **2002**, *21*, 1788-1806.

two types of activation could work cooperatively, resulting in high activity for producing cyclohexane derivatives. Our bifunctional Zr-[L1Ir]-catalyst has zirconium as Lewis acid and iridium which can act as the active metal. Herein we study the catalytic activity in hydrogenation of aromatic compounds, under mild conditions (in ethanol at 6 bar of H_2 and 60-90 °C) by simultaneous activation of molecular hydrogen with iridium and the aromatic substrate with zirconium as Lewis acid.

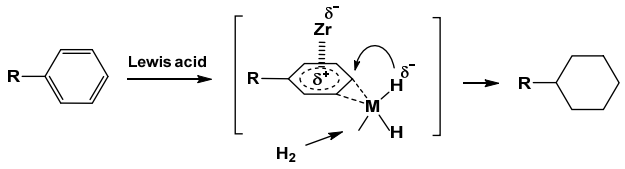

Scheme 2.6. General reaction pathway for the hydrogenation of aromatic compounds.

We selected aniline as model compound to explore the aromatic hydrogenation reaction catalyzed with Zr-BDC-NH_2-[L1Ir], founding a selectivity toward the formation of cyclohexanamine at 60 °C after 10 h of reaction. However, when temperature was increased to 90 °C alkylation of amine to *N*-ethylcyclohexanamine was the major product. At this temperature, reaction in isopropanol or 2-butanol also conducted to *N*-isopropylcyclohexanamine or *N*-(pentan-2-yl)cyclohexanamine,[139] respectively. To avoid the generation of these by-products, we chose *t*-butanol as solvent or a temperature of 60 °C and 6 bar H_2.

Zr-BDC-NH_2-[L1Ir] was also tested in the hydrogenation of a series of other representative monosubstituted benzenes with electron withdrawing or donating groups. Substrates with electron donating groups are hydrogenated faster than those with electron withdrawing groups (Table 2.1 and Figure 2.13). We found that Zr-BDC-NH_2-[L1Ir] catalyzes the quantitative hydrogenation of aromatic hydrocarbons such as toluene and phenol, which was selectively reduced to cyclohexanol with only traces of cyclohexanone or ethyl benzoate detected (Table 2.1, entries 4, 6, 7). Meanwhile, styrene is quickly reduced to ethylbenzene (Table 2.2, entry 1), which was further hydrogenated to ethylcyclohexane at 90 °C (Table 2.1, entry 8). Nitrobenzene and benzonitrile were transformed to cyclohexylamine and cyclohexylmethanamine respectively in good yield and selectivity (table 2.1,

entry 3, 9). Bromobenzene or diethyl phthalate did not react under these reaction conditions, even at 90 °C (table 2.1, entries 10, 11) while methyl 2-methoxybenzoate yields the corresponding cyclohexane carboxylate beside a 20% of hydrogenolysis of the C-O bond (table 2.1, entry 12). Comparing the soluble Ir-complexes, used as reference catalysts (Table 2.1, entry 1), with the corresponding supported on Zr-BDC-NH_2-[L1Ir]BF_4 MOF, a considerable increase on the reactivity was observed.

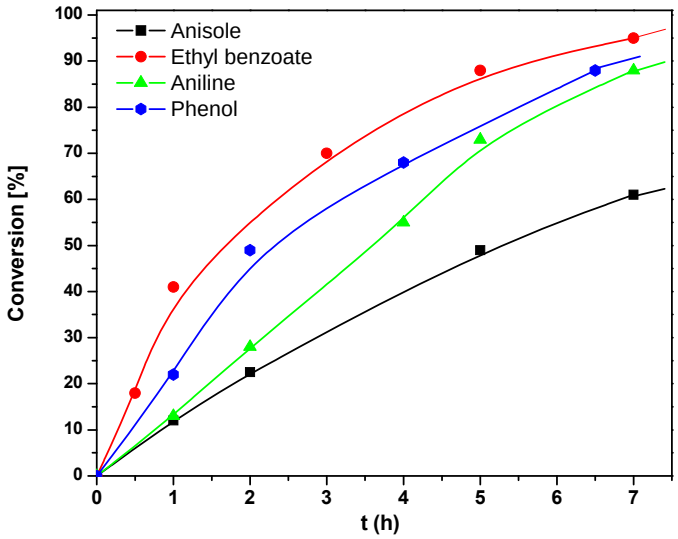

Figure 2.13. Kinetic profile for the Zr-BDC-NH_2-[L1Ir]BF_4-catalyzed aromatic hydrogenation.

Table 2.1. Hydrogenation of aromatic substrates.[a]

	Cat. (mol%)[b]	substrate	product	Conv. (%) (h)	TOF (h^{-1})[d]
1	[L1Ir] (1)			100 (8)	42
2	Zr-BDC-NH_2-[L1Ir]BF_4 (0.20)			85 (5) 98 (24)	85
3	Zr-BDC-NH_2-[L1Ir]BF_4 (0.20)			90 (10)	80
4	Zr-BDC-NH_2-[L1Ir]BF_4 (0.20)			100 (5)	98
5	Zr-BDC-NH_2-[L1Ir]BF_4 (0.20)	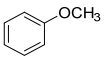	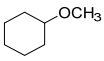	49 (6) 65 (24)	60
6	Zr-BDC-NH_2-[L1Ir]BF_4 (0.20)			85 (6)	110
7	Zr-BDC-NH_2-[L1Ir]BF_4 (0.20)	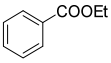	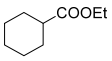	90 (5)	235
8	Zr-BDC-NH_2-[L1Ir]BF_4 (0.20)			90 (22)[c]	10
9	Zr-BDC-NH_2-[L1Ir]BF_4 (0.20)		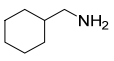	75 (24)[c]	8
10	Zr-BDC-NH_2-[L1Ir]BF_4 (0.20)			traces (20)	-
11	Zr-BDC-NH_2-[L1Ir]BF_4 (0.20)	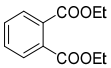	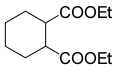	0 (24)	12
12	Zr-BDC-NH_2-[L1Ir]BF_4 (0.20)	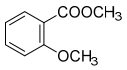	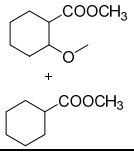	67 + 17 (19)	n.d.

[a]Reaction conditions: solvent: ethanol or isopropanol, T: 60 °C, P(H_2): 6 bar; [b]based on Ir; [c]Reaction in *t*-butanol at 90 °C, reaction in isopropanol (90 °C) yields 60% of *N*-alkylated product, [d]mmolsubs/mmol cat. h.

In order to determinate the selectivity of different functional groups against arenes, we explored the catalyzed-hydrogenation for other unsaturated carbon bonds (C=C, C=O) and cyano and nitro groups attached to an aromatic ring (Table 2.2). Thus, olefinic double bonds of styrene and α-methylstyrene were fully converted to ethylbenzene and isopropylbenzene, respectively. Furthermore, carbonyl compounds such benzaldehyde or acetophenone yield their corresponding alcohols, and benzonitrile or nitrobenzene their corresponding amines. In all cases these groups were hydrogenated before the reduction of arene was initiated.

Table 2.2. Hydrogenation experiments with Zr-BDC-NH_2-[L1Ir]BF_4.[a]

Entry	Substrate	Product	Conv. (%) (h)	TOF (h^{-1})
1		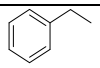	100 (0.5)	935
2			100 (2)	325
3	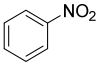	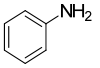	100 (0.5)	1000
4		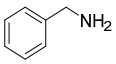	100 (24)	13
5		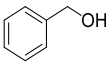	85 (2)	850
6		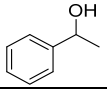	20(24) 100 (20)[b]	10

[a] 2 mol% of catalyst based on Ir; P(H_2): 2 bar; 40 °C; [b]90 °C.

After the hydrogenation reaction, Zr-BDC-NH_2-[L1Ir]BF_4 was separated from the reaction mixture by centrifugation, thoroughly washed with ethanol and reutilized as catalyst in subsequent runs under identical reaction conditions. The results, included in Figure 2.15, indicate that after the first cycle the activity slightly decreases, thus no efficiency loss is observed in the arene hydrogenation for up to five runs. Moreover, the filtrate solutions collected at the end of each catalytic run were analyzed by ICP-MS and in none of them Ir was detected, confirming the absence of iridium in the solution. In contrast, FT-IR spectra of the recovered solid catalyst a band at ≈2000 cm^{-1} appears corresponding to the γ(Ir-H) bond (Figure 2.14).

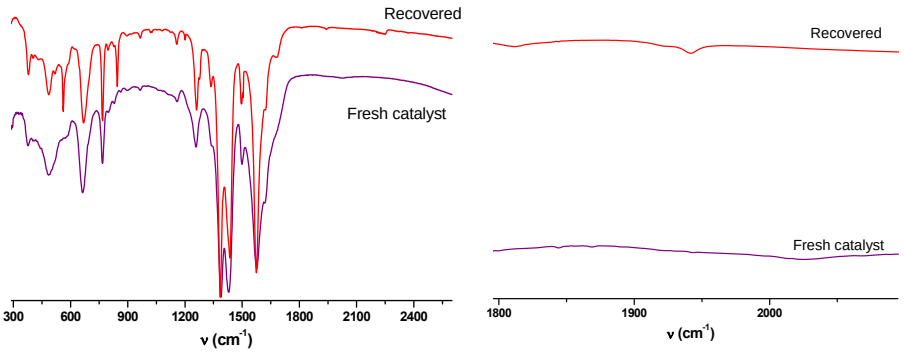

Figure 2.14. FT-IR of fresh and recovered catalysts after the hydrogenation of aniline.

A control experiment was also performed to show that the hydrogenation reactions are stopped by the removal of Zr-BDC-NH_2-[L1Ir]BF_4 from the reaction solution (Figure 2.15). Moreover, they provide easy separation and high reusability performance in these reactions by keeping their stability against leaching throughout the catalytic runs.

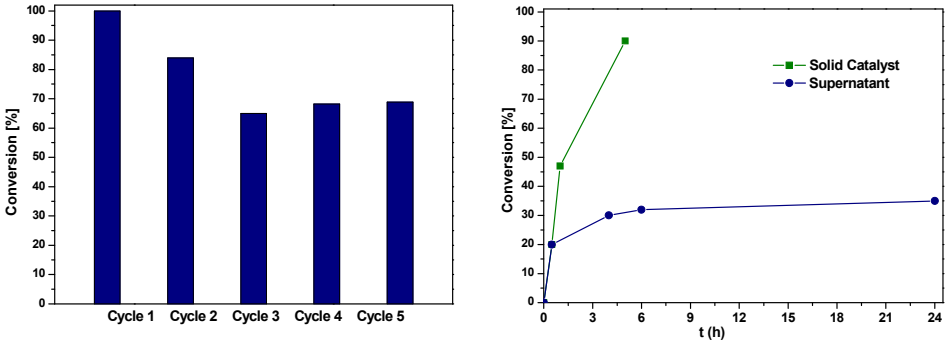

Figure 2.15. a) Recycling experiments for the catalyzed hydrogenation of aniline and b) hot filtration test for the hydrogenation of ethyl benzoate.

The characterization of the isolated samples after five catalytic runs in the hydrogenation of aniline reveals that (i) the crystallinity of the host Zr-BDC framework is mainly retained as depicted in the PXRD patterns in Figure 2.16, and (ii) there is some bulk iridium formed within the framework of Zr-BDC, at the end of the fifth catalytic run (SEM and TEM images in figure 2.17 and 2.18). Higher SEM and TEM resolution for Zr-BDC-NH_2-[L1Ir]BF_4 crystallites is difficult to adquire due to local damage by the electron beam, which causes distortion and movement.

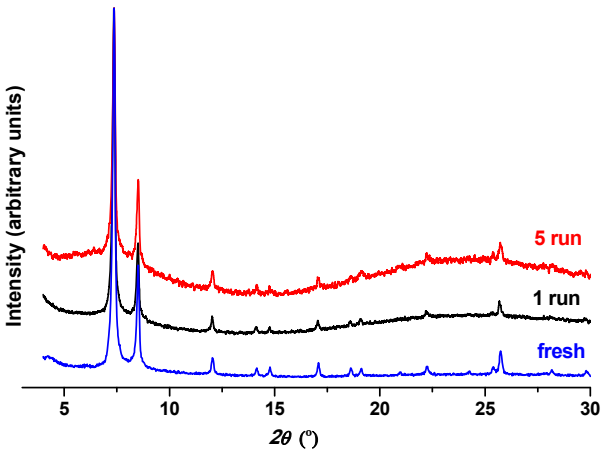

Figure 2.16. PXRD for fresh catalyst and recovered after 1 run and 5 run.

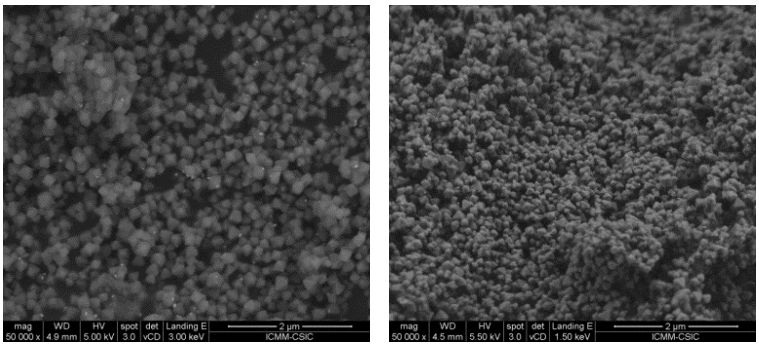

Figure 2.17. SEM images fresh (a) and recovered catalyst (b)

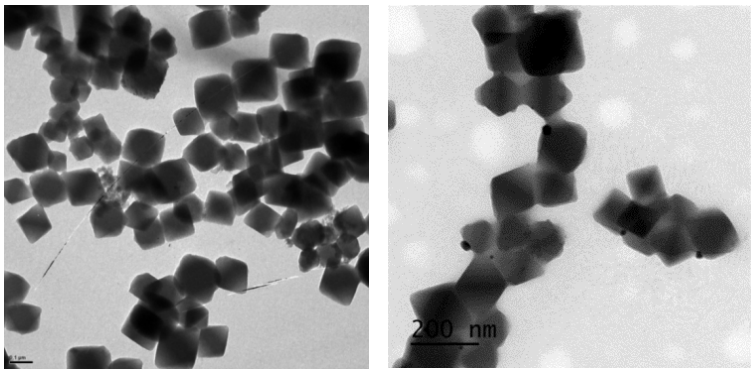

Figure 2.18. TEM images fresh (a) and recovered catalyst (b)

Recent studies have shown that metal-organic frameworks are also considered as suitable host materials for controlling growth of catalytic clusters or nanoparticles within MOF cavities.[74a,74b,74d,15c] Nowadays, it has been already demonstrated that the zeolitic imidazole framework (ZIF-8 MOF) or MIL101(Cr) can act as a suitable host material for Au,[83a,139] Ag,[140] Ni,[141] Ir[142] and Pd[143] nanoparticles. Our chemically robust Zr-based MOF (Zr-BDC-NH_2) might also result a host matrix to stabilize guest iridium nanoparticles (IrNPs).

In order to demonstrate of some IrNPs could be formed durung the catalytic cycles, we performed the following experiment: We reduced the Zr-BDC-NH_2-[L1Ir]BF_4 with $NaBH_4$ (ethanol at 273 K for 2 h) or H_2 (6 bar, 120 °C) in order to promote the generation of IrNPs supported on the Zr-MOF (Zr-MOF-IrNPs) and we found that PXRD analysis (Figure 2.19) showed the typical reflections of Zr-BDC-NH_2(100), which confirms the stability of the support under the chosen catalytic conditions. Moreover, the reduced catalysts were not active for the hydrogenation reaction of aniline and any product formation was not observed after 24 h. In fact, when the hydrogenation of aniline was performed with Zr-BDC-NH_2-[L1Ir]BF_4 at 120 °C, recycling is not possible because the activity considerably decreases after the first run.

[139] H.-L. Jiang, B. Liu, T. Akita, M. Haruta, H. Sakurai and Q. Xu *J. Am. Chem. Soc.* **2009**, *131*, 11302-11303; G. Lu, S. Li, Z. Guo, O. K. Farha, B. G. Hauser, X. Qi, Y. Wang, X. Wang, S. Han, X. Liu, J. S. DuChene, H. Zhang, Q. Zhang, X. Chen, J. Ma, S. C. J. Loo, W. D. Wei, Y. Yang, J. T. Hupp and F. Huo *Nat. Chem.* **2012**, *4*, 310-316.

[140] H.-L. Jiang, T. Akita, T. Ishida, M. Haruta and Q. Xu *J. Am. Chem. Soc.* **2011**, *133*, 1304-1306.

[141] P.-Z. Li, K. Aranishi and Q. Xu *Chem. Commun.* **2012**, *48*, 3173-3175.

[142] M. Zahmakiran *Dalton Trans.* **2012**, *41*, 12690-12696.

[143] J. Hermannsdörfer, M. Friedrich and R. Kempe *Chem. Eur. J.* **2013**, *19*, 13652-13657.

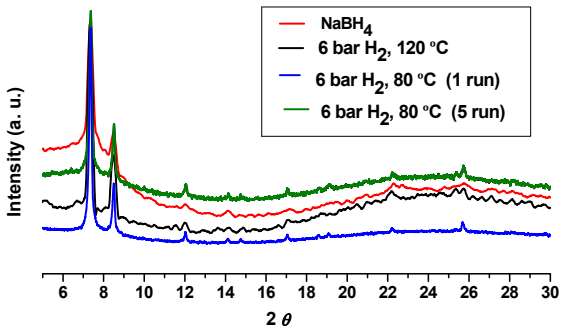

Figure 2.19. PXRD for Zr-BDC-NH_2-[L1Ir]BF_4: a) recovered after the first run, b) recovered after the fifth run, c) Zr-MOF-IrNPs after 6 bar H_2 at 120 °C and d) Zr-MOF-IrNPs obtained from reduction with $NaBH_4$.

The morphology of the different Ir-Zr-MOF samples was furhter examined by dynamic light scattering (DLS) (annexes), SEM (annexes) and TEM (annexes). TEM images of the materials obtained by reduction with $NaBH_4$ or by hydrogenation at 120 °C, which are inactive in hydrogenation reactions, show larger IrNPs and in a bigger amount. Meanwhile, TEM images of the recovered catalysts in operation conditions (60 °C/6 bar) show that most of the particles have a similar size to that found in the fresh catalyst, which seems to corroborate the view that the molecular structure of heterogenized complexes was preserved. This fact could be confirmed as well by FT-IR in which a band corresponding to Ir-H bond can be observed. All these experimental findings are in agreement with the hypothesis that the presence of larger particles could be responsible for the decrease of activity after first cycle of reactions.

X-ray photoelectron spectroscopy (XPS) analysis was performed on the fresh and recovered Zr-BDC-NH_2-[L1Ir]BF_4 MOF solids. The samples were kept in vacuum overnight prior to XPS measurements. The spectra were calibrated with respect to the C 1s peaks in each sample. The survey scan XPS spectrum of the Zr-BDC-NH_2-[L1Ir]BF_4 MOF samples (annexes) shows the presence of iridium in addition to the Zr-BDC framework elements (Zr, C, N). XPS analysis showed N 1s (399.1 eV) and C 1s signals, the latter comprising sp^2 carbon (284.6 eV), and sp^3 carbon neighboring oxygen (287.9 eV). The XPS core level for the iridium (Ir(4f) region) showed no difference in peak positions between the fresh catalyst and the solid recovered from the reaction (peaks at 64.8 and

62.1 eV, readily assigned to Ir $4f_{7/2}$ and Ir $4f_{5/2}$) indicating the $Ir^{\delta+}$ oxidation state in all the samples[128,144] (Figure 2.20).

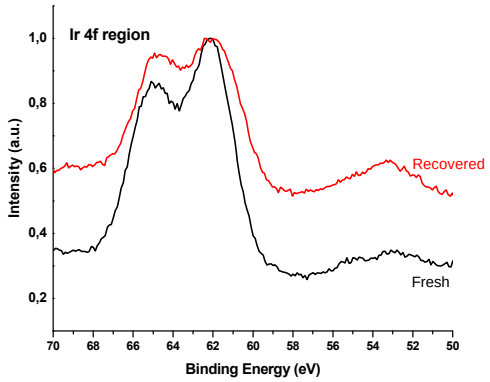

Figure 2.20. XPS Ir (4f) region for the initial and recovered catalyst.

Part B: Multistep reactions

2.3.2.2. Catalyst screening for alkylation of amines with alcohols.

a) Reaction with auxiliary H_2

Since Ir complexes have shown to be active for performing the *N*-alkylations of amines with alcohols, we used the Zr-BDC-NH_2-[L1Ir]BF_4 MOF catalyst for this type of reaction taking advantage of the large pores of the Zr-BDC-NH_2 (2.69 nm) which would allow free diffusion of reactants and products. Thus, the use of Zr-BDC-NH_2 could be considered an efficient way to heterogenize the Ir complex.

N-alkylation reaction of amines was performed in 2-propanol (1 bar H_2 pressure; 1 bar = 100 kPa) with the neutral [L1IrCl] complex as homogeneous catalyst, obtaining good conversion and selectivities (Table 2.3, entries 1 and 2). Meanwhile, the catalytic evaluation of Ir-MOF catalysts was performed by mixing them with nitrobenzene in 2-propanol in an Autoclave Engineers reactor (100 mL) at 80 °C under 4-6 bar H_2 pressure. Under these reaction conditions using our heterogeneous Zr-BDC-NH_2-[L1Ir]Cl (0.4 mol%) catalyst, the *N*-alkylation of the amine with the alcohol occurs with high conversion and selectivity; in fact, both of them higher than those obtained with the

[144] C. Wang, J.-L. Wang and W. Lin *J. Am. Chem. Soc.* **2012**, *134*, 19895-19908.

homogeneous catalyst. The activity of the homogeneous catalyst could be increased significantly with the substitution of the chloride ligand by a less coordinating counterion such as $[BF_4]^-$. With the use of this anion, activity was also higher for the Zr-BDC-NH_2-[L1Ir]BF_4 catalyst, which was again similar to the activity of the homogeneous catalyst. The temperature could be lowered to 50 °C; however, longer reaction time was needed to obtain high conversion.

After identifying the potential of Zr-BDC-NH_2-[L1Ir]BF_4 as a catalyst for *N*-alkylation of amines, we investigated the scope and limitations of this transformation. Various primary or secondary alcohols were coupled with aniline, producing monoalkylated amines in high yields. Although primary alcohols easily react to produce the corresponding amines in a few hours, secondary alcohols proved to be less reactive and longer reaction times were required.

For the *N*-alkylation of aniline with ethanol (Table 2.3, entries 1, 8, 9) the supported Zr-BDC-NH_2-[L1Ir]BF_4 catalyst was superior to the corresponding soluble Ir-complex, indicating both that the Ir complex moiety in the heterogeneous catalyst is crucial and the support material Zr-MOF also plays an important role in promoting the reaction. This effect can be related to the Lewis acidity of the Zr-cluster, which promotes the imine formation and introduces an additional benefit from the point of view of increasing H_2 concentration, and/or stabilizing the reaction transition state, as previously reported.[145]

[145] B. Pugin, H. Landert, F. Spindler and H.-U. Blaser *Adv. Synth. Catal.* **2002**, *344*, 974-979; C. González-Arellano, A. Corma, M. Iglesias and F. Sánchez *Adv. Synth. Catal.* **2004**, *346*, 1316-1328.

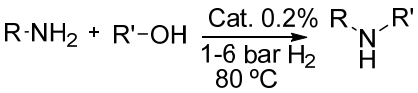

Table 2.3. N-alkylation of amines with alcohols[a] over Ir-Zr-MOF supported catalysts.

Entry	Cat. (mol%)	PH_2 (bar)	R	R'	Yield [%] (h)[b]
1	[L1Ir]Cl (3)	1	Ph	Et	100 (6)
2	[L1Ir]Cl (3)	4	Ph	*i*Pr	99 (20)
3	Zr-BDC-NH_2-[L1Ir]Cl (0.4)	4	Ph	*i*Pr	100 (20)
4	Zr-BDC-NH_2-[L1Ir]BF_4 (0.4)	6	Cy	*i*Pr	70 (20)
5	Zr-BDC-NH_2-[L1Ir]BF_4 (0.25)	6	Ph	2-Bu	100 (24)
6	Zr-BDC-NH_2-[L1Ir]BF_4 (0.25)	6	Cy	2-Bu	85 (24)
7	Blank	6	Ph	Et	5 (24)
8	Zr-BDC-NH_2-[L1Ir]BF_4 (0.2)	4	Ph	Et	100 (10)
9	Zr-BDC-NH_2-[L1Ir]BF_4 (0.2)	4	Ph	Et	100 (4)
10	Zr-BDC-NH_2-[L1Ir]BF_4 (0.2)	4	Bn	*i*Pr	100 (23)
11	Zr-BDC-NH_2-[L1Ir]BF_4 (0.2)	4	Bn	*i*Pr	70 (4)

[a] Reaction conditions: Autoclave Engineers reactor, amine substrate (1 mmol), alcohol (40 mL), T: 80 °C. [b] Yields are based on amine substrates.

b) Reaction in the absence of H_2

Comparing all the catalysts examined before, Zr-BDC-NH_2-[L1Ir]BF_4 has demonstrated the best catalytic performance. Therefore, we decided to use this system for the *N*-alkylation of amines in the absence of H_2 by using a hydrogen borrowing mechanism (scheme 2.7).[146]

[146] A. Corma, T. Ródenas and M. J. Sabater *Chem. Eur. J.* **2010**, *16*, 254-260; P. Rubio-Marques, A. Leyva-Perez and A. Corma *Chem. Commun.* **2013**, *49*, 8160-8162; A. Corma, T. Ródenas and M. J. Sabater *J. Catal.* **2011**, *279*, 319-327; A. J. A. Watson and J. M. J. Williams *Science* **2010**, *329*, 635-636; S. Bähn, S. Imm, L. Neubert, M. Zhang, H. Neumann and M. Beller *ChemCatChem* **2011**, *3*, 1853-1864.

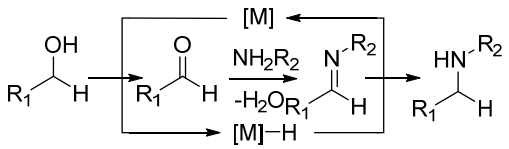

Scheme 2.7. *N*-alkylation of amines with alcohols in the absence of H_2 and base (R_1: Et, iPr, Bz; R_2: Ph, C_5H_{11}).

The reaction was conducted with 0.2 mol% Zr-BDC-NH_2-[L1Ir]BF_4 (based on Ir) and the scope of *N*-alkylation was explored with different combinations of substrates (primary, as 1-hexylamine; reactive cyclic secondary amines, such a piperidine; and alcohols). Excess amount of alcohol was used not only as a reactant but also as a solvent. Various amines reacted with different alcohols in the presence of Zr-BDC-NH_2-[L1Ir]BF_4 affording moderate to excellent yields of the corresponding *N*-alkylated products (Table 2.4). For instance, the reaction of 1-hexylamine and piperidine with ethanol gives the desired product in high yields (Table 2.4, entries 1 and 3) whereas the reaction with an aliphatic secondary alcohols such as 2-butanol occurs only with 1-hexylamine (Table 2.4, entry 2). The reaction with tertiary *tert*-butanol does not occur.

The reaction of piperidine or hexylamine with benzyl alcohol occurs at 120 °C in high yields (Table 2.4, entries 6, 8); however, the reaction with aniline is unsuccessful even at higher temperature (180 °C) (entry 9), and the application of microwave heating is necessary to achieve results comparable with those achieved using thermal heating for other substrates (entries 10 and 11). The reaction does not proceed in the absence of a catalyst or with Zr-BDC-NH_2-L1 (before forming the iridium complex), which suggests that the reaction proceeds through direct involvement of Ir.

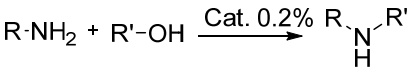

Table 2.4. N-alkylation of amines with alcohols catalyzed by Zr-BDC-NH_2-[L1Ir]BF_4.

entry	Alcohol	Amine	T (°C)	t (h)	Yield [%][d]	TOF (h^{-1})[e]
1		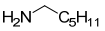	80[a]	2	100	940
2		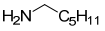	80[a]	24	100	22
3			80[a]	2	100	450
4			80[a]	2	100	570
5	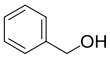		80[a]	6	10	-
6			120[b]	2	100	202
7	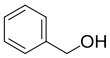	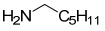	80[b]	6	10	-
8			120[b]	0.5	100	980
9			180[b]	24	10	-
10	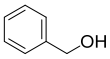		125[c]	2	42	105
11			150[c]	2.5	90	180
12			150[c]	2	0	-

[a] Autoclave Engineers reactor, 0.20 mol% catalyst (based on Ir), amine substrate (1 mmol), alcohol (40 mL); [b] Glas microreactor SUPELCO, 0.20 mol% catalyst (based on Ir), amine substrate (1 mmol), alcohol (2mL); [c] Microwave reactor; [d] Products were characterized by NMR, mass spectra, yields of isolated products are based on amine substrates; [e] mmol subs./mmol cat. h.

The accepted mechanism for alkylation of amines with alcohols in the absence of H_2 involves three steps: (1) alcohol dehydrogenation, (2) reaction of the resulting carbonyl with the amine to form the imine, and (3) hydrogenation of the imine with the hydride-complex formed in the first step (**scheme 2.7**). In the reaction of the alcohols with amines, we could not detect the intermediate imine product. This result indicates that either the hydrogenation of the imine formed in an external cycle is fast or the entire catalytic cyclic occurs with all the intermediates attached to the catalyst. In our case, supported by the presence of an hemilabile amino group in the ligand,[147] the intermediate

[147] M. V. Jiménez, J. Fernández-Tornos, J. J. Pérez-Torrente, F. J. Modrego, S. Winterle, C. Cunchillos, F. J. Lahoz and L. A. Oro *Organometallics* **2011**, *30*, 5493-5508; C. del Pozo, A. Corma, M. Iglesias and F. Sanchez *Green Chem.* **2011**, *13*, 2471-2481.

aldehyde remains coordinated to the Ir-complex and reacts with the amine to give the hemiaminal group, which is also attached to the catalyst; dehydration to the imine and reduction to the product amine would also occur without breaking the coordination to the catalyst, as has been proposed by Yamaguchi[148] and Madsen et al.[149]

In order to support this mechanistic approach, we performed the reaction of aniline (1.0 mmol) with benzaldehyde (1.0 mmol) in benzylic alcohol in the presence of catalytic amounts of Zr-BDC-NH_2-[L1Ir]BF_4, at 100 °C for 1 h, obtaining *N*-benzylaniline quantitatively [Eq. (1 in scheme 2.8] (see annexes). Moreover, the reduction of benzylideneaniline (1.0 mmol) in the presence of catalytic amounts Zr-BDC-NH_2-[L1Ir]BF_4 with 2-propanol as sacrificial alcohol to form the iridium hydride intermediate, resulted in the formation of traces of *N*-benzylaniline [Eq. (2) in scheme 2.8]; whereas the preformed imine is reacted exactly under the same reaction conditions with 4 bar H_2 pressure (see annexes). This result suggests that uncoordinated imine could not undergo transfer hydrogenation with the present catalytic system. Thus, the fact that the imine was never detected using the MOF catalyst is in agreement with a reaction mechanism in which the entire catalytic cycle occurs with all the intermediates attached to the catalyst.[149-150]

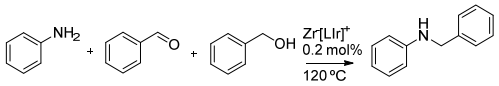

Eq.1.

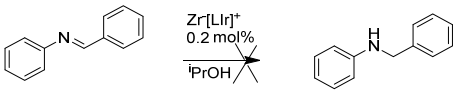

Eq.2.

Scheme 2.8. Mechanistic studies.

A complementary experiment was performed to check if the metal or metal complex leaching occurs during the reaction and whether the leached species

[148] K.-i. Fujita, Y. Enoki and R. Yamaguchi *Tetrahedron* **2008**, *64*, 1943-1954.
[149] P. Fristrup, M. Tursky and R. Madsen *Org. Biomol. Chem.* **2012**, *10*, 2569-2577.

are totally or partially responsible of the catalyst activity. Then, the reaction of hexylamine with ethanol was stopped by hot filtration of the catalyst at 30% of the amine formation. No further reaction occurred if the filtrate was used to continue the reaction (Figure 2.21). This result indicates that the catalytic process is heterogeneous. Furthermore, the inductively coupled plasma analysis of the filtrate confirms that the Ir content was below the detection limit (<0.10 ppm). The used catalyst was also analyzed by using XRD, SEM and TEM techniques, and the results presented in figures 2.22, 2.23 and 2.24, indicating that the catalyst remains structurally stable during the catalytic process.

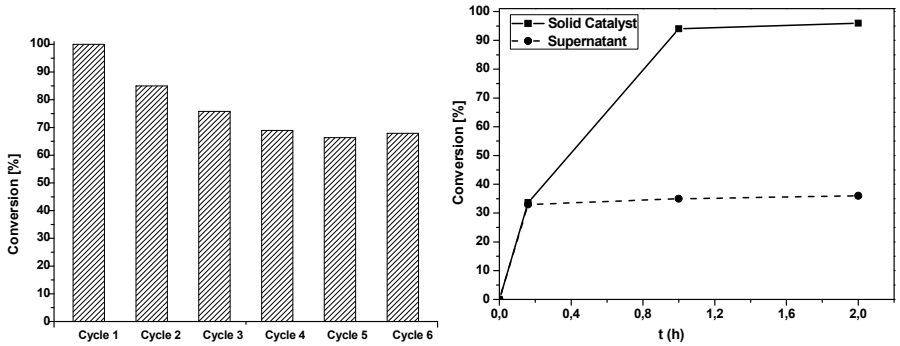

(a) (b)

Figure 2.21. Recycling experiment (a) and hot filtration (b).

From the point of view of their reusability, the results presented in figure 2.21 indicate a decrease in activity during the first four cycles, which remains stable or decays much more slowly after the forth cycle. The used catalyst was also studied by FTIR spectroscopy, and the presence of new bands related to amino groups indicates that some of the reaction products can remain adsorbed on the catalyst probably affecting to the lost of activity observed, especially in the initial cycles.

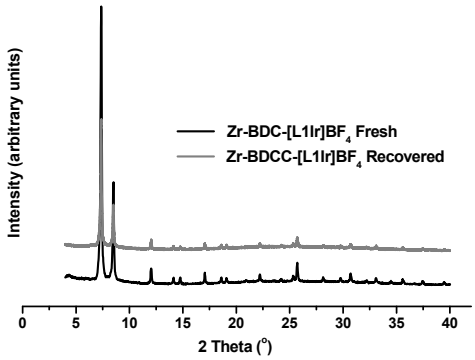

Figure 2.22. Powder X-ray diffraction.

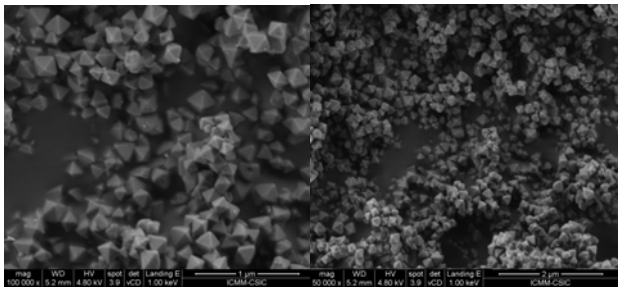

a) **b)**

Figure 2.23. SEM images for a) Fresh Zr-BDC-NH_2-[L1Ir]BF_4 and b) Zr-BDC-NH_2-[L1Ir]BF_4 recovered from the reaction.

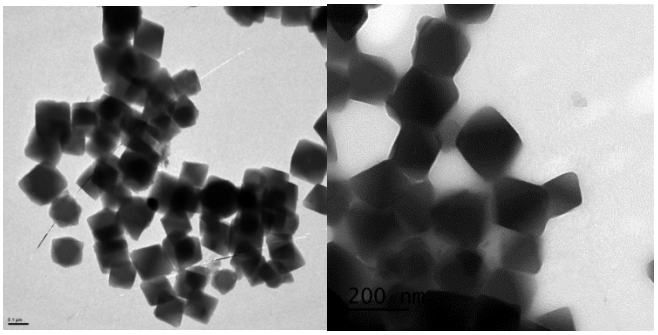

a) **b)**

Figure 2.24. TEM images for a) Fresh Zr-BDC-NH_2-[L1Ir]BF_4 and b) Recovered Zr-BDC-NH_2-[L1Ir]BF_4.

In summary, the direct *N*-alkylation of amines with alcohols was performed with a multifunctional heterogeneous catalyst based on a Ir-Zr-MOF. This system has demonstrated to be efficient and environmentally benign for the synthesis of various organic amines in air and in the absence of a base. Moreover, the catalyst was recovered and reused without significant loss of activity, and only water was produced as a byproduct.

2.3.2.3. Iridium MOF catalyst for reductive amination of aldehydes: comparison with homogeneous catalysts

Compounds containing a nitro group are of interest as building blocks for agrochemicals, dyes, pharmaceuticals, and ligands.[150] In particular, nitroarenes are one of the most readily available starting materials in organic synthesis since they can be produced from a wide range of aromatic starting materials.[151] One example is the hydrogenation of nitroarenes into anilines and further transformation by alkylation, reductive alkylation, hydroamination, etc. to obtain their derivatives including heterocyclic compounds.[152]

Development of catalysts that allow performing one-pot multistep reactions is of interest since it avoids intermediate separation and purification steps with the corresponding benefits in energy saving and minimization of waste. In this sense, the reductive amination reaction is one important transformation that allows the direct conversion of carbonyl compounds into amines using simple operations.[153] The reaction offers compelling advantages over other amine

[150] J. K. Landquist, in *Comprehensive Heterocyclic Chemistry*, Vol.; Ed.Rees), Pergamon, Oxford, **1984**, pp. 143-183; W. M. Horspool, in *PATAI'S Chemistry of Functional Groups*, Vol., John Wiley & Sons, Ltd **2009**; M. North *Angew. Chem. Int. Ed.* **2005**, *44*, 2053-2055.

[151] N. Ono, in *The Nitro Group in Organic Synthesis*, Vol., John Wiley & Sons, Inc. **2002**, pp. 3-29.

[152] R. S. Downing, P. J. Kunkeler and H. van Bekkum *Catal. Today* **1997**, *37*, 121-136; H.-U. Blaser, C. Malan, B. Pugin, F. Spindler, H. Steiner and M. Studer *Adv. Synth. Catal.* **2003**, *345*, 103-151; A. Corma, P. Serna, P. Concepción and J. J. Calvino *J. Am. Chem. Soc.* **2008**, *130*, 8748-8753; P. M. Reis and B. Royo *Tetrahedron Lett.* **2009**, *50*, 949-952.

[153] B. Sreedhar, P. S. Reddy and D. K. Devi *J. Org. Chem.* **2009**, *74*, 8806-8809; R. P. Tripathi, S. S. Verma, J. Pandey and V. K. Tiwari *Curr. Org. Chem.* **2008**, *12*, 1093-1115; B. M. Trost and I. Fleming *Comprehensive Organic Synthesis: Reduction*, Vol. 8; Elsevier

syntheses including: shortness, wide commercial availability of substrates, mild reaction conditions, and no need to isolate the imine intermediate. The resulting secondary amines and their derivatives are highly versatile building blocks for various organic substrates and are extremely important pharmacophores in numerous biologically active compounds owing to their interesting physiological activities.[154] Several reagents for reductive amination have been recently reported.[155] Although the reductive alkylation of amines with aldehydes is a common process, only few papers describe the reaction under hydrogenation conditions. For example, a Pd/C[156] catalyst has been reported to be active although the substrate scope is limited to aliphatic aldehydes. Imine formation from aldehydes and nitroarenes has been reported

---

Science & Technology Books, **1991**; E. W. Baxter and A. B. Reitz, in *Org. React.*, Vol. 59, John Wiley & Sons, Inc. **2004**, p. 1.

[154] B. Merla and N. Risch *Synthesis* **2002**, *2002*, 1365-1372; E. M. Gordon, R. W. Barrett, W. J. Dower, S. P. A. Fodor and M. A. Gallop *J. Med. Chem.* **1994**, *37*, 1385-1401.

[155] V. A. Tarasevich and N. G. Kozlov *Russ. Chem. Rev.* **1999**, *68*, 55-72; I. V. Mićović, M. D. Ivanović, D. M. Piatak and V. D. Bojić *Synthesis* **1991**, *1991*, 1043-1045; B.-C. Chen, J. E. Sundeen, P. Guo, M. S. Bednarz and R. Zhao *Tetrahedron Lett.* **2001**, *42*, 1245-1246; T. Suwa, E. Sugiyama, I. Shibata and A. Baba *Synthesis* **2000**, *2000*, 789-800; O.-Y. Lee, K.-L. Law, C.-Y. Ho and D. Yang *J. Org. Chem.* **2008**, *73*, 8829-8837; D. Imao, S. Fujihara, T. Yamamoto, T. Ohta and Y. Ito *Tetrahedron* **2005**, *61*, 6988-6992; V. I. Tararov, R. Kadyrov, T. H. Riermeier and A. Borner *Chem. Commun.* **2000**, 1867-1868; C. F. Lane *Synthesis* **1975**, *1975*, 135-146; A. F. Abdel-Magid, K. G. Carson, B. D. Harris, C. A. Maryanoff and R. D. Shah *J. Org. Chem.* **1996**, *61*, 3849-3862; M. D. Bomann, I. C. Guch and M. DiMare *J. Org. Chem.* **1995**, *60*, 5995-5996; S. Bhattacharyya, K. A. Neidigh, M. A. Avery and J. S. Williamson *Synlett* **1999**, *1999*, 1781-1783; B. C. Ranu, A. Majee and A. Sarkar *J. Org. Chem.* **1998**, *63*, 370-373; S. Bhattacharyya, K. A. Neidigh, M. A. Avery and J. S. Williamson *Synlett* **1999**, *1999*, 1781-1783; I. Saxena, R. Borah and J. C. Sarma *J. Chem. Soc., Perkin Trans. 1* **2000**, 503-504.

[156] M. O. Sydnes and M. Isobe *Tetrahedron Lett.* **2008**, *49*, 1199-1202; M. O. Sydnes, M. Kuse and M. Isobe *Tetrahedron* **2008**, *64*, 6406-6414; Y.-L. Jiang, Y.-Q. Hu, S.-Q. Feng, J.-S. Wu, Z.-W. Wu, Y.-C. Yuan, J.-M. Liu, Q.-S. Hao and D.-P. Li *Synth. Commun.* **1996**, *26*, 161-164; X. Zhou, Z. Wu, L. Lin, G. Wang and J. Li *Dyes Pigm.* **1998**, *36*, 365-371; Y. J. Jung, J. W. Bae, E. S. Park, Y. M. Chang and C. M. Yoon *Tetrahedron* **2003**, *59*, 10331-10338; J. W. Bae, Y. J. Cho, S. H. Lee, C.-O. M. Yoon and C. M. Yoon *Chem. Commun.* **2000**, 1857-1858; H. Sajiki, T. Ikawa and K. Hirota *Org. Lett.* **2004**, *6*, 4977-4980; H. Sajiki, T. Ikawa and K. Hirota *Org. Process Res. Dev.* **2005**, *9*, 219-220; R. Nacario, S. Kotakonda, D. M. D. Fouchard, L. M. V. Tillekeratne and R. A. Hudson *Org. Lett.* **2005**, *7*, 471-474; D. M. D. Fouchard, L. M. V. Tillekeratne and R. A. Hudson *Synthesis* **2005**, *2005*, 17-18; C. R. Reddy, K. Vijeender, P. B. Bhusan, P. P. Madhavi and S. Chandrasekhar *Tetrahedron Lett.* **2007**, *48*, 2765-2768; S. Chandrasekhar, C. Narsihmulu and V. Jagadeshwar *Synlett* **2002**, *2002*, 0771-0772.

with Au/TiO_2 catalysts[157] or Au/Fe_2O_3,[158] as well. More recently, it has been reported palladium nanoparticles supported on gum acacia[154a] and a polymer-supported palladium catalyst[159] promote reductive *N*-alkylation of nitroarenes using molecular hydrogen as reductant and methanol as solvent. In the present work, we report the application of Zr-BDC-NH_2-[L1Ir]BF_4 catalyst for the atom economic synthesis of mono *N*-alkylamines through reductive amination of aldehydes with nitroarenes in the presence of hydrogen. The process firstly involves a chemoselective reduction with hydrogen of the nitro compound to the corresponding amine in the presence of the carbonyl substrate on the iridium site. Then, in a consecutive step, the condensation between the aromatic amine and the carbonyl group would occur on the acid sites of the catalyst (MOF) (Scheme 2.9). Finally, the hydrogenation of the resulting imine with the Ir-complexes gives the secondary amine.

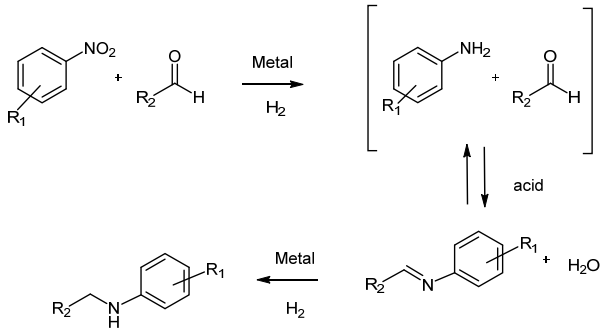

Scheme 2.9. One-pot synthesis of secondary amines by using [Ir]-catalysts.

Catalytic evaluation of both Ir-MOF-based catalysts was performed by mixing them with the nitroarenes and carbonyl compounds in isopropanol in a batch reactor. A series of initial experiments using benzaldehyde and nitrobenzene as model reactants allowed us to establish the adequate reaction conditions for obtaining secondary amines in high yields within a reasonable reaction time. After that, the reaction was extended to different aldehydes and

[157] L. L. Santos, P. Serna and A. Corma *Chem. Eur. J.* **2009**, *15*, 8196-8203; M. J. Climent, A. Corma, S. Iborra and L. L. Santos *Chem. Eur. J.* **2009**, *15*, 8834-8841.
[158] Y. Yamane, X. Liu, A. Hamasaki, T. Ishida, M. Haruta, T. Yokoyama and M. Tokunaga *Org. Lett.* **2009**, *11*, 5162-5165.
[159] M. M. Dell'Anna, P. Mastrorilli, A. Rizzuti and C. Leonelli *Appl. Catal., A* **2011**, *401*, 134-140.

nitroarenes. Under optimized reaction conditions, the scope of the reaction was explored with structurally and electronically diverse aldehydes and different nitroarenes. As shown in Table 2.5, various aldehydes were reductively aminated with nitrobenzene under 6 bar pressure of molecular hydrogen. The aldehydes used for this study included aromatic and aliphatic aldehydes. Irrespective of the electronic nature of the substituent, aromatic aldehydes react well to give the corresponding products in good yields (Table 2.5, entries 1-6). Furthermore, aliphatic aldehydes underwent the reductive amination rapidly and gave the products in excellent yield without formation of byproducts (Table 2.5, entries 7-9).

Table 2.5. MOF-[LIr]-catalyzed one-pot reductive amination of aldehydes with nitrobenzene under H_2 atmosphere in isopropanol[a].

entry	Catalyst	R	R'	Conv. (%)[b]	Sel. (%) Amine (B)
1	[L1Ir]	Ph	H	100	66
2	IRMOF-3-[L1Ir]	Ph	H	98	99
3	Zr-BDC-NH_2-[L1Ir]BF_4	Ph	H	99	99
4	Zr-BDC-NH_2-[L1Ir]BF_4	Ph	4-I	90	70 (98, 48h)
5	Zr-BDC-NH_2-[L1Ir]BF_4	Ph	4-Br	80 (95, 48h)	65 (97, 48h)
6	Zr-BDC-NH_2-[L1Ir]BF_4	OMePh	H	99	99
7	Zr-BDC-NH_2-[L1Ir]BF_4	C_6H_{13}	H	99	99
8	Zr-BDC-NH_2-[L1Ir]BF_4	C_6H_{13}	4-I	98	100
9	Zr-BDC-NH_2-[L1Ir]BF_4	C_6H_{13}	*o*-OCH_3	100	99

[a]Reaction conditions: nitrobenzene (1.0 mmol), aldehyde (1.5 mmol), [Ir] (1 mol %), isopropanol (1 mL), PH_2: 6 bar, T: 100 °C, time: 24 h. [b]Referred to nitrobenzene.

To study whether the reaction using solid [Ir]-MOF catalysts occurred on the solid or was catalyzed by Ir species potentially leached in the liquid phase, two separate experiments were conducted with benzaldehyde and nitrobenzene. In the first experiment, the reaction catalyzed by Zr-BDC-NH_2-[L1Ir]BF_4 was finished after 7 h, and the conversion of nitrobenzene was found to be 20%. At this point, the catalyst was separated from the reaction mixture and the reaction was continued with the filtrate for an additional 24 h. period. In the second experiment, the reaction was terminated after 7 h at 20% conversion and the catalyst was removed. The reaction was then continued with the filtrate for additional 17 h. In both cases, the conversion within the filtrates remained almost unchanged. Ir was not detected in the filtrate in either experiment by Inductively Coupled Plasma Atomic Emission Spectroscopy (ICP-

AES). These studies demonstrate that the Ir bound to the support during the reaction is active and the reaction proceeds on the solid.

As can be seen from the results in Table 2.6, Zr-BDC-NH_2-[L1Ir]BF_4 can be recovered by simple filtration in air and reused without significant loss of catalytic activity, at least after 4 cycles, whereas IRMOF-3-[L1Ir] and soluble complexes could be used only once, since they were completely deteriorated at the end of the first catalytic run.

Table 2.6. Recycling experiments with MOF-based-$[LIr]^+$ catalysts.

cycle	catalyst	t (h)	Conv. (%)	Sel. (%) Amine (B)	cycle
1	Zr-BDC-NH_2-[L1Ir]BF_4	24	99	99	1
2		24	99	99	2
3		24	99	99	3
4		24	99	99	4
1	IRMOF-3-[L1Ir]	24	98	99	1
2		24	-	-	2

Cat. 1 mol% based on Ir, T: 100 °C, PH_2: 6 bar.

Hot filtration tests for Zr-BDC-NH_2-[L1Ir]BF_4 proved that the catalytic activity was exclusively associated to the solid, and no reaction occurred when the catalyst was removed from the reaction media. The overall structure of the material remained intact after the catalytic experiments (figure 2.25) and we can concluding that the catalyst is stable under the selected reaction conditions.

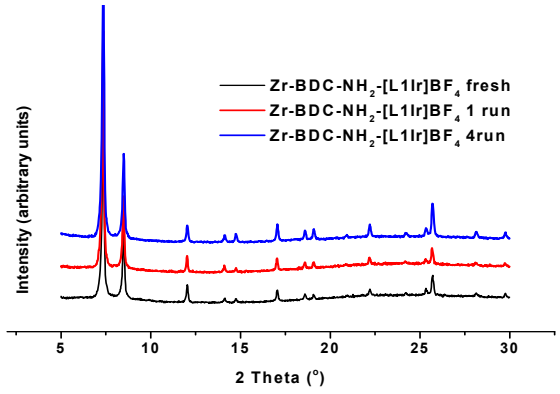

Figure 2.25. PXRD of Zr-BDC-[LIr]BF_4 after four runs.

SEM images of the fresh and the recovered materials also show that the morphology was maintained after the reaction (Fig. 2.26).

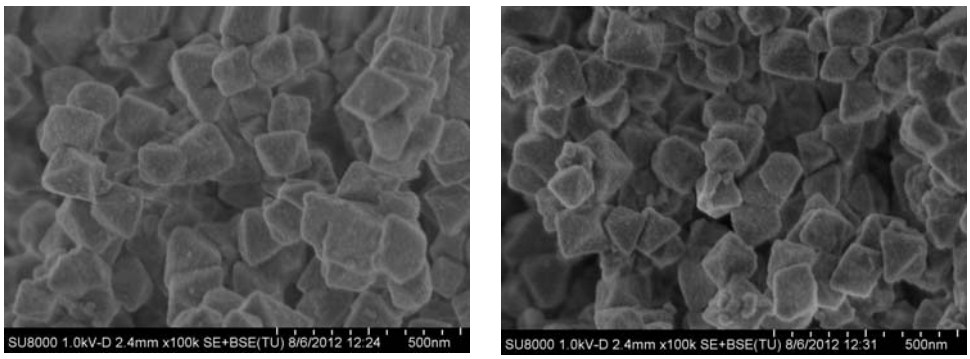

Figure 2.26. SEM images of Zr-BDC-NH_2-[L1Ir]BF_4 fresh (a) and Zr-BDC-NH_2-[L1Ir]BF_4 recycled (b).

Figure 2.27 shows representative TEM images conducted to analyze whether particles are formed during the catalytic experiments, observing no evidence for the formation of nanoparticles. Nevertheless, it should be considered that the content of Ir in the sample is very low.

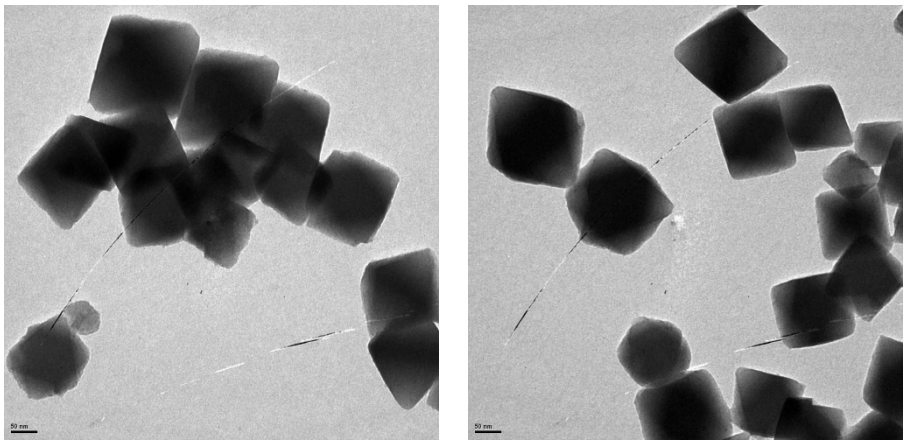

Figure 2.27. TEM images of Zr-BDC-NH_2-[L1Ir]BF_4: (a) fresh and (b) recovered after reaction.

2.3.2.4. Zr base catalyzed condensation with Rh-catalyzed hydrogenation

To examine the catalytic ability of (NNN)-M-Zr-MOF materials, several reactions have been performed: 1) Knoevenagel-type condensation for base properties, 2) cascade condensation-olefin-nitro hydrogenation reactions for the ability to operate as a multifunctional system, and 3) one-pot cascade reaction.

a) Base catalytic properties

Several studies on the use of MOFs as solid catalysts (with acid[75,81b,160] and base[80a,161] properties) for condensation reactions[162] have been reported. In the perfectly crystalline Zr-BDC-type MOF with the $[Zr_6O_4(OH_4)]^{12+}$ cluster and twelve bidentate linkers, Zr has a maximum coordination number of 8,[50] which, after dihydroxylation, has a coordination number of 7 that makes the Zr act as a Lewis acid on different reactions.[163] Of these reactions, cross-aldol condensations have been catalyzed by Zr-BDC-type MOFs.[164]

Ethyl nitroacetate was an ideal methylene compound used to obtain α-nitrocinnamates and acrylates, which are versatile building blocks in organic synthesis owing to their reactivity as good Michael acceptors and owing to the possibility of converting either the nitro or the ester group into other

[160] C.-D. Wu, A. Hu, L. Zhang and W. Lin *J. Am. Chem. Soc.* **2005**, *127*, 8940-8941; B. Gómez-Lor, E. Gutiérrez-Puebla, M. Iglesias, M. A. Monge, C. Ruiz-Valero and N. Snejko *Chem. Mater.* **2005**, *17*, 2568-2573; T. Sato, W. Mori, C. N. Kato, E. Yanaoka, T. Kuribayashi, R. Ohtera and Y. Shiraishi *J. Catal.* **2005**, *232*, 186-198; B. Chen, N. W. Ockwig, A. R. Millward, D. S. Contreras and O. M. Yaghi *Angew. Chem. Int. Ed.* **2005**, *44*, 4745-4749; A. Vimont, J.-M. Goupil, J.-C. Lavalley, M. Daturi, S. Surblé, C. Serre, F. Millange, G. Férey and N. Audebrand *J. Am. Chem. Soc.* **2006**, *128*, 3218-3227.

[161] J. S. Seo, D. Whang, H. Lee, S. I. Jun, J. Oh, Y. J. Jeon and K. Kim *Nature* **2000**, *404*, 982-986; T. Uemura, R. Kitaura, Y. Ohta, M. Nagaoka and S. Kitagawa *Angew. Chem. Int. Ed.* **2006**, *45*, 4112-4116; D. M. Shin, I. S. Lee and Y. K. Chung *Cryst. Growth Des.* **2006**, *6*, 1059-1061; Y. K. Hwang, D.-Y. Hong, J.-S. Chang, H. Seo, M. Yoon, J. Kim, S. H. Jhung, C. Serre and G. Férey *Appl. Catal., A* **2009**, *358*, 249-253; D. J. Lun, G. I. N. Waterhouse and S. G. Telfer *J. Am. Chem. Soc.* **2011**, *133*, 5806-5809.

[162] A. Dhakshinamoorthy, M. Opanasenko, J. Čejka and H. Garcia *Adv. Synth. Catal.* **2013**, *355*, 247-268.

[163] P. Valvekens, F. Vermoortele and D. De Vos *Catal. Sci. Technol.* **2013**, *3*, 1435-1445.

[164] F. Vermoortele, M. Vandichel, B. Van de Voorde, R. Ameloot, M. Waroquier, V. Van Speybroeck and D. E. De Vos *Angew. Chem. Int. Ed.* **2012**, *51*, 4887-4890.

functional groups.[165] The synthesis of functionalized α-nitroalkenes often required multistep synthesis, even in presence of toxic and expensive reagents ($TiCl_4$).[166a,166] The preparation of nitroalkenes using $ZrCl_4$ (which is a stronger Lewis acid, cheaper, and environmentally friendly than the previously used $TiCl_4$) as a catalyst and Et_3N as a base has been reported.[167] Taking this work into consideration, and given that the Zr-BDC-NH_2 MOF has Zr^{IV} Lewis acid in the structure and the ligand (BDC-NH_2) has amino groups or their derivatives, we believed that these bifunctional systems could act as catalysts for the synthesis of α-nitrocinnamates. Thus, we report the use of the efficient Zr-BDC-NH_2 MOF derivatives as catalysts for the condensation reaction between aldehydes and malononitrile and ethyl cyanoacetate catalyzed by basic sites, and we have obtain 100% conversion of adduct after 6 h (Table 2.7, entries 8, 9, 16-18). We have also performed the one-pot synthesis of α-nitrocinnamates with Zr-BDC-NH_2 (catalysts with basic and Lewis acid sites). The results are reported in Table 2.7.

[165] W. Lehnert *Tetrahedron* **1972**, *28*, 663-666; M. T. Shipchandler *Synthesis* **1979**, *1979*, 666-686; B. Shen and J. N. Johnston *Org. Lett.* **2008**, *10*, 4397-4400.
[166] R. S. Fornicola, E. Oblinger and J. Montgomery *J. Org. Chem.* **1998**, *63*, 3528-3529; J. P. G. Versleijen, A. M. van Leusen and B. L. Feringa *Tetrahedron Lett.* **1999**, *40*, 5803-5806.
[167] S. Fioravanti, L. Pellacani and M. C. Vergari *Org. Biomol. Chem.* **2012**, *10*, 524-528.

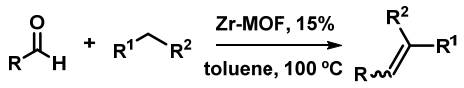

Table 2.7. Zr-BDC(BPDC)-catalyzed Knoevenagel-type condensation [a].

entry	Catalyst	R	R_1, R_2	Yield (%)	E/Z ratio[d]
1	IRMOF-3	Ph	NO_2, COOEt	25	50:50
2	Zr-BDC-NH_2	Ph	NO_2, COOEt	90	50:50
3	Zr-BPDC-NH_2	Ph	NO_2, COOEt	100	40:60
4	Zr-BPDC-NH_2	4-FPh	NO_2, COOEt	100	50:50
5	Zr-BPDC-NH_2	4-NO_2Ph	NO_2, COOEt	50	50:50
6	Zr-BPDC-NH_2	4-OMePh	NO_2, COOEt	60	40:60
7	Zr-BPDC-NH_2	C_6H_{13}	NO_2, COOEt	65	50:50
8	Zr-BPDC-NH_2	Ph	CN, CN	100	-
9	Zr-BPDC-NH_2	Ph	CN, COOEt	100	20:80
10	Zr-BDC-NH_2L2	Ph	NO_2, COOEt	100	40:60
11	Zr-BDC-NH_2L3	Ph	NO_2, COOEt	100	40:60
12	Zr-BDC-NH_2L3	4-FPh	NO_2, COOEt	100	30:70
13	Zr-BDC-NH_2L3	4-OMePh	NO_2, COOEt	20	40:60
14	Zr-BDC-NH_2L3	2,4,6-OMePh	NO_2, COOEt	10	40:60
15	Zr-BDC-NH_2L3	C_6H_{13}	NO_2, COOEt	100	50:50
16	Zr-BDC-NH_2L2	Ph	CN, CN	100[b]	-
17	Zr-BDC-NH_2L2	Ph	CN, COOEt	100[b]	100
18	Zr-BDC-NH_2L3	Ph	CN, COOEt	85[c]	100
19	Zr-BDC-NH_2-[L3Ir]BF_4	Ph	NO_2, COOEt	30	50:50
20	Zr-BDC-NH2-[L3Rh] BF_4	Ph	NO_2, COOEt	100	50:50

[a] All reactions were performed with the substrates impregnated in toluene using 15 weight % (5 mol%, based on Zr) for 24 h, T: 100 ºC. [b] 6 h. [c] 4h. [d] Determined by ^{1}H NMR analysis.

The activity of the Zr-BDC-NH_2 catalyst for the condensation reactions was then compared with that of Zr-BPDC-NH_2, and post functionalized Zr-BDC-NH_2-L2/Zr-BPDC-NH_2-L2 or Zr-BDC-NH_2-L3/Zr-BPDC-NH_2-L3. Notably, a higher reaction rate was achieved for the pincer-functionalized Zr-MOFs. As shown in Table 2.7, the expected α-nitrocinnamates and acrylates were obtained as E/Z

mixtures in good to excellent yields and the Z isomer was always the major isomer. It is known that for the reaction catalyzed by $ZrCl_4/Et_3N$,[168] 4 mmol of $ZrCl_4$ per 2 mmol of benzaldehyde are necessary, whereas in our case, a much lower amount of Zr was used because the reaction was performed with 5-15 weight% of Zr-MOF (2-5 mmol% based on Zr).

We then decided to investigate the scope and limitations of the reaction of a range of aldehydes, and active methylene compounds with our new catalysts in toluene (Table 2.7). As shown in the table, ethyl cyanoacetate or malononitrile and benzaldehyde furnished the product in high yields and lower reaction time compared with ethyl nitroacetate. Aromatic aldehydes provided the expected products in good yields, but were not affected by electronic factors. In addition, the reaction with aliphatic aldehydes such as n-heptanal gave the expected product in good yields.

The heterogeneity and recyclability of Zr-BDC-NH_2-L2 in the condensation of benzaldehyde and ethyl nitroacetate were examined. After stirring the reaction mixture for 3 h in the presence of catalyst, Zr-BDC-NH_2-L2 was removed through filtration. After the removal of Zr-BDC-NH_2-L2, the reaction did not proceed, which revealed the catalytic activity of (NNN)-Zr-MOF derivatives. The catalyst demonstrated good recyclability, is easily isolated from the reaction suspension through filtration, and can be reused without loss of activity for at least three cycles and gave yields of approximately 90% (see data in annexes).

Analysis of the PXRD results of the reused catalyst revealed that Zr-BDC-NH_2-L2 and Zr-BDC-NH_2-L3 could maintain their crystallinity during the reaction, which indicates the high stability of (NNN)-Zr-BDC derivatives (figure 2.28a). The Zr-BPDC catalysts were also recycled and activity was maintained (see data in annexes), even though crystallinity was lost significantly. Thus, Zr-BDC-NH_2-L3 seems to be a suitable catalyst compared to Zr-BPDC-NH_2-L3 on the basis of the stability issue (Figure 2.28b).

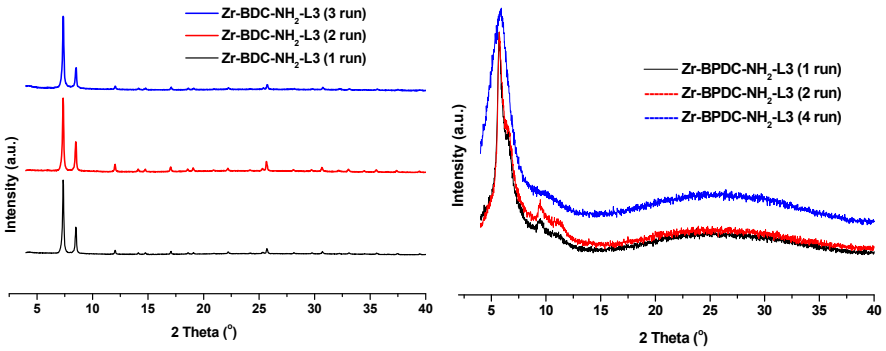

Figure 2.28. PXRD of (a) Zr-BDC-NH_2-L3 after recycling; (b) Zr-BPDC-NH_2-L3 after recycling.

Zr-BDC-NH_2 derivatives as catalysts for cascade olefination/hydrogenation reactions of aldehydes

Organic-chemical synthesis performed through one-pot, tandem, domino or cascade reactions[126] has become a significant area of research in organic chemistry[125b,127a-d] because such processes improve atom and process economies. The success of multistep sequential or multicomponent one-pot transformations requires a balance of equilibrium and a suitable sequence of reversible and irreversible steps.[168]

The development of catalysts for one-pot multistep reactions is important, as chemists aim at minimizing the use of reagents and solvents as well as reducing intermediate separation and purification steps.[4a,4b,127e,127f,169] An example of a multistep sequential process using differentiated bifunctional acid-metal catalysts was the cyclization of citronellal followed by hydrogenation to yield menthol in an one-pot synthesis[170] or the acetal hydrolysis followed by condensation and subsequent hydrogenation.[171] As mentioned above, α-nitrocinnamates and acrylates are versatile building

[168] I. Ugi *J. Prakt. Chem.* **1997**, *339*, 499-516.
[169] U. Diaz, D. Brunel and A. Corma *Chem. Soc. Rev.* **2013**, *42*, 4083-4097.
[170] F. Iosif, S. Coman, V. Parvulescu, P. Grange, S. Delsarte, D. D. Vos and P. Jacobs *Chem. Commun.* **2004**, 1292-1293; F. Neaţu, S. Coman, V. I. Pârvulescu, G. Poncelet, D. Vos and P. Jacobs *Top. Catal.* **2009**, *52*, 1292-1300; P. Mertens, F. Verpoort, A.-N. Parvulescu and D. De Vos *J. Catal.* **2006**, *243*, 7-13.
[171] N. T. S. Phan, C. S. Gill, J. V. Nguyen, Z. J. Zhang and C. W. Jones *Angew. Chem. Int. Ed.* **2006**, *45*, 2209-2212.

blocks in organic synthesis due to the possibility of converting either the nitro or the ester group into other functional groups. To examine the catalytic ability of Zr-BPDC-NH_2 derivatives as multifunctional catalysts, we chose as a model the reaction between an aldehyde and ethyl nitroacetate that yields product A (ethyl 2-nitro-3-phenylacrylate), which, in the presence of hydrogen, gives product B (ethyl 2-nitro-3-phenylpropanoate) and/or C (ethyl 2-amino-3-phenylpropanoate) the metal-catalyzed reaction (scheme 2.10). We have obtained the final products B and C by using either a two-step reaction or a one-pot reaction.

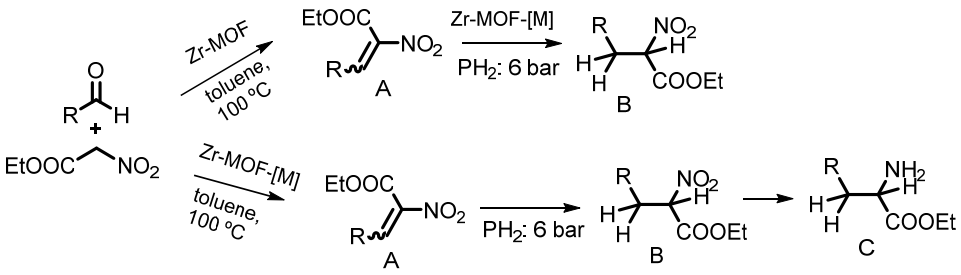

Scheme 2.10. M-Zr-MOF-catalyzed cascade condensation-olefin-nitro hydrogenation reaction. R = Ar; M = Rh, Ir.

To obtain these products, in the first case, Zr-BPDC-NH_2-L-catalyst was suspended in toluene, and benzaldehyde and ethyl nitroacetate were added. The condensation product of these reactants, product A, formed, and the aldehyde was completely consumed within 24 h (Table 2.8). The product was isolated by simple filtration, added to a suspension of Zr-BPDC-NH_2-[L3Rh] in toluene; the reaction mixture was then transferred to an autoclave (heated to 80 °C under 6 bar hydrogen for 10 h; 1 bar = 0.1 MPa), which yielded the corresponding benzyl amine (product C in scheme 2.10; Table 2.8, entry 1) as the sole product. If the reaction was performed in the presence of Zr-BDC-NH_2-L3 + Zr-BDC-NH_2-[L3Rh]BF_4, then only product B was formed (without the isolation of the corresponding acrylate) in high yield (table 2.8, entries 8, 9).

Table 2.8. MOF-[L3M]-catalyzed cascade reaction between aldehydes and ethyl nitroacetate (olefination)[a]-alkene hydrogenation-nitro hydrogenation reactions.[b]

Catalyst	Reaction mode	R	Conv. (%)[c]	t (h)	Catalyst	Sel. (%)	
						B	C
1	Zr-BPDC-NH_2 + Zr-BPDC-NH_2-[L3Rh]BF_4	Two step[d]	Ph	100	48	5	95
2	Zr-BPDC-NH_2-[L3Rh]BF_4	One-pot[e]	Ph	100	30	100	-
3					48	40	60
4					72	10	90
5	Zr-BPDC-NH_2-[L3Rh]BF_4	One-pot[f]	Ph	100	44	97	3
6					72	20	80
7	Zr-BPDC-NH_2-[L3Rh]BF_4 + DIOP	One-pot[e]	Ph	100	48	60	40
8	Zr-BDC-NH_2-L3 + Zr-BDC-NH_2-[L3Rh]BF_4	Two step[d]	Ph	100	48	95	5
9	Zr-BDC-NH_2-[L3Rh]BF_4	One-pot[e]	Ph	100	34	100	-
10	Zr-BDC-NH_2-[L3Rh]BF_4	One-pot[e]	4Me-Ph	100	48	100	-
11	Zr-BDC-NH_2-[L3Rh]BF_4	One-pot[e]	4F-Ph	100	44	98	-

[a] T: 110 °C, solvent: toluene, 1mL; [b] all reactions were performed in toluene using 1 mol % catalyst (based on rhodium); [c] Determined by GC and ^{1}H NMR, based on ethyl nitroacetate. [d] Two steps: glass reactor + autoclave Engineers; [e] one-pot reaction: glass reactor with manometer; [f]Autoclave Engineers, dec.

We found that the one-pot reaction of benzaldehyde and ethyl nitroacetate in the presence of a catalytic amount of Zr-BPDC-NH_2-[L3Rh]BF_4 derivative in toluene at 100 °C yielded product A, with 100% conversion after 24 h. Then, hydrogen (5 bar) was incorporated to the reaction media and the hydrogenation of the resulting double bond was completed after 6 h. If desired, the process can proceed, and finally, the reduction of NO_2 occurs, which yields the corresponding benzyl amino derivative (Scheme 2.10, Table 2.8, entries 4, 6). Next, the Zr-BDC-NH_2-[L3Rh]BF_4-catalyzed reaction can selectively lead to the reduction of the double bond, which yields the corresponding ethyl 2-nitro-3-phenylpropanoate or 2-nitro-3-(p-tolyl)-propanoate if the substrate is 4-methylbenzaldehyde (Table 2.8, entries 9-11). The same reaction catalyzed by Zr-BDC-NH_2-[LIr] gave only 30 % yield (product

selectivity = 50%) and the Ir catalyst decomposes under reaction conditions (Table 2.8, entry 12).

Notably, the reaction of benzaldehyde and ethyl nitroacetate in the presence of Zr-BDC-NH_2-[L3Rh]BF_4 with 0.11 mol% of catalyst (containing Rh) gives selectively the corresponding hydrogenated product in 97% yield after 44 h (total condensation-alkene hydrogenation reactions). If the reaction continues, the hydrogenation of the nitro group can be achieved after an additional 24 hours.

To study the effect of the chiral amino group for asymmetric induction in cascade reactions, we measured the optical rotation of product C obtained through the cascade reaction but we have not seen enantioselectivity in this reaction, even in the presence of a chiral diphosphine as DIOP [DIOP = 2,3-(isopropylidenedioxy)-2,3-dihydroxy-1,4-bis(diphenylphosphanyl)butane)]
(Table 2.8, entry 7).

Control experiments confirmed that intact Zr-BDC-NH_2-[L3Rh]BF_4 catalyst was responsible for the observed catalytic activity, because once the solid catalyst is removed through filtration at low conversion the reaction stopped (hot filtration experiment; annexes). Moreover, no evidence was found for the dissolution of the catalyst. To test the recyclability of the Zr-BDC-NH_2-[L3Rh]BF_4 catalyst, this was subject to four cycles for the one-pot reaction (Table x in annexes). The reaction was driven to completion in each cycle. The decreased activity of the catalyst was evident from an increase in the required time for the reaction completion, which was correlated with a slight loss of long-range crystallinity (Figure 2.29a). The recyclability of the Zr-BPDC catalysts was also studied, and it has been found that the stability of these catalysts is much lower than that of the Zr-BDC-NH_2-[L3Rh]BF_4 catalyst. The crystallinity of Zr-BPDC-NH_2-[LRh]BF_4 decreased significantly after five recycles (Figure 2.29b).

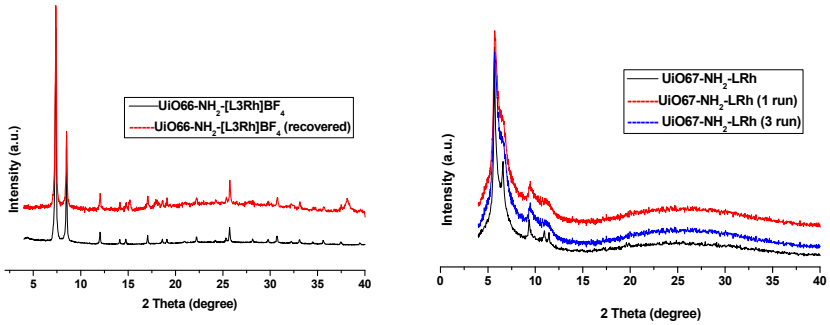

Figure 2.29. a). PXRD patterns of Zr-BDC-NH_2-[L3Rh] before and after recycling. b). PXRD of Zr-BPDC-NH_2-[L3Rh] before and after recycling.

2.4. Conclusions

- Multifunctional catalysts based on Zr-based metal organic frameworks containing guest-accesible NNN-pincer groups have been prepared.

- These catalysts can act as a bifunctional acid and base catalyst with the Zr (Lewis) and amine and amide groups located in the linkers, and by incorporating a transition metal trough coordination with the guest-accessible NNN-pincer group.

Part A

- The use of the iridium pincer complex active phase and Zr-MOF as a support has allowed us to obtain a new catalyst for the direct hydrogenation of aromatic compounds at low temperatures and initial hydrogen pressures. This catalyst is versatile and can be easily recycled with high conversion efficiendy for up to five cycles and represent an attractive choice for green industrial and synthetic applications.

Part B

- The Ir-Zr-based metal-organic framework is a highly efficient catalyst for producing higher amines from amines and alcohols with notable advantages such a broad substrate scope, high atom economy (only water is a byproduct), reusability of the catalyst, environmentally benign, higher yields of the desired products, and a simple workup procedure, which makes it an attractive and useful methodology for organic synthesis.

- A simple and efficient method for the synthesis of N-alkyl amines via reductive amination in the presence of hydrogen using a new readily recoverable hybrid catalyst that combines the catalytic activity of transition metal complexes with the architecture of metal organic frameworks. This protocol can be used to generate a diverse range of N-alkyl amines in good to excellent yields.

- The Rh-Zr meltal organic framework is an efficient catalyst for one-pot cacade condensation-hydrogentation reactions. The simple method for catalyst preparation, its easy recovery, and its reusability is expected to contribute to the use of the catalyst for t he development of benign chemical processes and products.

2.5. Experimental section

2.5.1. Synthesis of NNN pincer ligands

The general scheme for preparation of aldehyde precursors is shown in scheme 2.11.

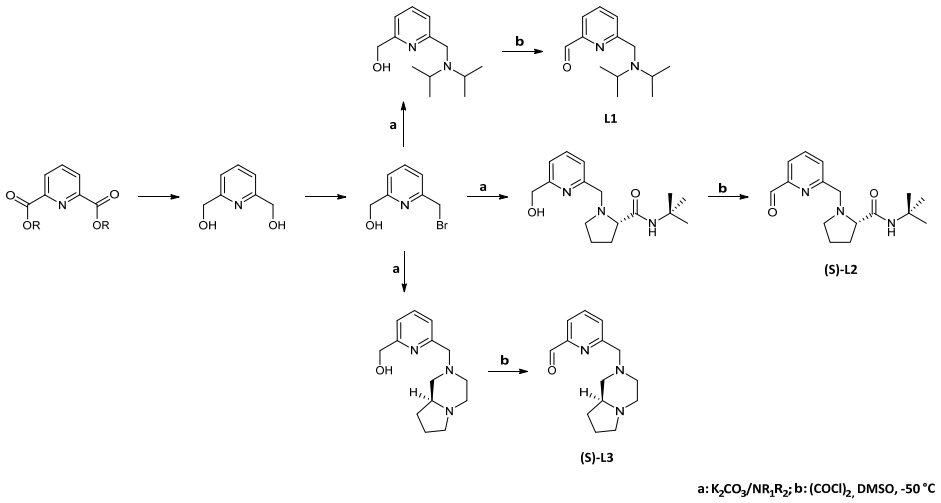

Scheme 2.11. Synthesis of precursors for pincer ligands.

Preparation of 2,6-bis-Hydroxymethylpyridine

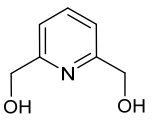

To a cooled solution of dimethyl 2,6-pyridinedicarboxylate (5.86 g, 30 mmol) in ethanol (160 mL) was added sodium borohydride (1,36 g, 36 mmol) in small portions at room temperature with efficient stirring, after 10 minutes, recently powdered calcium chloride (4 g, 36 mmol) was added in small portions and evolution of hydrogen could be detected. The reaction mixture was stirred overnight for total reduction, then the solvent was evaporated under reduced pressure and the residue dissolved into a saturated potassium carbonate solution (80 mL) and stirred at room temperature for 2-4 hours. Then, water was evaporated and the residue dried (40 °C / 1mmHg under P_2O_5). Finally the dry residue was extracted continuously with chloroform (180 mL) for at least 96 hours (at 24 h only 50% had been extracted). The crude product was obtained almost pure

and could be used in the next reaction. Yield: 92%. **m.p.**: 112-114 °C (lit. m.p.: 114-116 °C).

Preparation of 2-bromomethyl-6-hydroxymethylpyridine

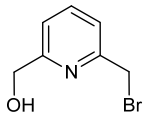

2,6-bis-hydroxymethylpyridine (7.2 g, 51.7 mmol) was heated at reflux with aqueous 48% HBr (80 mL) for 16-24 h until the reaction was completed. The evolution of reaction could be follow by TLC ($CHCl_3$/MeOH, 95:5). The reaction mixture was ice-cooled and neutralized by slow addition of aqueous 40% NaOH and thoroughly extracted with methylene chloride (8 x 30 mL). The organic extracts were dried on anhydrous sodium sulphate and purified by flash chromatography on silica using $CHCl_3$/MeOH 1% to 10% as eluent. Firstly we obtained 3.3 g (43%) of 2,6-dibromethylpyridine following by 4.3 g (57%) of pure 2-bromomethyl-6-hydroxymethylpyridine.

Preparation of (N)-tert-butylprolinamide

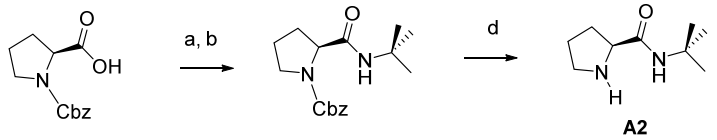

Scheme 2.12. Synthesis of (N)-tert-butylprolinamide.

(S)-N-Carbobenzoxy-tert-butylprolinamide

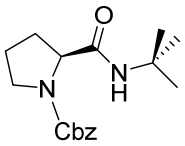

A flask was charged with (3.7 g, 13 mmol) of (S)-1-(benzyloxycarbonyl)pyrrolidine-2-carboxylic acid, 1.51 g (13 mmol) of triethylamine and 60 mL of THF. The resulting mixture was cooled to 0 °C. A solution of (1.64 g, 13 mmol) ethylclhoroformate in THF (30 mL) was added dropwise to the solution. The mixture was stirred for 1-2 h. Then, a solution of (0.95, 13 mmol) tert-butylamine was added dropwise to the mixture, stirred at room temperature for 2 h and filtered through a pad of celite. The reaction mixture was concentrated to dryness under reduced pressure, the residue was dissolved in AcOEt and successively washed with Na_2CO_3 (2M), water, brine and dried with anhydrous MgSO4. After solvent removal via rotary

evaporation to obtain 3.74 g of (S)-N-Carbobenzoxy-tert-butylprolinamide as a white solid. Yield: 82%. **m. p.** 81 °C (from cyclohexane-ethyl acetate).

$[\alpha]^{25}_{D}$= +40.5 (EtOH, 1).

Anal. Found.: C, 66.91; H, 7.80; N, 9.12. **$C_{17}H_{24}N_2O_3$ calc.**: C, 67.10; H, 7.89; N, 9.21 %.

IR (KBr, cm^{-1}): 1660 (s) $\nu_{(C=O)amide}$; 1704 (s) $\nu_{(C=O)Cbz}$; 3340 (m) $\nu_{(NH)}$.

^{1}H NMR (300 MHz, $CDCl_3$, 25 °C, ppm): δ = 7.35 (arom, 5H); 5.20 (CH_2-O, 2H); 3.91 (CH-CONH, 1H); 3.1 (CH_2-N, 2H); 2.2 (CH_2-CH-CONH, 2H); 1.9 (CH_2-CH_2-N, 2H);1.3 (CH_3, 9H).

^{13}C NMR (125 MHz, $CDCl_3$, 25 °C, ppm): δ= 170.78 (CONH); 155.51 (OCO); 136.51 (C1-phenyl); 128.35 (C2, C6-phenyl); 127.92 (C4-phenyl); 127.76 (C3, C5-phenyl); 67.06 (CH_2O); 61.19 (HC-CONH); 50.81 (C-CH_3); 47.09 (CH_2-N); 28.89 (CH_2-CH-CONH); 28.50 (CH_3); 24.0 (CH_2- CH_2N).

(S)-tert-Butylprolinamide

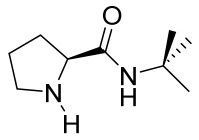

A mixture of (S)-N-carbobenzoxy-tert-butylprolinamide (5 g, 0.016 mol), cyclohexene (2 g, 0.024 mol) and 0.1 g of commercial Pd/C (10%) in 30 mL of ethanol was heated under reflux for 15-30 min in an argon atmosphere, cooled and filtered. The catalyst was washed wih ethanol, and filtrate and washed liquids were evaporated under reduced pressure to give 2.7 g of amide (S)-tert-butylprolinamide as a white crystalline solid. Yield: 98%. **m. p.** 92-93 °C (cyclohexane-toluene).

Anal. Found.: C, 63.78; H, 10.42; N, 16.65. **$C_9H_{18}N_2O$ calc.**: C, 63.90; H, 10.60; N, 16.57 %.

IR (KBr, cm^{-1}): 3340 (m), 3270 (m) $\nu_{(NH)}$ 1660 (s) $\nu_{(C=O)}$.

^{1}H NMR (300 MHz, $CDCl_3$, 25 °C, ppm): δ = 7.7 (NH, NHCO, 2H); 3.84-3.79 (CH-CONH, 1H); 3.3-3.2 (CH_2N, 2H); 2.36-2.02 (CH_2-CH-CONH, 2H); 1.97-1.84 (CH_2-CH_2-NH, 2H); 1.55 (CH_3, 9H).

^{13}C NMR (125 MHz, $CDCl_3$, 25 °C, ppm): δ= 173.79 (CONH); 60.97 (CH-CONH); 49.80 (CH-CH_3); 46.88 (CH_2-NH); 30.41 (CH_2-CHCONH); 28.48 (CH_3); 25.79 (CH_2-CH_2NH).

Preparation of (S)-octahydropyrrolo[1,2-a]-pyrazine

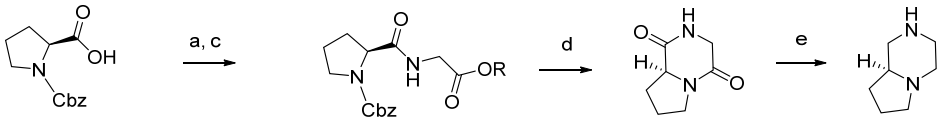

A3

Scheme 2.13. Synthesis of (S)-octahydropyrrolo[1,2-a]-pyrazine.

(S)-N-benzyloxycarbonyl(methoxycarbonylmethyl)prolinamide

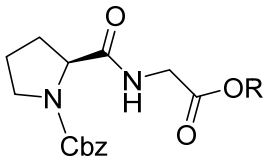

A solution of (S)-1-((benzyloxy)carbonyl)pyrrolidine-2-carboxylic acid (4.99 g, 20 mmol) and N-ethyl-N-isopropylpropan-2-amine (2.84 g, 22 mmol) in CH_2Cl_2 (40 mL) was cooled at -15 °C. Ethyl cloroformate (2.279 g, 21 mmol) in CH_2Cl_2 (5 mL) was added dropwise with vigorous stirring and the pasty reaction mixture stirred for an additional 30 min. A solution of N-ethyl-N-isopropylpropan-2-amine (2.58 g, 20 mmol) and methyl 2-aminoacetate hydrochloride (2.396 g, 19 mmol) CH_2Cl_2 (20 mL) were added. The reaction mixture was stirred 1 h at -15 °C and 12 h at r.t. When the reaction was completed, water (30 mL) was added with vigorous stirring. The phases were separated and the aqueous layer was extracted with AcOEt (3x20 mL). The organic layers were successively washed with $NaHCO_3$ 10%, brine, HCl 5% and brine (30 mL each time) and dried with anhydrous $MgSO_4$. After solvent removal via rotary evaporation not to exceed 35 °C to obtain (S)-N-benzyloxycarbonyl(methoxycarbonylmethyl)prolinamide (6.17 g, 96.3%) suitable for the next reaction. Yield = 92%.

MS (m/z): 320 [M^+]; 289, 204, 185, 160, 91.

^{1}H NMR (300 MHz, $CDCl_3$, 25 °C, ppm): δ = 7.35-7.32 (m, 5HAr); 5.20, 5.13 (AB, 2H, CH_2O J_{HH} = 12.2 Hz); 4.31 (m, 1H, CHCO); 4.02, 3.55 (m, m, 1H, 1H Pyrr); 3.72 (s, 2H, NCH_2CO); 3.74 (s, 2H, -CH_2-Py).

(S)-hexahydropyrrolo[1,2-a]pyrazine-1,4-dione

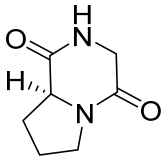

A mixture of (S)-N-benzyloxycarbonyl(methoxycarbonylmethyl)prolinamide (6.14 g, 19.17 mol), cyclohexene (15.74 g, 192 mmol) and 0.041 g of commercial Pd/C (10%) in 25 mL of methanol was heated under reflux for 3-4 days in an argon atmosphere, cooled and filtered. The catalyst was washed with methanol, and filtrate and wash liquids were evaporated under reduced pressure to give (S)-hexahydropyrrolo[1,2-a]pyrazine-1,4-dione as a white solid. Yield= 78%. **M.p.** = 210-212 °C (lit. 213-214 °C).

MS (m/z): 154 [M^+]; 111, 83.

^{1}H NMR (300 MHz, $CDCl_3$, 25 °C, ppm): δ = 7.03 (broad s, 1H, NH); 4.12 (br, d, 2H); 3.86 (dd, JHH = 16.4 Hz, JHH = 4.5 Hz); 3.75-3.05 (m, 2H); 2.40-2.38 (m, 1H); 2.25-1.90 (m, 3H).

(S)-octahydropyrrolo[1,2-a]pyrazine

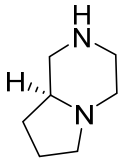

(S)-hexahydropyrrolo[1,2-a]pyrazine-1,4-dione (0.910 g, 5.9 mmol) was slowly added to a solution of $LiAlH_4$ (0.896 g, 23.61 mmol) in anhydrous THF (24 mL) under argon and refluxed for 20 min. Water (0.9 mL), NaOH 15% (0.9 mL) and water (2.7 mL) were successively added (slowly and carefully) to the mixture and stirred for 3 hours. The solid was removed by filtration and washed with cool THF (10 mL); the liquid extracts were dried with anhydrous $MgSO_4$. The solvent was evaporated under reduced pressure via rotary evaporation without overpass 80 mbar and 35 °C. The residue was distilled in bulb-to-bulb oven 50-55 °C/0.03mm/Hg to give a colourless liquid, that was stored under argon at low temperature (< -10 °C). MS for (S)-octahydropyrrolo[1,2-a]pyrazine.HBr (ES+, m/z): 127 [M+1], 333-335 [$2MBr^+$].

Synthesis of 2-formyl-6-diisopropylaminomethylpyridine, (L1):

2-hydroxymethyl-6-diisopropylaminomethylpyridine

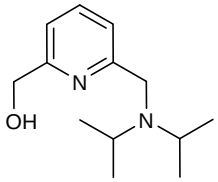

Diisopropylamine (0.92 g, 1.28 ml, 9 mmol) was added to a stirred mixture of 2-bromomethyl-6-hydroxymethylpyridine (1.22 g, 6 mmol) and powdered potassium carbonate (12.45 g, 90 mmol) in acetonitrile (60 mL) at room temperature. After the reaction was completed, 4-6 hours (TLC, chloroform: methanol, 90/10), the reaction mixture was filtered on celite, washed with acetonitrile and evaporated under reduced pressure. The residue was dissolved in ethyl acetate (50 mL) and washed with water and saturated solution of NaCl. The 2-hydroxymethyl-6-diisopropylaminomethylpyridine (1.13 g, 85%) was used without purification in next step. An analytical sample was achieved by column chromatography on silica gel using ethyl acetate/methanol, 95:5.

Anal. Calc. for $C_{13}H_{22}N_2O$ (222.2): C, 70.2; H, 10.0; N, 12.6. **Found**: C, 70.0; H, 9.9; N, 12.5 %.

MS (m/z): 221[M^+-H], 207 [M^+-H-Me], 179 [M^+-H-iPr] 165, 123[M^+-iPr2N].

IR (KBr, cm^{-1}): 3368, 3248 ν_{OH}, 2962 (vs), 2928, 2868 ν_{CHalip}, 1597(s), 1577 (m) $\nu_{C=C}$, $\nu_{C=N}$; 1456 (m), 1382 (m), 1364 (s) ν_{CH}, 1205 (m), 1180 ν_{C-C}.
^{1}H NMR (300 MHz, $CDCl_3$, 25 °C, ppm): δ = 7.63 (t, $1H_{Py}$, J_{HH} = 4.5 Hz); 7.52 (d, $2H_{Py}$, J_{HH} = 4.55 Hz), 7.04 (d, $2H_{Py}$, J_{HH} = 4.5 Hz); 4.77 (br, 1H, OH), 4.72 (s, 2H, CH_2O), 3.80 (m, 2H, -CH_2-); 3.09 (sept, 2H, 2 –CH_{iPr}, J_{HH} = 6.6 Hz); 1.05 (d, 12H, 4 -CH_{3iPr}, J_{HH} = 6.6 Hz).

^{13}C NMR (125 MHz, $CDCl_3$, 25 °C, ppm): δ = 158.8 (CPy); 157.5 (CPy); 137.0 (CHPy); 118.1 (CHPy); 118.0 (CHPy); 63.9 (CH_2O); 51.2 (-CH_2-); 49.2 (2C, 2 -CH_{iPr}); 20.7 (4 -CH_{3iPr}).

2-formyl-6-diisopropylaminomethylpyridine, (L1)

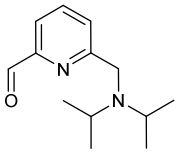

To a solution of oxalyl chloride (200 µL, 2.4 mmol) in dichloromethane (5 mL, at -55 °C) was successively added with efficient stirring DMSO (340 µL, 4.8 mmol) in dichloromethane (1 mL) and, two minutes later, 2-hydroxymethyl-6-diisopropylaminomethylpyridine (444 mg, 2 mmol) in dichloromethane (2 mL). After 15 minutes at -55 °C triethylamine (1.4 mL, 10 mmol) was added and stirred five minutes more, reaction mixture was slowly heated to room temperature and allows standing for 4 hours. The reaction was quenched for slow addition of water (10 mL). The organic phase was separated and aqueous phase extracted with dichloromethane (3 x 5 mL), the combined organic extracts were washed with water (10 mL) and brine (15 mL) and dried on anhydrous magnesium sulphate. The solvent was eliminated under reduced pressure to yield 2-formyl-6-diisopropylaminomethylpyridine (320 mg, 73%) almost pure. An analytical sample was obtained by chromatography on silica gel with chloroform:methanol, 99:1 as eluent.

Anal. Calc. for $C_{13}H_{20}N_2O$ (220.3): C, 70.9; H, 9.2; N, 12.7. **Found**: C, 70.6; H, 10.0; N, 12.8%.

MS (m/z): 221[M^+], 163 [M^+-iPr] 121[M^+-iPr2N] 106 [M^+-iPr_2NCH_2], 100.

IR (KBr, cm^{-1}): 2966 (vs) ν_{CHalip}, 1714 (vs) $\nu_{C=O}$, 1590 (s) $\nu_{C=C}$, $\nu_{C=N}$; 1452 (m), 1382 (m), 1364 (s) ν_{CH}, 1204 (m) ν_{C-C}.

^{1}H NMR (300 MHz, $CDCl_3$, 25 °C, ppm): δ = 10.04 (s, 1H, O=CH); 7.91 (broad s, $1H_{Py}$); 7.81-7.79 (broad, $2H_{Py}$); 3.88 (s, 2H, -CH_2-); 3.06 (sept, 2H, 2 –CH_{iPr}, J_{HH} = 6.6 Hz); 1.04 (d, 12H, 4 -CH_{3iPr}, J_{HH} = 6.6 Hz).
^{13}C NMR (125 MHz, $CDCl_3$, 25 °C, ppm): δ = 193.7 (C=O); 165.3 (C_{Py}); 151.7 (C_{Py}); 137.1 (CH_{Py}); 126.5 (CH_{Py}); 119.7 (CH_{Py}); 51.2 (-CH_2-); 49.1 (2C, 2 -CH_{iPr}); 20.8 (4 -CH_{3iPr}).

Synthesis of (S)-2-formyl-6-((2-(tert-butylcarbamoyl)-pyrrolidin-1-yl)-methyl)pyridine, (S)-L2:

(S)-2-hydroxymethyl-6-((2-(tert-butylcarbamoyl)pyrrolidin-1-yl)methyl)pyridine

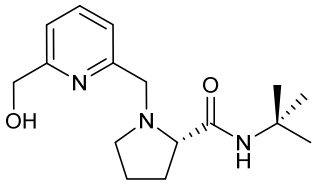

(S)-tert-Butylprolinamide (0.63 g, 4 mmol) was added to a stirred mixture of 2-bromomethyl-6-hydroxymethylpyridine (0.81 g, 4 mmol) and powdered potassium carbonate (8.3 g, 60 mmol) in acetonitrile (40 mL) at room temperature. After 2-4 hours the reaction was completed, (TLC, chloroform: methanol, 90/10), filtered on celite, washed with acetonitrile and evaporated under reduced pressure. The residue was dissolved in ethyl acetate (50 mL) and washed with water and saturated solution of NaCl. The (S)-2-hydroxymethyl-6-((2-(tert-butylcarbamoyl)pyrrolidin-1-yl)methyl)pyridine (0.89, 76%) was obtained nearly pure and was used in next step. An analytical sample was achieved by column chromatography on silica gel using ethyl acetate/methanol, 90:10.

Anal. Calc. for $C_{16}H_{25}N_3O_2$ (291.2): C, 66.0; H, 8.7; N, 14.4. **Found**: C, 65.8; H, 8.4; N, 14.3%.

MS (m/z): 291 [M^+], 191 [M^+ - CONHtBu], 123. IR (KBr, cm^{-1}): 3376 (s), 3316 (s) ν_{NH} ν_{OH}, 1646 (vs), 1535 (s) ν_{CO-NH}, 1456 (m), 1228 (m), 1094 (m), 1077 (m) ν_{C-C}.

^{1}H NMR (300 MHz, $CDCl_3$, 25 °C, ppm): δ = 7.65 (t, 1H_{Py}, J_{HH} = 7.2 Hz); 7.33 (br s, 1H, -NH); 7.17 (d, 2H_{Py}, J_{HH} = 7.2 Hz); 4.75 (s, 2H, CH_2OH); 4.08 (broad, 1H, OH); 3.92 (d, 1H, -CH_2-Py, AB, J_{HH} = 13.2 Hz); 3.69 (d, 1H, -CH2-Py, AB, J_{HH} = 13.2 Hz); 3.15 (dd, 1H, -CH2pyrr, J_{HH} = 5.3, 9.8 Hz); 3.07 (m, 1H, -CH_{pyrr}); 2.45 (dt, 1H, -CH_{2pyrr}, J_{HH} = 6.8, 9.4 Hz); 2.21-1.84 (m, 2H, -CH_{2pyrr}); 1.80-1.62 (m, 2H, 2 -CH_{2pyrr}); 1.26 (s, 9H, 3 -CH_3).

^{13}C NMR (125 MHz, $CDCl_3$, 25 °C, ppm): δ = 174.2 (CO); 159.4 (C_{Py}); 157.9 (C_{Py}); 137.7 (CH_{Py}); 121.8 (CH_{Py}); 119.4 (CH_{Py}); 68.4 (-CHN_{pyrr}-CO); 64.4 (-CH_2OH); 61.6 (-CH_2-); 54.9 (-CH_{2pyrr}); 50.5 (CtBu); 31.1 (-CH_{2pyrr}); 29.1 (3 -CH_3); 24.5 (-CH_{2pyrr}).

(S)-2-formyl-6-((2-(tert-butylcarbamoyl)pyrrolidin-1-yl)methyl)pyridine, (S)-L2:

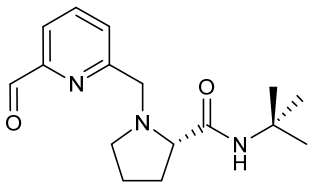

To a solution of oxalyl chloride (262 µL, 3.1 mmol) in dichloromethane (6.5 mL) at -55 °C was successively added with efficient stirring a dichloromethane solution (2 mL)of DMSO (440 µL, 6.2 mmol) and, two minutes later, (S)-2-hydroxymethyl-6-((2-(tert-butylcarbamoyl)pyrrolidin-1-yl)methyl)pyridine (750 mg, 2.58 mmol) in dichloromethane (3 mL). After 15 minutes of stirring at -55 °C triethylamine (1.8 mL, 12.9 mmol) was added and stirred five minutes more, temperature was slowly increased to room temperature and the reaction mixture allows to stand for 4 hours. The reaction was quenched for slow addition of water (20 mL). The organic phase was separated and aqueous phase extracted with dichloromethane (3 x 10 mL), the combined organic extract was washed with water (20 mL) and brine (20 mL) and dried on anhydrous magnesium sulphate. The solvent was eliminated under reduced pressure to yield (S)-2-formyl-6-((2-(tert-butylcarbamoyl)pyrrolidin-1-yl)methyl)pyridine (694 mg, 93%) nearly pure. An analytical sample was obtained by chromatography on silica gel with chloroform:methanol, 95:5 as eluent.

Anal. Calc. for $C_{16}H_{23}N_3O_2$ (289.4): C, 66.4; H, 8.0; N, 14.5. **Found**: C, 66.1; H, 8.0; N, 14.2%.

MS (m/z): 289 [M^+], 189 [M^+ - CONHtBu], 121.

IR (KBr, cm^{-1}): 3323 (s) ν_{NH}, 1714 (vs) $\nu_{CO\text{-}ald}$, 1670 (vs) $\nu_{CO\text{-}NH}$, 1518 (s), 1363 (m), 1229 (m) $\nu_{C\text{-}C}$.

^{1}H NMR (300 MHz, $CDCl_3$, 25 °C, ppm): δ = 10.06 (s, 1H, -CHO); 7.85 (m, $1H_{Py}$); 7.48 (dd, $1H_{Py}$, J_{HH} = 2.4, 6.5 Hz); 7.44 (br s, 1H, -NH); 4.02 (d, 1H, -CH_2-, ABXY, J_{HH} = 13.4 Hz); 3.74 (d, 1H, -CH_2-, ABXY, J_{HH} = 13.4 Hz); 3.18 (dd, 1H, -CH_{2pyrr}, J_{HH} = 5.3, 9.8 Hz); 3.04 (m, 1H, -CH_{pyrr}); 2.46 (dt, 1H, -CH_{2pyrr}, J_{HH} = 6.8, 9.4 Hz); 2.30-2.16 (m, 1H, -CH_{2pyrr}); 1.93-1.85 (m, 1H, -CH_{2pyrr}); 1.81-1.70 (m, 2H, 2 -CH_{2pyrr}); 1.29 (s, 9H, 3 -CH_3).

^{13}C NMR (125 MHz, $CDCl_3$, 25 °C, ppm): δ = 193.4 (CHO); 173.4 (CO); 159.5 (C_{Py}); 152.8 (C_{Py}); 137.5 (CH_{Py}); 127.0 (CH_{Py}); 120.1 (CH_{Py}); 68.0 (-CHN_{pyrr}-

CO); 60.8 (-CH_2-); 54.1 (-CH_{2pyrr}); 50.2 (CtBu); 30.6 (-CH_{2pyrr}); 28.7 (3 -CH_3); 24.0 (-CH_{2pyrr}).

Synthesis of (S)-2-formyl-6-(octahydropyrrolo[1,2-a]-pyrazin-2-ylmethyl)pyridine, (S)-L3:

(S)-2-hydroxymethyl-6-(octahydropyrrolo[1,2-a]-pyrazin-2-ylmethyl)pyridine

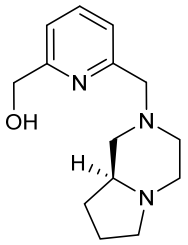

(S)-octahydropyrrolo[1,2-a]pyrazine (0.60 g, 4 mmol) was added to a stirred mixture of 2-bromomethyl-6-hydroxymethylpyridine (0.81 g, 4.8 mmol) and powdered potassium carbonate (8.29 g, 60 mmol) in acetonitrile (60 mL) at room temperature. After 4-6 hours the reaction was completed, (TLC, silica pre-treated with eluent + 2% Et_3N, chloroform: methanol, 90/10), filtered through celite, washed with acetonitrile and evaporated under reduced pressure. The residue was dissolved in ethyl acetate (50 mL) and washed with water and saturated solution of NaCl. The (S)-2-hydroxymethyl-6-(octahydropyrrolo[1,2-a]-pyrazin-2-ylmethyl)pyridine (0.81 g, 82%) was used in next step without purification. An analytical sample was achieved by column chromatography on silica gel silica pre-treated with eluent + 2% Et_3N using ethyl acetate/methanol, 95:5.

Anal. Calc. for $C_{14}H_{21}N_3O$ (247.17): C, 68.0; H, 8.6; N, 17.0. **Found**: C, 67.7; H, 8.7; N, 17.0%. MS (m/z): 247 [M^+]; 151, 125, 123, 96.

IR (KBr, cm^{-1}): 3350 (s) 2966 (vs) ν_{OH}, 2937 (s), 2808(vs) ν_{CH}; 1658 (m), 1593 (m), 1577 (m) $\nu_{C=C}$, $\nu_{C=N}$, 1456 (m) ν_{CH}.

^{1}H NMR (300 MHz, $CDCl_3$, 25 °C, ppm): δ = 7.65 (t, $1H_{Py}$); 7.30 (d, $1H_{Py}$, J_{HH} = 7.7 Hz); 7.12 (d, $1H_{Py}$, J_{HH} = 7.5 Hz); 5.30 (br, 1H, OH); 4.73 (s, 2H, CH_2O); 3.74 (s, 2H, -CH_2-Py); 3.06, 2.14 (m, m, 1H, 1H, -CH_{2pyrr}); 2.99, 2.35 (m, m, 1H, 1H, -$CH_{2pyrazine}$); 2.97, 2.00 (m, m, 1H, 1H -$CH_{2pyrazine}$); 2.84, 2,35 (m, m, 1H, 1H, -$CH_{2pyrazine}$); 2.13 (1H, -CH_{pyrr}); 1.82, 1.71 (m, m, 1H, 1H, -CH_{2pyrr}); 1.75, 1.38 (m, m, 1H, 1H, -CH_{2pyrr}).

^{13}C NMR (125 MHz, $CDCl_3$, 25 °C, ppm): δ = 158.3 (C_{Py}); 157.6 (C_{Py}); 137.0 (CH_{Py}); 121.6 (CH_{Py}); 118.6 (CH_{Py}); 64.0 (-CH_2O-); 63.9 (-CH_2-Py); 62.8 (-CHN_{pyrr}-$C_{pyrazine}$); 58.2 (-$CH_{2pyrazine}$); 53.4 (-CH_{2pyrr}); 52.7 (-$CH_{2pyrazine}$); 51.4 (-$CH_{2pyrazine}$); 27.2 (-CH_{2pyrr}); 21.3 (-CH_{2pyrr}).

(S)-2-formyl-6-(octahydropyrrolo[1,2-a]-pyrazin-2-ylmethyl)pyridine (S)L3

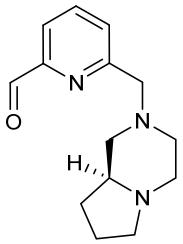

To a solution of oxalyl chloride (150 µL, 1.75 mmol) in dichloromethane (4 mL) at -55 °C was successively added with efficient stirring DMSO (250 µL, 3.5 mmol) in dichloromethane (1 mL) and, two minutes later, (S)-2-hydroxymethyl-6-(octahydropyrrolo[1,2-a]-pyrazin-2-ylmethyl)pyridine (370 mg, 1.5 mmol) in dichloromethane (1.5 mL). After 15 minutes of stirring at -55 °C triethylamine (1.1 mL, 7.5 mmol) was added and stirred five minutes more, temperature was slowly increased to room temperature and the reaction mixture allows to stand for 4 hours. The reaction was quenched for slow addition of water (15 mL). The organic phase was separated and aqueous phase extracted with dichloromethane (2 x 10 mL), the combined organic extract was washed with water (15 mL) and brine (15 mL) and dried on anhydrous magnesium sulphate. The solvent was eliminated under reduced pressure to yield (S)-2-formyl-6-(octahydropyrrolo[1,2-a]-pyrazin-2-ylmethyl)pyridine (331 mg, 90%) pure. An analytical sample was obtained by chromatography on silica gel with chloroform:methanol, 99:1 as eluent.

Anal. Calc. for $C_{14}H_{19}N_3O$ (245.15): C, 68.5; H, 7.8; N, 17.1. Found: C, 68.2; H, 8.1; N, 16.8 %.

MS (m/z): 245 [M^+]; 117, 123, 121.

IR (KBr, cm^{-1}): 2966 (vs) ν_{OH}, 2935 (s), 2802(vs) ν_{CH}; 1713 (vs) $\nu_{C=O}$, 1592 (m) $\nu_{C=C}$, $\nu_{C=N}$, 1457 (m) ν_{CH}, 1338 (m), 1163 (s) ν_{C-C}.

^{1}H NMR (300 MHz, $CDCl_3$, 25 °C, ppm): δ = 10.08 (s, 1H CHO); 7.85 (d, $1H_{Py}$); 7.83 (d, $1H_{Py}$, J_{HH} = 3.8 Hz); 7.69 (dd, $1H_{Py}$, J_{HH} = 5.1 Hz); 3.8, 3.1 (AB, 2H, -CH_2-Py); 3.08, 2.14 (m, m, 1H, 1H -CH_{2pyrr}); 2.96, 2.35 (m, m, 1H, 1H, -$CH_{2pyrazine}$); 2.97, 2.02 (m, m, 1H, 1H, -$CH_{2pyrazine}$); 2.86, 2,38 (m, m, 1H, 1H, -

$CH_{2pyrazine}$); 2.13 (1H, -CH_{pyrr}); 1.82, 1.71 (m, m, 1H, 1H, -CH_{2pyrr}); 1.75, 1.38 (m, m, 1H, 1H, -CH_{2pyrr}).

^{13}C NMR (125 MHz, $CDCl_3$, 25 °C, ppm): δ = 193.3 (CHO); 165.3 (C_{Py}); 151.7 (C_{Py}); 137.1 (CH_{Py}); 126.5 (CH_{Py}); 119.7 (CH_{Py}); 62.8 (-CHN_{pyrr}-$C_{pyrazine}$); 58.3 (-$CH_{2pyrazine}$); 53.9 (-CH_2-Py); 53.4 (-CH_{2pyrr}); 52.2 (-$CH_{2pyrazine}$); 51.4 (-$CH_{2pyrazine}$); 27.3 (-CH_{2pyrr}); 21.6 (-CH_{2pyrr}).

(E)-2-(tert-Butyliminomethyl)-6-diisopropylaminomethylpyridine, (L1'):

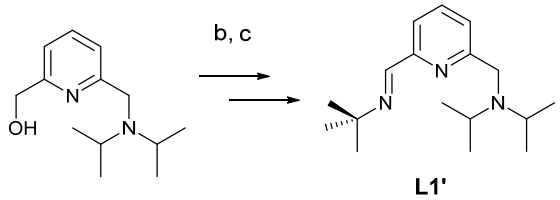

L1'

b: $(COCl)_2$, DMSO, -50 °C; c: *t*-$BuNH_2$/ AcN

To a stirred solution of 2-formyl-6-diisopropylaminomethylpyridine (440 mg, 2 mmol) in ethanol (25 ml), was added tert-butylamine (230 µl, 2.2 mmol) and freshly activated molecular sieves 4 Å (2g), after stirring for 14-16 hours at room temperature the reaction mixture was filtered through celite, concentrated under reduced pressure to yield pure (E)-2-(tert-butyliminomethyl)-6-diisopropylaminomethylpyridine (545 mg, 99%).

Anal. Calc. for $C_{17}H_{29}N_3$ (275.4): C, 74.1; H, 10.6; N, 15.3. Found: C, 74.3; H, 10.8; N, 15.6. %.

MS (*m/z*): 275 [M^+], 218 [M^+-*t*-Bu], 176 [M^+-Et_2N], 162, 120.

IR (KBr, cm^{-1}): ν_{CHalip} 2967 (vs), 1645 (m), 1589 (m) $\nu_{C=C}$, $\nu_{C=N}$; 1454 (m), 1382 (m), 1363 (s) ν_{CH}, 1205 (m) ν_{C-C}.

^{1}H NMR (300 MHz, $CDCl_3$, 25 °C, ppm): δ = 8.32 (s, 1H, N=CH); 7.84 (t, $1H_{Py}$, J_{HH} = 4.4 Hz); 7.64 (d, $2H_{Py}$, J_{HH} = 4.7 Hz); 3.80 (m, 2H, -CH_2-); 3.03 (sept, 2H, 2 –CH_{iPr}, JHH = 6.6 Hz); 1.28 (s, 9H, 3 -CH_{3tBu}); 1.00 (d, 12H, 4 -CH_{3iPr}, J_{HH} = 6.6 Hz).

^{13}C NMR (125 MHz, $CDCl_3$, 25 °C, ppm): δ = 163.7 (C_{Py}); 156.8 (N=CH); 154.3 (C_{Py}); 136.7 (CH_{Py}); 122.6 (CH_{Py}); 118.2 (CH_{Py}); 57.7 (C_{tBu}); 51.4 (-CH_2-); 48.9 (2C, 2 -CH_{iPr}); 29.6 (3 -CH_{3tBu}); 20.7 (4 -CH_{3iPr}).

Synthesis of [IrL1'Cl] (L1'Ir)

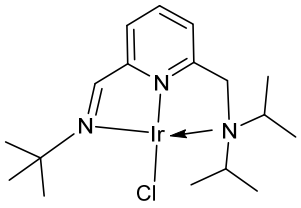

In a 100 mL round-bottomed Schlenk flask 50 mg (0.18 mmol) of the ligand (L1') was dissolved in 5 ml of CH_2Cl_2 under N_2. This solution was then treated with a red solution of 60.6 mg (0.091 mmol) $[Ir(C_8H_{12})Cl]_2$ in 20 ml CH_2Cl_2. The solution was stirred for an additional hour. The solvent was removed in vacuum until 5 mL, pentane was added to the mixture and an orange solid obtained. After drying the residue for several hours in vacuum, the analytically pure product was obtained in 70% yield (63.9 mg; 0.13 mmol).

Anal. Calc. for $C_{25}H_{41}ClIrN_3$ (611.3): C, 49.1; H, 6.8; N, 6.9; Ir, 31.4; Found: C, 48.5; H, 6.4; N, 6.4 Ir, 30.5%.

MS (ES^+, *m/z*): 612.3 (M^+, 10), 576.3 ([Ir(cod)(L1')]+, 40), 276 ($L1'^+$, 100).

IR (KBr, cm^{-1}): ν_{CHarom} 3092 (w); ν_{CHalip} 2974 (s), 2937 (m) 2882 (m); $\nu_{C=C}$, $\nu_{C=N}$ 1700 (m), 1635 (s) 1594 (s), 1465 (s); ν_{CH} 1397 (s), 1379 (s), 1367 (s); ν_{C-C}, 1209 (s), 1153 (s), 1095 (m); $\nu_{CHout\ plane}$ 806 (m), 776 (m); ν_{CH} 556 (m), 503 (m).

^{1}H NMR (300 MHz, $CDCl_3$): δ = 8.89 (s, 1H, N=CH); 8.13 (d, 1H_{Py}, J= 7.9 Hz,); 7.79 (t, 1H_{Py}, J= 7.7 Hz); 7.48 (d, 1H_{Py}, J= 7.5 Hz,); 5.28 (d, 1H, -CH_2-, J_{HH} = 18.4 Hz); 4.41 (d, 1H, -CH_2-, J_{HH}= 18.4); 3.40 (br); 3.15 (q, 2H, -CH_{iPr}, J_{HH} = 6.6 Hz); 2.32 (br); 1.75 (s, 9H, 3 -CH_{3tBu}); 1.12 (d, 6H, -CH_{3iPr}, J_{HH} = 2.2 Hz); 1.09 (d, 6H, -CH_{3iPr}, J_{HH} = 2.1 Hz);

^{13}C NMR (125 MHz, $CDCl_3$, 25 °C, ppm): δ = 166.7 (N=CH); 160.2 (C_{Py}); 154.4 (C_{Py}); 136.3 (CH_{Py}); 125.3 (CH_{Py}); 123.8 (CH_{Py}); 61.7(C_{tBu}); 53.6 (-CH_2-); 48.9 (2C, 2 -CH_{iPr}); 31.4 (3 -CH_{3tBu}); 21.05, 20.08 (4 -CH_{3iPr}).

Synthesis of [IrL1']X (X = BF4):

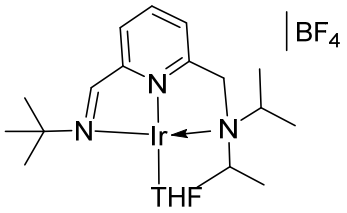

A solution of 70 mg (0.11 mmol) of the complex $[Ir(C_8H_{12})Cl]_2$ in 15 mL THF was placed in Schlenk tube, $AgBF_4$ (22.3 mg, 0.11 mmol) was added and immediately AgCl appears in the reaction media. The mixture was stirred for 1 h, AgCl was removed and ligand L1' (30.3 mg, 0.11 mmol) was added to the filtrate upon which the color of the solution changed to orange. After 3h at 40 °C the solvent was removed in vacuum and the residue was washed in portions with 15 mL of pentane. After five hours drying in vacuum, the orange product was obtained in 90% yield (68 mg, 0.10 mmol).

MS (ES^+, *m/z*): 659.3 [M^+, [Ir(cod)(L1')]BF_4, 20), 592.3 ([Ir(cod)(L1')(H_2O)], 10), 276 ($L1'^+$, 80).

2.5.2. Postmodification of MOFs

Synthesis of Zr-BDC-NH_2-L1: $[Zr_6O_4(BDC\text{-}NH_2)_{6-x}L1_x]$ (L1 = 2-formyl-6-diisopropylaminomethylpyridine)

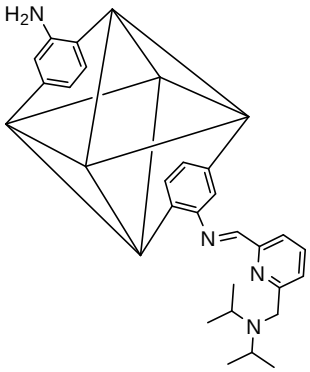

Zr-BDC-NH_2 (1.5 g, 1.6 mmol) was dispersed in 15 mL CH_2Cl_2. To this slurry, a solution of aldehyde (375.0 mg, 1.7 mmol) in CH_2Cl_2 (5 mL) was dropwise added at room temperature, and the mixture was stirred for additional 6 h. The sample was collected by centrifugation, washed twice with CH_2Cl_2, and dried in air at 70 °C.

Elemental analysis was performed on samples outgassed under vacuum (100 °C, 12 h). $Zr_6O_4(OH)_4(BDC\text{-}NH_2)_{5.7}(BDC\text{-}L1)_{0.3}$: (corresponding to ~5% amine functionalization): C, 34.35; H, 2.19; N, 5.09; Calculated: C, 34.35; H, 2.19; N, 5.09%. Found: C, 34.45; H, 2.64; N, 5.07%. The level of functionalization is 5% of the total -NH_2 groups.

^{13}C NMR (CP MAS): 17.8 (CH_{3iPr}), 45.8 (CH_{iPr}), 50.6 (CH_2), 116.1, 123.0, 132.1, 138.5, 151.4, 162.8 (imine C=N), 171.2 (COO).

Synthesis of Zr-BDC-NH_2-L1Ir: [Zr_6O_4(BDC-NH_2)$_{6-x}$(BDC-L1IrCl)$_x$]

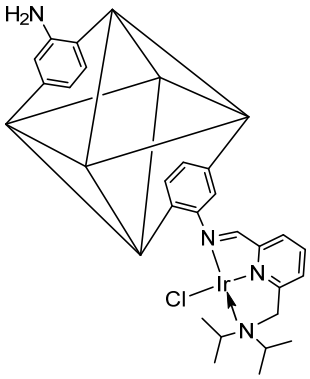

Zr-BDC-NH_2-L1 (1 g) was dispersed in 15 mL CH_2Cl_2. To this slurry, a solution of [IrCl(cod)]$_2$·(200 mg, 0.3 mmol) in 15 mL CH_2Cl_2 was added at room temperature, and the mixture was stirred at reflux for 12 h. The sample was collected by centrifugation, washed twice with CH_2Cl_2, and dried in air at 70-80 °C.

Elemental analysis was performed on samples outgassed under vacuum (100 °C, 4 h). $Zr_6O_4(OH)_4$(BDC-NH_2)$_{5.7}$([BDC-L1IrCl])$_{0.3}$: Calculated: C, 32.48; H, 2.15; N, 4.82%. Found: C, 34.12; H, 2.39; N, 4.82%.

The amount of iridium in the final solid was determined by **ICP-AES**. Calculated: Ir, 3.15%; Found: Ir, 3.11%.

^{13}C NMR (CP MAS): 17.9, 21.2 (CH_{3iPr}), 45.7 (CH_{iPr}), 116.9, 123.2, 131.7, 138.5, 151.4, 165.6 (imine C=N), 171.4 (COO).

ESI-MS analysis: Due to the stability of Zr-BDC MOFs in acidic media, hydrofluoric acid (HF) was chosen to digest the materials, taking into account the high affinity of Zr for fluoride The samples were digested in hydrofluoric acid (HF) due to the high affinity of Zr for fluoride. The starting Zr-BDC-NH_2 was also digested and used as reference. The negative mode mass spectra obtained showed a base peak at m/z 180 that corresponds to H_2BDC-NH_2 (annexes, [H_2BDC-NH_2 + H]$^-$). The negative mode mass spectra obtained for H_2BDC-NH_2L clearly shows a base peak at m/z 383 (annexes, [H_2BDC-L + H]$^-$), which corresponds to the modified ligand. The spectra of H_2BDC-[LIr] show a peak at m/z 677 (annexes, {[H_2BDC-[LIr(MeOH)]BF_3 + H}$^-$). Last, HF cleaves also the Zr cluster itself, and the fluoro complex [ZrF_5]$^-$ is readily discerned (annexes).

Synthesis of Zr-BDC-NH_2-[L1Ir]$^+$: [$Zr_6O_4(OH)_4$(BDC-NH_2)$_{6-x}$([L1Ir]BF4)$_x$]

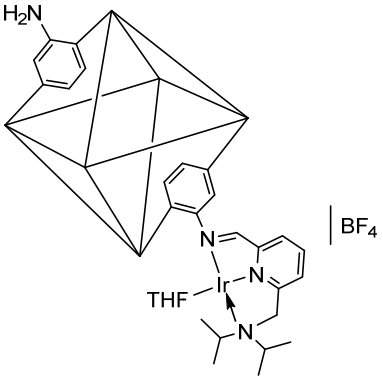

$AgBF_4$ (8.7 mg, 0.044 mmol) was added to a solution of $[IrCl(cod)]_2$·(15 mg, 0.022 mmol) in 10 mL THF at room temperature, and the mixture was stirred for 1 h; then, AgCl was filtered and the solution containing $[Ir(COD)]BF_4$ added to a suspension of Zr-BDC-NH_2-L1 (100 mg) in 10 mL THF. The mixture was stirred for 10 h; the solid was collected by centrifugation, washed twice with THF, and dried in air at 70 °C.

Elemental analysis was performed on samples outgassed under vacuum (100 °C, 4 h). $Zr_6O_4(OH)_4$(BDC-NH_2)$_{5.7}$L1$_{0.1}$([L1Ir]BF_4)$_{0.2}$. Calculated: C, 32.70; H, 2.17; N, 4.85%. Found: C, 32.92; H, 2.56; N, 4.54%.

The amount of iridium in the final solid was determined by **ICP-AES**. Calculated: Ir, 2.11%; Found: Ir, 1.85%.

Zr-BDC-NH_2-L2: [Zr_6O_4(BDC-NH_2)$_{6-x}$L2$_x$] (L2= (S)-2-formyl-6-((2-(tert-butylcarbamoyl)-pyrrolidin-1-yl)-methyl)pyridine).

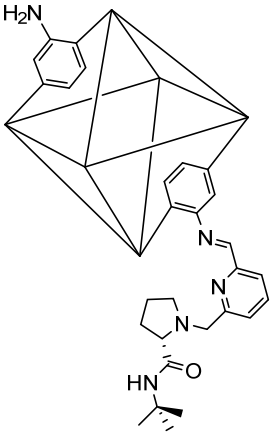

Zr-BDC-NH_2 (275 g, 0.64 mmol) was dispersed in 15 mL CH_2Cl_2. To this slurry, a solution of aldehyde (221 mg, 0.64 mmol) in CH_2Cl_2 (5 mL) was dropwise added at room temperature, and the mixture was stirred for additional 24 h. The sample was collected by centrifugation, washed twice with CH_2Cl_2 and dried in air at 70 °C.

Elemental analysis was performed on samples outgassed under vacuum (100 °C, 12 h). $Zr_6O_4(OH)_4$(BDC-NH2)$_5$(BDC-L2): (corresponding to ~17% amine functionalization): Calculated: C, 38.56; H, 2.79; N, 5.53%. Found: C, 37.6; H, 3.02; N, 5.59%.

^{13}C-NMR (CP MAS): 23.1, 28.8 (CH_{3tBu}), 35.7, 52.2 (CH_2), 118.1, 124.4, 132.9, 139.8, 151.8, 172.1 (COO), 173.2 (COO, CONH).

Zr-BDC-NH_2-[L2Ir]BF_4: [$Zr_6O_4(OH)_4$(BDC-NH_2)$_{6-x}$([L2Ir]$_x$ BF4)].

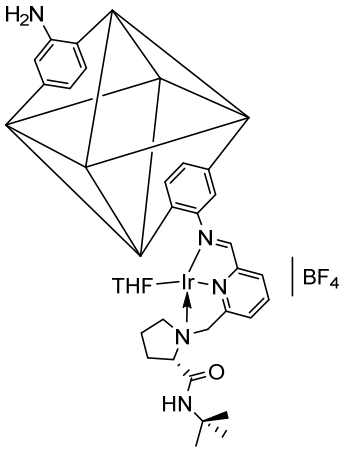

$AgBF_4$ (23.2 mg, 0.12 mmol) was added to a solution of $[IrCl(cod)]_2$·(40 mg, 0.06 mmol) in 10 mL THF at room temperature, and the mixture was stirred for 1 hour; then, AgCl was filtered and the solution containing $[Ir(COD)]BF_4$ added to a suspension of Zr-BDC-NH_2-L2 (200 mg) in 10 mL THF. The mixture was stirred for 10 h; the solid was collected by centrifugation, washed twice with THF and dried in air at 70 °C.

Elemental analysis was performed on samples outgassed under vacuum (100 °C, 4 h). $Zr_6O_4(OH)_4$(BDC-NH_2)$_5$L2$_{0.6}$([L2Ir]BF_4)$_{0.4}$ Calculated: C, 36.55; H, 2.64; N, 5.25%. Found: C, 35.62; H, 2.56; N, 5.54%.

The amount of iridium in the final solid was determined by **ICP-AES**. Calculated: Ir, 3.6%; Found: Ir, 3.2%.

^{13}C-NMR (CP MAS): 27.8 (CH_{3tBu}), 45.9 (CH_2), 51.9, 57.8 (CH_2), 118.0, 123.9, 132.3, 138.6, 150.6, 161.4 (imine C=N), 171.4 (COO).

Zr-BDC-NH_2-L3: [Zr_6O_4(BDC-NH_2)$_{6-x}$L3$_x$] (L3= (S)-2-formyl-6-(octahydropyrrolo[1,2-a]-pyrazin-2-ylmethyl)pyridine).

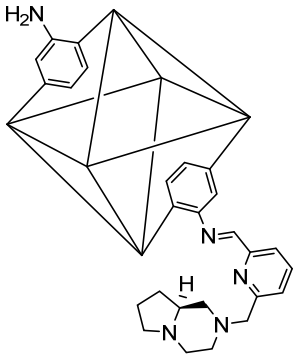

Zr-BDC-NH_2 (1.5 g, 1.6 mmol) was dispersed in 15 mL CH_2Cl_2. To this slurry, a solution of aldehyde (416.5 mg, 1.7 mmol) in CH_2Cl_2 (5 mL) was dropwise added at room temperature, and the mixture was stirred for additional 6 h. The sample was collected by centrifugation, washed twice with CH_2Cl_2 and dried in air at 70 °C.

Elemental analysis was performed on samples outgassed under vacuum (100 °C, 12 h). $Zr_6O_4(OH)_4(BDC\text{-}NH_2)_{5.7}(BDC\text{-}L3)_{0.3}$: (corresponding to ~5% amine functionalization): Calculated: C, 34.61; H, 2.18; N, 5.07%. Found: C, 33.58; H, 2.64; N, 5.08%.

^{13}C-NMR (CP MAS): 21.5, 28.8, 34.1, 39.2, 45.8, 51.7 (CH_2), 116.9, 117.7, 123.2, 131.6, 138.6, 150.9, 161.8 (imine C=N), 171.2, 172.4 (COO).

Zr-BDC-NH_2-[L3Rh]BF_4: [$Zr_6O_4(OH)_4(BDC\text{-}NH_2)_{6-x}$([L3Rh]$BF_4$)$_x$].

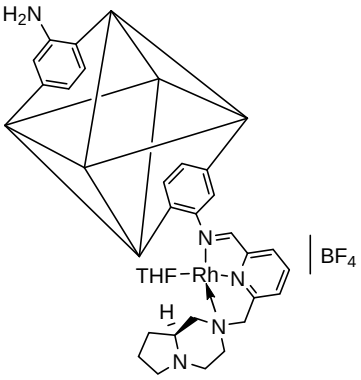

Following a similar procedure as for Zr-BDC-NH_2-[L2Ir]: $AgBF_4$ (10.0 mg, 0.051 mmol), $[RhCl(cod)]_2$·(12.7 mg, 0.025 mmol) we obtained a yellow solid.

Elemental analysis $Zr_6O_4(OH)_4(BDC\text{-}NH_2)_{5.7}(BDC\text{-}L3)_{0.15}(BDC\text{-}[L3Rh]BF_4)_{0.15}$: Calculated: C, 34.08; H, 2.15; N, 5.00%. Found: C, 32.43; H, 2.93; N, 4.68%.

The amount of rhodium in the final solid was determined by **ICP-AES**. Calculated: Rh, 0.83%; Found: Rh, 0.76% (0.07 mmol/g).

^{13}C-NMR (CP MAS): 25.9, 34.3, 51.4 (CH_2), 116.9, 120.1, 132.9, 138.1, 149.3, 170.3 (COO).

UiO66–NH2-[L3Ir]BF4: [Zr6O4(OH)4(BDC-NH2)6-x([L3Ir]BF4)x].

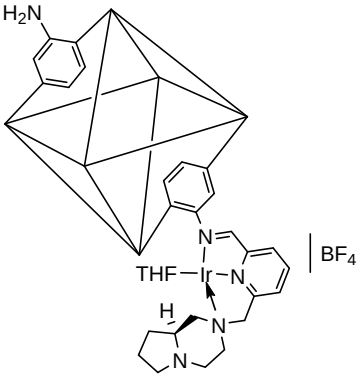

Following a similar procedure as for Zr-BDC-NH_2-[L2Ir]: $AgBF_4$ (8.7 mg, 0.044 mmol), $[IrCl(cod)]_2$·(15 mg, 0.022 mmol) resulted:

Elemental analysis $Zr_6O_4(OH)_4(BDC\text{-}NH2)_{5.7}(BDC\text{-}L3)_{0.1}([L3Ir]BF_4)_{0.2}$ Calculated: C, 33.58; H, 2.11; N, 4.92%. Found: C, 32.92; H, 2.56; N, 4.54%.

The amount of iridium in the final solid was determined by **ICP-AES**. Calculated: Ir, 2.05%; Found: Ir, 2.40 % (0.12 mmol/g).

^{13}C-NMR (CP MAS): 24.7, 45.9 (CH_2), 67.1, 116.8, 118.4 (sh), 123.3, 131.9, 138.4, 151.0, 161.2 (imine C=N), 171.5 (COO).

Zr-BPDC-NH_2-L3: [$Zr_6O_4(OH)_4$(BPDC-NH_2)$_{6-x}$(L3)$_x$].

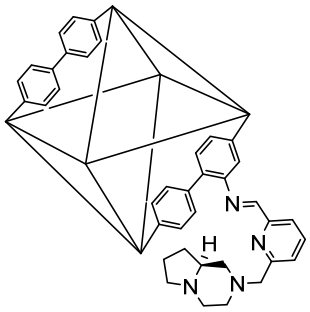

Following a similar procedure as for Zr-BPDC-NH_2-L3: Zr-BPDC-NH_2 (1.5 g, 0.7 mmol) was dispersed in 15 mL CH_2Cl_2. To this slurry, a solution of aldehyde (416.5 mg, 2.0 mmol) in CH_2Cl_2 (5 mL) was dropwise added at room temperature, and the mixture was stirred for additional 6 h. The sample was collected by centrifugation, washed twice with CH_2Cl_2 and dried in air at 70 °C.

Elemental analysis was performed on samples outgassed under vacuum (100 °C, 12 h). $Zr_6O_4(OH)_4$(BPDC-NH_2)$_{5.8}$(BPDC-L3)$_{0.2}$: (corresponding to ~3.5% amine functionalization): Calculated: C, 46.07; H, 3.27; N, 3.95; Found: C, 45.02; H, 3.65; N, 3.71%.

^{13}C-NMR (CP MAS): 32.3, 36.5, 119.7, 122.0, 130.3, 143.0, 172.2 (COO).

Zr-BPDC-NH_2-[L3Rh]BF_4: [$Zr_6O_4(OH)_4$(BPDC-NH_2)$_{6-x}$([L3Rh]BF_4)$_x$].

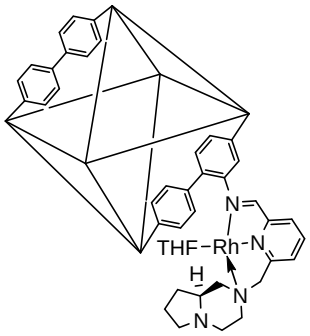

BF_4

Following a similar procedure as for Zr-BPDC-NH_2-[L3Rh]: $AgBF_4$ (8.7 mg, 0.044 mmol), $[RhCl(cod)]_2$·(11 mg, 0.022 mmol) we obtained a yellow solid.

Elemental analysis $Zr_6O_4(OH)_4$(BPDC-NH_2)$_{5.8}$(BPDC-L3)$_{0.1}$(BPDC-L3Rh)$_{0.1}$: Calculated: C, 45.69; H, 3.24; N, 3.92; Found: C, 47.82; H, 2.86; N, 3.49%.

The amount of rhodium in the final solid was determined by **ICP-AES**. Calculated: Rh, 0.45%; Found: Rh, 0.50% (0.05 mmol/g).

^{13}C-NMR (CP MAS): 31.6, 119.4, 130.3, 143.2, 172.7 (COO).

Synthesis of IRMOF-3, [$Zn_4O(BDC\text{-}NH_2)_3$]. (BDC-NH_2 = 2-aminoterephthalate):

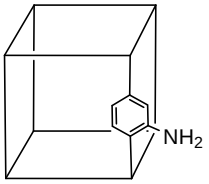

Triethylamine (1.6 g, 15.81 mmol) was dropwise added to a mixture of $Zn(NO_3)_2{\cdot}6H_2O$ (1.21 g, 4.07 mmol) and BDC-NH_2 (0.371 g, 2.05 mmol) in DMF (40 mL) and stirred for 2 h at room temperature. The resulting pale yellow solid was collected by centrifugation and washed twice with DMF. The solid was thrice immersed in $CHCl_3$ during three days, and the solid was finally dried in air at 60 °C. This washing procedure removes most of the DMF solvent molecules, although the presence of an IR absorption band at 1660 cm^{-1} in the spectrum of the washed sample indicates that some adsorbed DMF still remains inside the pores. The structure of the material was confirmed by X-ray diffraction, prior and after washing with $CHCl_3$.

Elemental analysis was performed on samples outgassed under vacuum (100 °C, 12 h). $Zn_4O(BDC\text{-}NH_2)_3$: Calculated: C, 35.35; H, 1.84; N, 5.16%. Found: C, 34.61; H, 1.87; N, 5.14%.

^{13}C-NMR (CP MAS): 116, 126, 132, 137, 149, 175 (COO) ppm (annexes)

Postsynthetic modification of IRMOF-3. IRMOF-3-L1, [$Zn_4O(BDC\text{-}NH_2)_{3\text{-}x}$(BDC-L1)$_x$].

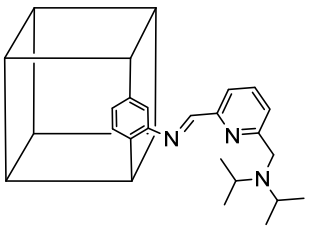

In a typical procedure, freshly prepared IRMOF-3 (1 g, 1.2 mmol) was dispersed in 15 mL CH_2Cl_2. To this slurry, a solution of aldehyde (500 mg, 4.1 mmol) in CH_2Cl_2 (15 mL) was dropwise added at room temperature, and the mixture was stirred for additional 30 min. The sample was collected by centrifugation, washed twice with CH_2Cl_2 and dried in air at 60 °C.

Elemental analysis was performed on samples outgassed under vacuum (100 °C, 12 h). $Zn_4O(BDC\text{-}NH_2)_{2.94}(L1)_{0.06}$ (corresponding to 2% amine functionalization): Calculated: C, 35.84; H, 1.97; N, 5.15%. Found: C, 32.40; H, 2.27; N, 5.04%. The level of functionalization is 2% of the total -NH_2 groups.

^{13}C-NMR (CP MAS): 18.2 (CH_{3iPr}), 30.9, 51.6 (CH_{iPr}), 117.3, 123.8, 132.9, 137.7, 150.0, 164.0 (imine C=N), 174.6 (COO) ppm (annexes).

Synthesis of IRMOF-3-LIr, $[Zn_4O(BDC\text{-}NH_2)_{3\text{-}x}([L1IrCl]_x)$.

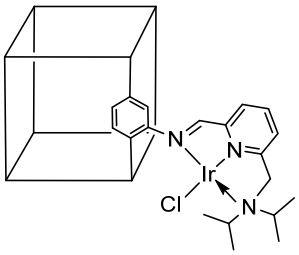

Sample IRMOF-3-L1 (1 g) was dispersed in 15 mL CH_2Cl_2. To this slurry, a solution of $[IrCl(cod)]_2$·(200 mg, 0.3 mmol) in 15 mL CH_2Cl_2 was dropwise added at room temperature, and the mixture was stirred for an additional hour. The sample was collected by centrifugation, washed twice with CH_2Cl_2 and dried in air at 60 °C.

Elemental analysis was performed on samples outgassed under vacuum (100 °C, 12 h). $Zn_4O(BDC\text{-}NH_2)_{2.94}(BDC\text{-}L1IrCl)_{0.06}$: Calculated: C, 35.25; H, 1.94; N, 5.06%. Found: C, 33.62; H, 2.49; N, 4.99%.

The amount of iridium in the final solid was determined by **ICP-AES**. Calculated: Ir, 1.39%. Found: Ir, 1.38%.

^{13}C-NMR (CP MAS): 19.0 (CH_{3iPr}), 30.8, 51.4 (CH_{iPr}), 118.2, 125.8, 132.8, 138.4, 150.3, 162.4 (imine C=N), 175.6 (COO) (annexes).

2.5.3. Catalytic mesurements

2.5.3.1. Hydrogenation of aromatics

General procedure: Hydrogenation of aromatics was performed in an Autoclave Engineers (100 mL). The reactants were added to the suspension of catalyst (2.4 mg, 0.2 mol% based on iridium) in ethanol (15-40 mL); the reactor was hermetically sealed, pressurized (6 bar H_2) and heated (60 °C) under continuous stirring (*ca.* 1000 rpm). Small liquid aliquots (≈100 µl) were taken. The progress of the reaction was monitored by GC-MS (annexes).

In particular, hydrogenation of aniline (50 µL, 0.5 mmol) was performed with 10.5 mg (1.05×10^{-3} mmol Ir) of ZrMOF-LIr in 2-propanol (15 mL). The reaction mixture was filtered, and the solvent was removed under reduced pressure to

give the crude product, pure for GC-MS. When the reaction is carried out with 10 times more substrate, the reaction is complete in 36 h.

The recycling of ZrMOF-LIr

After completion of the reaction the catalyst was recovered by separation of solid MOF-Ir from liquid after extensively centrifuging. The recovered catalyst was washed with ethanol for three times, dried at 80 °C for 12 h and reused. The ZrMOF-LIr catalyst showed consistent activity for four cycles.

The hot filtration test of ZrMOF-LIr catalyst

A mixture of ZrMOF-LIr (6.7 mg, 7.0 x 10^{-4} mmol Ir), ethyl benzoate (50 µL, 0.35 mmol), and ethanol (15 mL) were put into a reactor (Autoclave Engineers) and the mixture was extensively stirred (*ca.* 1000 rpm) at 60 °C, 6 bar H2 for 0.5 h. The conversion was ~20%. Then the solid catalyst was quickly separated after filtration of the reactant mixtures. The liquid was kept at 60 °C with extensive stirring for 24 h. The conversion was 35%. It is found that the blank thermal reaction without any catalyst for this reaction at 60 °C was *ca.* 8% (annexes).

2.5.3.2. N-Alkylation of amines with alcohols

Method a: The N-alkylation reaction was performed in an Autoclave Engineers (100 mL). The amines were added to the suspension of catalyst (0.2 mol% iridium) in alcohol (40 mL). The reactor was hermetically sealed, pressurized with H_2 (4 bar) and heated under continuous stirring. Small liquid aliquots (≈100 µl) were taken. The progress of the reaction was monitored by using GC-MS. The reaction mixture was filtered, and the solvent was removed under reduced pressure to give the crude product.

Method b: N-alkylation was performed in a glass microreactor (2.0 mL, Supelco Analytical) equipped with a magnetic bar, and sensors for both temperature and pressure control. The amine (1 mmol) was added to the catalyst suspension (19.2 mg, 2 x 10^{-3} mmol Ir) in alcohol (1 mL). The reactor was hermetically sealed and heated at 80-120 °C under continuous stirring. Small liquid aliquots (≈10 µl) were taken. The progress of the reaction was monitored by using GC-MS. After disappearance of the amine, the reaction

mixture was cooled to room temperature (RT). The catalyst was removed by filtration and rinsed with ethyl acetate; the removal of solvent in vacuum yielded a crude residue. All the products were identified on the basis of NMR and mass spectral data.

The recycling of Zr-[LIr]BF_4-MOF

After completion of the reaction, the catalyst was recovered through the separation of solid Ir-MOF from the liquid by extensive centrifugation. The recovered catalyst was washed thruce with CH_2Cl_2 and then ether, and finally the catalyst was dried at 100 °C for 12 h and reused. The Zr-[LIr]BF_4-MOF catalyst showed consistent activity for five cycles.

The hot filtration test of Zr-[LIr]BF_4-MOF catalyst

A mixture of Zr-[LIr]BF_4 (2.4 mg, 2 x 10^{-4} mmol Ir), amine (2.2 µL, 0.02 mmol), and alcohol (1.0 mL) was placed in a closed glass reactor (2.0 mL, Supelco) and stirred vigorously at 80 °C for 30 min. The conversion was approximately 30%. Then, the solid catalyst was quickly separated after filtration of the reactant mixtures. And the liquid was kept at 80 °C under vigorous stirring for 2 h. The conversion was 32%. The conversion of the blank thermal reaction without any catalyst for this reaction at 80 °C was approximately 2%.

2.5.3.3. Synthesis of secondary amines

Selective domino hydrogenation of nitroaromatics in the presence of aldehydes was performed in a closed glass microreactor (2.0 mL, Supelco) equipped with a magnetic bar, and sensors for both temperature and pressure control. The reactor had also connections to allow gas supply, and also an outlet for samples to be taken at different time intervals. The reactants nitroarene (2.2 µL for nitrobencene, 0.02 mmol)) and aldehyde (3.5 µL for benzaldehyde, 0.03 mmol) were added to the suspension of catalyst (2.4 mg, 2 x 10^{-4} mmol iridium) in isopropanol (1 mL). The reactor was hermetically sealed, pressurized with hydrogen at six bars, and heated at 100 °C under continuous stirring. Small liquid aliquots (≈100 µl) were taken. The progress of the reaction was monitored by GC-MS. The reaction mixture was filtered, and the solvent was removed under reduced pressure to give the crude product. It

was purified by column chromatography on silica gel using hexane-ethyl acetate mixture as eluent.

The recycling of IRMOF-3-LIr, ZrMOF-LIr in the domino reaction

The stability of MOF-Ir was investigated in the selective formation of secondary amines. IRMOF-3-LIr decomposes after 1 run (annexes) whereas ZrMOF-LIr was recovered unaltered after at least 4 run (annexes).
After completion of the reaction, the catalyst was recovered by the separation of solid Ir-MOF from liquid after an extensive centrifugation. Washing the recovered catalyst with CH_2Cl_2 for three times and then ether, the catalyst was dried at 60 °C for 12 h and reused. The ZrMOF-LIr catalyst showed consistent activity for four cycles.

The hot filtration test of ZrMOF-LIr catalyst
A mixture of ZrMOF-LIr (2.4 mg, 2 x 10^{-4} mmol Ir), nitrobenzene (2.2 µL, 0.02 mmol), benzaldehyde (3.5 µL, 0.03 mmol), and isopropanol (1.0 mL) was put into a closed glass reactor (2.0 mL, Supelco) and was extensively stirred (*ca.* 1000 rpm) at 100 °C for 2 h. The conversion is 20%. Then, the solid catalyst was quickly separated after filtration of the reactant mixtures. And the liquid was kept at 100 °C with extensively stirring for 24 h. The conversion was 22%. It is found that the blank thermal reaction without any catalyst for this reaction at 100 °C is *ca.* 2% (annexes).

2.5.3.4. Zr base catalyzed condensation with Rh-catalyzed hydrogenation

Knoevenagel-type condensation reactions: The condensation reaction between benzaldehyde and ethyl nitroacetate with Zr-BDC-NH_2 and Zr-BPDC-NH_2 derivatives as catalysts was performed in a magnetically stirred round bottom flask. A mixture of catalyst (15 mg, 5 mol%), benzaldehyde (0.2 mL, 1.9 mmol), was placed into a 15 mL flask. The reactants in the flask were stirred for 5 min to disperse the Zr-MOF. Ethyl nitroacetate (23 mg, 1.8 mmol) was then added, and the resulting mixture was stirred at 100 °C. Reaction conversion was monitored by withdrawing aliquots from the reaction mixture at different time intervals, filtering through a short silica gel pad, analyzing by using GC-MS. Finally, the reaction mixture was filtered and the solvent was removed under reduced pressure to give the crude product. The crude product

was purified by column chromatography on silica gel using hexane-ethyl acetate mixture as an eluent. The Zr-MOF catalyst was separated from the reaction mixture by simple centrifugation, washed with toluene, dried under vacuum, and reused. For the leaching test, a catalytic reaction was stopped after 4 h, analyzed by using GC, and centrifuged to remove the solid catalyst. The reaction solution was then stirred for 24 h.

Cascade reactions:

1) Two-step reaction: Glass reactor + Autoclave Engineers device: The condensation reaction was performed as described above in the presence of Zr-BDC-NH_2-L2Rh as catalyst (1 mol% based on Rh or containing Rh). Upon the completion of the reaction, the content was transferred to an autoclave reactor. Then, we added toluene (40 mL), purged with nitrogen, and pressurized with hydrogen (80 °C, 6 bar).

2) One-pot reaction: The condensation reaction was performed as described above in presence of the Zr-BDC-NH_2-L2Rh catalyst (1 mol% based on Rh or containing Rh). Upon the completion of the reaction, hydrogen (6 bar) was introduced and the progress of reaction was followed by using GC-MS. The one-pot reaction was also performed in an Autoclave Engineers device.

Recycling Experiments: At the end of the process, the reaction mixture was centrifuged and the catalyst residue washed to completely remove any remaining products and/or reactants. The solid was reused, and any change in the catalytic activity was observed.

Chapter 3

Mixed-metal MOFs

3.1. Introducción

Introduction of various metal cations in metal-organic frameworks provides an interesting strategy to tune the properties of porous materials towards practical applications. Mixed-metal MOFs may be synthesized by direct synthesis under solvothermal conditions, by post-synthesis metal exchange (PSE),[172] or by secondary building unit rational design.[173]

The metathesis of metal ions or ligands from MOFs has been previously reported.[174] This strategy has important implications for the stability and easier preparation of these materials, been named as post-synthetic exchange. Cation and anion exchange reactions have been observed with nanoparticles[175] and other materials,[176] but observation of such phenomena in MOFs is relatively recent. For example, the exchange of cations in MOF occurs[177] by exposure to solutions containing metal ions, finding that ion exchange of the metals at the secondary building units occurs without significant changes in the framework structure.

Titanium MOFs is one of the most interesting candidates due to the large abundance of the metal, its cheap price, low toxicity and photocatalytic properties. However, to date, scarce porous titanium MOFs have been reported, except MIL-125[178] and NTU-9.[179] The difficulties to synthesize

[172] Y. Han, J.-R. Li, Y. Xie and G. Guo *Chem. Soc. Rev.* **2014**, *43*, 5952-5981.
[173] S. Wongsakulphasatch, F. Nouar, J. Rodriguez, L. Scott, C. Le Guillouzer, T. Devic, P. Horcajada, J. M. Greneche, P. L. Llewellyn, A. Vimont, G. Clet, M. Daturi and C. Serre *Chem. Commun.* **2015**, *51*, 10194-10197.
[174] M. Kim, J. F. Cahill, Y. Su, K. A. Prather and S. M. Cohen *Chem. Sci.* **2012**, *3*, 126-130; C. K. Brozek and M. Dinca *Chem. Soc. Rev.* **2014**, *43*, 5456-5467.
[175] D. H. Son, S. M. Hughes, Y. Yin and A. Paul Alivisatos *Science* **2004**, *306*, 1009-1012.
[176] J. a. Zhao, L. Mi, J. Hu, H. Hou and Y. Fan *J. Am. Chem. Soc.* **2008**, *130*, 15222-15223; H. Fei, M. R. Bresler and S. R. J. Oliver *J. Am. Chem. Soc.* **2011**, *133*, 11110-11113; H. Fei, C. H. Pham and S. R. J. Oliver *J. Am. Chem. Soc.* **2012**, *134*, 10729-10732.
[177] S. Das, H. Kim and K. Kim *J. Am. Chem. Soc.* **2009**, *131*, 3814-3815; T. K. Prasad, D. H. Hong and M. P. Suh *Chem. Eur. J.* **2010**, *16*, 14043-14050; Z. Zhang, L. Zhang, L. Wojtas, P. Nugent, M. Eddaoudi and M. J. Zaworotko *J. Am. Chem. Soc.* **2012**, *134*, 924-927; G. Mukherjee and K. Biradha *Chem. Commun.* **2012**, *48*, 4293-4295; Q. Yao, J. Sun, K. Li, J. Su, M. V. Peskov and X. Zou *Dalton Trans.* **2012**, *41*, 3953-3955; H. Wang, W. Meng, J. Wu, J. Ding, H. Hou and Y. Fan *Coord. Chem. Rev.* **2016**, *307, Part 2*, 130-146.
[178] M. Dan-Hardi, C. Serre, T. Frot, L. Rozes, G. Maurin, C. Sanchez and G. Férey *J. Am. Chem. Soc.* **2009**, *131*, 10857-10859.

titanium MOFs directly prompted to search for new synthetic strategies. Interestingly, PSE could be considered an alternative to obtain certain Ti-MOFs that cannot or are difficult to be directly synthesized.

Recently, it has been reported that a series of porous titanium MOFs can be successfully synthesized by this PSE strategy.[180] The incorporation of the smaller Ti atom in the water and high temperature stable Zr-based UiO-66, enhances adsorption capacity[181] and maintains the very high thermal, chemical[182] and structural stability of UiO-66 during water adsorption/desorption cycles.[183] Ti-UiO-66 also shows exceptional gas permeability in mixed matrix membranes.[184] Moreover, Cohen *et al*. have reported that a mixed-ligand (terephthalic acid / 2-aminoterephthalic acid), mixed-metal (Zr-Ti) UiO-66-derivative results an effective photocatalyst for CO_2 reduction under visible light irradiation.[185] Ti-substituted (Zr-Ti) UiO-66-NH_2 also showed enhanced photocatalytic performance via a Ti-mediated electron transfer mechanism.[186]

In the first part of this chapter, a facile preparation of a series of Zr(Ti)-MOFs by introduction of Ti(IV) ions into the Zr-frameworks with mixed-ligands will described and the resultant mixed-ligand, mixed-metal Zr(Ti)-MOFs will be tested in terms of maintain thermal, chemical and structural stability. The resultant materials will be evaluated as Lewis acid catalysts for cascade reactions involving the Meerwein-Ponndorf-Verley (MPV) reduction followed by etherification, reactions of cyclization of citronellal, and isomerization of α-pinene oxide.

---

[179] J. Gao, J. Miao, P.-Z. Li, W. Y. Teng, L. Yang, Y. Zhao, B. Liu and Q. Zhang *Chem. Commun.* **2014**, *50*, 3786-3788.
[180] M. Kim, J. F. Cahill, H. Fei, K. A. Prather and S. M. Cohen *J. Am. Chem. Soc.* **2012**, *134*, 18082-18088.
[181] C. Hon Lau, R. Babarao and M. R. Hill *Chem. Commun.* **2013**, *49*, 3634-3636.
[182] V. Bon, V. Senkovskyy, I. Senkovska and S. Kaskel *Chem. Commun.* **2012**, *48*, 8407-8409.
[183] Q. Yang , H. Jobic, F. Salles, D. Kolokolov , V. Guillerm, C. Serre and G. Maurin *Chem. Eur. J.* **2011**, *17*, 8882-8889.
[184] S. J. D. Smith, B. P. Ladewig, A. J. Hill, C. H. Lau and M. R. Hill *Sci. Rep.* **2015**, *5*, 7823.
[185] Y. Lee, S. Kim, J. K. Kang and S. M. Cohen *Chem. Commun.* **2015**, *51*, 5735-5738.
[186] D. Sun, W. Liu, M. Qiu, Y. Zhang and Z. Li *Chem. Commun.* **2015**, *51*, 2056-2059.

Ce is another attractive candidate for substitution of Zr into UiO-66 derivatives: Ce^{4+} adopts eight coordination in its common oxide CeO_2, and the properties of CeO_2-ZrO_2 solid solutions are well established in redox catalysis and for their oxygen storage properties.[187] In the literature we can found mixed lanthanide frameworks with highly tuneable luminiscent properties[188], and some examples of Ce(III) doped Zr-based MOFs for NO_2 adsorption,[189] catalytic decomposition of methanol into CO_2[190] and aerobic oxidation of benzyl alcohol.[191]

In the second part of this chapter, we described the synthesis of bimetallic Zr(Ce)-MOFs by direct synthesis under solvothermal conditions. These materials were applied as catalyst in the direct synthesis of imines from alcohols and amines.

[187] R. D. Monte and J. Kaspar *J. Mater. Chem.* **2005**, *15*, 633-648.
[188] K. A. White, D. A. Chengelis, K. A. Gogick, J. Stehman, N. L. Rosi and S. Petoud *J. Am. Chem. Soc.* **2009**, *131*, 18069-18071.
[189] A. M. Ebrahim and T. J. Bandosz *ACS Appl. Mater. Interfaces* **2013**, *5*, 10565-10573.
[190] F. Nouar, M. I. Breeze, B. C. Campo, A. Vimont, G. Clet, M. Daturi, T. Devic, R. I. Walton and C. Serre *Chem. Commun.* **2015**, *51*, 14458-14461.
[191] M. Lammert, M. T. Wharmby, S. Smolders, B. Bueken, A. Lieb, K. A. Lomachenko, D. D. Vos and N. Stock *Chem. Commun.* **2015**, *51*, 12578-12581.

3.2. Objectives

- Synthesis of bimetallic Zr(Ti)-MOFs by a post-synthesis method and Zr(Ce)-MOFs by direct synthesis. Characterization of the obtained materials.

- Study of the catalytic activity of Zr(Ti) MOFs in three different reactions: cascade Meerwein-Ponndorf-Verley (MPV) reduction and etherification, cyclization of citronellal and isomerization of α-pinene oxide.

- Study of Catalytic activity of Zr(Ce)-MOFs for the direct synthesis of imines from alcohols and amines.

- Recycling experiments.

3.3. Results and Discussion

3.3.1. Synthesis and characterization of the Zr(Ti) MOFs

Ti(IV) would be attractive as a lighter, highly oxophilic metal that should impart a lower density with improved stability as well as unique photochemical properties.[192] Scarce Ti-based MOFs have been reported, and in general they react easily with water and oxygen.[179193] Thus, the introduction of the Ti(IV) cation into the highly stable UiO-MOFs (Zr-BDC, Zr-BPDC, Zr-NDC and the corresponding mixed-carboxylic acid-amino carboxylic acid-ligands) was an attractive challenge (Scheme 3.1 shows an illustration of titanium incorporation into Zr(NDC)-MOFs).

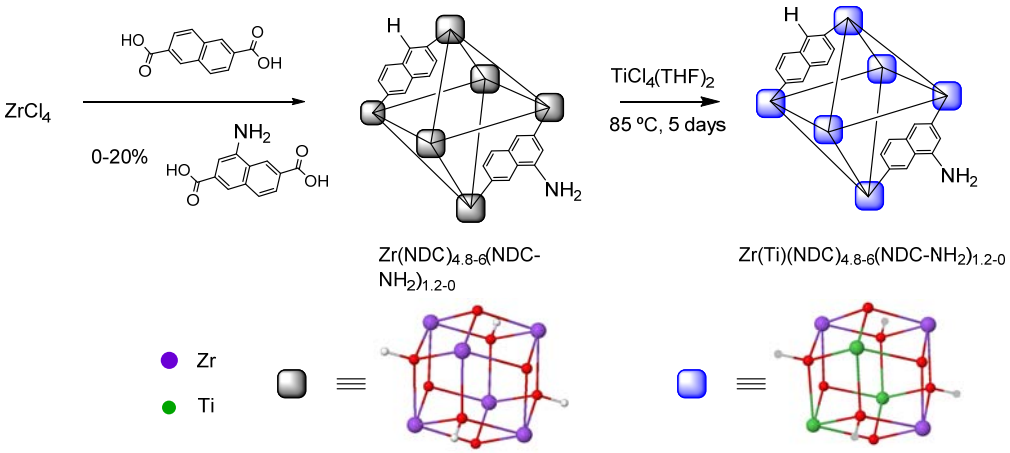

Scheme 3.1. Synthesis of Zr(Ti)NDC-MOFs.

Zr(Ti)-MOFs were prepared by exposure of the parent Zr-MOFs[89b] ($Zr_6O_4(OH)_4(R\text{-}COO_2)_6$ ($R\text{-}COO_2$ is BDC, NDC or BPDC) to dimethylformamide (DMF) solutions of $TiCl_4(THF)_2$ (THF: tetrahydrofurane) for 5 days at 85 °C.[181] After removing the solid by centrifugation and washing with fresh DMF and THF, the amount of statistical incorporated Ti(IV) was quantified by scanning

[192] N. N. Greenwood and A. Earnshaw *Chemistry of the Elements*, Vol.; Elsevier Science, **2012**.
[193] Y. Fu, D. Sun, Y. Chen, R. Huang, Z. Ding, X. Fu and Z. Li *Angew. Chem. Int. Ed.* **2012**, *51*, 3364-3367.

electron microscopy-energy dispersive X-ray analysis (SEM-EDX) and total X-ray fluorescence (TXRF) spectroscopy and the Zr/Ti ratio were 3.1 for Zr(Ti)-BDC-NH_2, 3.0 for Zr(Ti)-BPDC-NH_2, 2.5 for Zr(Ti)-NDC-NH_2 and 2.6 for Zr(Ti)-NDC (annexes). The results give metal compositions of $Zr_{4.5}Ti_{1.5}$ for Zr(Ti)-BDC-NH_2, $Zr_{4.4}Ti_{1.6}$ for Zr(Ti)-BPDC-NH_2, $Zr_{4.3}Ti_{1.7}$ for Zr(Ti)-NDC-NH_2 and $Zr_{4.4}Ti_{1.6}$ for Zr(Ti)-NDC. For mixed ligands-MOFs, the ratio between ligands was obtained by elemental analysis of nitrogen and confirmed by UV-visible spectroscopy and corresponds to a 20% of amino ligand content. FTIR spectra of NH_2-derivatives confirm the absence of DMF by the absence of their well-defined ν(C=O) band at 1660 cm^{-1} (annexes). Zr(Ti)-NDC show in the FTIR spectra the characteristic ν(Zr-O) bands at 682, 642 cm^{-1} and ν(Ti-O) at 665 cm^{-1} (annexes).

^{1}H NMR of digested Zr-NDC-MOFs confirmed the presence of both NDC and NDC-NH_2 linkers (annexes). Hydrofluoric acid was employed to digest the materials, because of the high affinity of Zr for fluoride. Electrospray ionization-mass spectrometry (ESI-MS) of digested Zr-MOFs was also performed (annexes).

The Zr(Ti)-MOFs shows excellent crystallinity, as evidenced by the powder X-ray difraction (PXRD) (Fig. 3.1). The good agreement between the XRD patterns of UiO-(Zr/Ti) and UiO-(Zr) indicates that the framework of parent Zr-MOF is not collapsed and rules out the possibility of the formation of Ti-based impurities; moreover, no diffraction peaks belonged to other titanium species could be observed. As observed, peaks in XRD patterns of Zr(Ti)-BDC-NH_2 shifted to higher reflection angles (2θ = 7.41) as compared to original Zr-BDC-NH_2, (2θ = 7.28), the 2θ value in Zr(Ti)-BPDC-NH_2 shifts from 5.77 to 5.80 and Zr(Ti)-NDC from 6.43 to 6.55 (from 6.30 to 6.36 for Zr(Ti)-NDC-NH_2) (annexes). This is also observed over inorganic solid solutions indicating that smaller Ti(IV) ion (0.605 Å) substitutes a larger Zr(IV) ion (0.72 Å) in Zr-O oxo-clusters.[194] Thus, we have obtained bimetallic Zr(Ti)-UiO based MOFs with very good stability and crystallinity. Hereafter we will only study the Zr-NDC series.

[194] Y.-F. Li, D. Xu, J. I. Oh, W. Shen, X. Li and Y. Yu *ACS Catal.* **2012**, *2*, 391-398; P. Jaiban, A. Rachakom, S. Jiansirisomboon and A. Watcharapasorn *Nanoscale Res. Lett.* **2012**, *7*, 1-5.

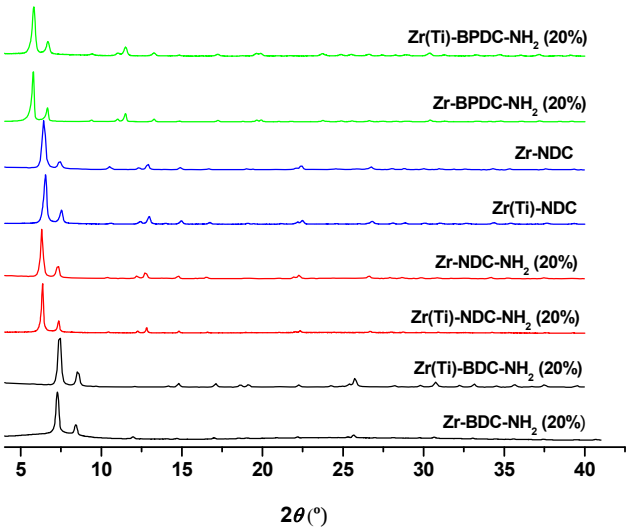

Figure 3.1. PXRD patterns of UiO- and Zr(Ti)-MOFs.

The X-ray photoelectron spectroscopy (XPS) of the elements of interest, Zr 3d and Ti 2p, are shown in Fig. 3.2. Fig. 3.2a presents the Ti 2p region showing two peaks at 458.7 eV and 464.5 eV, corresponding to Ti $2p_{3/2}$ and Ti $2p_{1/2}$ respectively, providing another confirmation of the successful incorporation of the Ti moiety in Zr-NDC. The spin energy separation is 5.8 eV. The peak position of Ti^{4+} is consistent with Ti^{4+} in an octahedral coordination environment.[195] The Zr 3d was shown in Figure 3.2b with two peaks at 182.7 and 185 eV, due to Zr $3d_{5/2}$ and Zr $3d_{3/2}$. These data are ver similar to that previously described for UiO66(Ti)-NH_2[187] and UiO66(Ti).[196]

[195] H. G. T. Nguyen, L. Mao, A. W. Peters, C. O. Audu, Z. J. Brown, O. K. Farha, J. T. Hupp and S. T. Nguyen *Catal. Sci. Technol.* **2015**, *5*, 4444-4451; F. Hayati, S. Chandren, H. Hamdan and H. Nur *Bull. Chem. React. Eng. & Catal.* **2014**, *9*, 28-38; L. Xu, D.-D. Huang, C.-G. Li, X. Ji, S. Jin, Z. Feng, F. Xia, X. Li, F. Fan, C. Li and P. Wu *Chem. Commun.* **2015**, *51*, 9010-9013.

[196] A. Wang, Y. Zhou, Z. Wang, M. Chen, L. Sun and X. Liu *RSC. Adv.* **2016**, *6*, 3671-3679.

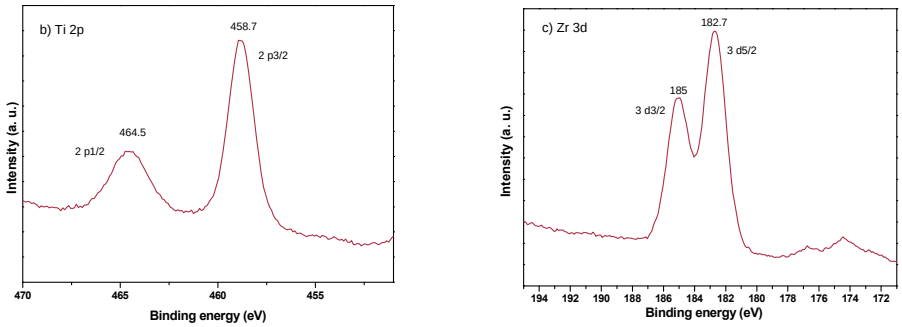

Figure 3.2. XPS spectra of Zr(Ti)-NDC-MOF: (a) Ti 2P and (b) Zr 3d regions.

The thermogravimetric analysis (TGA) of Zr(Ti)-NDC showed a high thermal stability with a thermal decomposition temperature similar to that of the parent Zr-NDC (>400 °C, annexes).

The porosity was investigated by the BET analysis (N_2, 77K) of Zr(Ti)-NDC (1068 $m^2 \cdot g^{-1}$ which is comparable to that of the parent Zr-NDC: ~1062 $m^2 \cdot g^{-1}$) (Table in annexes). PXRD patterns collected after the N_2 sorption experiments indicate that all other samples remain intact after activation; although some peak broadening was observed (annexes).

Similar to parent Zr-NDC and Zr-NDC-NH_2, the UV-visible diffuse-reflectance spectra of Zr(Ti)-NDC and Zr(Ti)-NDC-NH_2 also show two main absorption peaks at around 290 and 350 nm (Figure 3.3). However, the peak at 350 nm, corresponding to the absorption of Zr-O clusters is broader,[187,197] that could be attributed to the absorption of new Ti-O oxo-clusters (annexes). In addition to the peak at 350 nm, a shoulder peak extending to ca. 400 nm also appears in Zr-NDC-NH_2 and Zr(Ti)-NDC-NH_2 which can be assigned to the amino group. A new band at 650 nm is also observed for Zr(Ti)-NDC-NH_2 probably due to a charge transferThese results indicate that Ti(IV) has been successfully incorporated in Zr-NDC and Zr-NDC-NH_2 MOFs.

The solid-state photoluminescence spectra of the Zr-NDC compounds were studied at room temperature. As shown in Figure 3.3, with excitation at 350 nm, the emission wavelength of the Zr-NDC[198] is red-shifted to 405 nm (475 nm for Zr-NDC-NH_2), while in the case of Zr(Ti)-NDC the emission wavelength

appears at 424 nm (504 nm for Zr(Ti)-NDC-NH_2). Thus, the introduction of a functional group (-NH_2) on the organic ligand, and other metal as Ti improved the luminescent behavior.

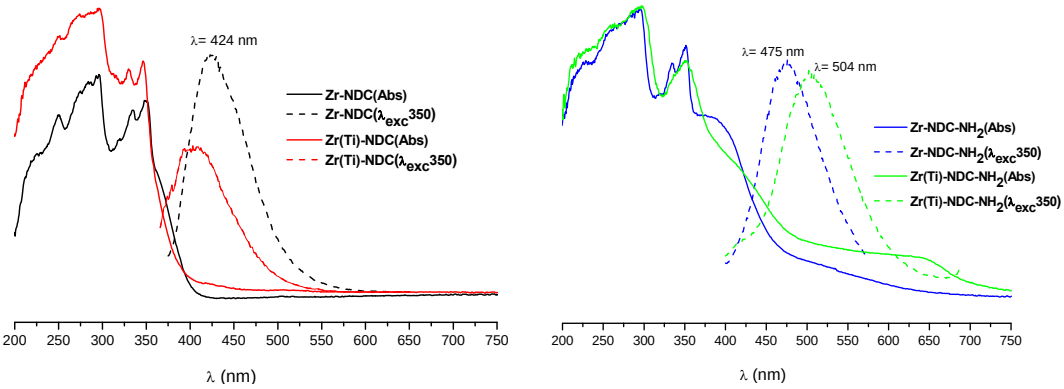

Figure 3.3. The solid-state UV-Visible absorption and emission spectra of Zr-NDC-compounds.

^{13}C CP/MAS-NMR spectra of evacuated Zr(Ti)-NDC samples (Figure 3.4) showed clearly all signals corresponding to the linkers at 172-171 (COO), 134.8-134.6 (CCOO), 132.8-132.5, 130.2-130.0, 127.4-127.1, and 125.7-125.4 ppm which are characteristic of the unique carbon atoms of NDC and NDC-NH_2 links, respectively, **C**-NH_2 resonance (for the mixed linker compounds) do not appears possibly due to their poor relaxation.

The morphology of Zr-NDC and Zr-NDC-NH_2 reveal some changes on the surface of crystals (from the defects by replacing a 8-coordinated Zr(IV) ion for an 6-coordinated Ti(IV) ion) although the reaction was performed at a temperature below 85 °C (annexes).

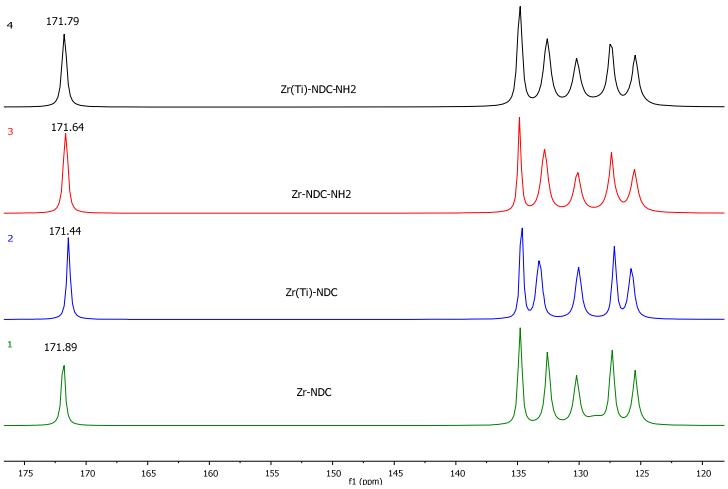

Figure 3.4. ^{13}C NMR of 1) Zr-NDC; 2) Zr(Ti)-NDC; 3) Zr-NDC-NH_2; 4) Zr(Ti)-NDC-NH_2.

3.3.2. Synthesis and characterization of the Zr(Ce) MOFs

The introduction of cerium can provides us redox properties in the framework. The synthesis of Zr(Ce)MOFs was carried out with BDC, BPDC and NDC as linkers to obtain different pore size materials. In order to obtain mixed-metal and mixed-linker MOFs, we have introduced different amount of NH_2-linker. Thus, we can observed how the reactivity changes depending on the functionalization of the linker and the amount of Ce in the structure. Zr(Ce)MOFs has been synthesized by direct synthesis under solvothermal conditions in a teflon lined vessel at 120 °C for 24 h (Scheme 3.2).[191] The amount of incorporated Ce was quantified by TXRF spectroscopy and the ratio Zr/Ce were 2.74 for ZrCe(20)-BDC-NH_2(100), which corresponds to a metal composition of $Zr_{4.4}Ce_{1.6}$. The amount of -NH_2 groups in the structure was calculated by elemental analysis of nitrogen (annexes).

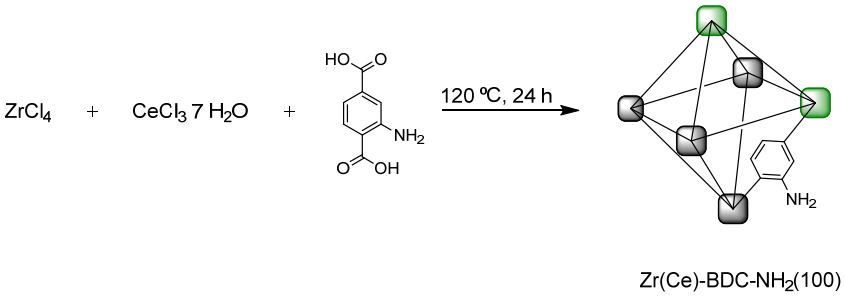

Scheme 3.2. Synthesis of ZrCe-BDC-NH_2(100) MOF by direct synthesis.

As observed in XRD patterns of ZrCe-BDC-NH_2(100) show peaks shifted to lower reflection angles compared to original Zr-MOFs. The value 2θ shifts from 7.39 to 7.32. New and distinct peaks are revealed on the diffraction pattern when the amount of Ce incorporated is bigger (2θ = 9.7 and 9.9), and they show the structural effect of the incorporation of Ce^{+3} in the Zr-MOF matrix. They might correspond to pure Ce-MOFs and the presence of several Ce species, such as $Ce(OH)_3$, $Ce(CO_3)_3$, and CeO_2. It is hypothesized that these new features are the result of the interactions of Ce with the Zr-O center or the organic linker via π-complexation or a chelation process (Figure 3.5)

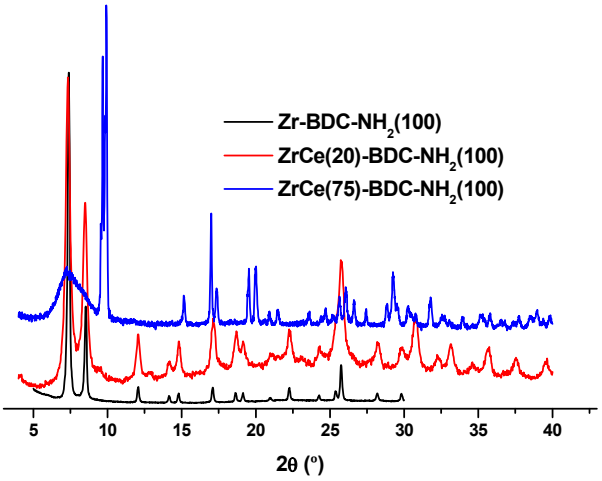

Figure 3.5. PXRD patterns of ZrCe-BDC-MOFs.

The thermogravimetric analysis shows a high thermal stability for these ZrCe compounds as we can observe in figure 3.6. The thermal decomposition of ZrCe(20)-BDC-NH_2(100) is lower (~ 350 °C) to that of Zr-MOFs

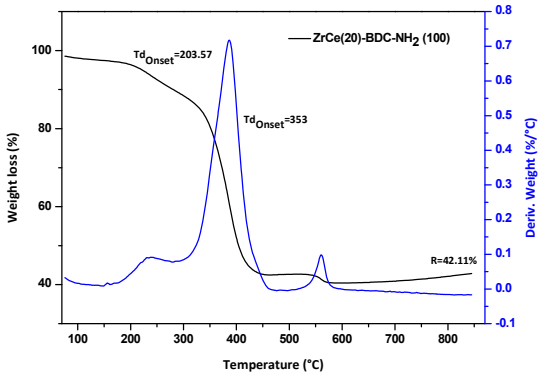

Figure 3.6. Thermograms of ZrCe-BDC-NH_2(100) MOF.

The BET surface areas was measured at 77 K under N_2, the surface is lower than the parent Zr-MOFs (333.15 $m^2 \cdot g^{-1}$), these results can be explained due to Ce^{3+} ion is bigger than Zr^{4+} ion. The isotherm is shown in figure 3.7. The UV-visible diffuse-reflectance spectra of ZrCe(20)-BDC-NH_2(100) shows two main absorption peaks 260 and 370 nm.

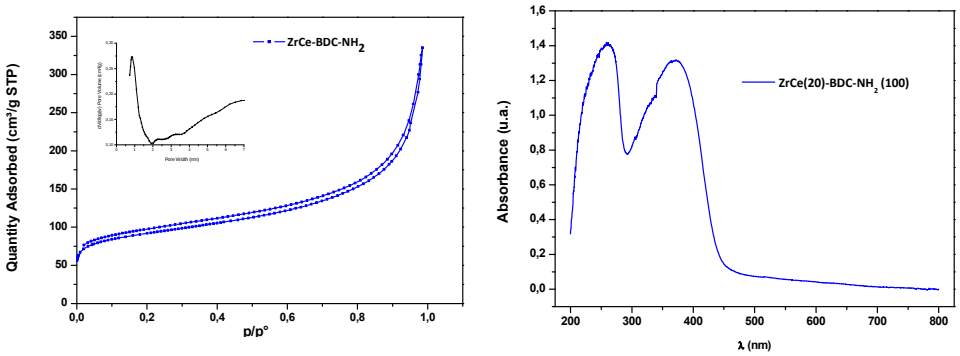

Figure 3.7. N_2 isotherm (left) and DRUV (right) of ZrCe-BDC-NH_2 MOF.

In order to know in which oxidation state is the cerium into the sample, XPS analysis was performed (Figure 3.8). The satellite peak located at the high

binding energy (around 917 eV) associated to the Ce 3d3/2, is characteristic of the presence of tetravalent Ce (Ce^{4+} ions) in Ce compounds. When tetravalent Cerium is abundant, the peak should be clearly visible. This satellite is not present in the sample. Therefore we can conclude that the Cerium Ce^{3+} specie is the most abundant in the material.

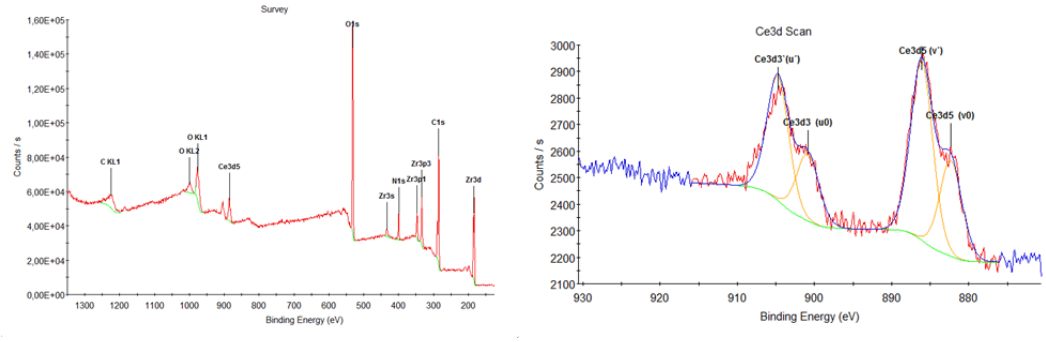

Figure 3.8. XPS spectra (survey scan) of of ZrCe-BDC-NH_2 MOF (left) and Ce region (right).

ZrCe-BDC-NH_2 MOF maintain a similar morphology to UiO-66 as can be observed from the TEM images (Figure 3.9).

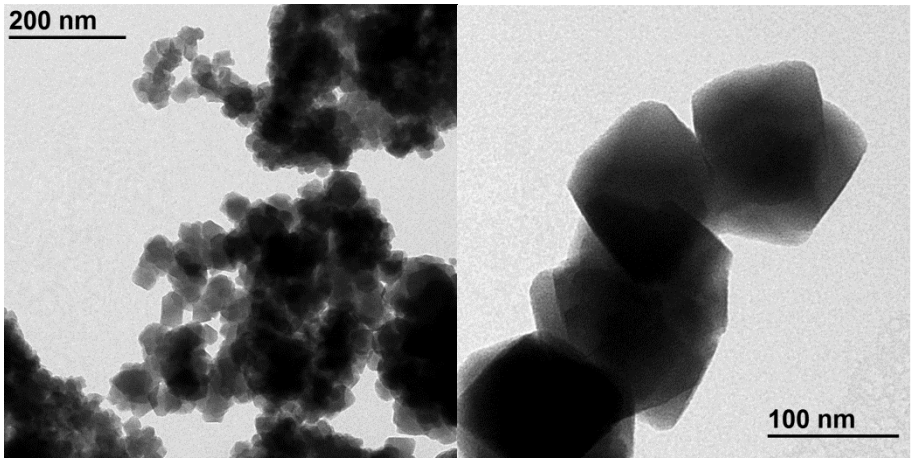

Figure 3.9. TEM images of ZrCe(20)-BDC-NH_2(100).

3.3.3. **Synthesis and characterization of the ZrCeTi MOFs**

At this point, we considered the possibility of achieve a trimetallic MOF in order to improve the acid and redox properties of the material. The synthetic route is shown in the scheme 3.3, the ZrCe-MOF is obtained by direct synthesis and then, by incorporation of titanium, the trimetallic material was obtained. The amount of each metal present in the structure was calculated by TXRF, obtaining compositions as $Zr_{4.2}Ce_{0.4}Ti_{1.4}$ for ZrCeTi-BDC-NH_2(100) and $Zr_{4.3}Ce_{0.2}Ti_{1.5}$ for ZrCeTi-NDC-NH_2(100). These results indicate that titanium is exchanged for the cerium which is in the structure. These are preliminary results, this project is still to be developed.

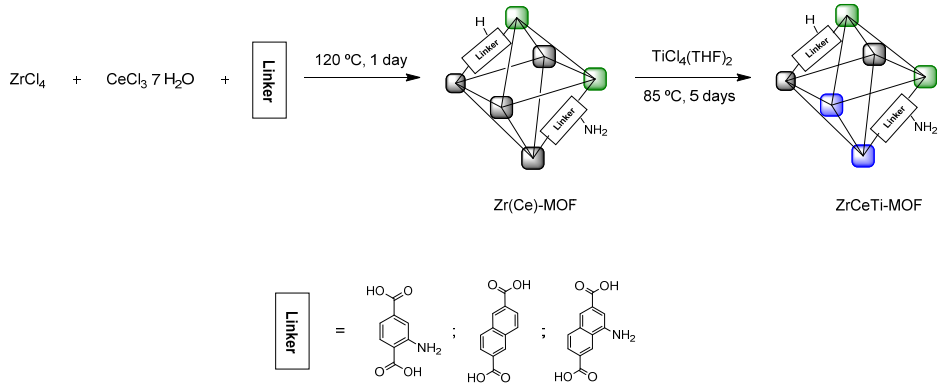

Scheme 3.3. Synthesis of ZrCeTi-MOFs.

3.3.4. Catalytic applications

3.3.4.1. Lewis acid catalyzed reactions with Zr(Ti)-MOFs

A recent work,[11] presents an extensive study in which the activity of MOFs has been compared, under the same reaction conditions, with their simple homogeneous representatives and other common inorganic-organic hybrid materials and inorganic solid catalysts to put into perspective the activity and selectivity of MOFs. This study shows that the preparation of mixed-multivariant-MOFs could be an alternative to the conventional Lewis acids catalysts. Based on this concept, now we study the influence of Ti on Zr-NDC-MOFs for catalyzing the cascade reaction involving the Meerwein-Ponndorf-Verley reduction of *p*-methoxybenzaldehyde with 2-butanol as hydrogen source (Scheme 3.4). Moreover they have also been studied in two acid-catalyzed model reactions, the carbon-carbon bond forming -Prins reaction (Scheme 3.5) and the isomerization of α-pinene oxide (Scheme 3.6).

To explore the Lewis acid sites, we investigated the ammonia temperature-programmed desorption (NH_3-TPD) (commonly used to determine the acidity of zeolites)[197] of the Zr-NDC and Zr(Ti)-NDC, indicating the presence of acid sites in the catalysts (Figure 3.10). Zr-NDC and Zr(Ti)-NDC showed weak to medium strength acidity.[198]

[197] N. Katada, H. Igi and J.-H. Kim *The Journal of Physical Chemistry B* **1997**, *101*, 5969-5977.
[198] J. Kim, S.-N. Kim, H.-G. Jang, G. Seo and W.-S. Ahn *Appl. Catal., A* **2013**, *453*, 175-180; T. Kajiwara, M. Higuchi, D. Watanabe, H. Higashimura, T. Yamada and H. Kitagawa *Chem. Eur. J.* **2014**, *20*, 15611-15617.

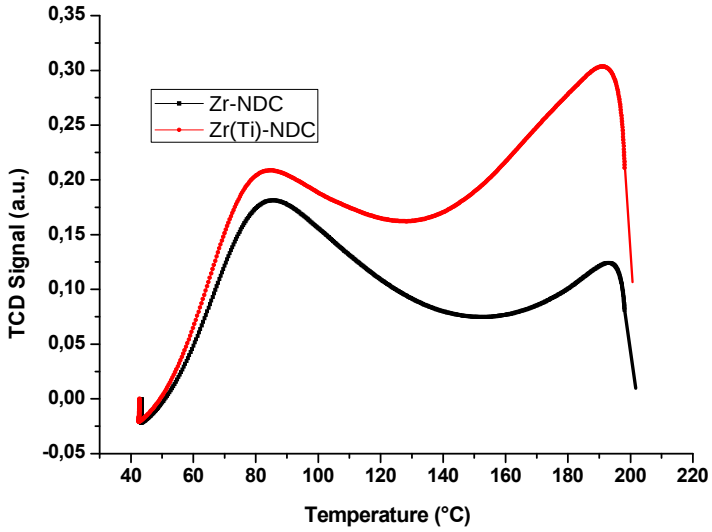

Figure 3.10. NH_3-TPD profiles of Zr-NDC and Zr(Ti)-NDC.

3.3.4.1.1. Cascade Meerwein-Ponndorf-Verley (MPV) reduction and etherification.

Etherification of oxygenated organic compounds is a fundamental organic transformation for the synthesis of fine chemicals.[199] 4-methoxybenzyl 1-methylpropyl ether (Scheme 3.4) has a fruity pear odor and is a potential fragrance compound, which is commercially prepared by etherification of 4-methoxybenzyl alcohol (which is obtained industrially by reduction of 4-methoxybenzaldehyde) with 2-butanol. Thus, the process requires two steps: a) the reduction of 4-methoxybenzaldehyde to the corresponding alcohol and b) the etherification reaction.[200] It would therefore be of interest to design a process that could carry out the aldehyde reduction and etherification in a one-pot process to produce the title ether in high yield and selectivity.[4c]

[199] O. Mitsunobu, in *Comprehensive Organic Synthesis*, Vol., Pergamon, Oxford, **1991**, pp. 1-31; C. Lee and R. Matunas, in *Comprehensive Organometallic Chemistry III*, Vol., Elsevier, Oxford, **2007**, pp. 649-693.

[200] K. Bauer, D. Garbe and H. Surburg *Common Fragrance and Flavor Materials: Preparation, Properties and Uses*, Vol.; Wiley, **2008**.

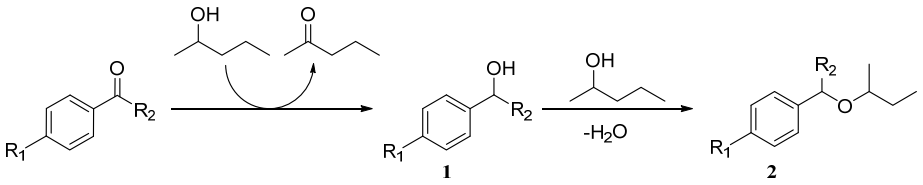

Scheme 3.4. Domino reaction of aldehydes with 2-butanol: MPV reduction of the aldehyde to alcohol with successive etherification.

Brønsted acids can catalyze the formation of ethers when starting from two alcohol molecules,[201] and sulfuric acid has been applied in homogeneous phase;[202] but are limited to primary ethers. In contrast, water stable Lewis acid catalysts as Sn- and Zr-containing silicate molecular sieves with framework single, isolated metal sites are active and selective for catalyzing MPV reduction of aldehydes as well as etherification of alcohols.[203] Thus, considering that Zr-NDC-MOFs show Lewis acidity, it could be of interest to find if they are able to promote efficiently the tandem reaction involving the MPV reduction of *p*-methoxybenzaldehyde with 2-butanol to *p*-methoxybenzyl alcohol, followed by its etherification with an excess of 2-butanol (Scheme 3.4), and how they compare with other solid Lewis acids such as Sn-, Zr-, Ta-Beta zeolites.[205,204]

Results in Table 3.1 show that the desired fragrance was obtained with Zr-NDC and Zr(Ti)-NDC, being the Zr(Ti) catalyst more active for the global process (yield > 90%). The linker NDC-NDC-NH_2 also has a beneficial effect on the final activity. The reaction proceeds under mild reaction conditions and all catalysts proved to be active for yielding the ether compound easyly with good yield. The selectivity for the one-pot process is high, and the desired ether was the only product observed. In this case, the intermediary alcohol rapidly reacts on the catalyst to give the corresponding ether. Substrate scope for the etherification reaction was explored by using Zr(Ti)-NDC as catalyst. Benzaldehyde readily reacted with 2-butanol to form the ether product 2,

[201] F. F. Roca, L. De Mourgues and Y. Trambouze *J. Catal.* **1969**, *14*, 107-113.
[202] L. Brandsma and J. F. Arens, in *The Ether Linkage (1967)*, Vol., John Wiley & Sons, Ltd. **2010**, pp. 553-615.
[203] A. Corma and M. Renz *Angew. Chem. Int. Ed.* **2007**, *46*, 298-300.
[204] A. Corma, F. X. Llabrés i Xamena, C. Prestipino, M. Renz and S. Valencia *J. Phys. Chem. C* **2009**, *113*, 11306-11315.

while aldehydes with electron withdrawing groups at the aromatic ring (see Table 3.1, entry 7) can be more difficult to react with Zr(Ti)-NDC.
Zr(Ti) is the most active catalyst for the both isolated reactions MPV reaction and etherification. When Zr-NDC was tested for their catalytic activity in the MPV reduction of cyclohexanone with 2-butanol it shows practically no activity and conversions of 5% were obtained after 1 h of reaction time. On the other hand, conversions of 20 and 60% were obtained with Zr(Ti) after 1 and 4 h of reaction time. When the etherification of 1-butanol with *p*-methoxybenzyl alcohol is carried out, 15 % conversion was observed for the Zr-NDC-catalyzed reaction and 83% for Zr(Ti)-NDC. These results together with our previous work,[205-206,205] indicate that in the case of domino reactions catalyzed by Lewis acid sites, MOFs offer the possibility to maximize the final yield by introducing more than one type of Lewis acid site in the framework. Indeed, a catalyst with Zr and Ti in the MOF maximize each one of two steps of the process to give the highest yield of the desired ether (see Table 3.1). A blank experiment with TiO_2 shows that it is inactive for this reaction and our experimental conditions (Table 3.1, entry 10).

Recycling experiments with Zr(Ti)-NDC-NH_2 catalyst show that the activity decreases after three cycles, and longer reaction times were necessary to obtain a high selectivity to the ether.

[205] A. Corma, M. a. T. Navarro and M. Renz *J. Catal.* **2003**, *219*, 242-246.

Table 3.1. Domino reaction of aldehydes with 2-butanol in the presence of Zr-NDC-catalysts.[a]

Entry	Catalyst	Aldehyde R	Conv. (h)	Selectivity (%)[b]	
				alcohol	ether
1	Zr(Ti)-NDC	OCH_3	90(4)	10	90
2	Zr(Ti)-NDC-NH_2	OCH_3	95(4)	-	100
3	Zr(Ti)-NDC-NH_2[c]	OCH_3	65(4) 98 (21)	1.5	98.5
4	Zr-NDC	OCH_3	19(4)	-	100
5	Zr-NDC-NH_2	OCH_3	30(4)	7	93
6	Zr(Ti)-NDC	H	97(4)	-	100
7	Zr(Ti)-NDC	F	85 (4)	58	42
8	Zr-Beta[205]	OCH_3	100 (8)	-	100
9	Sn-Beta[205]	OCH_3	71 (8)	-	100

[a] Reaction conditions: 0.16 mmol of aldehyde was dissolved in 1 mL of 2-butanol, a 5 mg sample of catalyst was added, and the reaction mixture was introduced on a MW oven (150 °C). Aliquots were taken periodically and analyzed by GC analysis. The conversions displayed were obtained after 4 h of reaction time. [b] Normalized to 100%. [c] Reaction mixture was stirred magnetically and heated to reflux.

3.3.4.1.2. Selective cyclization of citronellal to isopulegol

After it was established that the incorporation of titanium sites into the Zr-NDC-MOF network generates new Lewis acid catalysts, the performance of these materials was explored for the cyclization of citronellal to isopulegol (Scheme 3.5). For this reaction the diastereoselectivity is an important issue, since it is relevant for the preparation of menthol.[206] With homogeneous Lewis acid catalysts high diastereoselectivities may be obtained especially by using $ZnBr_2$ or aluminum tris(2,6-diphenylphenoxide).[207] Several solid acid materials for the above reaction have been also explored, such as zeolites containing isolated and well-defined Lewis acid centers, such as Sn and Zr atoms.[208,208]

[206] M. Boronat, A. Corma and M. Renz, in *Turning Points in Solid-State, Materials and Surface Science: A Book in Celebration of the Life and Work of Sir John Meurig Thomas*, Vol., The Royal Society of Chemistry **2008**, pp. 639-650.
[207] G. Heydrich, G. Gralla, K. Ebel and M. Friedrich, Vol. Ed.^(Eds., Google Patents **2011**.
[208] A. Corma and M. Renz *Chem. Commun.* **2004**, 550-551; M. Boronat, P. Concepcion, A. Corma, M. T. Navarro, M. Renz and S. Valencia *Phys. Chem. Chem. Phys.* **2009**, *11*, 2876-2884.

More recently MOF materials as $Cu_3(BTC)_2$[209] [BTC = benzene-1,3,5-tricarboxylate] or UiO-66(Zr)[210] yield also high diastereoselectivities to isopulegol.

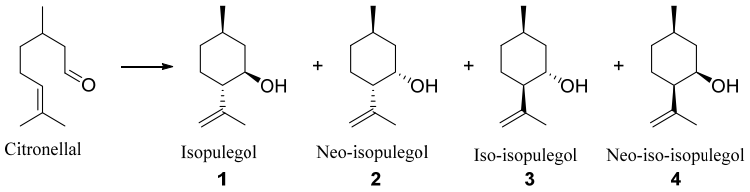

Scheme 3.5. Cyclization of citronellal to isopulegol and its isomers.

Here, the citronellal cyclization to isopulegol has been studied with Zr-NDC and Zr(Ti)-NDC catalysts and the results compared with those obtained with other MOFs and inorganic solid acids as MCM-41(Ti), and Sn-beta zeolite. (±) Citronellal was submitted to a Zr-NDCs-catalyzed Prins reaction at different temperatures and catalyst loadings in toluene (each catalyst was previously activated at 493 K). Results in Table 3.2, show that in all cases, the selectivity for the four diastereomeric pulegols with respect to other products was > 98% and selectivity for the desired isopulegol diastereomer was in the order of 65-75% with respect to the other three diastereomers.

Zr(Ti)-NDC shows better performance than Zr-NDC at different temperatures and catalyst loading. For these heterogeneous catalysts, the diastereoselectivity for (±)-isopulegol decreased slightly at higher temperatures, although the overall selectivity to cyclization improved (Table 3.2). Zr-MOFs with NDC-NH_2 linker are less active than NDC-derivatives. The cyclization of citronellal also proceeds smoothly without any solvent being the rate of reaction higher without solvent, which could be explained by a dilution effect. The diastereoselectivity for (±)-isopulegol was similar without solvent and in toluene, 63 and 66%, respectively. Under the same reaction conditions $Cu_3(BTC)_2$ shows a similar selectivity than Zr(Ti)-NDC catalysts. A comparison

[209] L. Alaerts, E. Séguin, H. Poelman, F. Thibault-Starzyk, P. A. Jacobs and D. E. De Vos *Chem. Eur. J.* **2006**, *12*, 7353-7363; M. Vandichel, F. Vermoortele, S. Cottenie, D. E. De Vos, M. Waroquier and V. Van Speybroeck *J. Catal.* **2013**, *305*, 118-129.

[210] F. Vermoortele, B. Bueken, G. Le Bars, B. Van de Voorde, M. Vandichel, K. Houthoofd, A. Vimont, M. Daturi, M. Waroquier, V. Van Speybroeck, C. Kirschhock and D. E. De Vos *J. Am. Chem. Soc.* **2013**, *135*, 11465-11468.

with data from literature for other MOF catalysts ($Cu_3(BTC)_2$, UiO-66, MIL-101(Cr), MOF-808-SO_4) reveals that Zr(Ti)-NDC displays similar rates and selectivities (Table 3.2). A comparison with other solid molecular sieve inorganic catalyst such as MCM-41(Ti) and Sn-beta shows that the inorganic solids are more active and Sn-beta presents better diastereoselectivity (83%).

Table 3.2. Selectivities to isopulegol obtained with different Zr-NDC-catalysts samples in toluene.[a]

Entry	Catalyst	T (°C)	Cat. (mg)	Conv. (%)	Sel.[b] (%)	Diastereosel.[c] (%)
1	Zr-NDC	100	10	47	99	68
2	Zr(Ti)-NDC	100	10	48	99	75
3	Zr-NDC	100	20	60	99	62
4	Zr(Ti)-NDC	100	20	90	99	69
5	Zr-NDC	150	5	58	98	69
6	Zr(Ti)-NDC	150	5	82	98	71
7	Zr-NDC-NH_2	150	5	56	99	60
8	Zr(Ti)-NDC-NH_2	150	5	65	99	62
9	Zr-NDC (untreated)	150	5	45	99	74
10	Zr(Ti)-NDC (untreated)	150	5	57	99	76
11	UiO-66-NH_2	150	5	15[d]	99	72
12	$Cu_3(BTC)_2$	150	5	50[d]	99	73
13	MCM-41(Ti)	150	5	90[d]	99	70
14	Sn-beta[210a]	80	50	>99	>98	83
15	Ti-Beta[210a]	80	50	35	>98	56
16	$Cu_3(BTC)_2$[211a]	110	100	80	-	65
17	UiO-66[165]	100	-	20	-	75
18	UiO-66-NH_2[165]	100	-	20	-	75
19	MIL-101(Cr)[115b]	80	-	>99	>99	74
20	MOF-808-1.3SO_4[211]	60	-	97	-	67
21	Zr-TUD-1[212]	80	-	99.6	99.6	65

[a] Reactions were carried out in toluene with citronellal (0.3mmol, 58 µL) added to 5, 10, 20 mg of catalyst preactivated at 200 °C, reaction time: 24 h. [b] Selectivity for the four diastereomeric pulegols with respect to other products. [c] Selectivity for the isopulegol diastereomer with respect to the other three diastereomers. [d] This work.

[211] J. Jiang, F. Gándara, Y.-B. Zhang, K. Na, O. M. Yaghi and W. G. Klemperer *J. Am. Chem. Soc.* **2014**, *136*, 12844-12847.

[212] A. Ramanathan, M. C. Castro Villalobos, C. Kwakernaak, S. Telalovic and U. Hanefeld *Chem. Eur. J.* **2008**, *14*, 961-972.

Finally, for preparative purposes, an experiment was scaled up by a factor of 10 and a conversion of 80% and diastereoselectivity of 60% were reached.

Cycle times of 24 h were chosen in order to ensure that a possible loss of activity of Zr(Ti)-NDC could be detected. Although the conversion decreased by about 15% in each consecutive batch experiment, the diastereoselectivity for (±)-isopulegol remained constant. The loss of activity might be partly attributed to successive treatments or blockage of pores. The catalyst was calcined at 300 °C (heating rate 1 °C·min^{-1}) for 2 h to remove any possible inhibitors. Activity of the Zr(Ti)-NDC was partially recovered up to 90-95%. Moreover, no leaching of zirconium or titanium could be detected (ICP-OES, detection limit 0.002 ppm). A hot filtration experiment was also performed and no reaction was observed in the filtrate upon removal of the catalyst after 8 h of reaction.

While comparison of X-ray diffraction patterns of Zr-NDC and Zr(Ti)-NDC catalysts before and after several reaction runs did not reveal significant differences (annexes).

3.3.4.1.3. Isomerization of α-pinene oxide.

The third test reaction for Lewis acid catalysis of Zr(Ti)-NDCs is the isomerization of α-pinene oxide, a highly sensitive substrate towards acids, which reacts to give a mixture of campholenic aldehyde (5), isopinocamphone (6), pinocarveol (7) and others products (Scheme 3.6). Campholenic aldehyde is a fragrance compound prepared in high yield when a suitable Lewis acid is used.[213] It has been seen that MOFs as $Cu_3(BTC)_2$,[211,214] UiO-66,[215] MIL-

[213] A. Corma and H. García *Chem. Rev.* **2003**, *103*, 4307-4366; J. Kaminska, M. A. Schwegler, A. J. Hoefnagel and H. van Bekkum *Rec. Trav. Chim. Pays-Bas* **1992**, *111*, 432-437; K. Wilson, A. Rénson and J. H. Clark *Catal. Lett.* **1999**, *61*, 51-55; P. J. Kunkeler, J. C. van der Waal, J. Bremmer, B. J. Zuurdeeg, R. S. Downing and H. van Bekkum *Catal. Lett.* **1998**, *53*, 135-138.
[214] A. Dhakshinamoorthy, M. Alvaro, H. Chevreau, P. Horcajada, T. Devic, C. Serre and H. Garcia *Catal. Sci. Technol.* **2012**, *2*, 324-330.
[215] F.-G. Xi, Y. Yang, H. Liu, H.-F. Yao and E.-Q. Gao *RSC. Adv.* **2015**, *5*, 79216-79223.

100(Fe),[216] Fe(BTC)[216] with well-defined Lewis acid exhibited moderate activity and selectivity for this reaction.

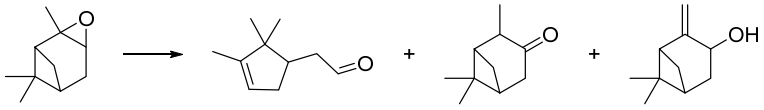

α-pinene oxide | campholenic aldehyde | isopinocamphone | pinocarveol

5 **6** **7**

Scheme 3.6. Isomerization of α-pinene oxide.

The acid-catalyzed isomerization of α-pinene oxide was investigated using here Zr-NDC and Zr(Ti)-NDCs as catalysts and 1,2-dichloroethane (DCE) as solvent, at 70 °C (data in other solvents and temperatures were included in supplementary, table S3). The added-value campholenic aldehyde product was formed in 50% yield at 80% conversion. The by-products include isopinocamphone, pinocarveol and traces of trans-carveol, (Scheme 3.6). Without catalyst the reaction is slow and selective to campholenic aldehyde is poor, indicating that Zr(Ti)-NDCs promote the reaction. All reported yields and selectivities were reproducible for at least three experiments and were constant until complete conversion. The catalytic performance of Zr(Ti)s for the reaction is strongly dependent on the type of solvent used as shown in annexes. Reactions were also carried out with other MOFs ($Cu_3(BTC)_2$, Fe-MIL-101) under the same conditions to compare the results with those obtained with Zr-NDC-MOFs. According to table 3.3, the conversion and selectivity towards campholenic aldehyde depends on the type of Zr-MOF showing Zr(Ti)-NDC the best activity and selectivity (entry 2). It is well known that Lewis acid sites favor the formation of campholenic aldehyde; therefore, it is reasonable to suggest that the better catalytic properties of Zr(Ti)-catalysts are determined by titanium. Another aspect for the catalytic properties may be the difference in the structure of Zr(Ti)-MOFs, which can affect the reagents accessibility to active sites. This could explain the better activity and selectivity observed, in the presence of Zr(Ti)-NDC with pores of 2.06 nm (1.48 nm for Zr-NDC). Zr(Ti)-NDC give better results than MIL101 (Fe) (entry 10), MIL100 (Fe)

[216] M. N. Timofeeva, V. N. Panchenko, A. A. Abel, N. A. Khan, I. Ahmed, A. B. Ayupov, K. P. Volcho and S. H. Jhung *J. Catal.* **2014**, *311*, 114-120; F. Vermoortele, R. Ameloot, L. Alaerts, R. Matthessen, B. Carlier, E. V. R. Fernandez, J. Gascon, F. Kapteijn and D. E. De Vos *J. Mater. Chem.* **2012**, *22*, 10313-10321.

(entries 15, 16) but better selectivity was found when $Cu_2(BTC)_3$ was the catalyst (entries 9, 14). A comparison with inorganic solids as Ti-beta shows that Zr(Ti)-NDC has a better catalytic activity but a lower selectivity towards campholenic aldehyde. MCM-41(Si/Al= 15) shows a similar behavior than Zr(Ti)-MOF.

Recycling experiments show that the activity of Zr(Ti)-NDC decreases upon recycling probably due to absoption of subproducts on the active sites, regeneration by washing with ethanol or calcination of catalyst at 200 °C only lead to a slightly increase of catalytic activity (conversion decreases about 30% per cycle and after calcination treatment, decreases by 20% in each batch).

Table 3.3. Zr-NDCs-catalyzed isomerization of α-pinene oxide.[a]

Entry	Catalyst	Conv. (%)(h)	Selectiv. (%)		
			5	**6**	**7**
1	Zr-NDC	74 (24)	51	19	30
2	Zr(Ti)-NDC	88 (24)	58	20	22
3	Zr-NDC-NH_2	56 (24)	43	28	29
4	Zr(Ti)-NDC-NH_2	55 (24)	50	17	33
5	UiO67-NH_2	68(24)	44	26	30
6	UiO67(Ti)-NH_2	75(24)	50	22	28
7	UiO66-NH_2	46(24)	42	24	34
8	UiO66(Ti)-NH_2	74 (24)	31	27	42
9	$Cu_2(BTC)_3$[b]	73 (24)	82	3.5	7
10	MIL101(Fe)[b]	62 (24)	48	10	34
11	MCM-41(Si/Al=15)[b]	94 (21)	60	-	-
12	UiO66[217]	100	45	-	-
13	$Cu_2(BTC)_3$[216]	8 (6)	48	41	-
14	$Cu_2(BTC)_3$[211a]	70 (40)[c]	80	-	-
15	MIL100(Fe)[216]	22 (6)[d]	45	40	-
16	MIL100(Fe)[218a]	96 (0.5)[e]	56	-	-
17	Ti-beta[215d]	29 (24)	81	-	-

[a] Reaction conditions: 5 mg cat, α-pinene oxide (0.13 mmol, 20 mg), 70 °C in 1,2-dichloroethane; yields and selectivity correspond to and overage value of three experiments. [b] This work. [c] Reactions were carried out at room temperature with 0.1 g of α-pinene oxide in 5 mL of solvent added to 0.1 g of $Cu_3(BTC)_2$. [d] Reaction conditions: 0.5 mL of α-pinene oxide, 50 mg catalyst activated at 150 ºC for 2 h under vacuum before use, 70 °C without solvent. [e] Reaction conditions: 1,2-dichloroethane, 5 mg catalyst, 30 °C.

3.3.4.2. Direct synthesis of imines from alcohols and amines

The direct synthesis of imines from alcohol and amine is already described with Ag supported on γ-Alumina[217], Cu/Al hydrotalcite[218], Ru[219] and has been recently described using CeO_2 as catalyst.[220] We have performed this reaction using ZrCe-MOFs as catalyst. In a first reaction step, the alcohol is oxidized to aldehyde and subsequently, a condensation between it and the amine takes place. The reduction of the imine towards the corresponding amine scarcely occurs in our case.

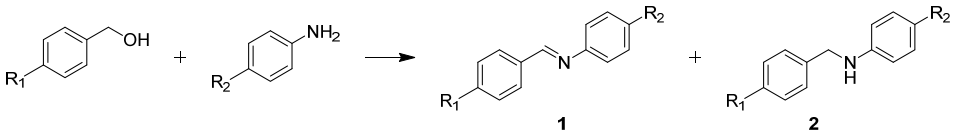

Scheme 3.7. Synthesis or imines starting from alcohol and amines.

ZrCe-BDC-NH_2(100) shows better reactivity than ZrCe-NDC-NH_2 as shown in table 3.4. When the material possess larger amount of cerium in its structures, a higher conversion is reached (entry 7). ZrCe-MOFs with higher amount of -NH_2 linker present more activity, this fact can clearly be seen when comparing entries 8 and 9. If alcohols or amines with electron withdrawing groups at the aromatic ring are used (entries 6, 12, 14 and 15) the conversion obtained is lower, being more pronounced in the case of substituents of the amine. Two blank experiments have been performed, in one of them, the reaction was carried out without catalyst (entry 1) and in the other Zr-NDC was used as catalyst, in both cases no conversion was obtained. If the reaction is performed with conventional heating, 40 hours more are necessary to achieve the same conversion compared with microwave activation.(entries 2 and 3).

[217] K. Shimizu, M. Nishimura and A. Satsuma *ChemCatChem* **2009**, *1*, 497-503.
[218] P. R. Likhar, R. Arundhathi, M. L. Kantam and P. S. Prathima *Eur. J. Org. Chem.* **2009**, *2009*, 5383-5389.
[219] V. R. Jumde, L. Gonsalvi, A. Guerriero, M. Peruzzini and M. Taddei *Eur. J. Org. Chem.* **2015**, *2015*, 1829-1833.
[220] M. Tamura and K. Tomishige *Angew. Chem. Int. Ed.* **2015**, *54*, 864-867.

Table 3.4. Synthesis of imines from alcohols and amines.[a]

Entry	Catalyst	R_1	R_2	%Conversion (h)	%Selectivity	
					1	2
1	-	H	H	0.8(6)	100	-
2	ZrCe(20)-BDC-NH_2 (100)[b]	H	H	76 (48)	98	2
3	ZrCe(20)-BDC-NH_2 (100)	H	H	73 (8)	94	6
4	ZrCe(20)-BDC-NH_2 (100)	CH_3O	H	90 (8)	82	18
5	ZrCe(20)-BDC-NH_2 (100)	CH_3	H	80(8)	93	7
6	ZrCe(20)-BDC-NH_2 (100)	Cl	H	62 (8)	100	-
7	ZrCe(75)-BDC-NH_2 (100)	H	H	86 (8)	100	-
8	ZrCe(20)-NDC-NH_2 (20)	H	H	9 (8)	93	7
9	ZrCe(50)-NDC-NH_2 (50)	H	H	84 (8)	91	9
10	ZrCe(50)-NDC-NH_2 (50)	CH_3O	H	62 (8)	62	38
11	ZrCe(50)-NDC-NH_2 (50)	CH_3	H	15(8)	100	-
12	ZrCe(50)-NDC-NH_2 (50)	Cl	H	37 (8)	100	-
13	ZrCe(50)-NDC-NH_2 (50)	NH_2	H	-(8)	-	-
14	ZrCe(50)-NDC-NH_2 (50)	H	Cl	4(8)	100	-
15	ZrCe(50)-NDC-NH_2 (50)	H	Br	9(8)	100	-
16	Zr-NDC	H	H	6 (8)	100	-
17	ZrCe(20)-UiO-67	H	H	8 (8)	99	1

[a] Reaction conditions: 0.1 mmol of alcohol and 0.2 mmol of amine were dissolved in 0.5 mL of xylene, 10 mg of catalyst was added, and the reaction mixture was introduced on a MW oven (150 °C). The conversions displayed were obtained after 8 h of reaction time. [b] Conventional heating.

The scaled up by a factor of 10 was carried out with both catalyst, with ZrCe(20)-BDC-NH_2(100) a conversion of 60% was obtained at 8 hours of reaction with a selectivity of 93% towards the imine. Recycling experiments show that the activity of ZrCe(20)-BDC-NH_2(100) remains after 6 cycles (Figure 3.11, left). We performed the XPS analysis of the recovered MOF and Ce^{3+} specie is still the most abundant in the structure since the satellite around 917 eV is not observed in the spectra (Figure 3.11, right).

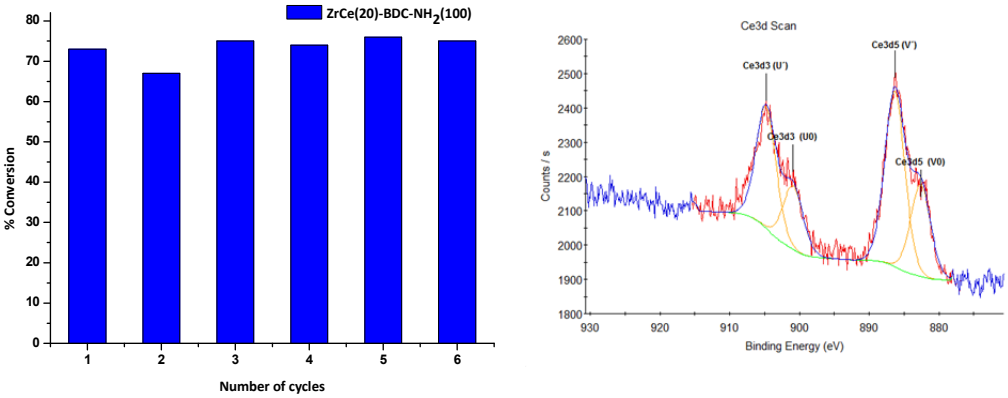

Figure 3.11. Recycling experiments (left) and Ce region of XPS spectra of Zr-Ce-BDC-MOF (right).

3.4. Conclusions

- We have obtained bimetallic Zr(Ti)-MOFs by incorporation of titanium atoms into Zr-MOFs and evaluated the effect of Ti on their Lewis acid catalytic properties.

- Mixed metal MOFs with cerium have benn synthesized to introduce the redox properties of these materials.

- Zr(Ti)-MOFs are active and selective catalysts for producing ethers of interest as fine chemicals starting from one aldehyde and one alcohol, through a domino reaction that involves a Meerwein-Ponndorf-Verley reduction of the aldehyde followed by etherification of the alcohol. No metal leaching has been detected during the reaction. They result also, effective catalysts in the cyclization of citronellal and for the isomerization of α-pinene oxide with higher activity and selectivity than parent Zr-NDC.

- ZrCe-MOFs have been tested in the formation of imines from alcohols and amines as catalysts, giving good conversions and good selectivity towards the imine.

3.5. Experimental section

3.5.1. Synthesis of ZrTi-MOFs

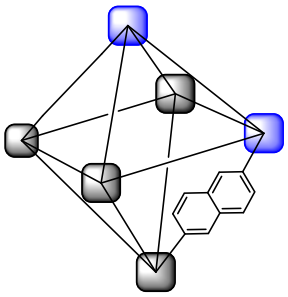

$TiCl_4(THF)_2$ (38 mg, 0.1 mmol) was dissolved in DMF (6mL). Zr-MOF (50 mg, 0.3 mmol equiv of linker) was placed in a vial, and the solution of titanium was added. This mixture was incubated at 85 °C in a pre-heated oven for 5 days. After cooling was centrifuged and the solids washed with 3x10 mL of DMF, 10 mL of MeOH and 10 mL of THF. The final solids were dried at 100 °C under vacuum to yield: $Zr_{4.5}Ti_{1.5}O_4(OH)_4(BDC)_{4.8}(BDC\text{-}NH_2)_{1.2}$, $Zr_{4.5}Ti_{1.5}O_4(OH)_4(BPDC)_{4.8}(BPDC\text{-}NH_2)_{1.2;}$ $Zr_{4.4}Ti_{1.6}O_4(OH)_4(NDC)_{6;}$ $Zr_{4.3}Ti_{1.7}O_4(OH)_4(NDC)_{4.8}(NDC\text{-}NH_2)_{1.2.}$

Table S1. Elemental analysis.

	%C (calc.)	%H (calc.)	%N (calc.)	Zr/Ti	
				EDX	TXRF
Zr-NDC	40.95 (43.75)	2.42 (2.65)	-		
Zr-NDC-NH_2	39.28 (43.36)	2.53 (2.69)	0.87 (0.84)	-	-
Zr(Ti)-NDC	36.18 (45.34)	3.09 (2.75)	-	2.50	2.64
Zr(Ti)-NDC-NH_2	32.28 (45.02)	2.09 (2.79)	1.23 (0.88)	2.47	2.50
UiO66(Ti)-NH_2				2.75	3.10
UiO67(Ti)-NH_2				2.82	3.00

3.5.2. Synthesis of ZrCe-MOFs.

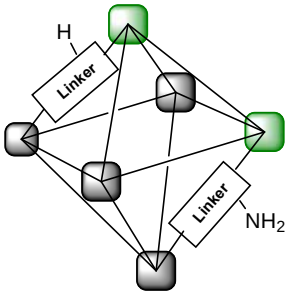

$ZrCl_4$ (466 mg, 2 mmol), $CeCl_3{\cdot}7H_2O$ (236 mg, 0.5 mmol for ~20% of functionalization) and 2.5 mmol of linker were dissolved in 12 mL of DMF and placed in a Teflon lined vessel. Then, the mixture was heated to 393 K for 24 hours. After cooling the solid was centrifuged and washed with 3x10 mL of DMF, 10 mL of MeOH and 10 mL of THF. The final solids were dried at 100 °C under vacuum to yield: $Zr_{4.4}Ce_{1.6}O_4(OH)_4(C_8H_5NO_4)_6$ and $Zr_2Ce_4O_4(OH)_4(C_{12}H_8O_4)_3(C_{12}H_9NO_4)_3$.

3.5.3. Synthesis of ZrCeTi-MOFs.

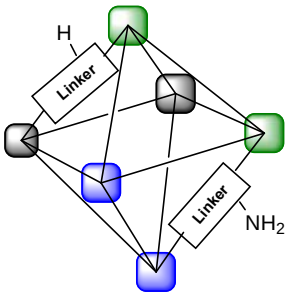

$TiCl_4(THF)_2$ (38 mg, 0.1 mmol) was dissolved in DMF (6mL). ZrCe-MOF (50 mg, 0.3 mmol equiv of linker) was placed in a vial, and the solution of titanium was added. This mixture was incubated at 85 °C in a pre-heated oven for 5 days. After cooling was centrifuged and the solids washed with 3x10 mL of DMF, 10 mL of MeOH and 10 mL of THF. The final solids were dried at 100 °C under vacuum to yield: $Zr_{4.2}Ce_{0.4}Ti_{1.4}\ O_4(OH)_4(C_8H_5NO_4)_6$ and $Zr_{4.3}Ce_{0.2}Ti_{1.5}\ O_4(OH)(C_{12}H_9NO_4)_6$.

3.5.4. Evaluation of Lewis acid catalysis

The catalytic performance of Zr(Ti)-MOFs was evaluated by using three reactions: a cascade etherification reaction, the cyclization of citronellal to isopulegol and the isomerization of α-pinene oxide.

General procedure for the domino etherification reaction starting from an aldehyde: MOF catalyst (5 mg) was added to a solution of 4-methoxybenzaldehyde (22 mg, 0.16 mmol) in 2-butanol (1 mL) in a microwave sealed-vessel equipped with a magnetic stirring bar, the reaction mixture was heated under reflux. This flask was irradiated in a Microwave Synthesis Reactor Anton Paar Monowave 300 for a total of 4 h according to the following heating program: step 1) 18 °C to 120 °C (1 min), step 2) hold at 120 °C (2 h), step 3) cool to 55 °C, step 4) 55 °C to 120 °C (1 min), step 5) hold at 120 °C (2 h), step 6) cool to 55 °C.

Cyclization of citronellal. In a schlenck under N2, 58 µL (0.3 mmol) of citronellal was added to the catalyst suspension (5 mg, preactivated at 220 °C for 2 h under vacuum) in toluene (0.5 mL). The reaction mixture was heated at 150 °C under continuous stirring for 24 h. At the end, the catalyst was separated by filtration and washed with toluene and then reused. The progress of the reaction was monitored by GC-MS.

Isomerization of α-pinene oxide. The reaction was performed in a glass microreactor (2.0 mL, Supelco Analytical). The catalyst (preactivated for 2 h at 220 °C under vacuum) was suspended (5 mg) in 0.5 mL of dichloroethane, and then 20 µL (0.13 mmol) of α-pinene oxide was added. This mixture was magnetically stirred at 70° C for 24 h. The products were identified by GC-MS. After the completion of the reaction, the catalytic mixture was separated by filtration and washed with dichloroethane. It was then reused for the above reaction at least 4 times.

Evaluation of Redox catalysis

The catalytic activity of ZrCe-MOFs was evaluated by the formation of imines starting from alcohols and amines.

Synthesis of imines Benzyl alcohol (0.1 mmol) and the amine (0.2 mmol) were dissolved in 0.5 mL of xylene and then, MOF catalyst (10 mg) was added in a microwave sealed-vessel equipped with a magnetic stirring bar, the reaction mixture was heated under reflux. This flask was irradiated in a Microwave Synthesis Reactor Anton Paar Monowave 300 for a total of 8 h according to the following heating program: step 1) 18 °C to 120 °C (1 min), step 2) hold at 120 °C (2 h), step 3) cool to 55 °C, step 4) 55 °C to 120 °C (1 min), step 5) hold at 120 °C (2 h), step 6) cool to 55 °C. This program was repeated twice.

Conclusions

We have performed the synthesis of different Zr-based MOFs derivatives with dicarboxylate linkers (BDC, NDC and BPDC). We have used different strategies to obtain multifunctional systems.

In the chapter 1, we synthesized Lewis acid/basic materials due to the combination of the acid properties of zirconium with the basicity of the amino groups present in the linker. These materials had shown to be good catalysts in C-C- coupling cascade reactions. Thus, we have carried out the one-pot synthesis of dicyanomethylene derivative dyes.

In chapter 2, we described the post-functionalization in the linker for heterogeneization of metal complexes in the MOF structure. We obtained transition-metal/Lewis acid/basic materials to be used in catalytic reactions. The Ir-Zr-based metal-organic frameworks are a highly efficient catalysts for direct hydrogenation of aromatic compounds at low temperatures and initial hydrogen pressures, for producing higher amines from amines and alcohols and for the synthesis of N-alkyl amines via reductive amination in the presence of hydrogen. The Rh-Zr meltal organic framework is an efficient catalyst for one-pot cacade condensation-hydrogentation reactions.

The strategy that we have followed in chapter 3 is the incorporation of other metals in the material structure. We introduced titanium to improve the Lewis acidity of the material. ZrTi-MOFs materials are active and selective catalysts for producing ethers of interest as fine chemicals starting from one aldehyde and one alcohol, through a domino reaction that involves a Meerwein-Ponndorf-Verley reduction of the aldehyde followed by etherification of the alcohol. They also result effective catalysts in the cyclization of citronellal and for the isomerization of α-pinene oxide with higher activity and selectivity than parent Zr-MOFs. In order to obtain lewis acid/redox properties in the same catalyst, ZrCe-MOFs have been synthesized. They were tested in the formation of imines from alcohols and amines as catalysts, giving good conversions and good selectivity towards the imine.

The recycling experiments demonstrate an interesting prospect for the long-term reusability of these materials, being the most stable derivatives those with BDC as linker. Moreover, they present other notable advantages such a broad substrate scope, simple workup procedure, which make them attractive and useful for organic synthesis.

Conclusiones

Hemos sintetizado varios derivados de MOFs de zirconio con diferentes ligandos (BDC, NDC and BPDC). Para obtener sistemas multifuncionales hemos utilizado diferentes estrategias en cada uno de los capítulos.

En el capítulo 1, hemos sintetizado materiales con propiedades ácido de Lewis/base debido a la combinación de las propiedades ácidas del zirconioy de la basicidad de los grupos amino presentes en los ligandos orgánicos del MOF. Estos materiales han demostrado ser buenos catalizadores en reaciones en cascada de acoplamiento C-C. Por tanto, nosotros hemos utilizado estos MOFs en la síntesis de colorantes derivados del dicianometileno.

En el capítulo 2, describimos la post-funcionalización en el ligando para heterogeneizar complejos metálicos en la estructura del MOF. Hemos obtenido materiales multifuncionales que presentan las propiedades de los complejos de metales de transición, acidez de Lewis y basicidad que pueden ser utilizados en diferentes reacciones catalíticas. Las redes metalo-orgánicas con Ir y Zr son eficientes catalizadores para la hidrogenación directa de compuestos aromáticos a baja temperatura y baja presión de hidrógeno, para produción aminas de mayor peso molecular partiendo de aminas y alcoholes y para la síntesis de aminas *N*-alquiladas mediantes aminación reductiva en presencia de hidrógeno. El MOF de Rh y Zr es un catalizador eficiente para la reacción en cascada 'one-pot' de condensación-hidrogenación.

La estragia seguida en el capítulo 3 es la incorporación de otros metales en la estructura del material. Hemos introducion titanio para mejorar la acidez de Lewis del material. Los ZrTi-MOFs son catalizadores activos y selectivos para la producción de éters interesantes como productos químicos finos partiendo de un aldehido y un alcohol mediante la reacción en cascada de reducción Meerwein-Ponndorf-Verley del aldehido seguida de una eterificación del alcohol. Estos materiales también son buenos catalizadores en la ciclación del citronelal y en la isomerización del óxido α-pineno con mayor actividad y selectividad que los Zr-MOFs. Con el fin de obtener materiales con propiedades redox/acidez de Lewis, hemos sintetizado ZrCe-MOFs. Estos materiales han sido probados en la formación de iminas partiendo de alcoholes y aminas, obteniendo buenas conversiones y buena selectividad hacia la formación de la imina.

Los experimentos de reciclado de los diferentes derivados obtenidos demuestran una perspectiva interesante para la reutilización a largo plazo de

estos materiales, siendo los derivados más estables aquellos que poseen BDC como ligando orgánico en su estructura. Además, presentan otras ventajas interesantes como fácil tratamiento después de la reacción y pueden ser utilizados para un gran número de sustratos, lo que los hace interesantes y útiles para ser utilizados en síntesis orgánica.

Annexes

Annexes of chapter 1

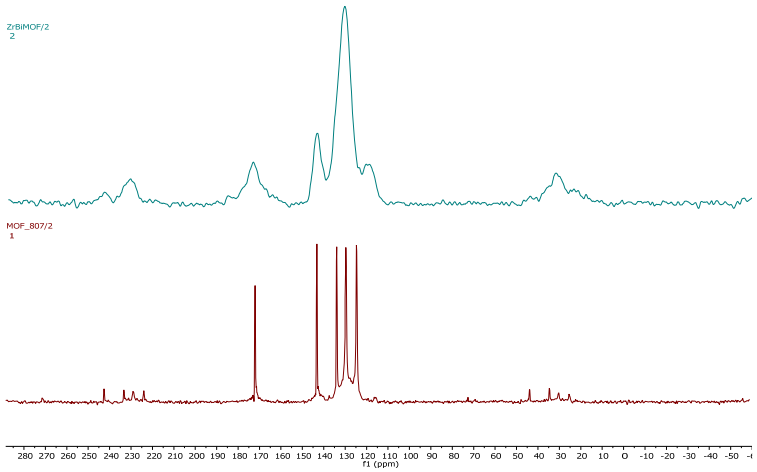

Figure A.1.1. ^{13}C-NMR for Zr-BPDC-NH_2(100), top and Zr-BPDC-NH_2(20) bottom.

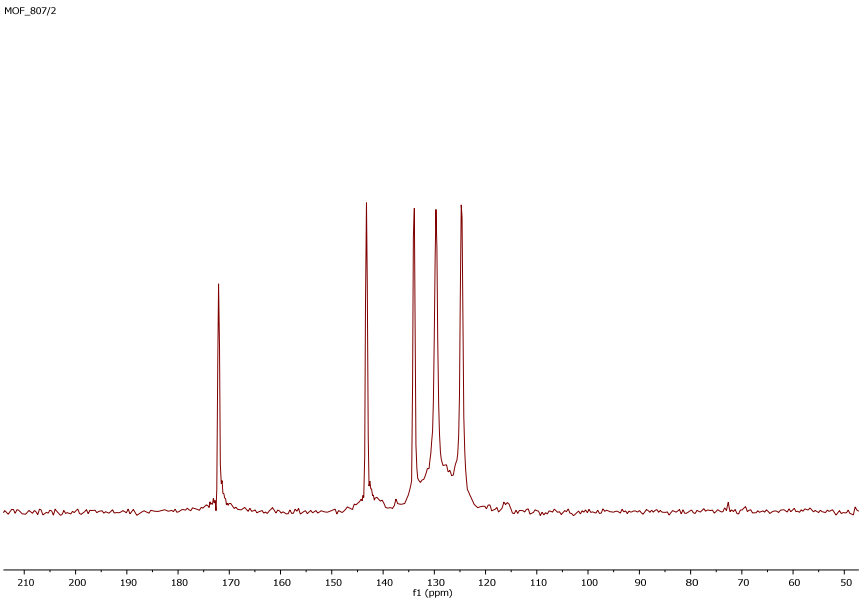

Figure A.1.2. ^{13}C-NMR for Zr-BPDC-NH_2(20%).

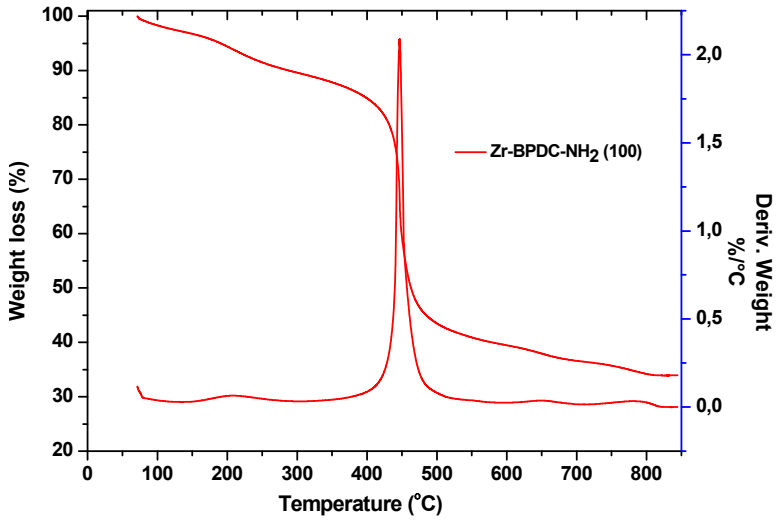

Figure A.1.3. TGA curves for Zr-BPDC-NH_2.

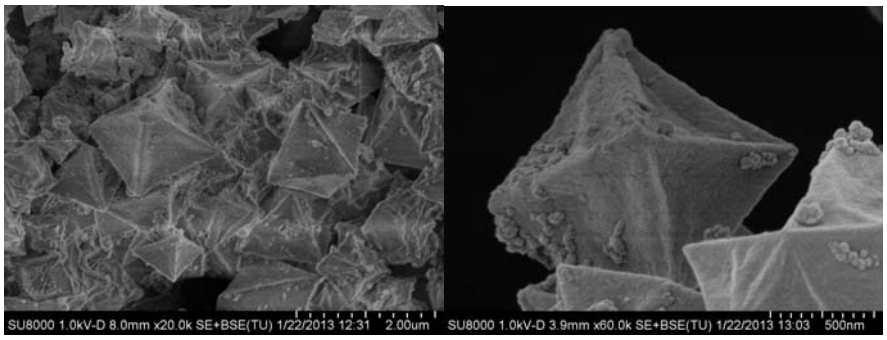

Figure A.1.4. SEM micrographs of samples Zr-BPDC-NH_2 (100%).

Table A.1.1. Textural properties.

	S (m^2/g)	Pore size (nm)	Pore volume (cm^3/g)
Zr-BPDC-NH_2(20)	1280.57	2.69	0.08

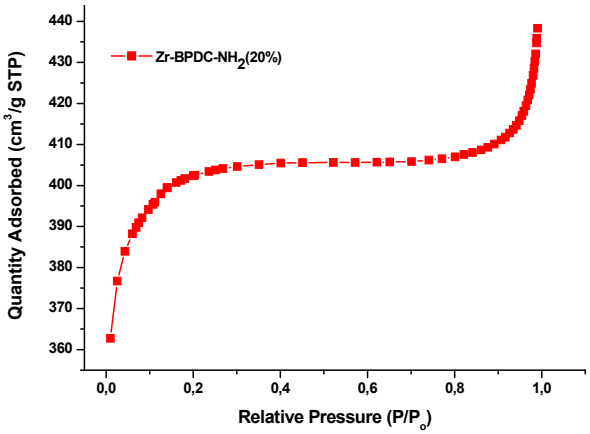

Figure A.1.5. N_2 isotherm of Zr-BPDC-NH_2(20).

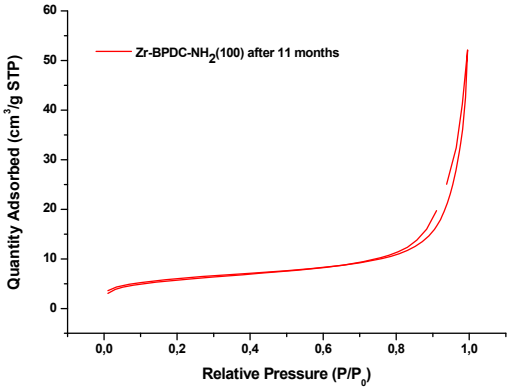

Figure A.1.6. N_2 isotherm of amorphous Zr-BPDC-NH_2(100) after 11 months.

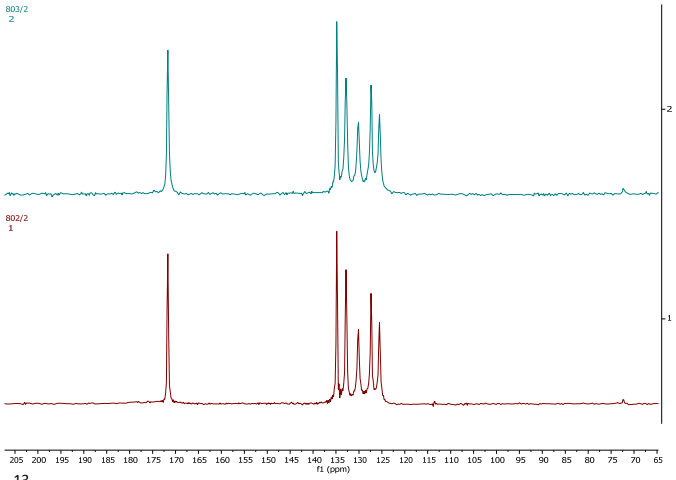

Figure A.1.7. ^{13}C-NMR for Zr-NDC-NH_2(20) top and Zr-NDC bottom.

Table A.1.2. Textural properties.

	S (m^2/g)	Pore size (nm)	Pore volume (cm^3/g)
Zr-NDC-NH_2	926.13	5.01	0.17
Zr-NDC-NH_2(20)	1053.59	5.05	0.14

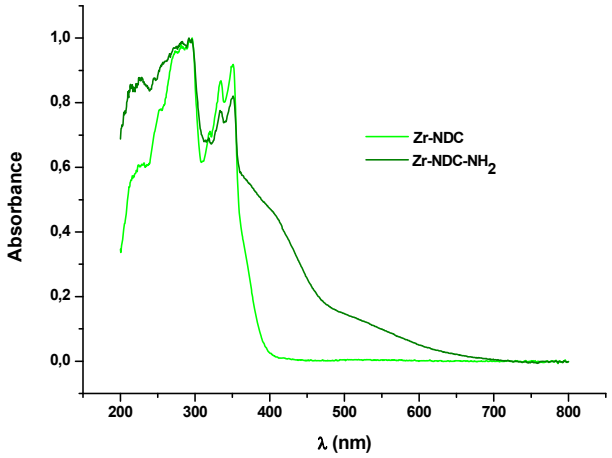

Figure A.1.8. Diffuse reflectance spectra.

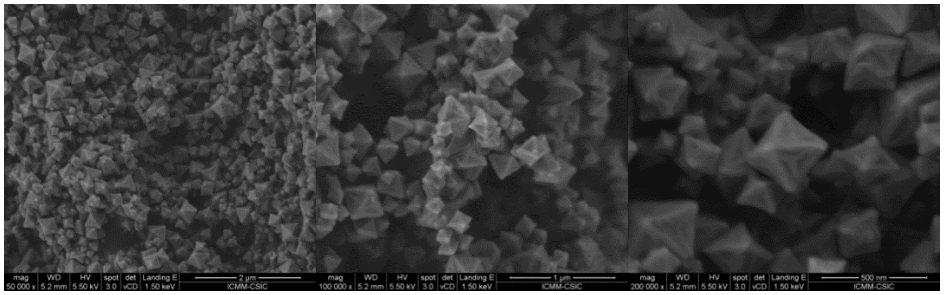

Figure A.1.9. SEM micrographs of samples $Zr_6O_4(OH)_4(NDC)_{6-x}(NDC\text{-}NH_2)_x$ (20%).

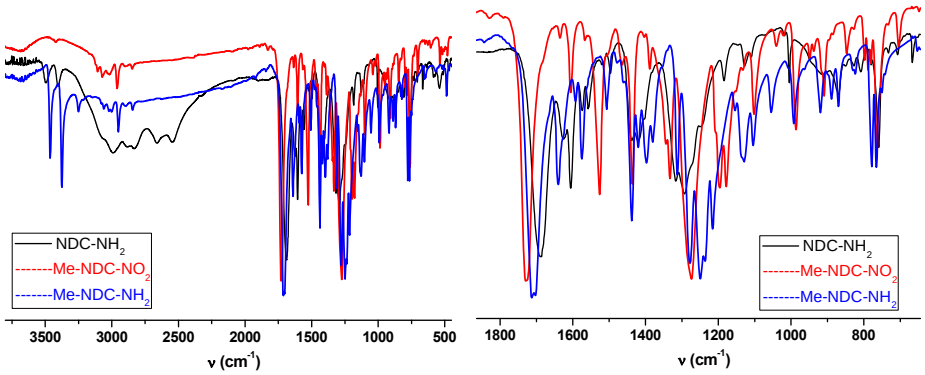

Figure A.1.10. FT-IR (normalized) for $NDC\text{-}NH_2$, $Me\text{-}NDC\text{-}NO_2$ and $Me\text{-}NDC\text{-}NH_2$.

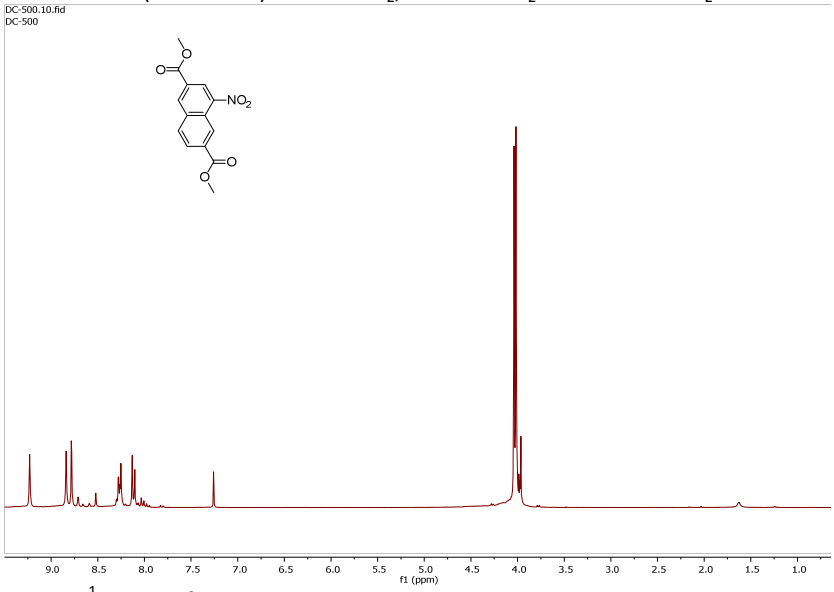

Figure A.1.11. ^{1}H-NMR of $Me\text{-}NDC\text{-}NO_2$.

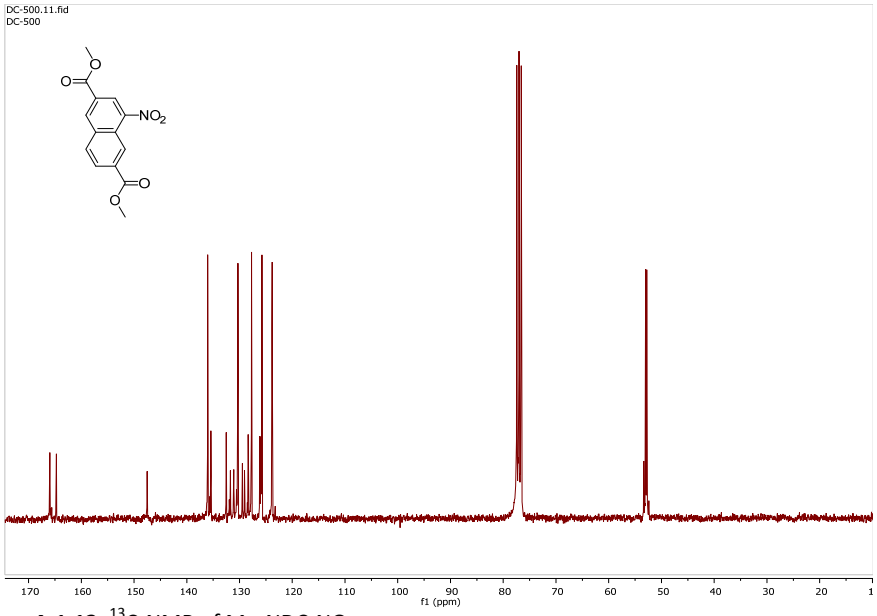

Figure A.1.12. ^{13}C-NMR of Me-NDC-NO_2.

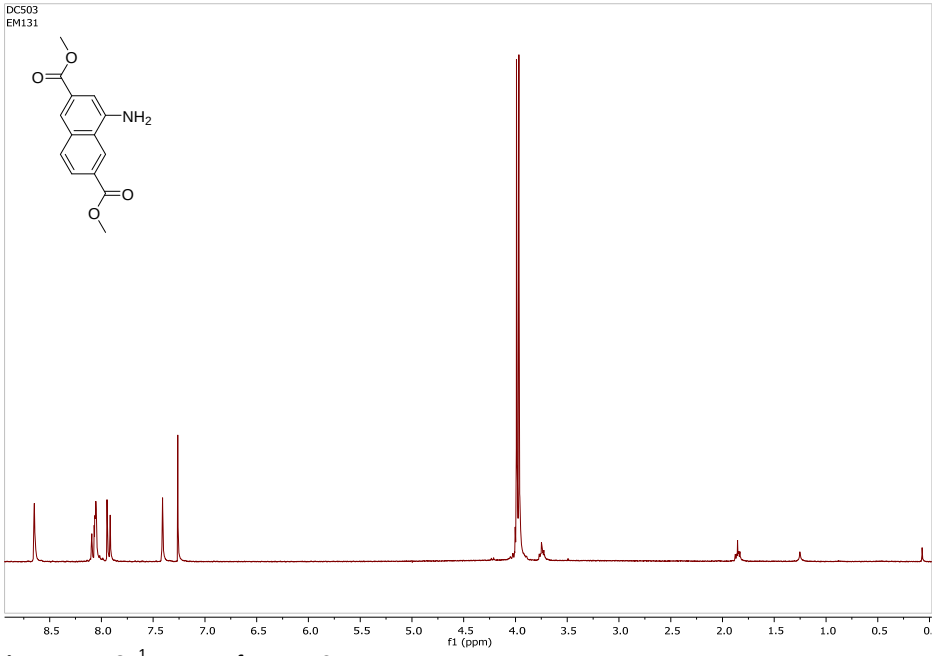

Figure A.1.13. ^{1}H-NMR of Me-NDC-NH_2.

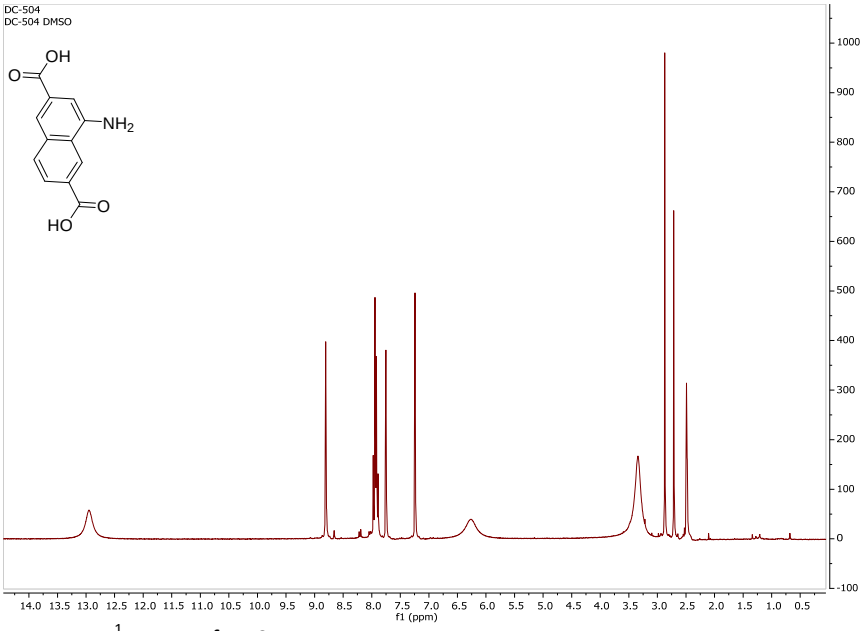

Figure A.1.14. ^{1}H-NMR of NDC-NH_2.

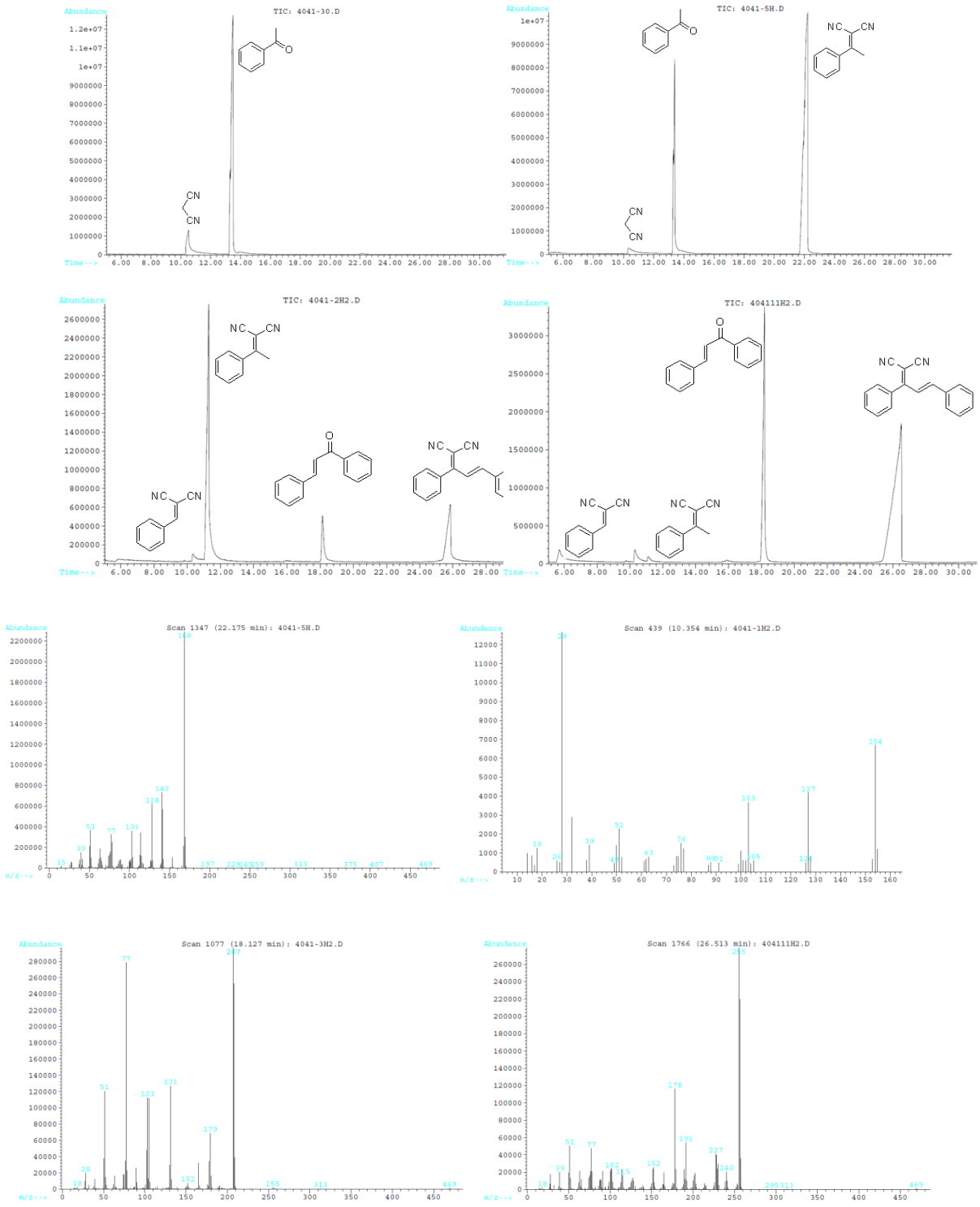

Figure A.1.15. GC-MS analysis for Zr-BPDC-NH_2 (20%)-catalyzed reaction.

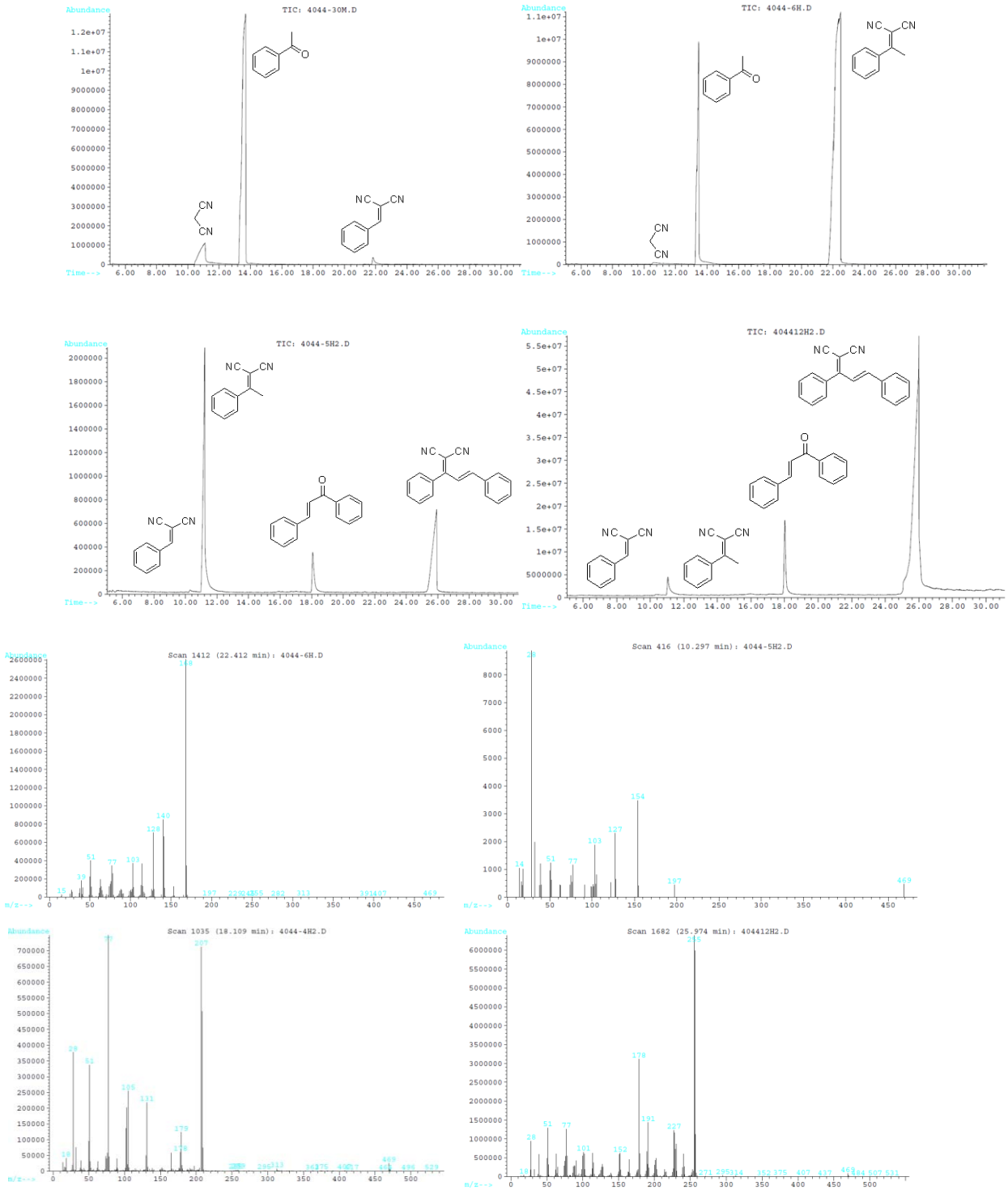

Figure A.1.16. GC-MS analysis for Zr-NDC-NH_2 (20%)-catalyzed reaction.

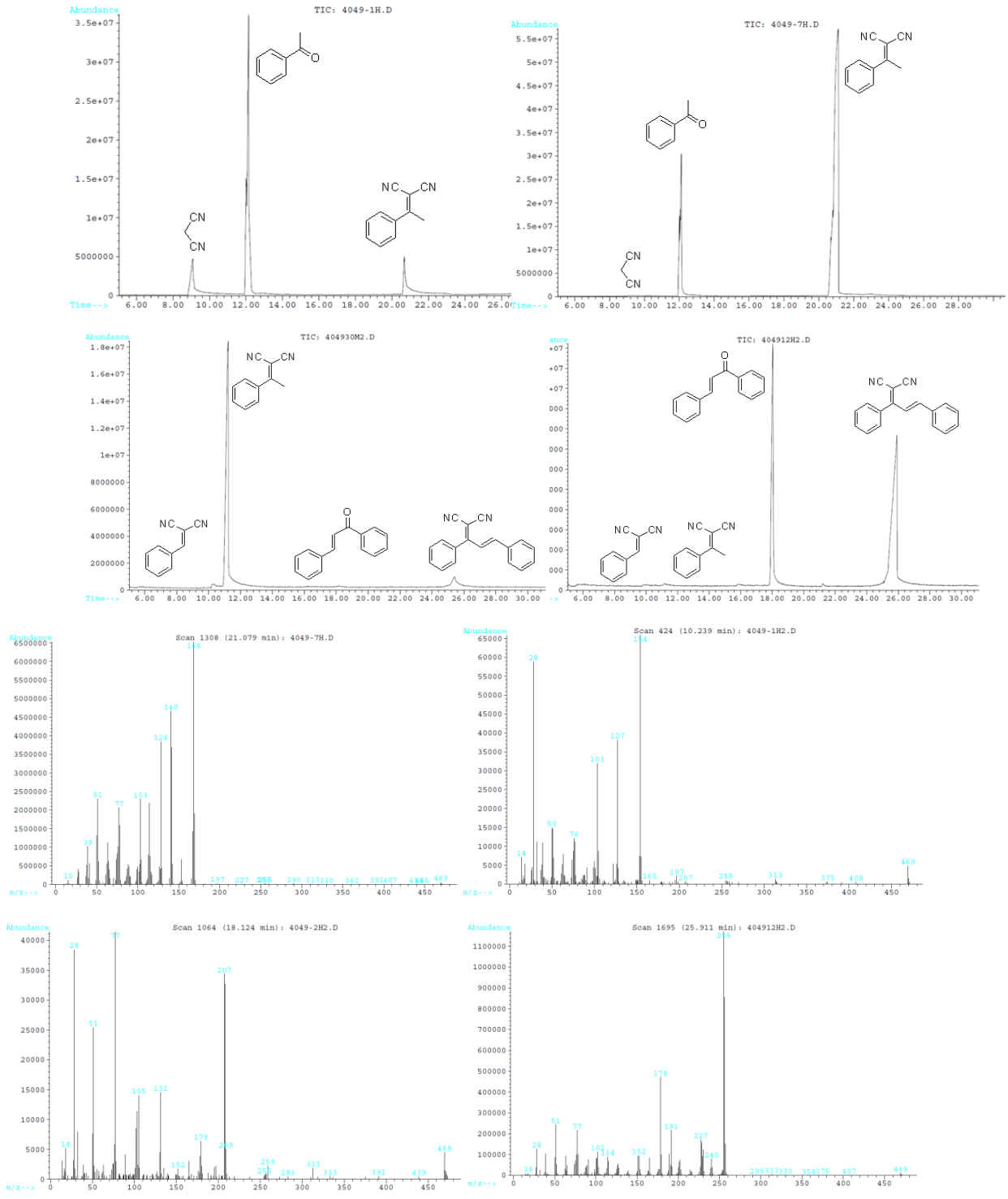

Figure A.1.17. GC-MS analysis for Zr-BDC-NH_2 (20%)-catalyzed reaction.

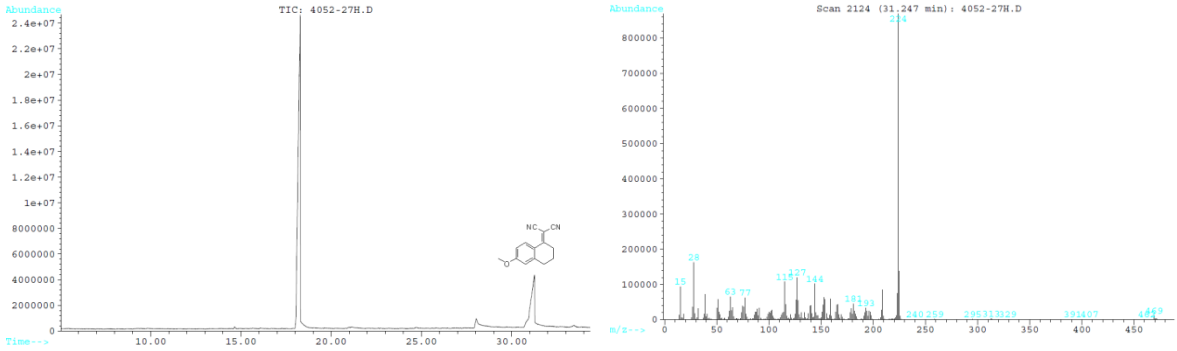

Figure A.1.18. GC-MS analysis for 6-methoxy-3,4-dihydronaphthalen-1(2H)-one with Zr-BPDC-NH_2 (20%)-catalyzed reaction.

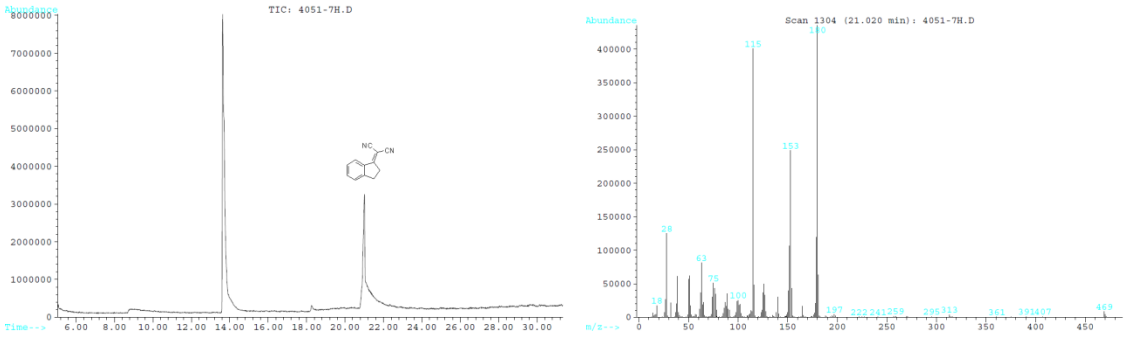

Figure A.1.19. GC-MS analysis for 1-indanone with Zr-BPDC-NH_2 (20%)-catalyzed reaction.

Annexes of chapter 2

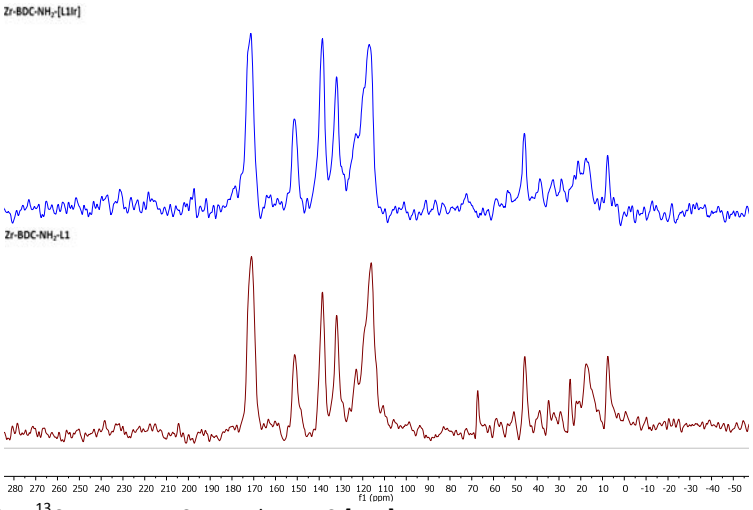

Figure A.2.1. ^{13}C NMR Zr-BDC-L1 and Zr-BDC-[L1Ir].

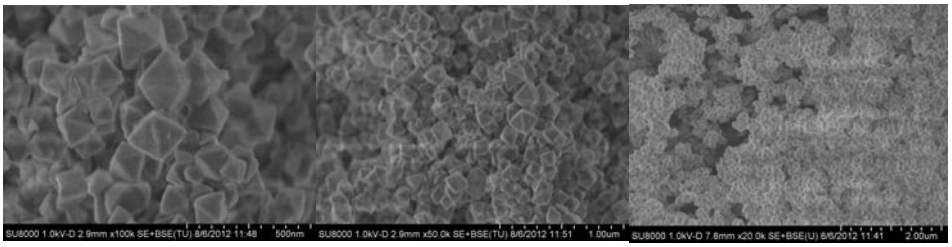

Figure A.2.2. SEM for Zr-BDC-NH_2-L1.

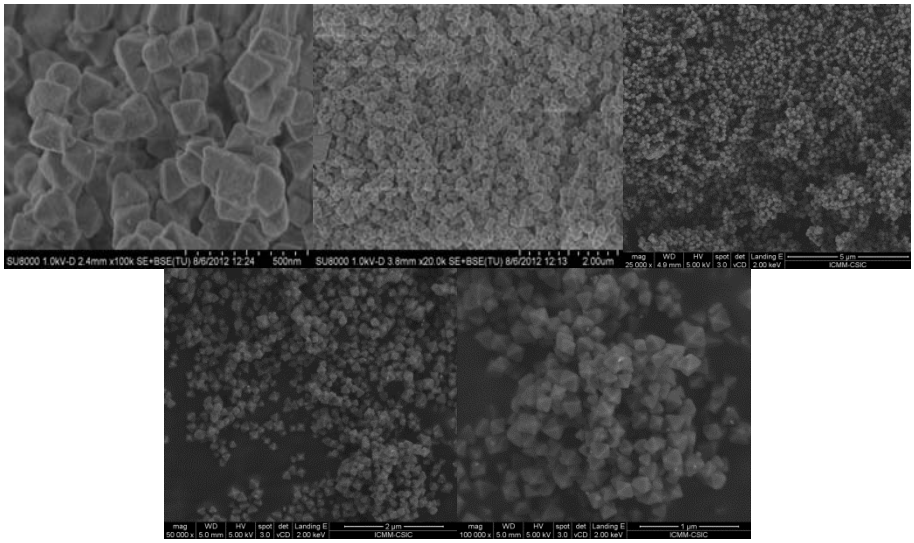

Figure A.2.3. SEM for fresh Zr-BDC-NH_2-[LIr]BF_4.

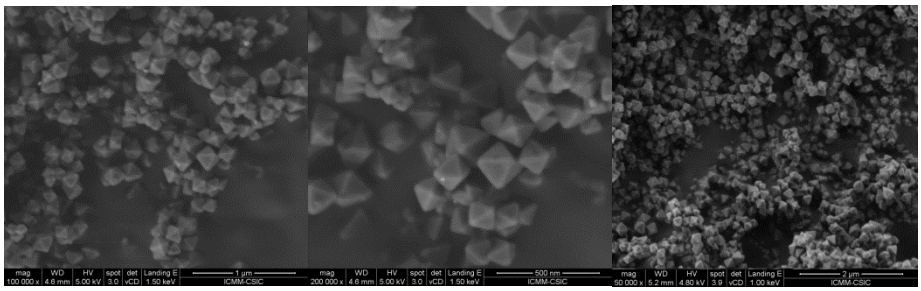

Figure A.2.4. SEM images for recovered Zr-BDC-NH_2-[LIr]BF_4.

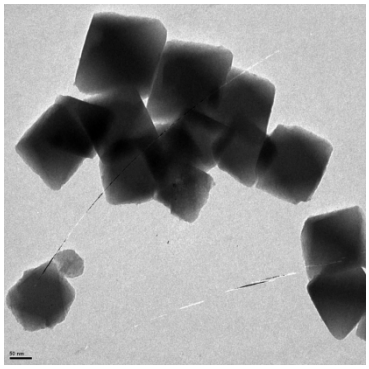

Figure A.2.5. TEM for fresh Zr-BDC-NH_2-[LIr]BF_4 catalyst.

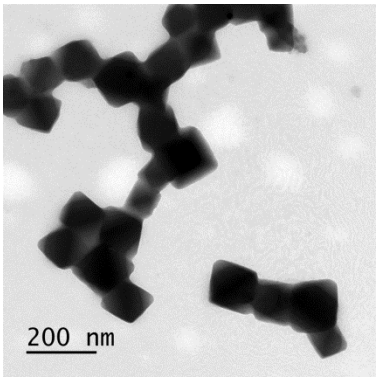

Figure A.2.6. TEM for Zr-BDC-NH_2-[LIr]BF_4 recovered from reaction.

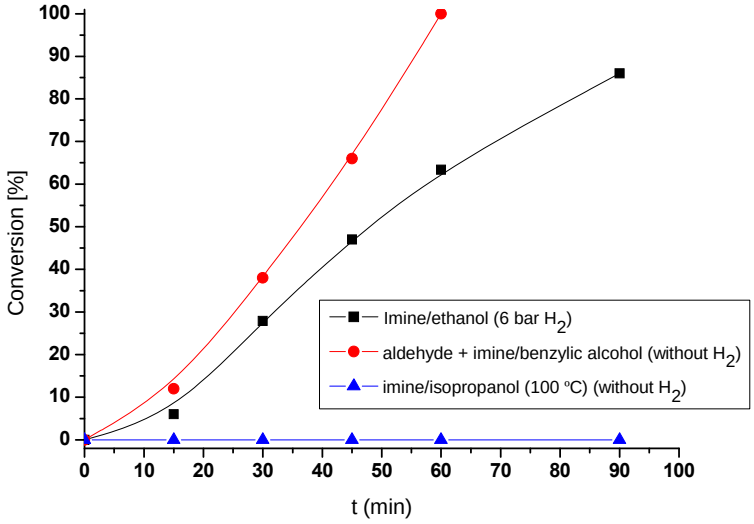

Figure A.2.7. Kinetic profiles for Zr-[LIr]BF_4-catalyzed reactions.

Morphology of Zr-BDC-NH_2-[L1Ir]BF4

The morphology of the different Ir-Zr-MOF samples was examined by dynamic light scattering (DLS) (Fig. A.2.8), SEM (Fig. A.2.9) and TEM (Fig. A.2.10). SEM images of Zr-[L1Ir]-MOF fresh obtained reveal particles with diameters between 200 nm and 300 nm; DLS measurements give values of 770 nm (note that DLS measures the hydrodynamic radius including a solvating shell, leading to larger particle sizes than obtained by direct imaging techniques). After reaction SEM images and DLS measurements of the recovered catalyst reveal

particles with a similar size to that from fresh one. However, when Zr-[LIr]-MOF reacted with NaBH4 we observe that particle size diminishes (~ 135-150 nm from SEM, 270 nm from DLS). In TEM images, the dark spots could be attributed to the presence of the grafted Iridium sites. Higher resolution images for these large crystallites are difficult to obtain, due to local damage by the electron beam and the fact that the increased thickness of the sample minimizes the contrast between the metal and the support. From TEM images we have measured the Ir particle size and we found (figure A.2.11) that in fresh obtained Zr-[LIr]-MOF catalyst, the size of the iridium particles ranges from 3.5 to 9 nm, whereas after the first run the recovered catalyst shows two patterns for the Ir-particle size: one from 5 to 9 nm and from 19 to 35 nm. Finally for Zr-[LIr]-MOF treated with $NaBH_4$, size ranges mainly between 20-40 nm.

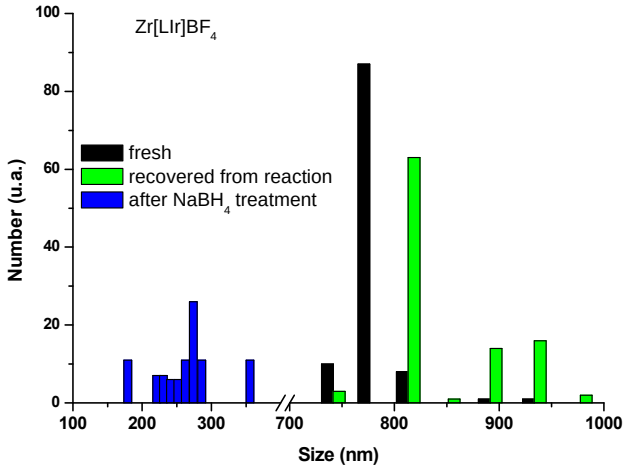

Figure A.2.8. DLS measurements of Zr-BDC-NH_2 particles as a function of treatment after synthesis: evolution of the size distribution of the reaction mixture (black: fresh prepared, green: recovered from the aniline hydrogenation, blue: treated with $NaBH_4$).

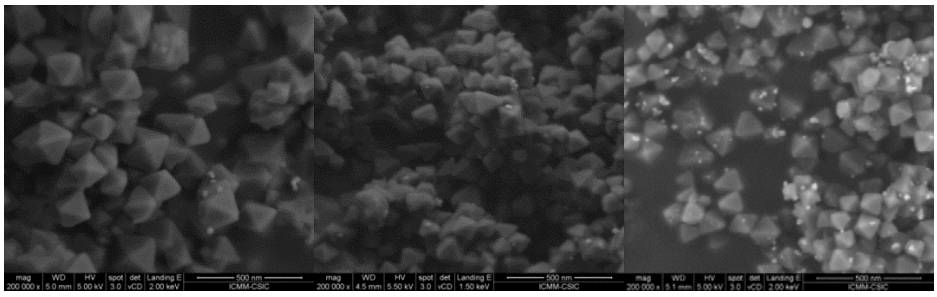

Figure A.2.9. SEM images for Zr-MOF-Ir samples: a) Fresh ; b) recovered after reaction and c) from $NaBH_4$.

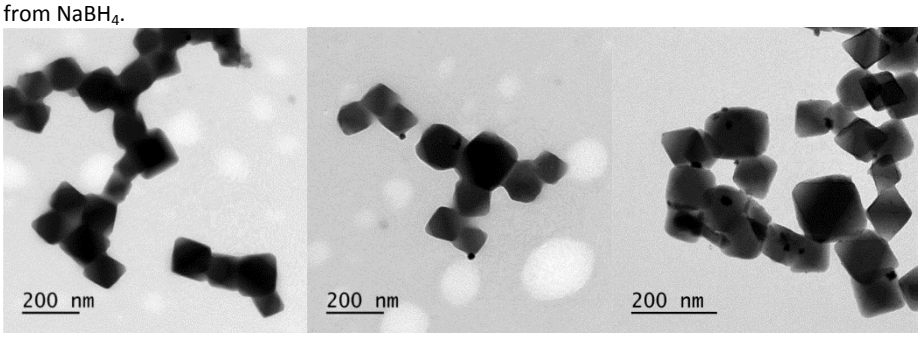

Figure A.2.10. TEM images for Zr-MOF-Ir samples: a) Fresh; b) Recovered after reaction and c) 6 bar H_2, 120 °C.

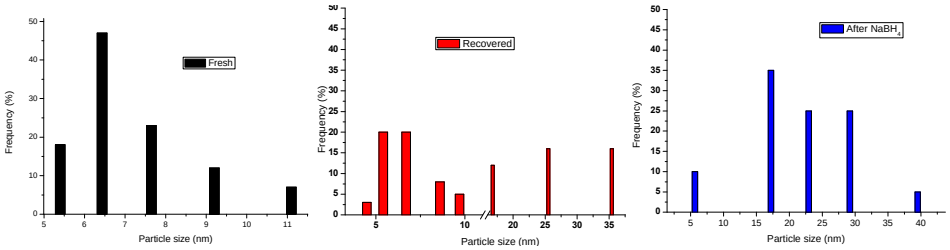

Figure A.2.11. TEM IrNPs size distribution.

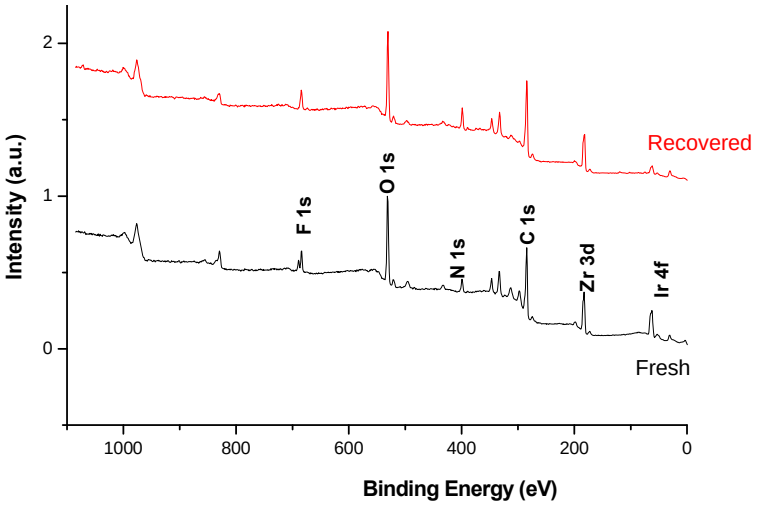

Figure A.2.12. XPS survey scans of a fresh and a used sample after a hydrogenation run.

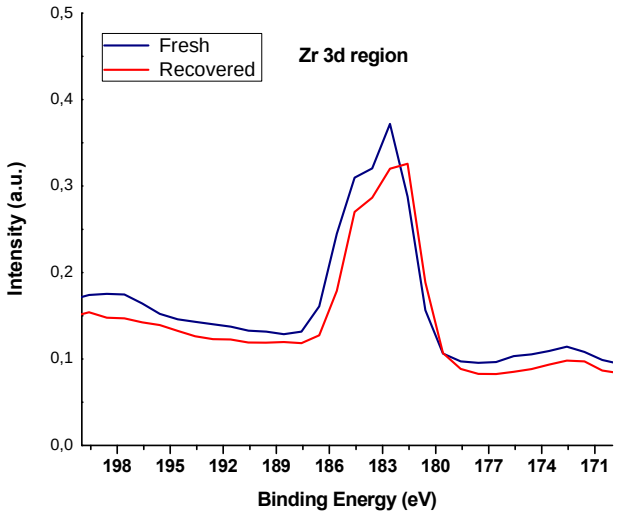

Figure A.2.13. XPS Zr(3d) region for the original catalyst and recovered after reaction.

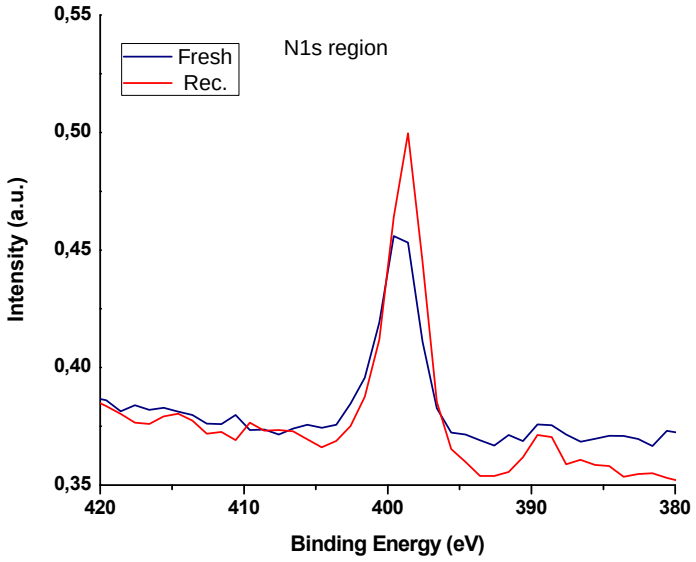

Figure A.2.14. XPS N(1s) region for the original catalyst and recovered after reaction.

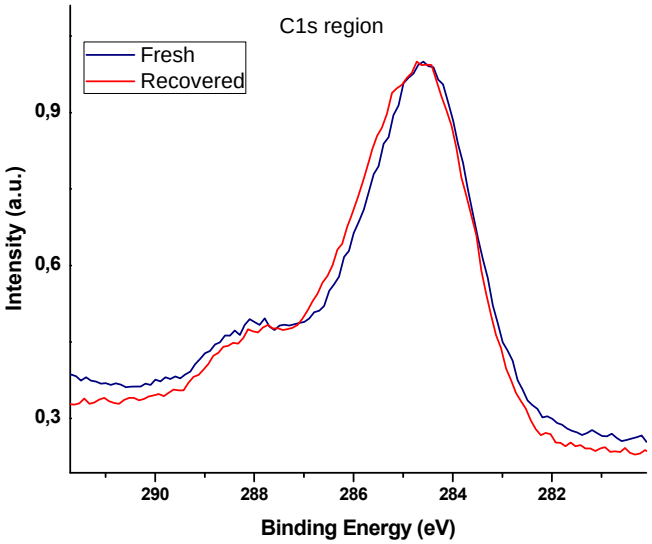

Figure A.2.15. XPS C(1s) region for the original catalyst and recovered after reaction.

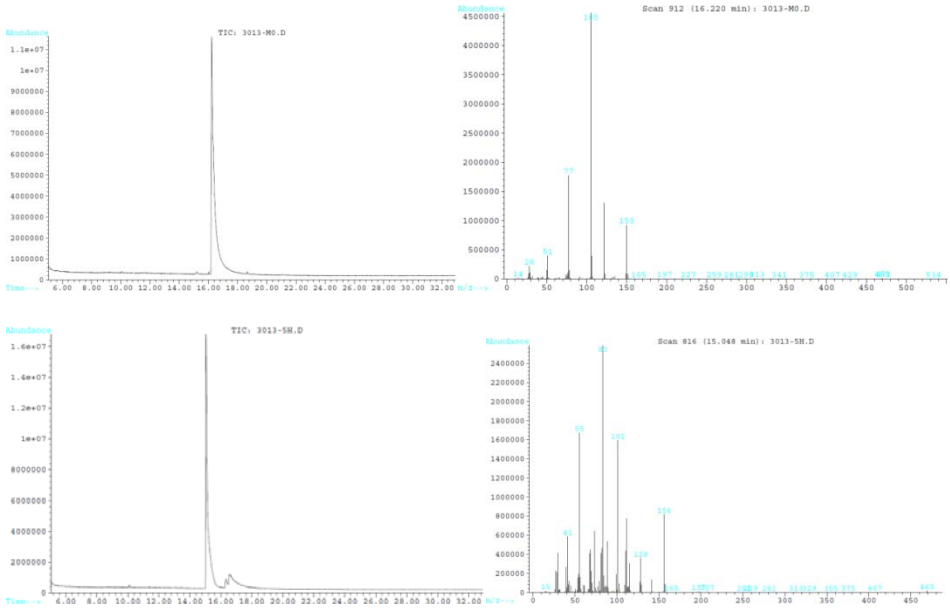

Figure A.2.16. GC-MS analysis for hydrogenation of Ethyl benzoate.

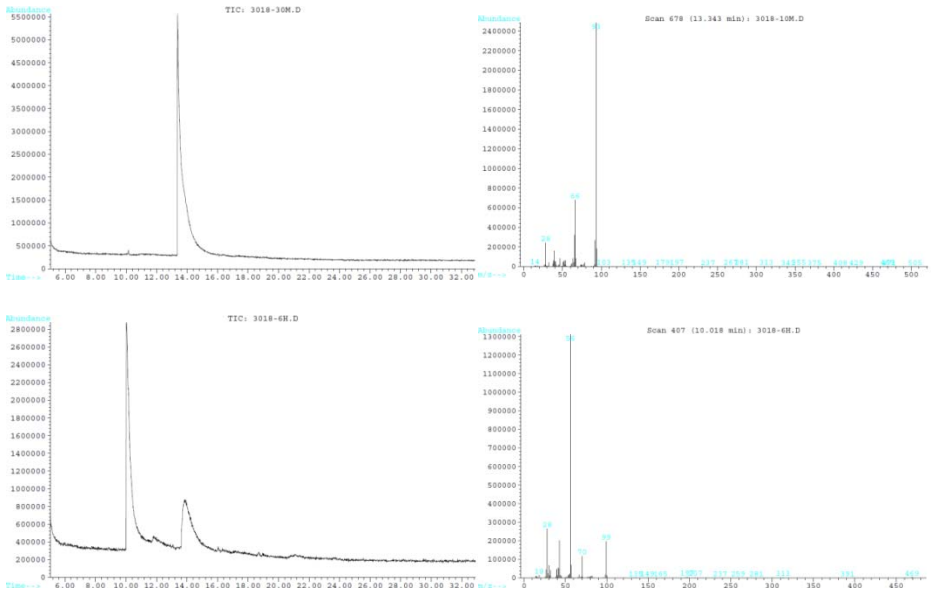

Figure A.2.17. GC-MS analysis for hydrogenation of aniline.

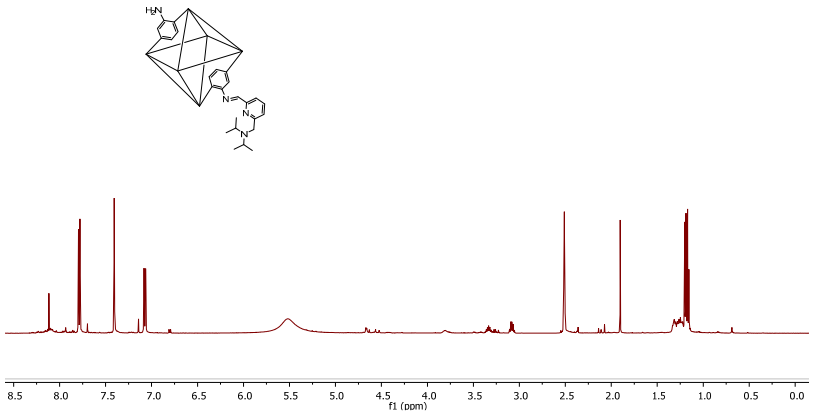

Figure A.2.18. ^{1}HNMR of Zr-BDC-NH_2-L1 (Digested sample).

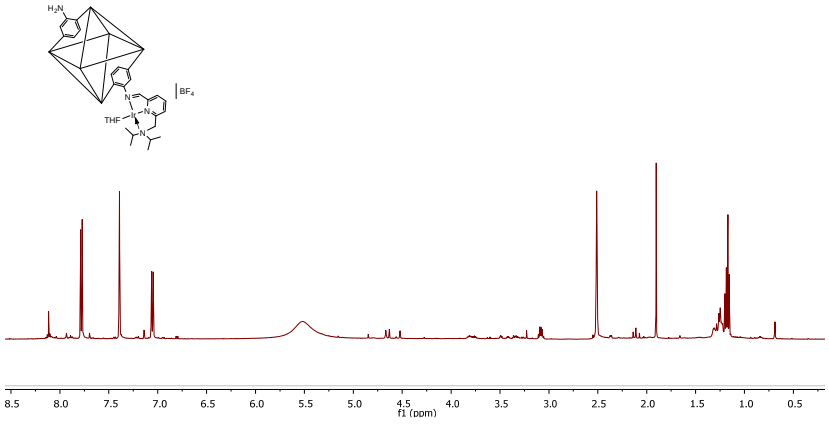

Figure A.2.19. ^{1}HNMR of Zr-BDC-NH_2-[L1Ir] (Digested sample).

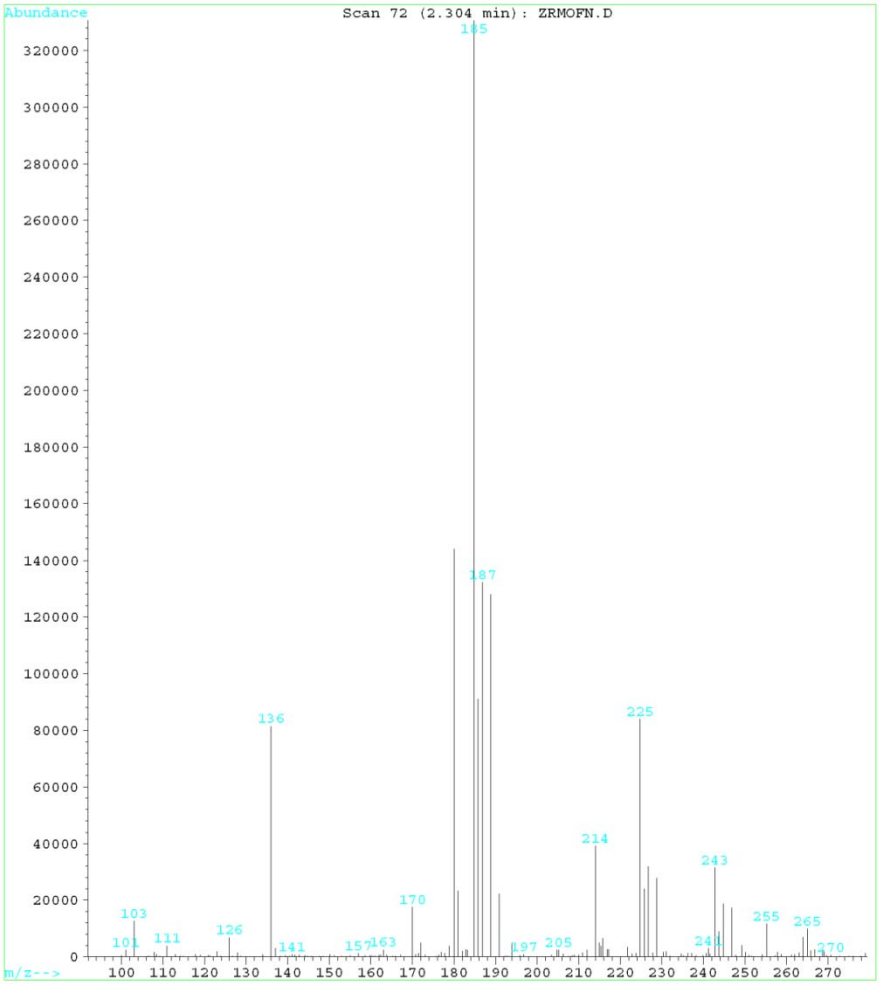

Figure A.2.20. ESI-MS of Zr-BDC-NH_2 (Digested sample).

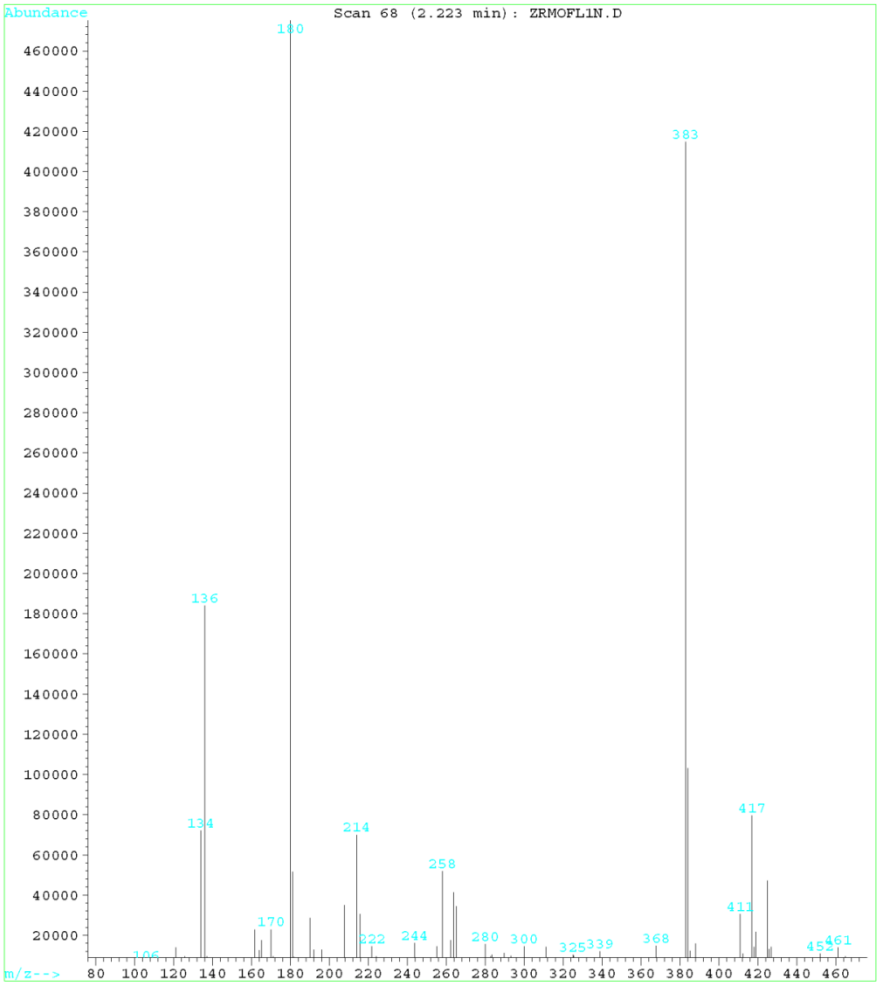

Figure A.2.21. ESI-MS of Zr-BDC-NH_2-L1 (Digested sample).

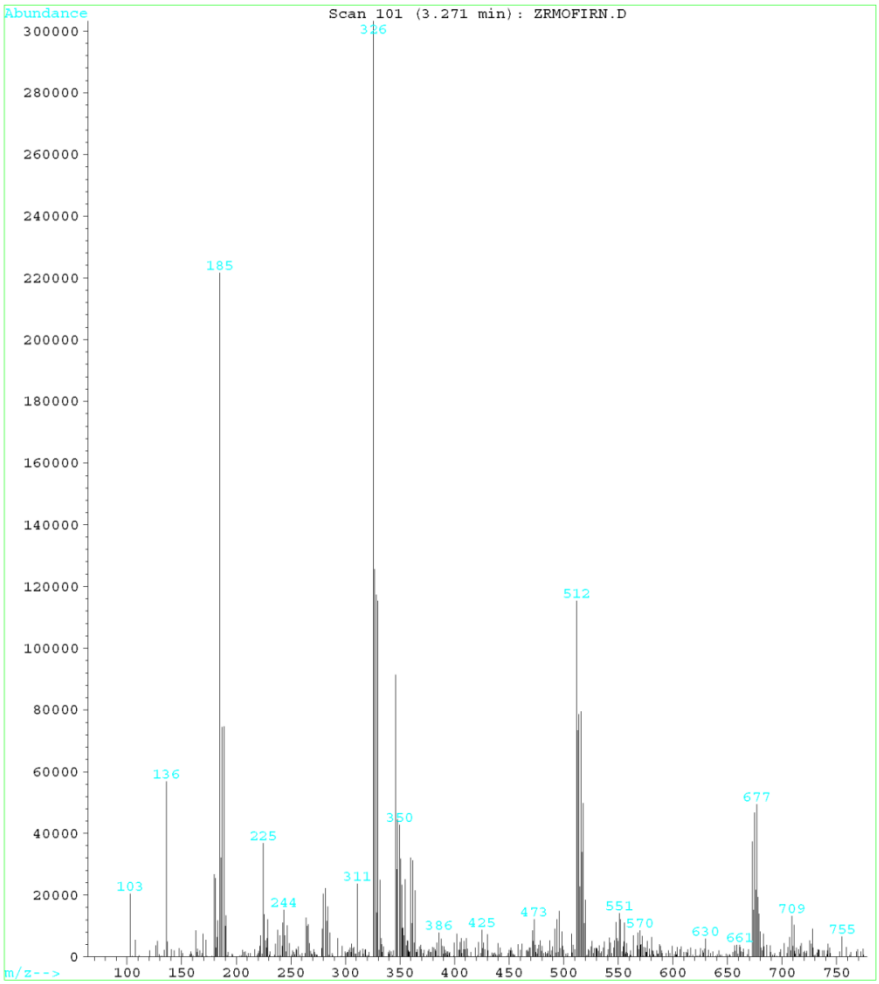

Figure A.2.22. ESI-MS of Zr-BDC-NH_2-[LIr] BF_4 (Digested sample).

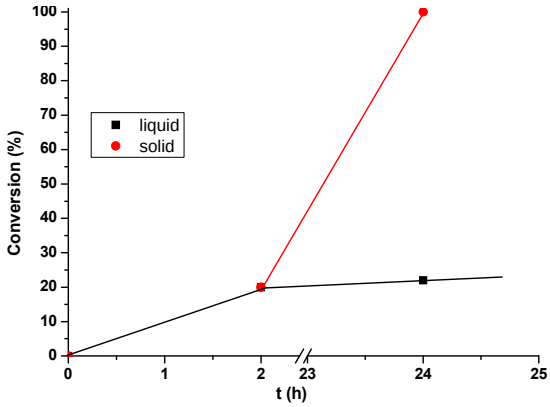

Figure A.2.23. Hot filtration experiment for one-pot reductive amination of benzaldehyde with nitrobenzene.

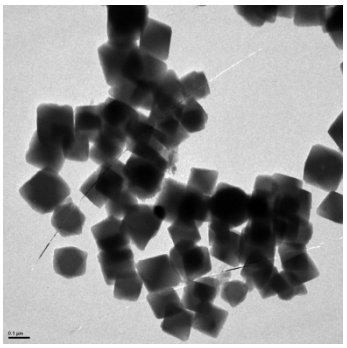

Figure A.2.24. Fresh Zr-BDC-NH_2-[LIr]BF_4.

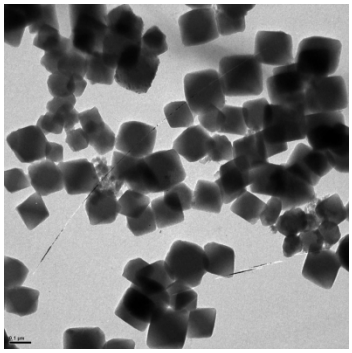

Figure A.2.25. Recovered Zr-BDC-NH_2-[LIr]BF_4

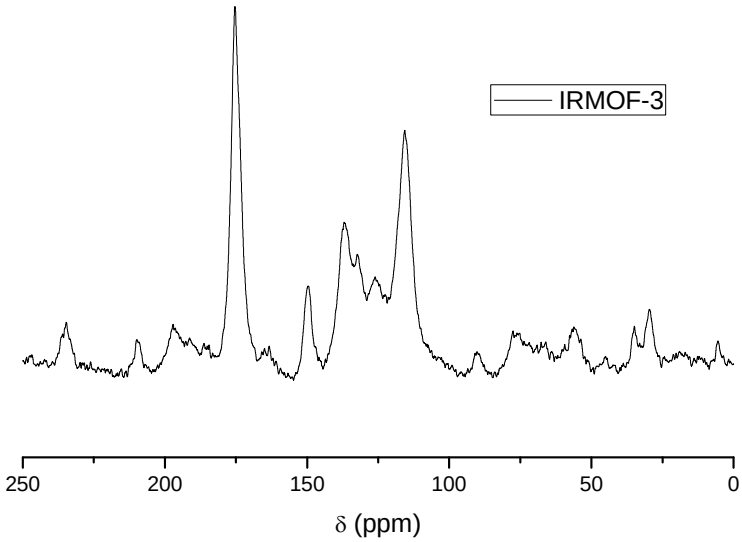

Figure A.2.26. ^{13}C NMR IRMOF-3.

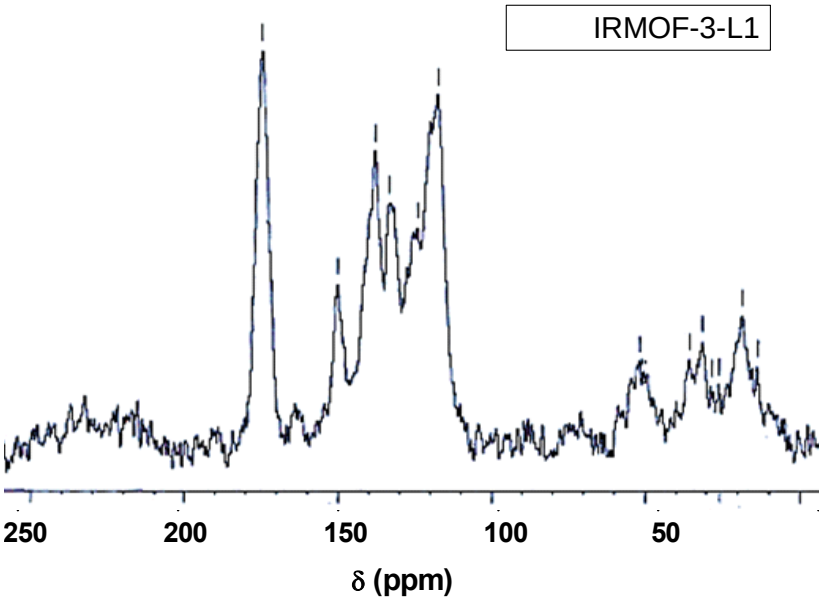

Figure A.2.27. ^{13}C NMR IRMOF-3-L.

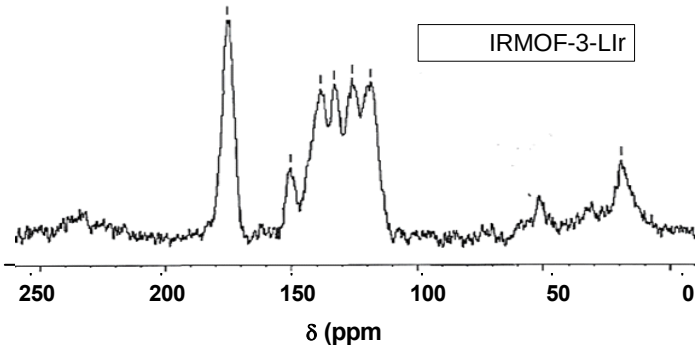

Figure A.2.28. ^{13}C NMR IRMOF-3-L-Ir.

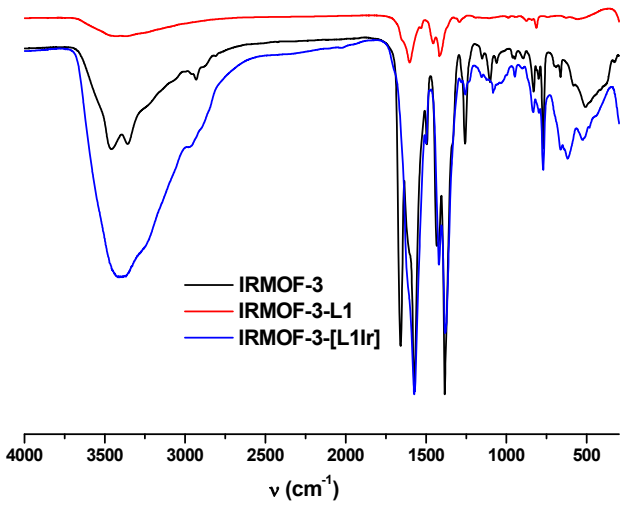

Figure A.2.29. FTIR spectra of IRMOF-3 and the post-synthetic modified IRMOF-3-L1, IRMOF-3-[L1Ir].

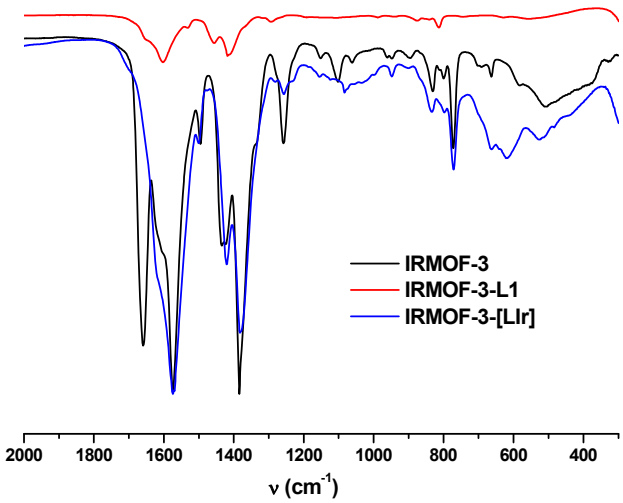

Fig. A.2.30. FTIR spectra of IRMOF-3 and the post-synthetic modified IRMOF-3-L1, IRMOF-3-[L1Ir]: MOF framework region and ν(C=O) region.

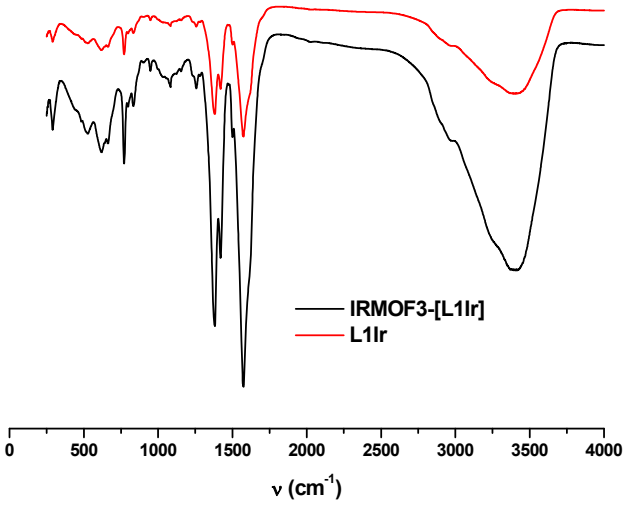

Figure A.2.31.FT-IR for L1Ir IRMOF-3-[L1Ir].

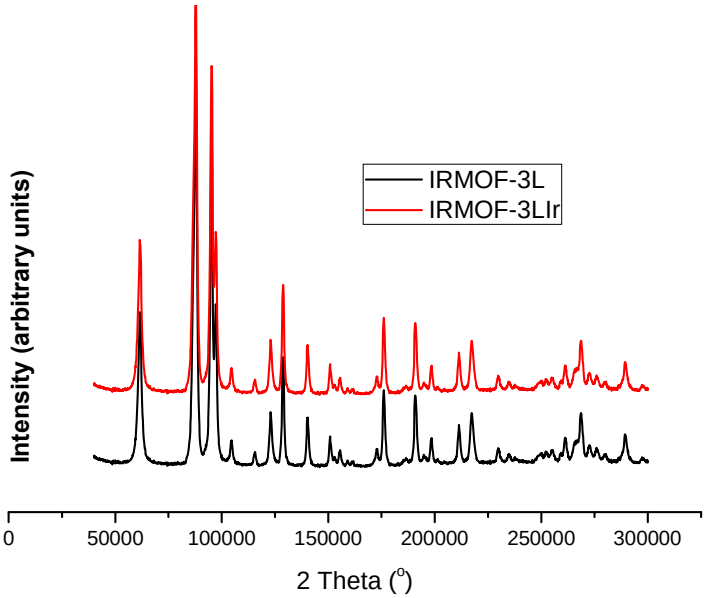

Figure A.2.32. PXRD for IRMOF-3-L1 and IRMOF-3-[L1Ir].

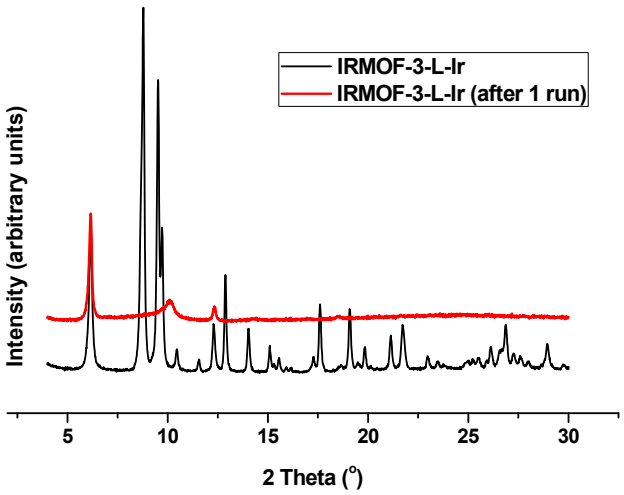

Figure A.2.33. PXRD of IRMOF-3-[L1Ir] after one run.

Figure A.2.34. ^{1}H NMR L1**.**

Figure A.2.35. ^{1}H NMR [L1Ir].

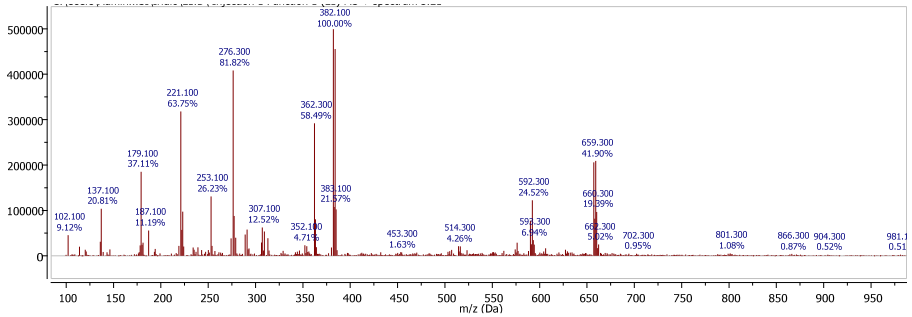

Figure A.2.36. ESI-MS [L1Ir][BF_4].

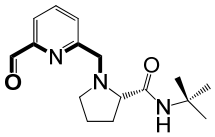

Figure A.2.37. ^{1}H NMR of (*S*)-N-(tert-butyl)-1-((6-formylpyridin-2-yl)methyl)pyrrolidine-2-carboxamide (**(*S*)-L2**).

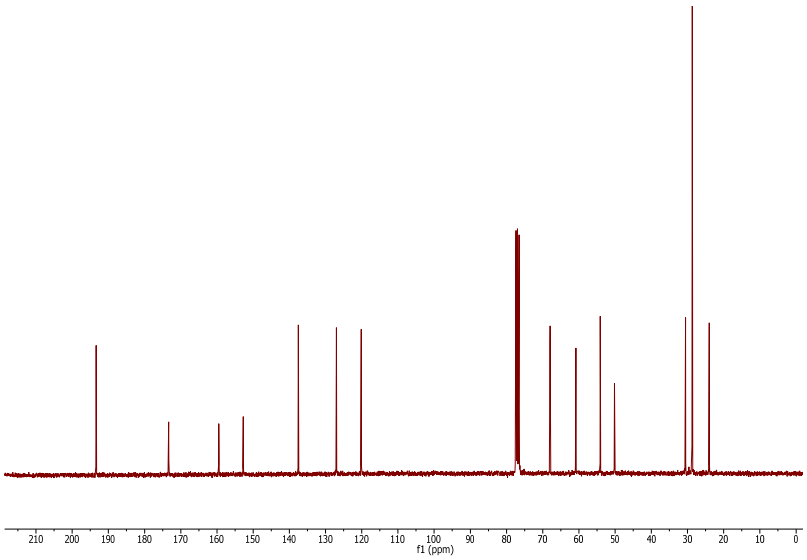

Figure A.2.38. ^{13}C NMR of (*S*)-N-(tert-butyl)-1-((6-formylpyridin-2-yl)methyl)pyrrolidine-2-carboxamide (**(*S*)-L2**).

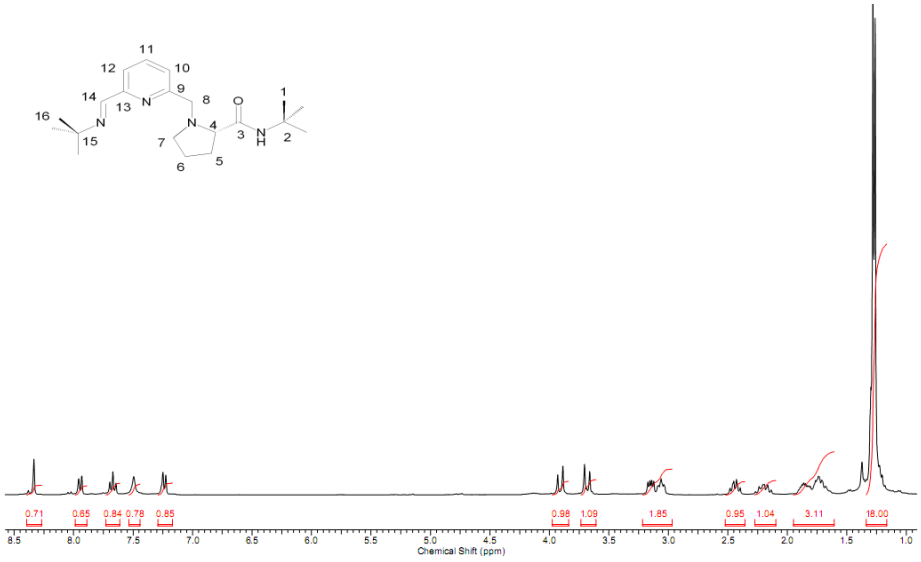

Figure A.2.39. ^{1}H NMR imine-L2.

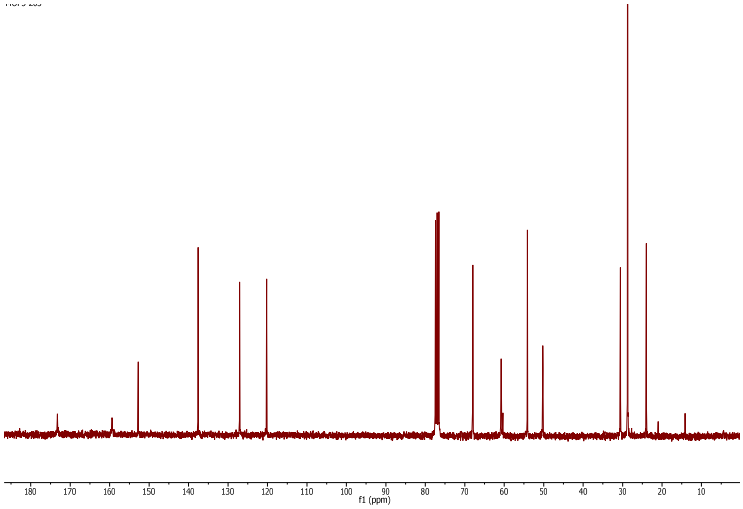

Figure A.2.40. ^{13}C NMR imine-L2.

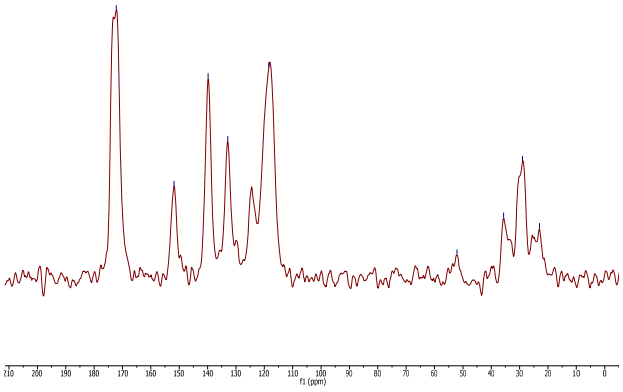

δ (ppm)

Figure A.2.41. ^{13}C NMR Zr-BDC-NH_2-L2.

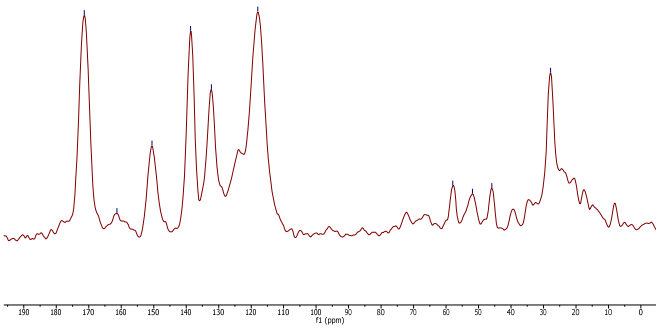

δ (ppm)

Figure A.2.42. ^{13}C NMR Zr-BDC-NH_2[L2Ir]BF_4.

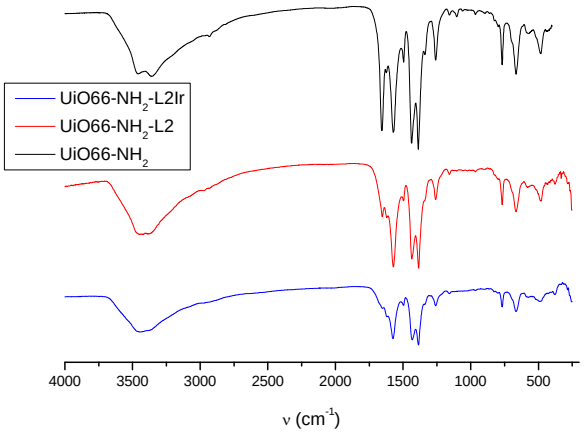

Figure A.2.43. FT-IR (normalized) for Zr-BDC-NH_2, Zr-BDC-NH_2-L2, Zr-BDC-NH_2[L2Ir]$^+$.

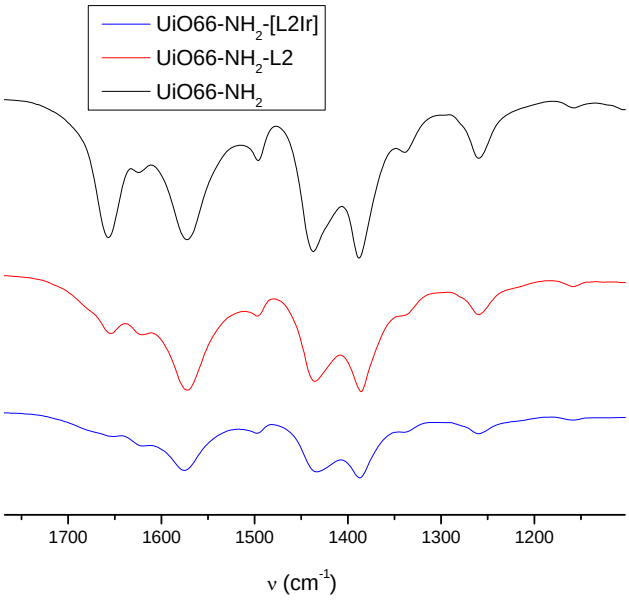

Figure A.2.44. FT-IR (normalized) for Zr-BDC-NH_2, Zr-BDC-NH_2-L2, Zr-BDC-NH_2[L2Ir]$^+$: MOF framework region and ν(C=O) region. (Note: for starting Zr-BDC-NH_2 peaks at 1657 cm^{-1} assigned to the C=O stretching vibration of residual DMF strongly adsorbed in the channels network).

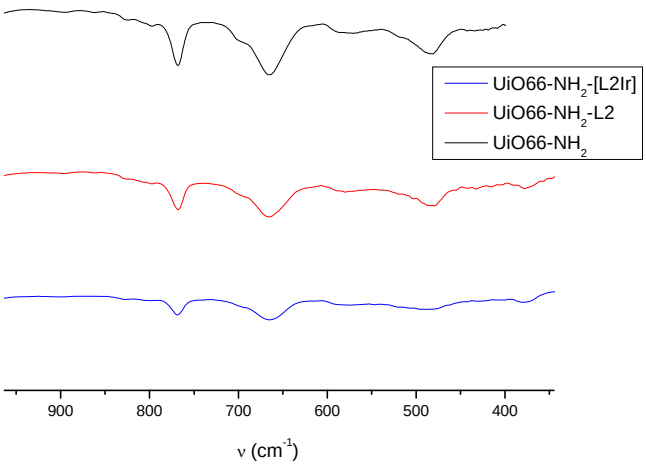

Figure A.2.45. FT-IR (normalized) for Zr-BDC-NH_2, Zr-BDC-NH_2-L2, Zr-BDC-NH_2[L2Ir]$^+$: Band at 760 cm^{-1}.

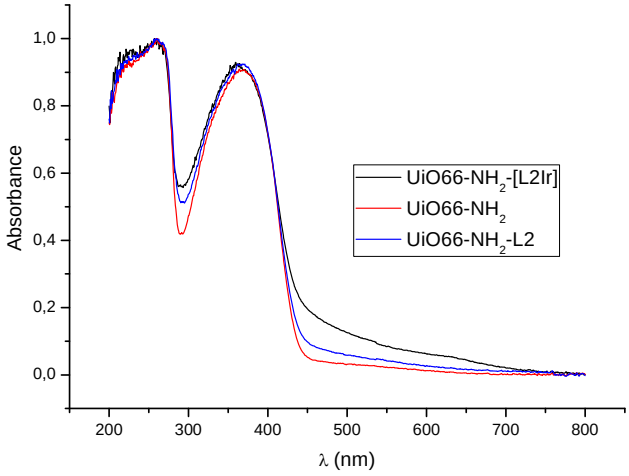

Figure A.2.46. DRUV- for Zr-BDC-NH_2, Zr-BDC-NH_2-L2, Zr-BDC-NH_2[L2Ir]$^+$.

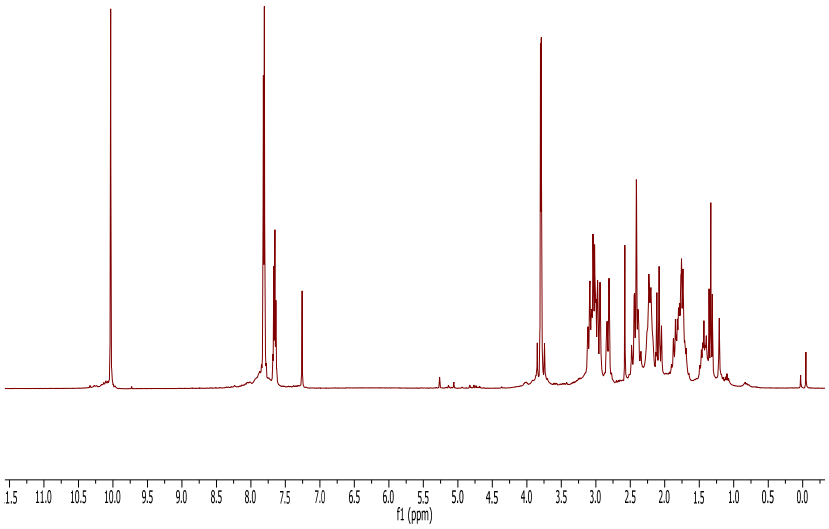

Figure A.2.47. ^{1}H NMR of (*S*)-6-((hexahydropyrrolo[1,2-a]pyrazin-2(1H)-yl)methyl)picolinaldehyde (**(*S*)-L3**).

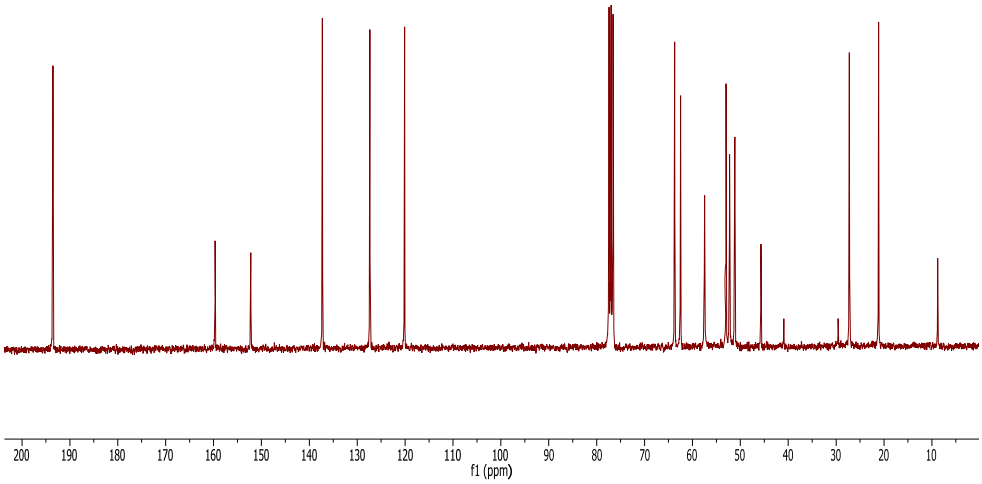

Figure A.2.48. ^{13}C NMR of (*S*)-6-((hexahydropyrrolo[1,2-a]pyrazin-2(1H)-yl)methyl)-picolinaldehyde (**(*S*)-L3**).

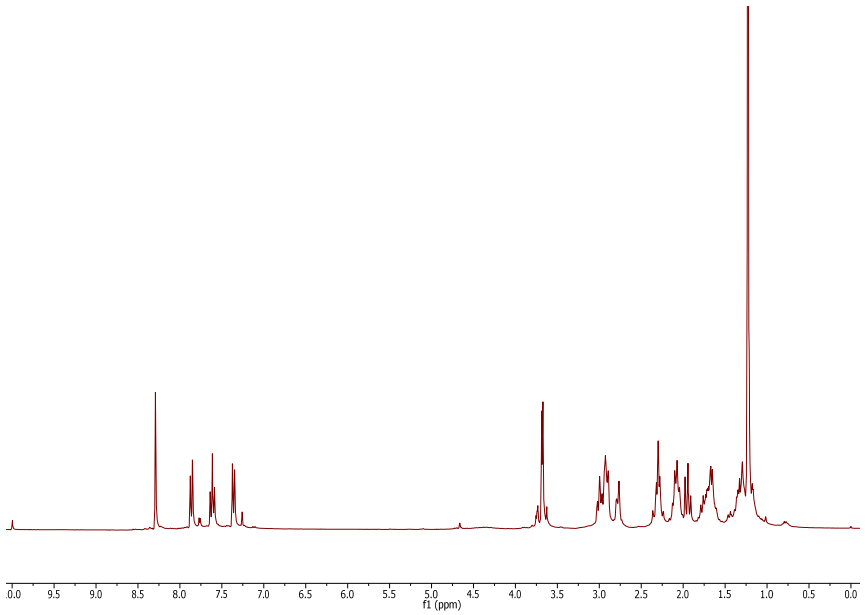

Figure A.2.49. ^{1}H NMR imine-L3.

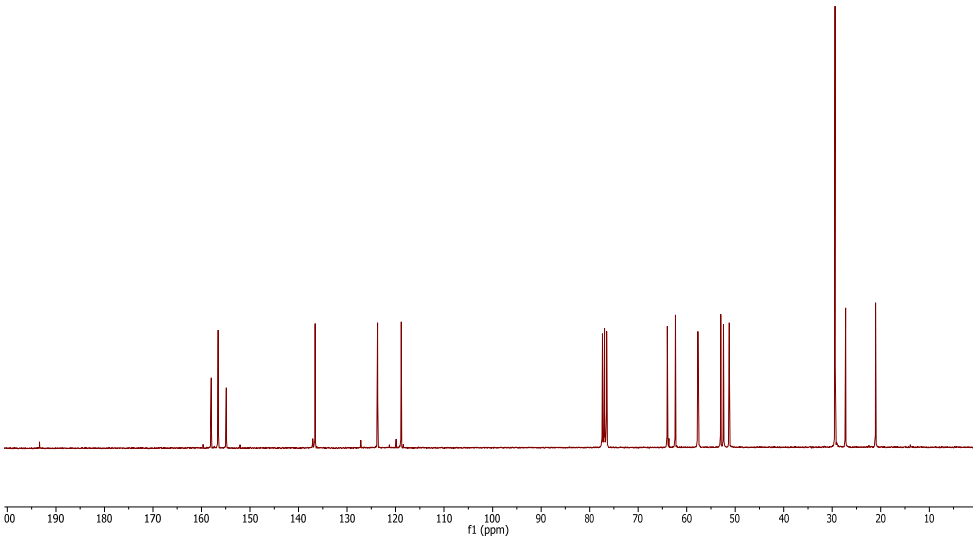

Figure A.2.50. ^{13}C NMR imine-L3.

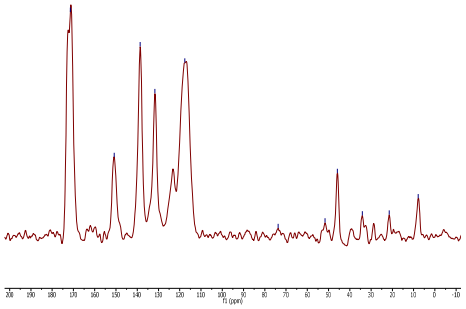

δ (ppm)

Figure A.2.51. ^{13}C NMR Zr-BDC-NH_2-L3.

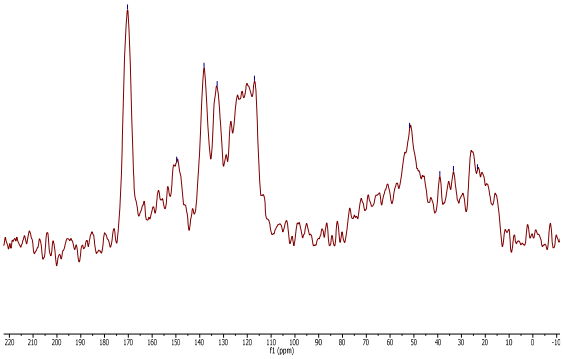

δ (ppm)

Figure A.2.52. ^{13}C NMR Zr-BDC-NH_2-[L3Rh]BF4.

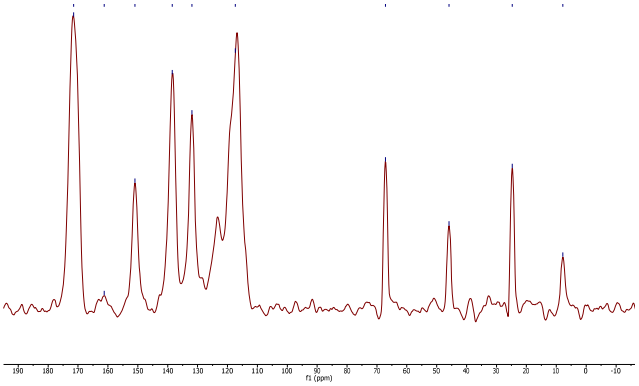

δ (ppm)

Figure A.2.53. ^{13}C NMR Zr-BDC-NH_2-[L3Ir]BF_4.

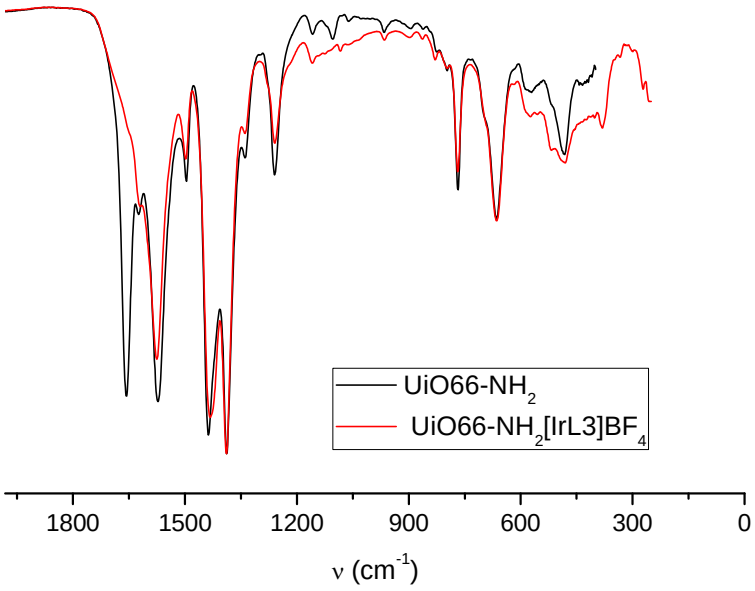

Figure A.2.54. FTIR spectra of Zr-BDC-NH_2 and the modified Zr-BDC-NH_2-L3.

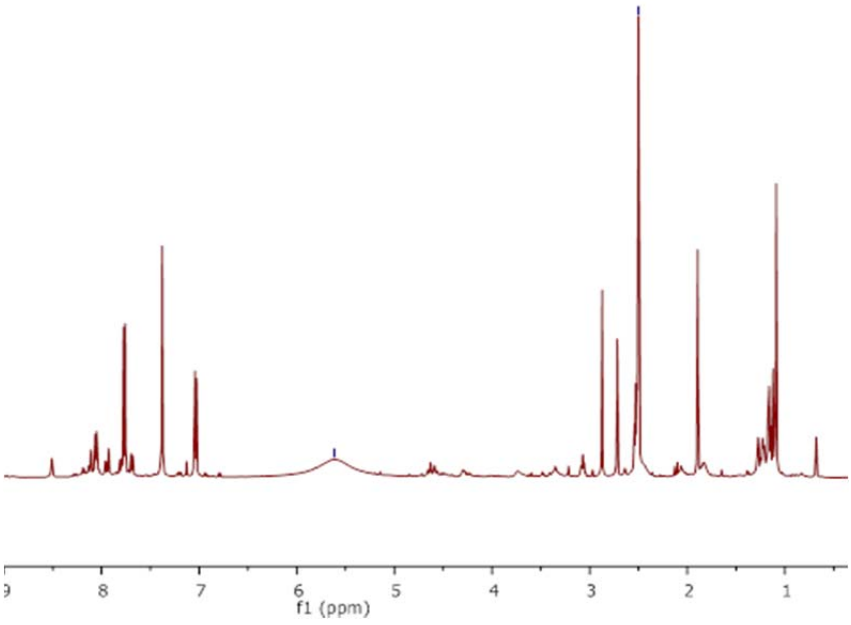

Figure A.2.55. ^{1}HNMR of Zr-BDC-NH_2-L2 (Digested sample).

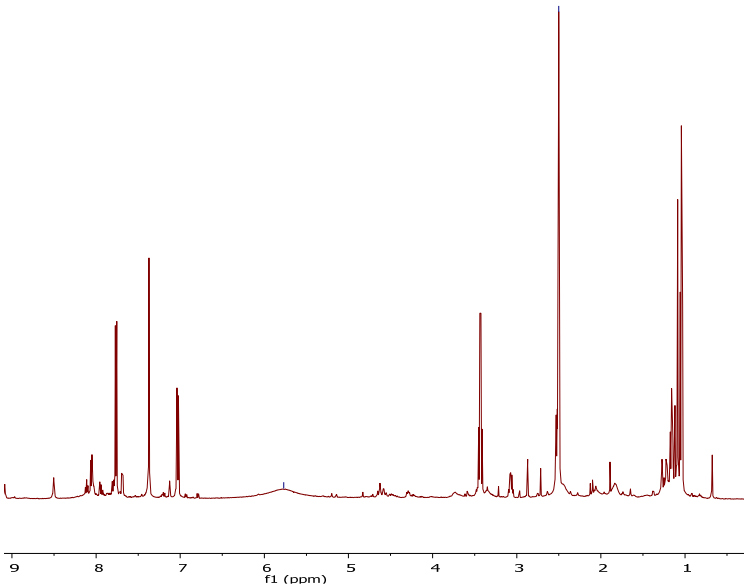

Figure A.2.56. ^{1}HNMR of Zr-BDC-NH_2-[L3Ir] (Digested sample).

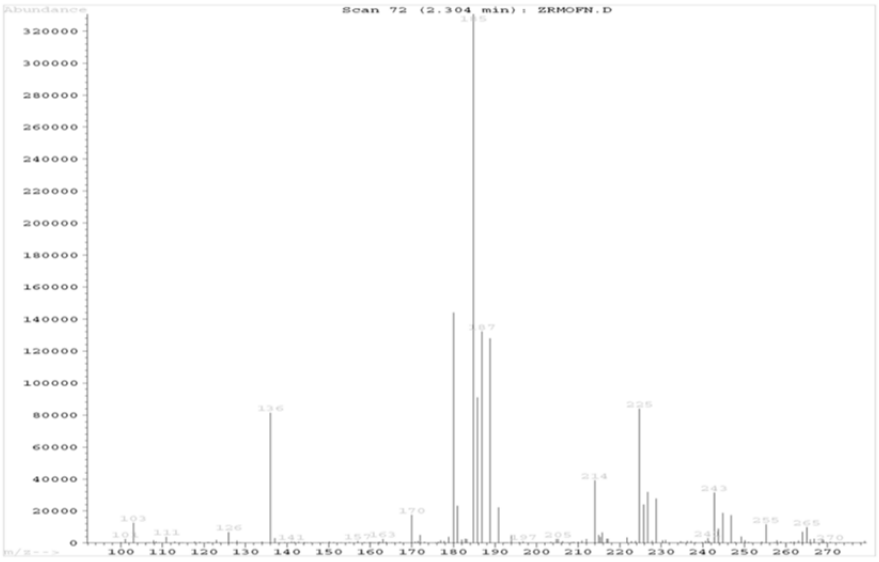

Figure A.2.57. ESI-MS of Zr-BDC-NH_2 (Digested sample).

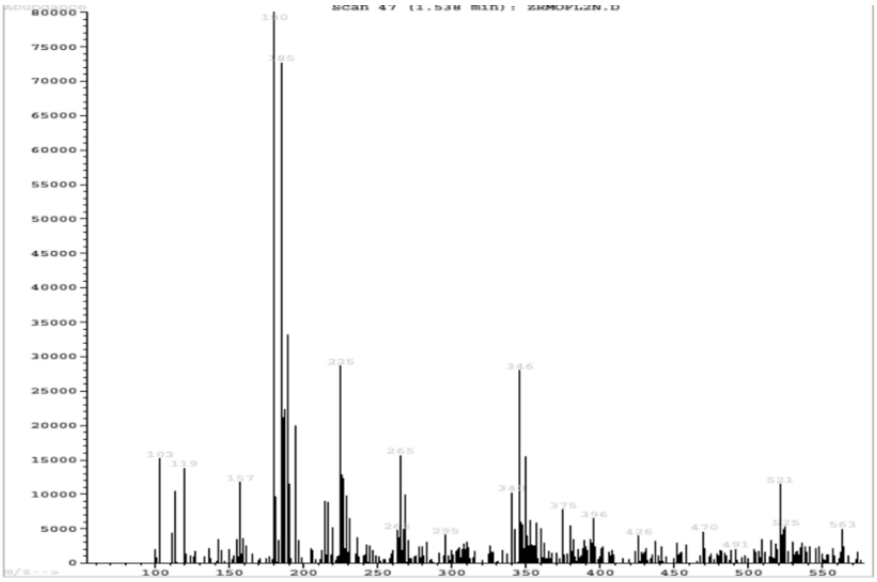

Figure A.2.58. ESI-MS of Zr-BDC-NH_2-L2 (Digested sample).

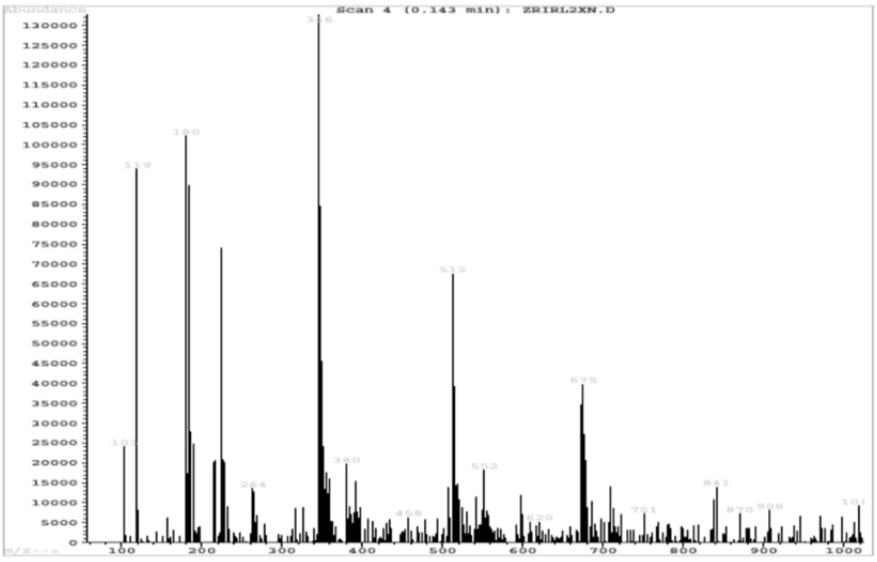

Figure A.2.59. ESI-MS of Zr-BDC-NH_2-[L2Ir]BF_4 (Digested sample).

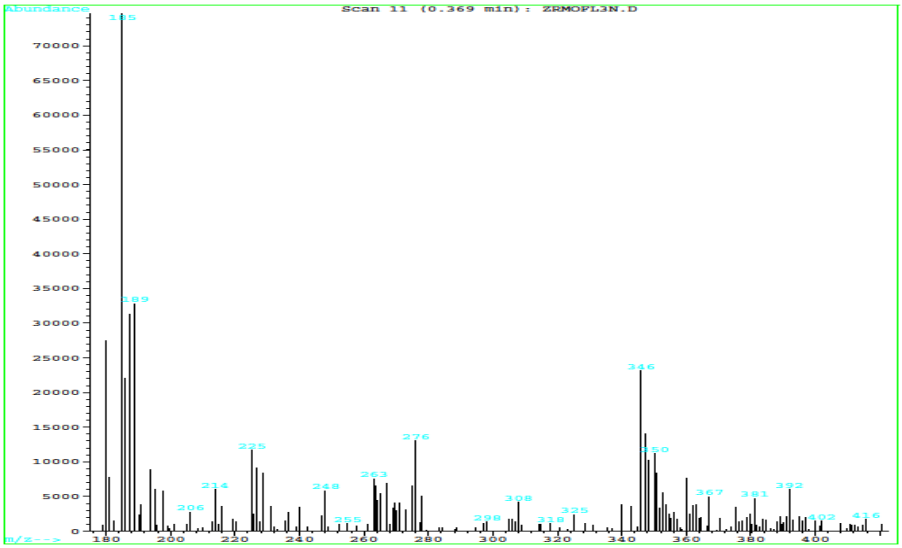

Figure A.2.60. ESI-MS of Zr-BDC-NH_2-L3 (Digested sample).

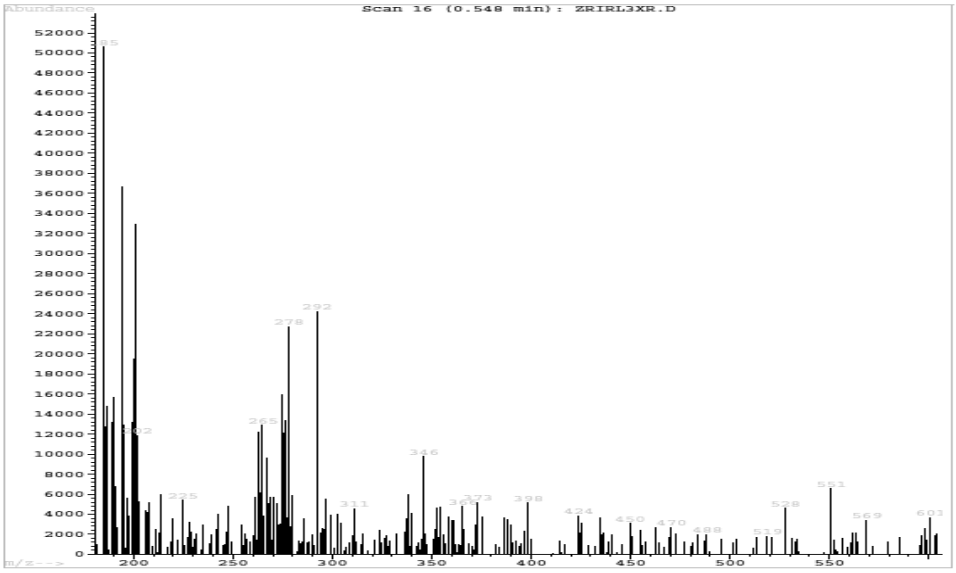

Figure A.2.61. ESI-MS of Zr-BDC-NH_2-[L3Ir]BF_4 (Digested sample).

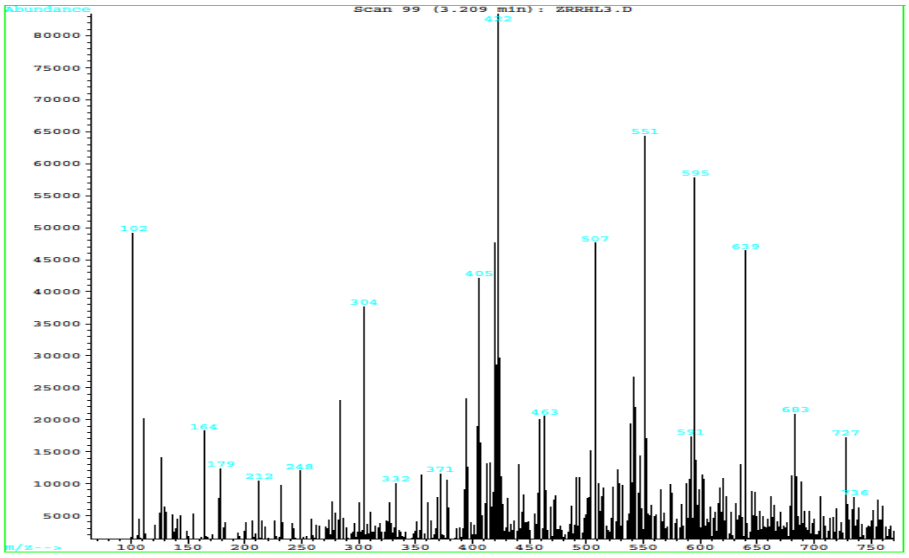

Figure A.2.62. ESI-MS of Zr-BDC-NH_2-[L3Rh]BF_4 (Digested sample).

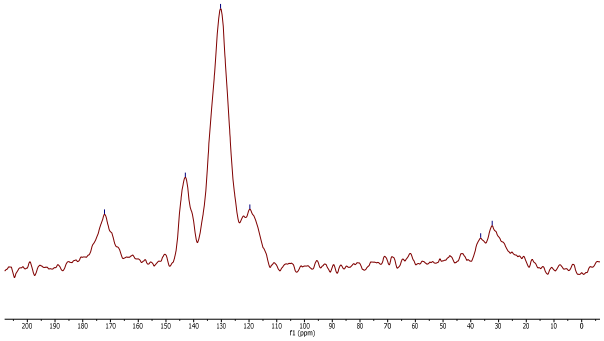

δ (ppm)

Figure A.2.63. ^{13}C NMR Zr-BPDC-NH_2-L3.

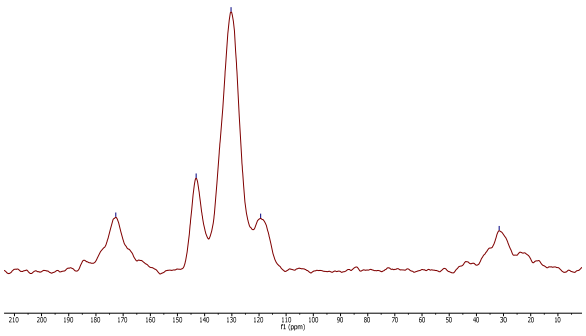

δ (ppm)

Figure A.2.64. ^{13}C NMR Zr-BPDC-NH_2-[L3Rh]BF_4.

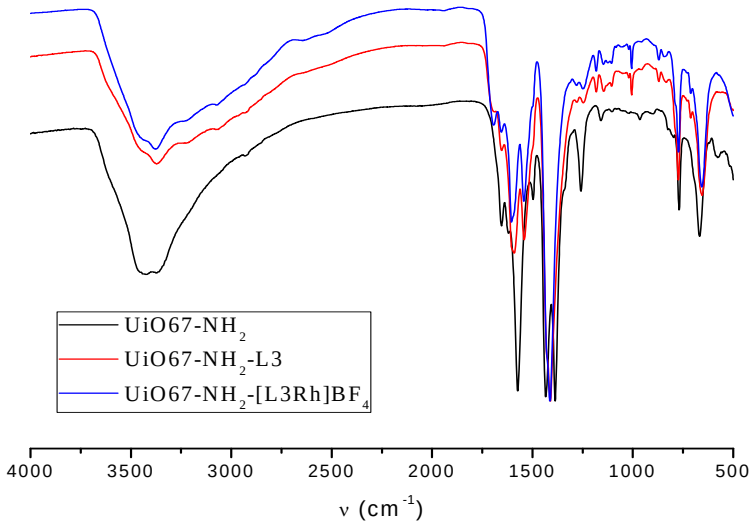

Figure A.2.65. FTIR spectra of Zr-BPDC-NH_2 and the modified Zr-BPDC-NH_2-L3.

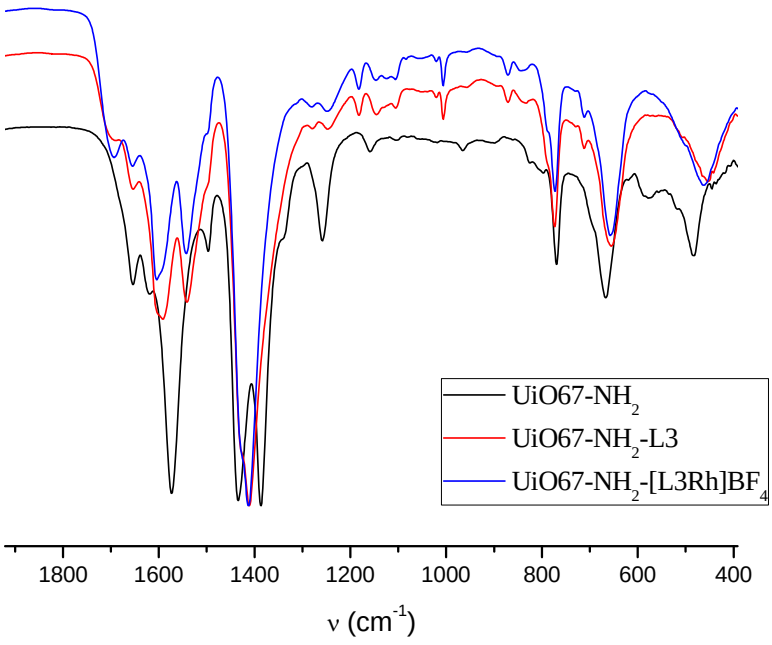

Figure A.2.66. FTIR spectra of Zr-BPDC-NH_2 and the modified Zr-BPDC-NH_2-L3.

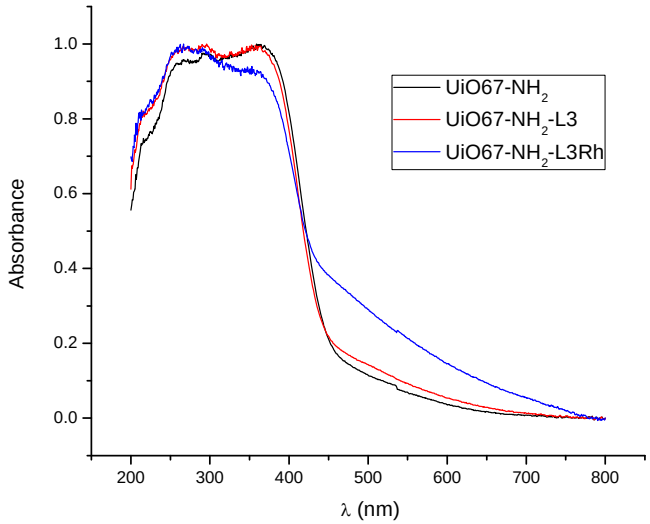

Figure A.2.67. DRUV spectra of Zr-BPDC-NH_2 and the modified Zr-BPDC-NH_2-L3.

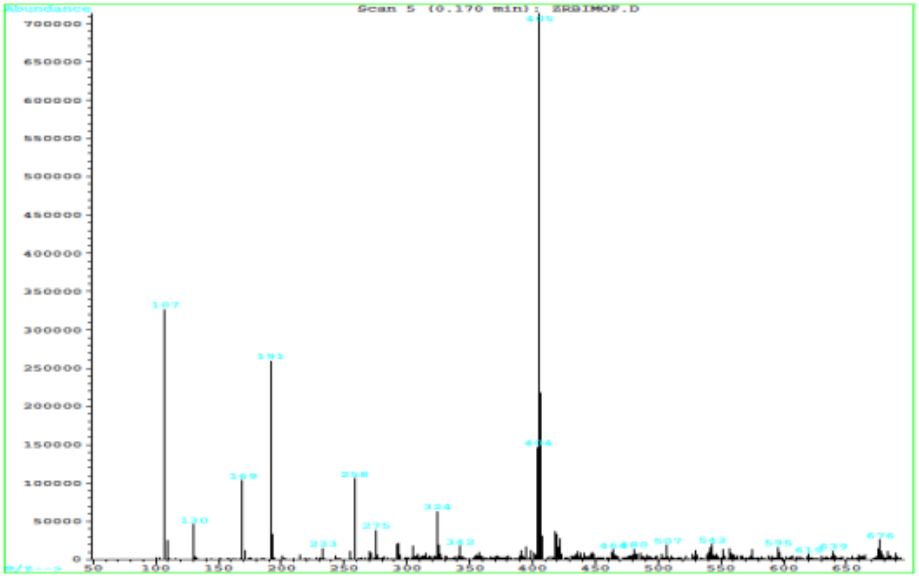

Figure A.2.68. ESI-MS of Zr-BPDC-NH_2 (Digested sample).

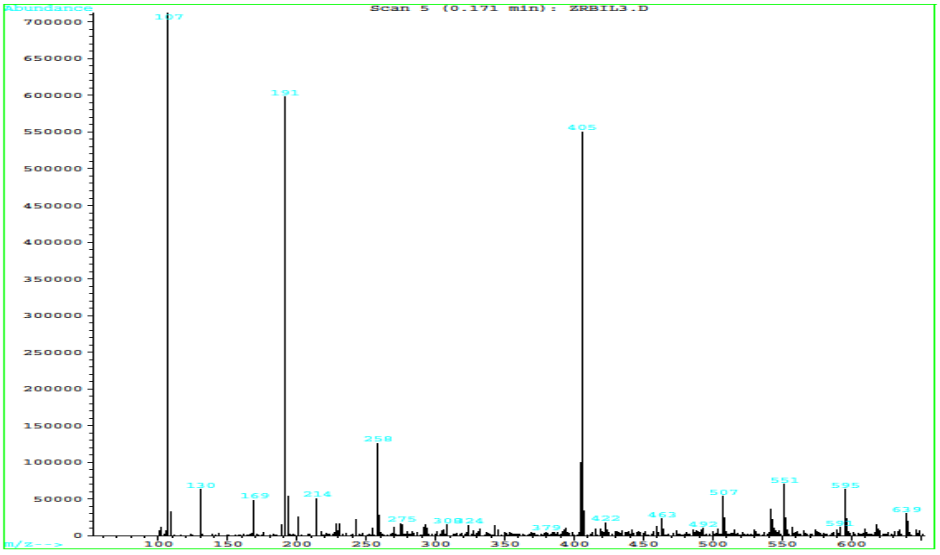

Figure A.2.69. ESI-MS of Zr-BPDC-NH_2-L3 (Digested sample).

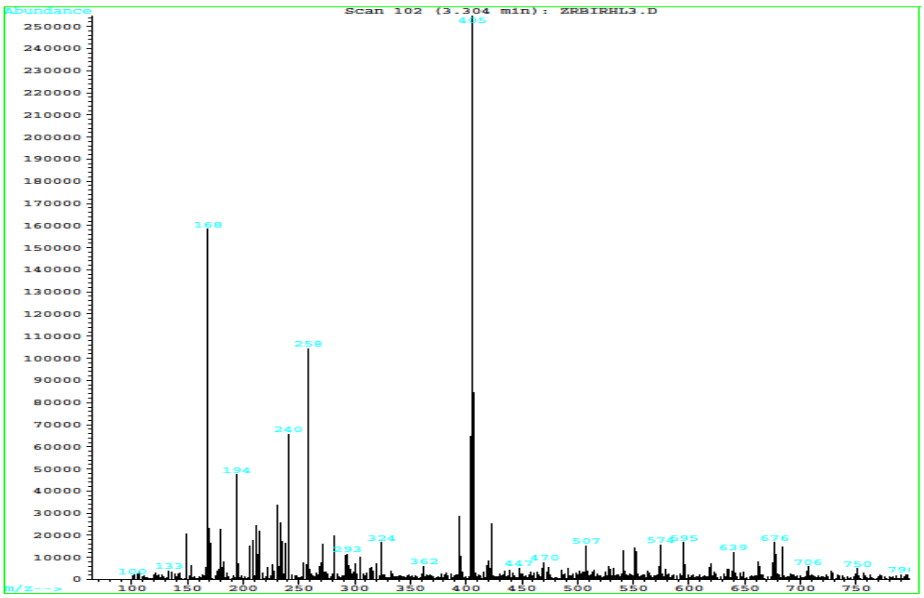

Figure A.2.70. ESI-MS of Zr-BPDC-NH_2-[L3Rh]BF_4 (Digested sample).

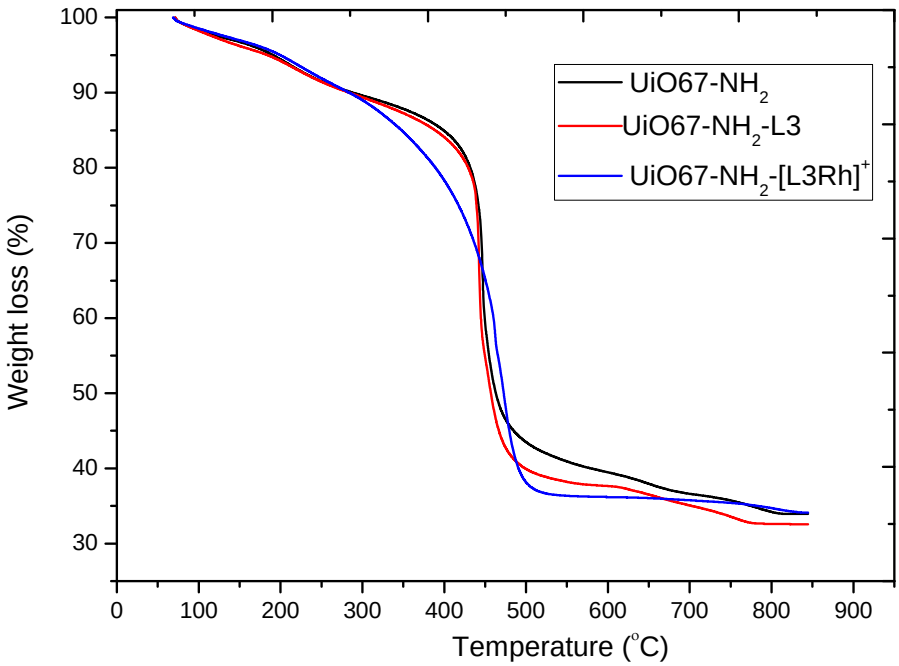

Figure A.2.71. TGA patterns of Zr-BPDC-NH_2, Zr-BPDC-NH_2-L3, Zr-BPDC-NH_2-[L3Rh].

Table A.2.1. Recycling experiments with Zr-BDC-NH_2-L2 and Zr-BPDC-NH_2-L2 catalysts.[1]

cycle	catalyst	t (h)	Conv. (%)	E/Z ratio[2]
1	Zr-BDC-NH_2-L2	24	90	50:50
2		24	87	50:50
3		24	85	50:50
1	Zr-BPDC-NH_2-L2	24	100	40:60
2		24	95	40:60
3		24	95	40:60
4			97	40:60

[1]Cat. 5 mol% based on Zr, T: 100 °C. [2]Determined by ^{1}H NMR analysis.

Table A.2.2. Recycling experiments with Zr-BDC-NH_2-L3Rh.[1]

cycle	catalyst	t (h)[2]	Conv. (%)
1	Zr-BDC-NH_2-L3Rh	34	100
2		36	100
3		36	100
4		40	100

[1]Cat. 1 mol% based on Rh, toluene: ml, T: 100 °C, PH_2: 6 bar. [2]condensation + alkene hydrogenation.

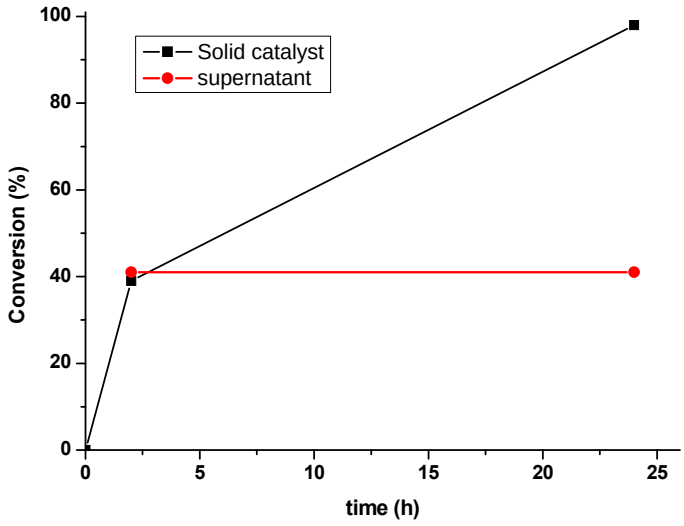

Figure A.2.72. Kinetic traces for the hydrogenation of ethyl 2-nitro-3-phenylacrylate in presence of **Zr-BDC-NH_2-[LRh]** and with the supernatant liquid.

Annexes of chapter 3

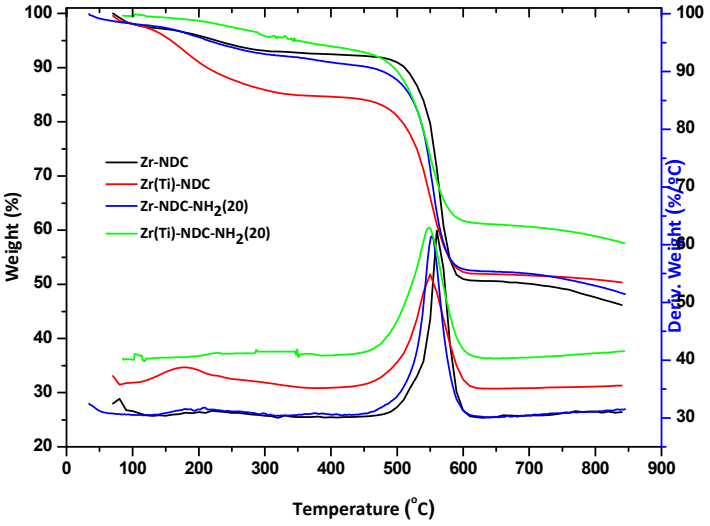

Figure A.3.1. Termograms of Zr-NDC series.

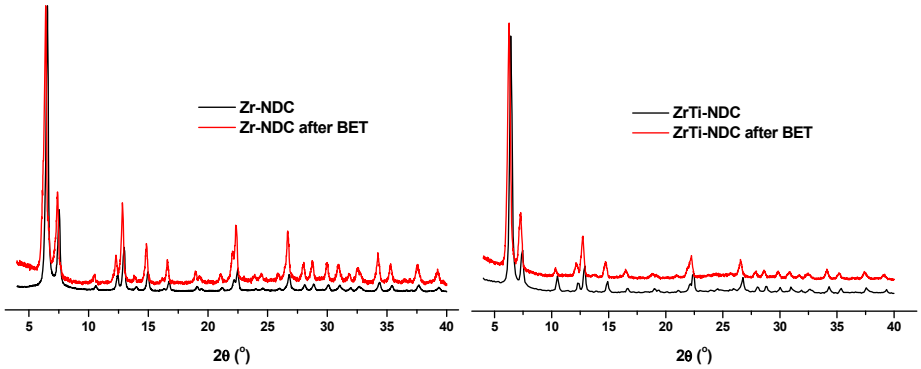

Figure A.3.2. PXRD patterns of Zr-NDC and Zr(Ti)-NDC fresh and after BET measurements.

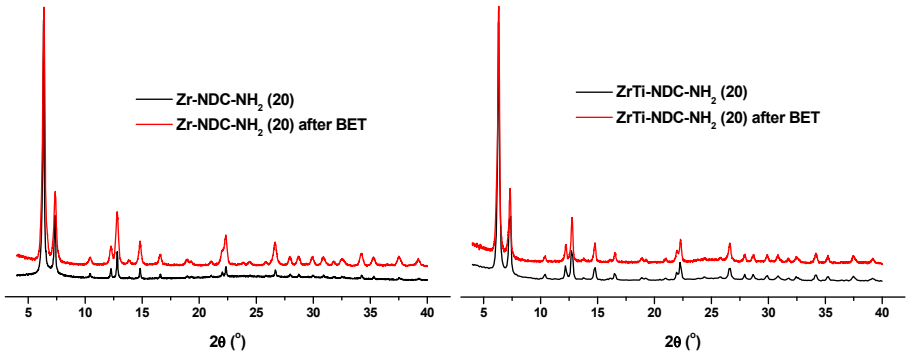

Figure A.3.3. PXRD patterns of Zr-NDC-NH_2(20) and Zr(Ti)-NDC-NH_2(20) fresh and after BET measurements.

Table A.3.1. Textural properties.

	BET ($m^2 \cdot g$)	Pore size (nm)	V (cm^3/g)
Zr-NDC	1068.7	1.48	0.27
Zr(Ti)-NDC	1062.6	2.07	0.53
Zr-NDC-NH_2	1372.9	1.68	0.48
Zr(Ti)-NDC-NH_2	1026.7	1.94	0.56

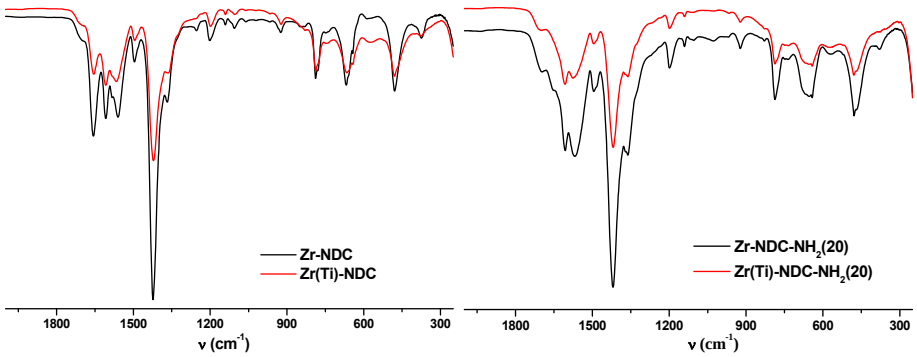

Figure A.3.4. FTIR spectra: the anti-symmetric (1590-1550 cm^{-1}) and symmetric (1390-1370 cm^{-1}) stretches of the carboxylate groups are present in the spectra of all four compounds, respectively.

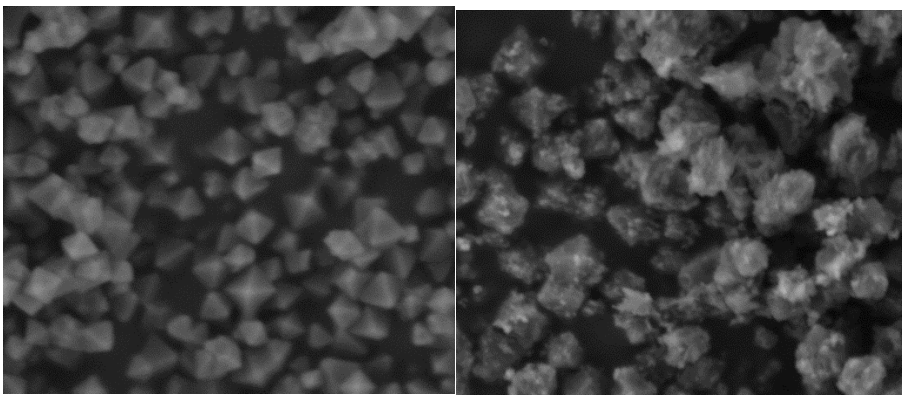

Figure A.3.5. SEM images of (a) Zr-NDC, (b) Zr(Ti)-NDC.

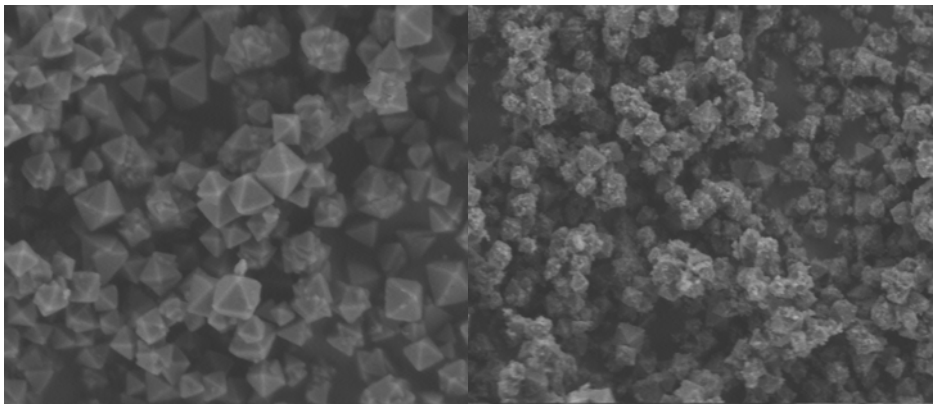

Figure A.3.6. SEM images of (a) Zr-NDC-NH_2(20), (b) Zr(Ti)-NDC-NH_2(20).

Table A.3.2. Isomerization of α-pinene oxide.

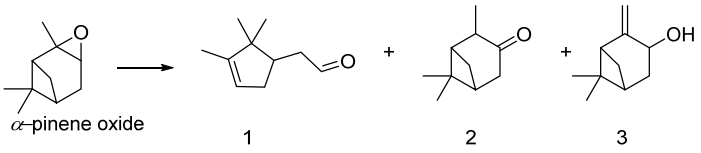

Catalyst	T (°C)	Solvent	% Conv. (h)	Sel. (%)		
				1	2	3
Zr-NDC	70	Toluene	37 (24)	47	22	31
Zr(Ti)-NDC	70	Toluene	65 (24)	51	21	28
Zr-NDC	70	-	61 (24)	48	30	22
Zr(Ti)-NDC	70	-	70 (24)	40	26	34
Zr-NDC	70	Dichloroethane	74 (24)	51	19	30
Zr(Ti)-NDC	70	Dichloroethane	88 (24)	55	20	25
Zr-NDC	100	Dichloroethane	64 (24)	45	20	35
Zr(Ti)-NDC	100	Dichloroethane	77 (24)	37	23	40
Zr-NDC	150	Dichloroethane	94 (6)	40	25	35
Zr(Ti)-NDC	150	Dichloroethane	97 (6)	29	16	55
Zr(Ti)-NDC	50	Dichloroethane	55(24)	40	29	31
Zr(Ti)-NDC	25	Dichloroethane	traces (24)	-	-	-

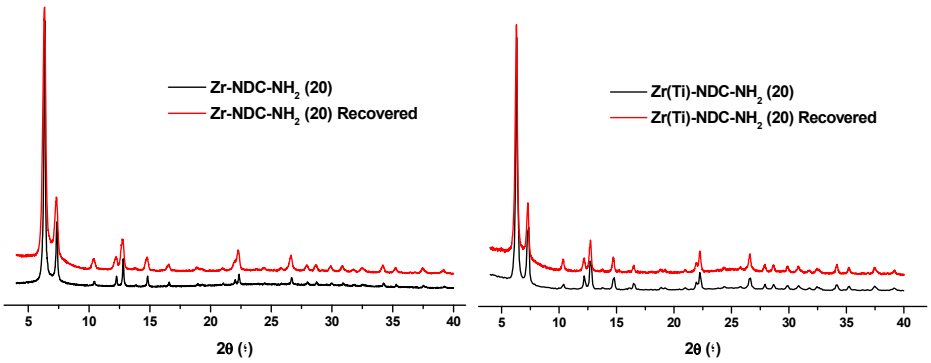

Figure A.3.7. PXRD of recovered Zr-NDC-NH_2(20) and Zr(Ti)-NDC-NH_2(20).

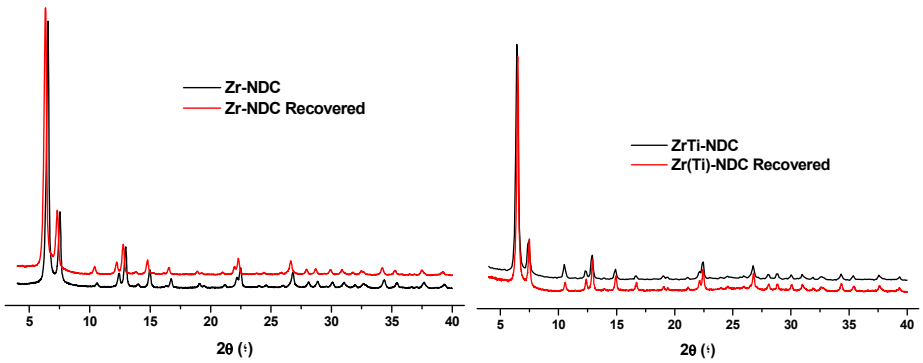

Figure A.3.8. PXRD of recovered Zr-NDC and Zr(Ti)-NDC.

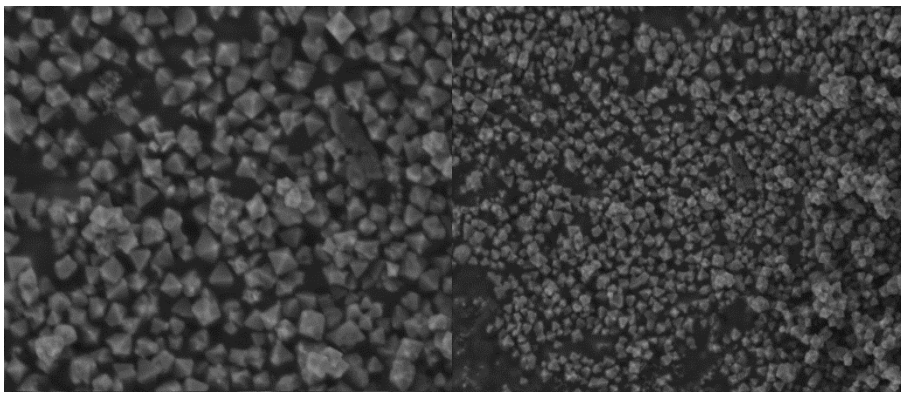

Figure A.3.9. SEM images of Zr-NDC (recovered).

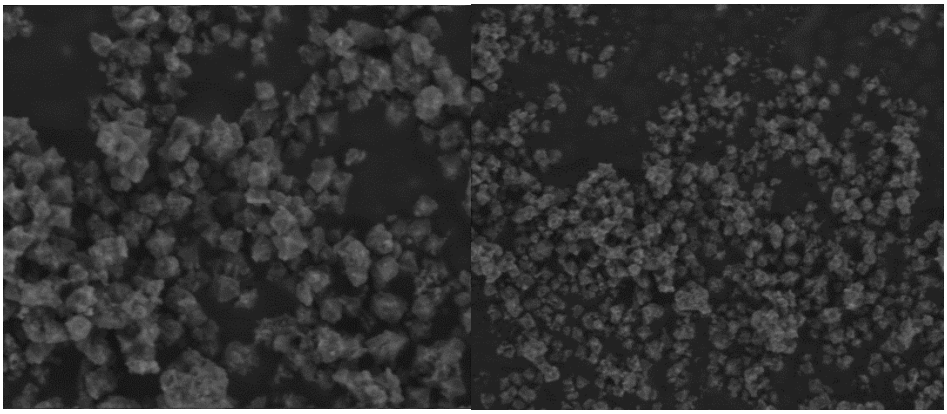

Figure A.3.10. SEM images of Zr(Ti)-NDC (recovered).

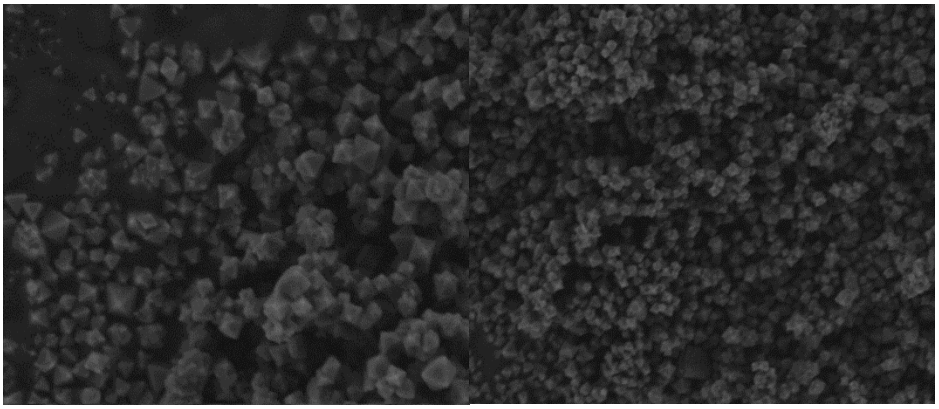

Figure A.3.11. SEM images of Zr-NDC-NH_2(20) (recovered).

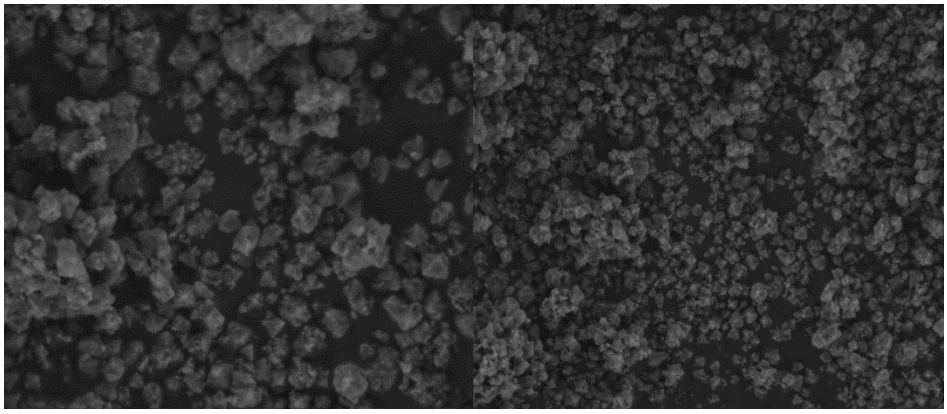

Figure A.3.12. SEM images of Zr(Ti)-NDC-NH_2(20) (recovered).

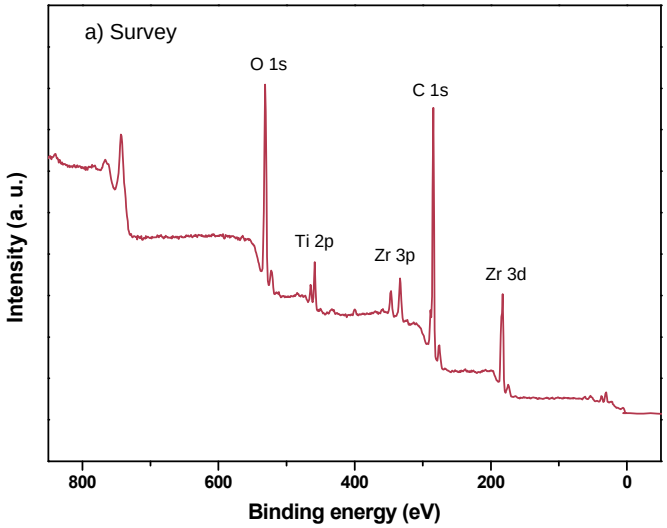

Figure A.3.13. XPS spectra (survey scan) of Zr(Ti)NDC-NH_2(20).

Figure A.3.14. The ^{1}H NMR spectrum of a solution obtained by the digestion of Zr-NDC and Zr-NDC-NH_2 in DMSO-d_6/HF_{aq} mixture.

Table A.3.3. Elemental analysis of Zr(Ce)-MOFs.

	$C_{exp.}$ %	$C_{theor.}$ %	$H_{exp.}$ %	$H_{theor.}$ %	$N_{exp.}$ %	$N_{theor.}$.%
ZrCe(20)-BDC-NH_2 (100)	28.99	31.8	3.24	1.89	4.67	4.64
ZrCe(20)-NDC-NH_2 (20)	38.62	40.98	3.11	2.72	3.35	3.32
ZrCe(50)-NDC-NH_2 (50)	38.78	38.23	2.93	2.58	3.73	3.72

Table A.3.4. Elemental analysis of ZrCeTi-MOFs.

	$C_{exp.}$ %	$C_{theor.}$ %	$H_{exp.}$ %	$H_{theor.}$ %	$N_{exp.}$ %	$N_{theor.}$.%
ZrCeTi-BDC-NH_2 (100)	28.66	33.36	2.00	12.72	4.91	3.32
ZrCeTi-NDC-NH_2 (100)	34.54	43.00	2.91	2.64	4.18	3.80

References

References

(1) Nicolaou, K. C. *Chem* **2016**, *1*, 331-334.

(2) Anastas, P. T., Kirchhoff, M. M. *Acc. Chem. Res.* **2002**, *35*, 686-694.

(3) Anastas, P. T., Kirchhoff, M. M., Williamson, T. C. *App. Catal., A* **2001**, *221*, 3-13.

(4) a) Climent, M. J., Corma, A., Iborra, S. *Chem. Rev.* **2011**, *111*, 1072-1133; b) Climent, M. J., Corma, A., Iborra, S. *RSC. Adv.* **2012**, *2*, 16-58; c) Climent, M. J., Corma, A., Iborra, S., Sabater, M. J. *ACS Catal.* **2014**, *4*, 870-891.

(5) Thomas, J. M., Thomas, W. J. *Principles and practice of heterogeneous catalysis*, Vol.; VCH, **1997**.

(6) Nelson, D. L., Cox, M. M. *Lehninger Principles of Biochemistry*, Vol.; W.H. Freeman, **2013**.

(7) Schmid, A., Dordick, J. S., Hauer, B., Kiener, A., Wubbolts, M., Witholt, B. *Nature* **2001**, *409*, 258-268.

(8) Bell, A. T. *Science* **2003**, *299*, 1688-1691.

(9) Corma, A. *Chem. Rev.* **1997**, *97*, 2373-2420.

(10) Yoon, M., Srirambalaji, R., Kim, K. *Chem. Rev.* **2012**, *112*, 1196-1231.

(11) Garcia-Garcia, P., Muller, M., Corma, A. *Chem. Sci.* **2014**, *5*, 2979-3007.

(12) Murray, L. J., Dinca, M., Long, J. R. *Chem. Soc. Rev.* **2009**, *38*, 1294-1314.

(13) a) Li, J.-R., Kuppler, R. J., Zhou, H.-C. *Chem. Soc. Rev.* **2009**, *38*, 1477-1504; b) Gücüyener, C., van den Bergh, J., Gascon, J., Kapteijn, F. *J. Am. Chem. Soc.* **2010**, *132*, 17704-17706.

(14) a) Yaghi, O. M., O'Keeffe, M., Ockwig, N. W., Chae, H. K., Eddaoudi, M., Kim, J. *Nature* **2003**, *423*, 705-714; b) Yaghi, O. M. *Nat. Mater.* **2007**, *6*, 92-93; c) Ma, L., Abney, C., Lin, W. *Chem. Soc. Rev.* **2009**, *38*, 1248-1256.

(15) a) Long, J. R., Yaghi, O. M. *Chem. Soc. Rev.* **2009**, *38*, 1213-1214; b) Tranchemontagne, D. J., Mendoza-Cortes, J. L., O'Keeffe, M., Yaghi, O. M. *Chem. Soc. Rev.* **2009**, *38*, 1257-1283; c) Jiang, H.-L., Xu, Q. *Chem. Commun.* **2011**, *47*, 3351-3370; d) Kuppler, R. J., Timmons, D. J., Fang, Q.-R., Li, J.-R., Makal, T. A., Young, M. D., Yuan, D., Zhao, D., Zhuang, W., Zhou, H.-C. *Coord. Chem. Rev.* **2009**, *253*, 3042-3066.

(16) McKinlay, A. C., Morris, R. E., Horcajada, P., Férey, G., Gref, R., Couvreur, P., Serre, C. *Angew. Chem. Int. Ed.* **2010**, *49*, 6260-6266.

(17) Stahl, G. E. *Experimenta, Observationes, Animadversiones, CCC numero Chymicae et Physicae*, Vol.; Ambrosius Haude, Berlin, **1731**.

(18) Buser, H. J., Schwarzenbach, D., Petter, W., Ludi, A. *Inorg. Chem.* **1977**, *16*, 2704-2710.

(19) Shibata, Y. *J. Coll. Sci., Imp. Univ. Tokyo* **1916**, *37*, 1-17.

(20) a) Bragg, W. L. *Proc. R. Soc. A* **1913**, *89*, 248-277; b) Bragg, W. H., Bragg, W. L. *Proc. R. Soc. A* **1913**, *89*, 277-291.

(21) Kinoshita, Y., Matsubara, I., Higuchi, T., Saito, Y. *Bull. Chem. Soc. Jpn.* **1959**, *32*, 1221-1226.

(22) Yaghi, O. M., Li, G., Li, H. *Nature* **1995**, *378*, 703-706.

(23) Yaghi, O. M., Li, H. *J. Am. Chem. Soc.* **1995**, *117*, 10401-10402.

(24) Riou, D., Ferey, G. *J. Mater. Chem.* **1998**, *8*, 2733-2735.

(25) a) Kitagawa, S., Matsuyama, S., Munakata, M., Emori, T. *J. Chem.Soc., Dalton Trans.* **1991**, 2869-2874; b) Kitagawa, S., Kawata, S., Nozaka, Y., Munakata, M. *J. Chem. Soc., Dalton Trans.* **1993**, 1399-1404.

(26) Kondo, M., Yoshitomi, T., Matsuzaka, H., Kitagawa, S., Seki, K. *Angew. Chem. Int. Ed.* **1997**, *36*, 1725-1727.

(27) Li, H., Eddaoudi, M., Groy, T. L., Yaghi, O. M. *J. Am. Chem. Soc.* **1998**, *120*, 8571-8572.

(28) Li, H., Eddaoudi, M., O'Keeffe, M., Yaghi, O. M. *Nature* **1999**, *402*, 276-279.

(29) Kaye, S. S., Dailly, A., Yaghi, O. M., Long, J. R. *J. Am. Chem. Soc.* **2007**, *129*, 14176-14177.

(30) Stock, N., Biswas, S. *Chem. Rev.* **2012**, *112*, 933-969.

(31) Grant Glover, T., Peterson, G. W., Schindler, B. J., Britt, D., Yaghi, O. *Chem. Eng. Sci.* **2011**, *66*, 163-170.

(32) Klinowski, J., Almeida Paz, F. A., Silva, P., Rocha, J. *Dalton Trans.* **2011**, *40*, 321-330.

(33) Prochowicz, D., Sokolowski, K., Justyniak, I., Kornowicz, A., Fairen-Jimenez, D., Friscic, T., Lewinski, J. *Chem. Commun.* **2015**, *51*, 4032-4035.

(34) Al-Kutubi, H., Gascon, J., Sudhölter, E. J. R., Rassaei, L. *ChemElectroChem* **2015**, *2*, 462-474.

(35) Tehrani, A. A., Safarifard, V., Morsali, A., Bruno, G., Rudbari, H. A. *Inorg. Chem. Commun.* **2015**, *59*, 41-45.

(36) Hu, Z., Castano, I., Wang, S., Wang, Y., Peng, Y., Qian, Y., Chi, C., Wang, X., Zhao, D. *Cryst. Growth Des.* **2016**, *16*, 2295-2301.

(37) a) Diring, S., Furukawa, S., Takashima, Y., Tsuruoka, T., Kitagawa, S. *Chem. Mater.* **2010**, *22*, 4531-4538; b) Zacher, D., Nayuk, R., Schweins, R., Fischer, R. A., Huber, K. *Cryst. Growth Des.* **2014**, *14*, 4859-4863.

(38) Guo, H., Zhu, Y., Wang, S., Su, S., Zhou, L., Zhang, H. *Chem. Mater.* **2012**, *24*, 444-450.

(39) a) Han, S., Huang, Y., Watanabe, T., Dai, Y., Walton, K. S., Nair, S., Sholl, D. S., Meredith, J. C. *ACS Comb. Sci.* **2012**, *14*, 263-267; b)

McKinstry, C., Cussen, E. J., Fletcher, A. J., Patwardhan, S. V., Sefcik, J. *Cryst. Growth Des.* **2013**, *13*, 5481-5486.

(40) Qiu, S., Zhu, G. *Coord. Chem. Rev.* **2009**, *253*, 2891-2911.

(41) Bosch, M., Zhang, M., Zhou, H.-C. *Adv. Chem.* **2014**, *2014*, 8.

(42) Zhang, J.-P., Huang, X.-C., Chen, X.-M. *Chem. Soc. Rev.* **2009**, *38*, 2385-2396.

(43) Kean, S. *The Disappearing Spoon: And Other True Tales of Madness, Love, and the History of the World from the Periodic Table of the Elements*, Vol.; Little, Brown, **2010**.

(44) Smith, J. V., Blackwell, C. S. *Nature* **1983**, *303*, 223-225.

(45) Schenk, H., Peschar, R. *Radiat. Phys. Chem.* **2004**, *71*, 829-835.

(46) Carson, F., Su, J., Platero-Prats, A. E., Wan, W., Yun, Y., Samain, L., Zou, X. *Cryst. Growth Des.* **2013**, *13*, 5036-5044.

(47) a) Eddaoudi, M., Li, H., Yaghi, O. M. *J. Am. Chem. Soc.* **2000**, *122*, 1391-1397; b) Kim, J., Chen, B., Reineke, T. M., Li, H., Eddaoudi, M., Moler, D. B., O'Keeffe, M., Yaghi, O. M. *J. Am. Chem. Soc.* **2001**, *123*, 8239-8247.

(48) a) Millange, F., Serre, C., Ferey, G. *Chem. Commun.* **2002**, 822-823; b) Serre, C., Millange, F., Thouvenot, C., Gardant, N., Pelle, F., Ferey, G. *J. Mater. Chem.* **2004**, *14*, 1540-1543.

(49) Chui, S. S.-Y., Lo, S. M.-F., Charmant, J. P. H., Orpen, A. G., Williams, I. D. *Science* **1999**, *283*, 1148-1150.

(50) Cavka, J. H., Jakobsen, S., Olsbye, U., Guillou, N., Lamberti, C., Bordiga, S., Lillerud, K. P. *J. Am. Chem. Soc.* **2008**, *130*, 13850-13851.

(51) Canivet, J., Fateeva, A., Guo, Y., Coasne, B., Farrusseng, D. *Chem. Soc. Rev.* **2014**, *43*, 5594-5617.

(52) Burtch, N. C., Jasuja, H., Walton, K. S. *Chem. Rev.* **2014**, *114*, 10575-10612.

(53) Low, J. J., Benin, A. I., Jakubczak, P., Abrahamian, J. F., Faheem, S. A., Willis, R. R. *J. Am. Chem. Soc.* **2009**, *131*, 15834-15842.

(54) Colombo, V., Galli, S., Choi, H. J., Han, G. D., Maspero, A., Palmisano, G., Masciocchi, N., Long, J. R. *Chem. Sci.* **2011**, *2*, 1311-1319.

(55) a) Serre, C. *Angew. Chem. Int. Ed.* **2012**, *51*, 6048-6050; b) Chen, T.-H., Popov, I., Zenasni, O., Daugulis, O., Miljanic, O. S. *Chem. Commun.* **2013**, *49*, 6846-6848; c) Nguyen, J. G., Cohen, S. M. *J. Am. Chem. Soc.* **2010**, *132*, 4560-4561; d) Wu, T., Shen, L., Luebbers, M., Hu, C., Chen, Q., Ni, Z., Masel, R. I. *Chem. Commun.* **2010**, *46*, 6120-6122.

(56) a) DeCoste, J. B., Peterson, G. W., Schindler, B. J., Killops, K. L., Browe, M. A., Mahle, J. J. *J. Mater. Chem., A* **2013**, *1*, 11922-11932; b) Jeremias, F., Lozan, V., Henninger, S. K., Janiak, C. *Dalton Trans.* **2013**, *42*, 15967-15973; c) Zhang, W., Huang, H., Liu, D., Yang, Q., Xiao, Y., Ma, Q., Zhong, C. *Microporous Mesoporous Mater.* **2013**, *171*, 118-124.

(57) Eddaoudi, M., Kim, J., Rosi, N., Vodak, D., Wachter, J., O'Keeffe, M., Yaghi, O. M. *Science* **2002**, *295*, 469-472.

(58) Hermes, S., Schröter, M.-K., Schmid, R., Khodeir, L., Muhler, M., Tissler, A., Fischer, R. W., Fischer, R. A. *Angew. Chem. Int. Ed.* **2005**, *44*, 6237-6241.

(59) Cohen, S. M. *Chem. Rev.* **2012**, *112*, 970-1000.

(60) Kim, M., Cahill, J. F., Su, Y., Prather, K. A., Cohen, S. M. *Chem. Sci.* **2012**, *3*, 126-130.

(61) Yuan, S., Qin, J.-S., Zou, L., Chen, Y.-P., Wang, X., Zhang, Q., Zhou, H.-C. *J. Am. Chem. Soc.* **2016**, *138*, 6636-6642.

(62) Deng, H., Doonan, C. J., Furukawa, H., Ferreira, R. B., Towne, J., Knobler, C. B., Wang, B., Yaghi, O. M. *Science* **2010**, *327*, 846-850.

(63) Wang, C., Xie, Z., deKrafft, K. E., Lin, W. *J. Am. Chem. Soc.* **2011**, *133*, 13445-13454.

(64) Koh, K., Wong-Foy, A. G., Matzger, A. J. *Chem. Commun.* **2009**, 6162-6164.

(65) a) Abrahams, B. F., Hoskins, B. F., Michail, D. M., Robson, R. *Nature* **1994**, *369*, 727-729; b) Kent, C. A., Mehl, B. P., Ma, L., Papanikolas, J. M., Meyer, T. J., Lin, W. *J. Am. Chem. Soc.* **2010**, *132*, 12767-12769.

(66) Vuong, G.-T., Pham, M.-H., Do, T.-O. *CrystEngComm* **2013**, *15*, 9694-9703.

(67) Burrows, A. D., Frost, C. G., Mahon, M. F., Richardson, C. *Angew. Chem. Int. Ed.* **2008**, *47*, 8482-8486.

(68) Evans, J. D., Sumby, C. J., Doonan, C. J. *Chem. Soc. Rev.* **2014**, *43*, 5933-5951.

(69) Hwang, Y. K., Hong, D.-Y., Chang, J.-S., Jhung, S. H., Seo, Y.-K., Kim, J., Vimont, A., Daturi, M., Serre, C., Férey, G. *Angew. Chem. Int. Ed.* **2008**, *47*, 4144-4148.

(70) Yamada, T., Kitagawa, H. *J. Am. Chem. Soc.* **2009**, *131*, 6312-6313.

(71) Dincă, M., Long, J. R. *J. Am. Chem. Soc.* **2007**, *129*, 11172-11176.

(72) a) Burnett, B. J., Barron, P. M., Hu, C., Choe, W. *J. Am. Chem. Soc.* **2011**, *133*, 9984-9987; b) Lee, C. Y., Farha, O. K., Hong, B. J., Sarjeant, A. A., Nguyen, S. T., Hupp, J. T. *J. Am. Chem. Soc.* **2011**, *133*, 15858-15861.

(73) Genna, D. T., Wong-Foy, A. G., Matzger, A. J., Sanford, M. S. *J. Am. Chem. Soc.* **2013**, *135*, 10586-10589.

(74) a) Farrusseng, D., Aguado, S., Pinel, C. *Angew. Chem. Int. Ed.* **2009**, *48*, 7502-7513; b) Lee, J., Farha, O. K., Roberts, J., Scheidt, K. A., Nguyen, S. T., Hupp, J. T. *Chem. Soc. Rev.* **2009**, *38*, 1450-1459; c) Gascon, J., Corma, A., Kapteijn, F., Llabrés i Xamena, F. X. *ACS Catal.* **2014**, *4*, 361-378; d) Corma, A., García, H., Llabrés i Xamena, F. X. *Chem. Rev.* **2010**, *110*, 4606-4655.

(75) Fujita, M., Kwon, Y. J., Washizu, S., Ogura, K. *J. Am. Chem. Soc.* **1994**, *116*, 1151-1152.

(76) a) Ma, L., Lin, W. In *Functional Metal-Organic Frameworks: Gas Storage, Separation and Catalysis*, Vol.; Ed.Schröder, M.), Springer Berlin Heidelberg **2010**, pp. 175-205; b) Mo, K., Yang, Y., Cui, Y. *J. Am. Chem. Soc.* **2014**, *136*, 1746-1749; c) Dang, D., Wu, P., He, C., Xie, Z., Duan, C. *J. Am. Chem. Soc.* **2010**, *132*, 14321-14323; d) Liu, Y., Xuan, W., Cui, Y. *Adv. Mater. (Weinheim, Ger.)* **2010**, *22*, 4112-4135.

(77) Chughtai, A. H., Ahmad, N., Younus, H. A., Laypkov, A., Verpoort, F. *Chem. Soc. Rev.* **2015**, *44*, 6804-6849.

(78) Vermoortele, F., Valvekens, P., De Vos, D. In *Metal Organic Frameworks as Heterogeneous Catalysts*, Vol., The Royal Society of Chemistry **2013**, pp. 268-288.

(79) Banerjee, M., Das, S., Yoon, M., Choi, H. J., Hyun, M. H., Park, S. M., Seo, G., Kim, K. *J. Am. Chem. Soc.* **2009**, *131*, 7524-7525.

(80) a) Hasegawa, S., Horike, S., Matsuda, R., Furukawa, S., Mochizuki, K., Kinoshita, Y., Kitagawa, S. *J. Am. Chem. Soc.* **2007**, *129*, 2607-2614; b) Mondloch, J. E., Farha, O. K., Hupp, J. T. In *Metal Organic Frameworks as Heterogeneous Catalysts*, Vol., The Royal Society of Chemistry **2013**, pp. 289-309.

(81) a) Zhang, X., Llabrés i Xamena, F. X., Corma, A. *J. Catal.* **2009**, *265*, 155-160; b) Cho, S.-H., Ma, B., Nguyen, S. T., Hupp, J. T., Albrecht-Schmitt, T. E. *Chem. Commun.* **2006**, 2563-2565.

(82) Falkowski, J. M., Liu, S., Lin, W. In *Metal Organic Frameworks as Heterogeneous Catalysts*, Vol., The Royal Society of Chemistry **2013**, pp. 344-364.

(83) a) Esken, D., Turner, S., Lebedev, O. I., Van Tendeloo, G., Fischer, R. A. *Chem. Mater.* **2010**, *22*, 6393-6401; b) Rosler, C., Fischer, R. A. *CrystEngComm* **2015**, *17*, 199-217.

(84) Van de Voorde, B., Stassen, I., Bueken, B., Vermoortele, F., De Vos, D., Ameloot, R., Tan, J.-C., Bennett, T. D. *J. Mater. Chem., A* **2015**, *3*, 1737-1742.

(85) Bai, Y., Dou, Y., Xie, L.-H., Rutledge, W., Li, J.-R., Zhou, H.-C. *Chem. Soc. Rev.* **2016**, *45*, 2327-2367.

(86) Lu, W., Wei, Z., Gu, Z.-Y., Liu, T.-F., Park, J., Park, J., Tian, J., Zhang, M., Zhang, Q., Gentle Iii, T., Bosch, M., Zhou, H.-C. *Chem. Soc. Rev.* **2014**, *43*, 5561-5593.

(87) Puchberger, M., Kogler, F. R., Jupa, M., Gross, S., Fric, H., Kickelbick, G., Schubert, U. *Eur. J. Inorg. Chem.* **2006**, *2006*, 3283-3293.

(88) Yang, Q., Wiersum, A. D., Llewellyn, P. L., Guillerm, V., Serre, C., Maurin, G. *Chem. Commun.* **2011**, *47*, 9603-9605.

(89) a) Kim, M., Cohen, S. M. *CrystEngComm* **2012**, *14*, 4096-4104; b) Schaate, A., Roy, P., Godt, A., Lippke, J., Waltz, F., Wiebcke, M., Behrens, P. *Chem. Eur. J.* **2011**, *17*, 6643-6651.

(90) Guillerm, V., Ragon, F., Dan-Hardi, M., Devic, T., Vishnuvarthan, M., Campo, B., Vimont, A., Clet, G., Yang, Q., Maurin, G., Férey, G., Vittadini, A., Gross, S., Serre, C. *Angew. Chem. Int. Ed.* **2012**, *51*, 9267-9271.

(91) a) Vermoortele, F., Ameloot, R., Vimont, A., Serre, C., De Vos, D. *Chem. Commun.* **2011**, *47*, 1521-1523; b) Gomes Silva, C., Luz, I., Llabrés i Xamena, F. X., Corma, A., García, H. *Chem. Eur. J.* **2010**, *16*, 11133-11138.

(92) Rosi, N. L., Eckert, J., Eddaoudi, M., Vodak, D. T., Kim, J., O'Keeffe, M., Yaghi, O. M. *Science* **2003**, *300*, 1127-1129.

(93) Devic, T., Horcajada, P., Serre, C., Salles, F., Maurin, G., Moulin, B., Heurtaux, D., Clet, G., Vimont, A., Grenèche, J.-M., Ouay, B. L., Moreau, F., Magnier, E., Filinchuk, Y., Marrot, J., Lavalley, J.-C., Daturi, M., Férey, G. *J. Am. Chem. Soc.* **2010**, *132*, 1127-1136.

(94) Chavan, S., Vitillo, J. G., Gianolio, D., Zavorotynska, O., Civalleri, B., Jakobsen, S., Nilsen, M. H., Valenzano, L., Lamberti, C., Lillerud, K. P., Bordiga, S. *Phys. Chem. Chem. Phys.* **2012**, *14*, 1614-1626.

(95) Burrows, A. D. *CrystEngComm* **2011**, *13*, 3623-3642.

(96) Lescouet, T., Kockrick, E., Bergeret, G., Pera-Titus, M., Farrusseng, D. *Dalton Trans.* **2011**, *40*, 11359-11361.

(97) Marx, S., Kleist, W., Huang, J., Maciejewski, M., Baiker, A. *Dalton Trans.* **2010**, *39*, 3795-3798.

(98) Siu, P. W., Brown, Z. J., Farha, O. K., Hupp, J. T., Scheidt, K. A. *Chem. Commun.* **2013**, *49*, 10920-10922.

(99) a) Garibay, S. J., Cohen, S. M. *Chem. Commun.* **2010**, *46*, 7700-7702; b) Kandiah, M., Nilsen, M. H., Usseglio, S., Jakobsen, S., Olsbye, U., Tilset, M., Larabi, C., Quadrelli, E. A., Bonino, F., Lillerud, K. P. *Chem. Mater.* **2010**, *22*, 6632-6640.

(100) Kim, M., Cahill, J. F., Prather, K. A., Cohen, S. M. *Chem. Commun.* **2011**, *47*, 7629-7631.

(101) Guillerm, V., Ragon, F., Dan-Hardi, M., Devic, T., Vishnuvarthan, M., Campo, B., Vimont, A., Clet, G., Yang, Q., Maurin, G., Férey, G., Vittadini, A., Gross, S., Serre, C. *Angew. Chem. Int. Ed.* **2012**, *124*, 9401-9405.

(102) Schoenecker, P. M., Carson, C. G., Jasuja, H., Flemming, C. J. J., Walton, K. S. *Ind. Eng. Chem. Res.* **2012**, *51*, 6513-6519.

(103) a) Sels, B. F., De Vos, D. E., Jacobs, P. A. *Catalysis Reviews* **2001**, *43*, 443-488; b) Tichit, D., Iborra, S., Corma, A., Brunel, D. In *Catalysts for Fine Chemical Synthesis*, Vol., John Wiley & Sons, Ltd **2006**, pp. 171-205.

(104) Corma, A., Iborra, S. In *Adv. Catal.*, Vol. Volume 49; (Eds.Bruce, C. G., Helmut, K.), Academic Press **2006**, pp. 239-302.

(105) a) Cavani, F., Trifirò, F., Vaccari, A. *Catal. Today* **1991**, *11*, 173-301; b) Vaccari, A. *Catal. Today* **1998**, *41*, 53-71.

(106) Climent, M. J., Corma, A., Fornés, V., Frau, A., Guil-López, R., Iborra, S., Primo, J. *J. Catal.* **1996**, *163*, 392-398.

(107) Corma, A., Fornés, V., Martín-Aranda, R. M., García, H., Primo, J. *Applied Catalysis* **1990**, *59*, 237-248.

(108) Gokhale, U. V., Seshadri, S. *Dyes Pigm.* **1986**, *7*, 389-394.

(109) a) Dworczak, R., Fabian, W. M. F., Pawar, B. N., Junek, H. *Dyes Pigm.* **1995**, *29*, 65-76; b) Fabian, W. M. F., Dworczak, R., Junek, H., Pawar, B. N. *Journal of the Chemical Society, Perkin Transactions 2* **1995**, 903-906.

(110) Climent, M. J., Corma, A., Guil-Lopez, R., Iborra, S. *Catal. Lett.* **2001**, *74*, 161-167.

(111) Corma, A. *Catalysis Reviews* **2004**, *46*, 369-417.

(112) a) Baleizão, C., Garcia, H. *Chem. Rev.* **2006**, *106*, 3987-4043; b) Corma, A., Díaz, U., García, T., Sastre, G., Velty, A. *J. Am. Chem. Soc.* **2010**, *132*, 15011-15021.

(113) Ferey, G. *Chem. Soc. Rev.* **2008**, *37*, 191-214.

(114) Wang, C., Zheng, M., Lin, W. *J. Phys. Chem. Lett.* **2011**, *2*, 1701-1709.

(115) a) Arnanz, A., Pintado-Sierra, M., Corma, A., Iglesias, M., Sánchez, F. *Adv. Synth. Catal.* **2012**, *354*, 1347-1355; b) Cirujano, F. G., Llabres i Xamena, F. X., Corma, A. *Dalton Trans.* **2012**, *41*, 4249-4254.

(116) a) Cirujano, F. G., Leyva-Pérez, A., Corma, A., Llabrés i Xamena, F. X. *ChemCatChem* **2013**, *5*, 538-549; b) Pan, Y., Yuan, B., Li, Y., He, D. *Chem. Commun.* **2010**, *46*, 2280-2282; c) Wu, P., Wang, J., Li, Y., He, C., Xie, Z., Duan, C. *Adv. Funct. Mater.* **2011**, *21*, 2788-2794; d) Llabrés i Xamena, F. X., Abad, A., Corma, A., Garcia, H. *J. Catal.* **2007**, *250*, 294-298; e) Llabrés i Xamena, F. X., Casanova, O., Galiasso Tailleur, R., Garcia, H., Corma, A. *J. Catal.* **2008**, *255*, 220-227; f) Gándara, F., Puebla, E. G., Iglesias, M., Proserpio, D. M., Snejko, N., Monge, M. Á. *Chem. Mater.* **2009**, *21*, 655-661; g) Monge, A., Gandara, F., Gutierrez-Puebla, E., Snejko, N. *CrystEngComm* **2011**, *13*, 5031-5044; h) D'Vries, R. F., Iglesias, M., Snejko, N., Alvarez-Garcia, S., Gutierrez-Puebla, E., Monge, M. A. *J. Mater. Chem.* **2012**, *22*, 1191-1198; i) Wang, Z., Chen, G., Ding, K. *Chem. Rev.* **2009**, *109*, 322-359; j) Wang, Z., Cohen, S. M. *Chem. Soc. Rev.* **2009**, *38*, 1315-1329.

(117) Tanabe, K. K., Cohen, S. M. *Chem. Soc. Rev.* **2011**, *40*, 498-519.

(118) a) Tanabe, K. K., Cohen, S. M. *Angew. Chem. Int. Ed.* **2009**, *48*, 7424-7427; b) Doonan, C. J., Morris, W., Furukawa, H., Yaghi, O. M. *J. Am. Chem. Soc.* **2009**, *131*, 9492-9493.

(119) Ingleson, M. J., Perez Barrio, J., Guilbaud, J.-B., Khimyak, Y. Z., Rosseinsky, M. J. *Chem. Commun.* **2008**, 2680-2682.

(120) Servalli, M., Ranocchiari, M., Van Bokhoven, J. A. *Chem. Commun.* **2012**, *48*, 1904-1906.

(121) Kandiah, M., Usseglio, S., Svelle, S., Olsbye, U., Lillerud, K. P., Tilset, M. *J. Mater. Chem.* **2010**, *20*, 9848-9851.

(122) Morris, W., Doonan, C. J., Yaghi, O. M. *Inorg. Chem.* **2011**, *50*, 6853-6855.

(123) a) Rybtchinski, B., Milstein, D. *Angew. Chem. Int. Ed.* **1999**, *38*, 870-883; b) Kanzelberger, M., Singh, B., Czerw, M., Krogh-Jespersen, K., Goldman, A. S. *J. Am. Chem. Soc.* **2000**, *122*, 11017-11018; c) Zhao, J., Goldman, A. S., Hartwig, J. F. *Science* **2005**, *307*, 1080-1082; d) Gusev, D. G., Fontaine, F.-G., Lough, A. J., Zargarian, D. *Angew. Chem. Int. Ed.* **2003**, *42*, 216-219; e) Agapie, T., Bercaw, J. E. *Organometallics* **2007**, *26*, 2957-2959; f) Ingleson, M., Fan, H., Pink, M., Tomaszewski, J., Caulton, K. G. *J. Am. Chem. Soc.* **2006**, *128*, 1804-1805; g) Ingleson, M. J., Pink, M., Caulton, K. G. *J. Am. Chem. Soc.* **2006**, *128*, 4248-4249; h) Gozin, M., Aizenberg, M., Liou, S.-Y., Weisman, A., Ben-David, Y., Milstein, D. *Nature* **1994**, *370*, 42-44; i) Grove, D. M., Van Koten, G., Mul, P., Van der Zeijden, A. A. H., Terheijden, J., Zoutberg, M. C., Stam, C. H. *Organometallics* **1986**, *5*, 322-326; j) Gusev, D. G., Maxwell, T., Dolgushin, F. M., Lyssenko, M., Lough, A. J. *Organometallics* **2002**, *21*, 1095-1100; k) Gusev, D. G., Madott, M., Dolgushin, F. M., Lyssenko, K. A., Antipin, M. Y. *Organometallics* **2000**, *19*, 1734-1739.

(124) a) Broadwater, S. J., Roth, S. L., Price, K. E., Kobaslija, M., McQuade, D. T. *Org. Biomol. Chem.* **2005**, *3*, 2899-2906; b) Tietze, L. F. *Chem. Rev.* **1996**, *96*, 115-136; c) Tietze, L. F., Beifuss, U. *Angew. Chem., Int. Ed.* **1993**, *32*, 131-163.

(125) a) Ajamian, A., Gleason, J. L. *Angew. Chem. Int. Ed.* **2004**, *43*, 3754-3760; b) Lee, J. M., Na, Y., Han, H., Chang, S. *Chem. Soc. Rev.* **2004**, *33*, 302-312.

(126) a) Fogg, D. E., dos Santos, E. N. *Coord. Chem. Rev.* **2004**, *248*, 2365-2379; b) Poli, G., Giambastiani, G. *J. Org. Chem.* **2002**, *67*, 9456-9459.

(127) a) Balme, G., Bossharth, E., Monteiro, N. *Eur. J. Org. Chem.* **2003**, *2003*, 4101-4111; b) Malacria, M. *Chem. Rev.* **1996**, *96*, 289-306; c) Parsons, P. J., Penkett, C. S., Shell, A. J. *Chem. Rev.* **1996**, *96*, 195-206; d) Wasilke, J.-C., Obrey, S. J., Baker, R. T., Bazan, G. C. *Chem. Rev.* **2005**, *105*, 1001-1020; e) Battistuzzi, G., Cacchi, S., Fabrizi, G. *Eur. J. Org. Chem.* **2002**, *2002*, 2671-2681; f) Negishi, E.-i., Copéret, C., Ma, S., Liou, S.-Y., Liu, F. *Chem. Rev.* **1996**, *96*, 365-394.

(128) a) C. D. Wanger, W. M. R., L. E. Davis, J. F. Moulder and G. E.Muilenberg *Handbook of X-ray Photoelectron Spectroscopy, Physical Electronics Division* **1981**, *3*; b) Campos, C., Torres, C., Oportus, M., Peña, M. A., Fierro, J. L. G., Reyes, P. *Catal. Today* **2013**, *213*, 93-100; c) Hintermair, U., Sheehan, S. W., Parent, A. R., Ess, D. H., Richens, D. T., Vaccaro, P. H., Brudvig, G. W., Crabtree, R. H. *J. Am. Chem. Soc.* **2013**, *135*, 10837-10851; d) Blanco, M., Álvarez, P., Blanco, C., Jiménez, M. V.,

Fernández-Tornos, J., Pérez-Torrente, J. J., Oro, L. A., Menéndez, R. *ACS Catal.* **2013**, *3*, 1307-1317.

(129) Rowsell, J. L. C., Yaghi, O. M. *J. Am. Chem. Soc.* **2006**, *128*, 1304-1315.

(130) Gascon, J., Aktay, U., Hernandez-Alonso, M. D., van Klink, G. P. M., Kapteijn, F. *J. Catal.* **2009**, *261*, 75-87.

(131) Huang, L., Wang, H., Chen, J., Wang, Z., Sun, J., Zhao, D., Yan, Y. *Microporous Mesoporous Mater.* **2003**, *58*, 105-114.

(132) a) Zhao, C., Kou, Y., Lemonidou, A. A., Li, X., Lercher, J. A. *Angew. Chem. Int. Ed.* **2009**, *48*, 3987-3990; b) Huang, J., Jiang, Y., van Vegten, N., Hunger, M., Baiker, A. *J. Catal.* **2011**, *281*, 352-360; c) Wang, Y., Yao, J., Li, H., Su, D., Antonietti, M. *J. Am. Chem. Soc.* **2011**, *133*, 2362-2365; d) Makowski, P., Demir Cakan, R., Antonietti, M., Goettmann, F., Titirici, M.-M. *Chem. Commun.* **2008**, 999-1001.

(133) a) Boxwell, C. J., Dyson, P. J., Ellis, D. J., Welton, T. *J. Am. Chem. Soc.* **2002**, *124*, 9334-9335; b) Hubert, C., Denicourt-Nowicki, A., Roucoux, A., Landy, D., Leger, B., Crowyn, G., Monflier, E. *Chem. Commun.* **2009**, 1228-1230.

(134) a) Bayram, E., Linehan, J. C., Fulton, J. L., Roberts, J. A. S., Szymczak, N. K., Smurthwaite, T. D., Özkar, S., Balasubramanian, M., Finke, R. G. *J. Am. Chem. Soc.* **2011**, *133*, 18889-18902; b) Yan, N., Yuan, Y., Dykeman, R., Kou, Y., Dyson, P. J. *Angew. Chem. Int. Ed.* **2010**, *49*, 5549-5553; c) Hubert, C., Denicourt-Nowicki, A., Beaunier, P., Roucoux, A. *Green Chem.* **2010**, *12*, 1167-1170; d) Motoyama, Y., Takasaki, M., Yoon, S.-H., Mochida, I., Nagashima, H. *Org. Lett.* **2009**, *11*, 5042-5045; e) Maegawa, T., Akashi, A., Yaguchi, K., Iwasaki, Y., Shigetsura, M., Monguchi, Y., Sajiki, H. *Chem. Eur. J.* **2009**, *15*, 6953-6963.

(135) a) Bayram, E., Zahmakıran, M., Özkar, S., Finke, R. G. *Langmuir* **2010**, *26*, 12455-12464; b) Zieliński, M., Pietrowski, M., Wojciechowska, M. *ChemCatChem* **2011**, *3*, 1653-1658.

(136) Guo, Z., Hu, L., Yu, H.-h., Cao, X., Gu, H. *RSC. Adv.* **2012**, *2*, 3477-3480.

(137) a) Toppinen, S., Rantakylä, T. K., Salmi, T., Aittamaa, J. *Ind. Eng. Chem. Res.* **1996**, *35*, 4424-4433; b) Lu, L., Rong, Z., Du, W., Ma, S., Hu, S. *ChemCatChem* **2009**, *1*, 369-371.

(138) a) Liu, H., Jiang, T., Han, B., Liang, S., Zhou, Y. *Science* **2009**, *326*, 1250-1252; b) Deshmukh, R. R., Lee, J. W., Shin, U. S., Lee, J. Y., Song, C. E. *Angew. Chem. Int. Ed.* **2008**, *47*, 8615-8617; c) Tarakeshwar, P., Lee, J. Y., Kim, K. S. *The Journal of Physical Chemistry A* **1998**, *102*, 2253-2255; d) Ahn, H., Nicholas, C. P., Marks, T. J. *Organometallics* **2002**, *21*, 1788-1806.

(139) Pintado-Sierra, M., Rasero-Almansa, A. M., Corma, A., Iglesias, M., Sánchez, F. *J. Catal.* **2013**, *299*, 137-145.

(140) a) Jiang, H.-L., Liu, B., Akita, T., Haruta, M., Sakurai, H., Xu, Q. *J. Am. Chem. Soc.* **2009**, *131*, 11302-11303; b) Lu, G., Li, S., Guo, Z., Farha, O. K., Hauser, B. G., Qi, X., Wang, Y., Wang, X., Han, S., Liu, X., DuChene, J. S., Zhang, H., Zhang, Q., Chen, X., Ma, J., Loo, S. C. J., Wei, W. D., Yang, Y., Hupp, J. T., Huo, F. *Nat. Chem.* **2012**, *4*, 310-316.

(141) Jiang, H.-L., Akita, T., Ishida, T., Haruta, M., Xu, Q. *J. Am. Chem. Soc.* **2011**, *133*, 1304-1306.

(142) Li, P.-Z., Aranishi, K., Xu, Q. *Chem. Commun.* **2012**, *48*, 3173-3175.

(143) Zahmakiran, M. *Dalton Trans.* **2012**, *41*, 12690-12696.

(144) Hermannsdörfer, J., Friedrich, M., Kempe, R. *Chem. Eur. J.* **2013**, *19*, 13652-13657.

(145) Wang, C., Wang, J.-L., Lin, W. *J. Am. Chem. Soc.* **2012**, *134*, 19895-19908.

(146) a) Pugin, B., Landert, H., Spindler, F., Blaser, H.-U. *Adv. Synth. Catal.* **2002**, *344*, 974-979; b) González-Arellano, C., Corma, A., Iglesias, M., Sánchez, F. *Adv. Synth. Catal.* **2004**, *346*, 1316-1328.

(147) a) Corma, A., Ródenas, T., Sabater, M. J. *Chem. Eur. J.* **2010**, *16*, 254-260; b) Rubio-Marques, P., Leyva-Perez, A., Corma, A. *Chem. Commun.* **2013**, *49*, 8160-8162; c) Corma, A., Ródenas, T., Sabater, M. J. *J. Catal.* **2011**, *279*, 319-327; d) Watson, A. J. A., Williams, J. M. J. *Science* **2010**, *329*, 635-636; e) Bähn, S., Imm, S., Neubert, L., Zhang, M., Neumann, H., Beller, M. *ChemCatChem* **2011**, *3*, 1853-1864.

(148) a) Jiménez, M. V., Fernández-Tornos, J., Pérez-Torrente, J. J., Modrego, F. J., Winterle, S., Cunchillos, C., Lahoz, F. J., Oro, L. A. *Organometallics* **2011**, *30*, 5493-5508; b) del Pozo, C., Corma, A., Iglesias, M., Sanchez, F. *Green Chem.* **2011**, *13*, 2471-2481.

(149) Fujita, K.-i., Enoki, Y., Yamaguchi, R. *Tetrahedron* **2008**, *64*, 1943-1954.

(150) Fristrup, P., Tursky, M., Madsen, R. *Org. Biomol. Chem.* **2012**, *10*, 2569-2577.

(151) a) Landquist, J. K. In *Comprehensive Heterocyclic Chemistry*, Vol.; Ed.Rees, C. W.), Pergamon, Oxford, **1984**, pp. 143-183; b) Horspool, W. M. In *PATAI'S Chemistry of Functional Groups*, Vol., John Wiley & Sons, Ltd **2009**; c) North, M. *Angew. Chem. Int. Ed.* **2005**, *44*, 2053-2055.

(152) Ono, N. In *The Nitro Group in Organic Synthesis*, Vol., John Wiley & Sons, Inc. **2002**, pp. 3-29.

(153) a) Downing, R. S., Kunkeler, P. J., van Bekkum, H. *Catal. Today* **1997**, *37*, 121-136; b) Blaser, H.-U., Malan, C., Pugin, B., Spindler, F., Steiner, H., Studer, M. *Adv. Synth. Catal.* **2003**, *345*, 103-151; c) Corma, A., Serna, P., Concepción, P., Calvino, J. J. *J. Am. Chem. Soc.* **2008**, *130*, 8748-8753; d) Reis, P. M., Royo, B. *Tetrahedron Lett.* **2009**, *50*, 949-952.

(154) a) Sreedhar, B., Reddy, P. S., Devi, D. K. *J. Org. Chem.* **2009**, *74*, 8806-8809; b) Tripathi, R. P., Verma, S. S., Pandey, J., Tiwari, V. K. *Curr. Org. Chem.* **2008**, *12*, 1093-1115; c) Trost, B. M., Fleming, I. *Comprehensive Organic Synthesis: Reduction*, Vol. 8; Elsevier Science & Technology Books, **1991**; d) Baxter, E. W., Reitz, A. B. In *Org. React.*, Vol. 59, John Wiley & Sons, Inc. **2004**, p. 1.

(155) a) Merla, B., Risch, N. *Synthesis* **2002**, *2002*, 1365-1372; b) Gordon, E. M., Barrett, R. W., Dower, W. J., Fodor, S. P. A., Gallop, M. A. *J. Med. Chem.* **1994**, *37*, 1385-1401.

(156) a) A. Tarasevich, V., G. Kozlov, N. *Russ. Chem. Rev.* **1999**, *68*, 55-72; b) Mićović, I. V., Ivanović, M. D., Piatak, D. M., Bojić, V. D. *Synthesis* **1991**, *1991*, 1043-1045; c) Chen, B.-C., Sundeen, J. E., Guo, P., Bednarz, M. S., Zhao, R. *Tetrahedron Lett.* **2001**, *42*, 1245-1246; d) Suwa, T., Sugiyama, E., Shibata, I., Baba, A. *Synthesis* **2000**, *2000*, 789-800; e) Lee, O.-Y., Law, K.-L., Ho, C.-Y., Yang, D. *J. Org. Chem.* **2008**, *73*, 8829-8837; f) Imao, D., Fujihara, S., Yamamoto, T., Ohta, T., Ito, Y. *Tetrahedron* **2005**, *61*, 6988-6992; g) Tararov, V. I., Kadyrov, R., Riermeier, T. H., Borner, A. *Chem. Commun.* **2000**, 1867-1868; h) Lane, C. F. *Synthesis* **1975**, *1975*, 135-146; i) Abdel-Magid, A. F., Carson, K. G., Harris, B. D., Maryanoff, C. A., Shah, R. D. *J. Org. Chem.* **1996**, *61*, 3849-3862; j) Bomann, M. D., Guch, I. C., DiMare, M. *J. Org. Chem.* **1995**, *60*, 5995-5996; k) Bhattacharyya, S., Neidigh, K. A., Avery, M. A., Williamson, J. S. *Synlett* **1999**, *1999*, 1781-1783; l) Ranu, B. C., Majee, A., Sarkar, A. *J. Org. Chem.* **1998**, *63*, 370-373; m) Saxena, I., Borah, R., Sarma, J. C. *J. Chem. Soc., Perkin Trans. 1* **2000**, 503-504.

(157) a) Sydnes, M. O., Isobe, M. *Tetrahedron Lett.* **2008**, *49*, 1199-1202; b) Sydnes, M. O., Kuse, M., Isobe, M. *Tetrahedron* **2008**, *64*, 6406-6414; c) Jiang, Y.-L., Hu, Y.-Q., Feng, S.-Q., Wu, J.-S., Wu, Z.-W., Yuan, Y.-C., Liu, J.-M., Hao, Q.-S., Li, D.-P. *Synth. Commun.* **1996**, *26*, 161-164; d) Zhou, X., Wu, Z., Lin, L., Wang, G., Li, J. *Dyes Pigm.* **1998**, *36*, 365-371; e) Jung, Y. J., Bae, J. W., Park, E. S., Chang, Y. M., Yoon, C. M. *Tetrahedron* **2003**, *59*, 10331-10338; f) Bae, J. W., Cho, Y. J., Lee, S. H., Yoon, C.-O. M., Yoon, C. M. *Chem. Commun.* **2000**, 1857-1858; g) Sajiki, H., Ikawa, T., Hirota, K. *Org. Lett.* **2004**, *6*, 4977-4980; h) Sajiki, H., Ikawa, T., Hirota, K. *Org. Process Res. Dev.* **2005**, *9*, 219-220; i) Nacario, R., Kotakonda, S., Fouchard, D. M. D., Tillekeratne, L. M. V., Hudson, R. A. *Org. Lett.* **2005**, *7*, 471-474; j) Fouchard, D. M. D., Tillekeratne, L. M. V., Hudson, R. A. *Synthesis* **2005**, *2005*, 17-18; k) Reddy, C. R., Vijeender, K., Bhusan, P. B., Madhavi, P. P., Chandrasekhar, S. *Tetrahedron Lett.* **2007**, *48*, 2765-2768; l) Chandrasekhar, S., Narsihmulu, C., Jagadeshwar, V. *Synlett* **2002**, *2002*, 0771-0772.

(158) a) Santos, L. L., Serna, P., Corma, A. *Chem. Eur. J.* **2009**, *15*, 8196-8203; b) Climent, M. J., Corma, A., Iborra, S., Santos, L. L. *Chem. Eur. J.* **2009**, *15*, 8834-8841.

(159) Yamane, Y., Liu, X., Hamasaki, A., Ishida, T., Haruta, M., Yokoyama, T., Tokunaga, M. *Org. Lett.* **2009**, *11*, 5162-5165.

(160) Dell'Anna, M. M., Mastrorilli, P., Rizzuti, A., Leonelli, C. *Appl. Catal., A* **2011**, *401*, 134-140.

(161) a) Wu, C.-D., Hu, A., Zhang, L., Lin, W. *J. Am. Chem. Soc.* **2005**, *127*, 8940-8941; b) Gómez-Lor, B., Gutiérrez-Puebla, E., Iglesias, M., Monge, M. A., Ruiz-Valero, C., Snejko, N. *Chem. Mater.* **2005**, *17*, 2568-2573; c) Sato, T., Mori, W., Kato, C. N., Yanaoka, E., Kuribayashi, T., Ohtera, R., Shiraishi, Y. *J. Catal.* **2005**, *232*, 186-198; d) Chen, B., Ockwig, N. W., Millward, A. R., Contreras, D. S., Yaghi, O. M. *Angew. Chem. Int. Ed.* **2005**, *44*, 4745-4749; e) Vimont, A., Goupil, J.-M., Lavalley, J.-C., Daturi, M., Surblé, S., Serre, C., Millange, F., Férey, G., Audebrand, N. *J. Am. Chem. Soc.* **2006**, *128*, 3218-3227.

(162) a) Seo, J. S., Whang, D., Lee, H., Jun, S. I., Oh, J., Jeon, Y. J., Kim, K. *Nature* **2000**, *404*, 982-986; b) Uemura, T., Kitaura, R., Ohta, Y., Nagaoka, M., Kitagawa, S. *Angew. Chem. Int. Ed.* **2006**, *45*, 4112-4116; c) Shin, D. M., Lee, I. S., Chung, Y. K. *Cryst. Growth Des.* **2006**, *6*, 1059-1061; d) Hwang, Y. K., Hong, D.-Y., Chang, J.-S., Seo, H., Yoon, M., Kim, J., Jhung, S. H., Serre, C., Férey, G. *Appl. Catal., A* **2009**, *358*, 249-253; e) Lun, D. J., Waterhouse, G. I. N., Telfer, S. G. *J. Am. Chem. Soc.* **2011**, *133*, 5806-5809.

(163) Dhakshinamoorthy, A., Opanasenko, M., Čejka, J., Garcia, H. *Adv. Synth. Catal.* **2013**, *355*, 247-268.

(164) Valvekens, P., Vermoortele, F., De Vos, D. *Catal. Sci. Technol.* **2013**, *3*, 1435-1445.

(165) Vermoortele, F., Vandichel, M., Van de Voorde, B., Ameloot, R., Waroquier, M., Van Speybroeck, V., De Vos, D. E. *Angew. Chem. Int. Ed.* **2012**, *51*, 4887-4890.

(166) a) Lehnert, W. *Tetrahedron* **1972**, *28*, 663-666; b) Shipchandler, M. T. *Synthesis* **1979**, *1979*, 666-686; c) Shen, B., Johnston, J. N. *Org. Lett.* **2008**, *10*, 4397-4400.

(167) a) Fornicola, R. S., Oblinger, E., Montgomery, J. *J. Org. Chem.* **1998**, *63*, 3528-3529; b) Versleijen, J. P. G., van Leusen, A. M., Feringa, B. L. *Tetrahedron Lett.* **1999**, *40*, 5803-5806.

(168) Fioravanti, S., Pellacani, L., Vergari, M. C. *Org. Biomol. Chem.* **2012**, *10*, 524-528.

(169) Ugi, I. *J. Prakt. Chem.* **1997**, *339*, 499-516.

(170) Diaz, U., Brunel, D., Corma, A. *Chem. Soc. Rev.* **2013**, *42*, 4083-4097.

(171) a) Iosif, F., Coman, S., Parvulescu, V., Grange, P., Delsarte, S., Vos, D. D., Jacobs, P. *Chem. Commun.* **2004**, 1292-1293; b) Neaţu, F., Coman, S., Pârvulescu, V. I., Poncelet, G., Vos, D., Jacobs, P. *Top. Catal.* **2009**, *52*, 1292-1300; c) Mertens, P., Verpoort, F., Parvulescu, A.-N., De Vos, D. *J. Catal.* **2006**, *243*, 7-13.

(172) Phan, N. T. S., Gill, C. S., Nguyen, J. V., Zhang, Z. J., Jones, C. W. *Angew. Chem. Int. Ed.* **2006**, *45*, 2209-2212.

(173) Han, Y., Li, J.-R., Xie, Y., Guo, G. *Chem. Soc. Rev.* **2014**, *43*, 5952-5981.

(174) Wongsakulphasatch, S., Nouar, F., Rodriguez, J., Scott, L., Le Guillouzer, C., Devic, T., Horcajada, P., Greneche, J. M., Llewellyn, P. L., Vimont, A., Clet, G., Daturi, M., Serre, C. *Chem. Commun.* **2015**, *51*, 10194-10197.

(175) Brozek, C. K., Dinca, M. *Chem. Soc. Rev.* **2014**, *43*, 5456-5467.

(176) Son, D. H., Hughes, S. M., Yin, Y., Paul Alivisatos, A. *Science* **2004**, *306*, 1009-1012.

(177) a) Zhao, J. a., Mi, L., Hu, J., Hou, H., Fan, Y. *J. Am. Chem. Soc.* **2008**, *130*, 15222-15223; b) Fei, H., Bresler, M. R., Oliver, S. R. J. *J. Am. Chem. Soc.* **2011**, *133*, 11110-11113; c) Fei, H., Pham, C. H., Oliver, S. R. J. *J. Am. Chem. Soc.* **2012**, *134*, 10729-10732.

(178) a) Das, S., Kim, H., Kim, K. *J. Am. Chem. Soc.* **2009**, *131*, 3814-3815; b) Prasad, T. K., Hong, D. H., Suh, M. P. *Chem. Eur. J.* **2010**, *16*, 14043-14050; c) Zhang, Z., Zhang, L., Wojtas, L., Nugent, P., Eddaoudi, M., Zaworotko, M. J. *J. Am. Chem. Soc.* **2012**, *134*, 924-927; d) Mukherjee, G., Biradha, K. *Chem. Commun.* **2012**, *48*, 4293-4295; e) Yao, Q., Sun, J., Li, K., Su, J., Peskov, M. V., Zou, X. *Dalton Trans.* **2012**, *41*, 3953-3955; f) Wang, H., Meng, W., Wu, J., Ding, J., Hou, H., Fan, Y. *Coord. Chem. Rev.* **2016**, *307, Part 2*, 130-146.

(179) Dan-Hardi, M., Serre, C., Frot, T., Rozes, L., Maurin, G., Sanchez, C., Férey, G. *J. Am. Chem. Soc.* **2009**, *131*, 10857-10859.

(180) Gao, J., Miao, J., Li, P.-Z., Teng, W. Y., Yang, L., Zhao, Y., Liu, B., Zhang, Q. *Chem. Commun.* **2014**, *50*, 3786-3788.

(181) Kim, M., Cahill, J. F., Fei, H., Prather, K. A., Cohen, S. M. *J. Am. Chem. Soc.* **2012**, *134*, 18082-18088.

(182) Hon Lau, C., Babarao, R., Hill, M. R. *Chem. Commun.* **2013**, *49*, 3634-3636.

(183) Bon, V., Senkovskyy, V., Senkovska, I., Kaskel, S. *Chem. Commun.* **2012**, *48*, 8407-8409.

(184) Yang , Q., Jobic, H., Salles, F., Kolokolov , D., Guillerm, V., Serre, C., Maurin, G. *Chem. Eur. J.* **2011**, *17*, 8882-8889.

(185) Smith, S. J. D., Ladewig, B. P., Hill, A. J., Lau, C. H., Hill, M. R. *Sci. Rep.* **2015**, *5*, 7823.

(186) Lee, Y., Kim, S., Kang, J. K., Cohen, S. M. *Chem. Commun.* **2015**, *51*, 5735-5738.

(187) Sun, D., Liu, W., Qiu, M., Zhang, Y., Li, Z. *Chem. Commun.* **2015**, *51*, 2056-2059.

(188) Monte, R. D., Kaspar, J. *J. Mater. Chem.* **2005**, *15*, 633-648.

(189) White, K. A., Chengelis, D. A., Gogick, K. A., Stehman, J., Rosi, N. L., Petoud, S. *J. Am. Chem. Soc.* **2009**, *131*, 18069-18071.

(190) Ebrahim, A. M., Bandosz, T. J. *ACS Appl. Mater. Interfaces* **2013**, *5*, 10565-10573.

(191) Nouar, F., Breeze, M. I., Campo, B. C., Vimont, A., Clet, G., Daturi, M., Devic, T., Walton, R. I., Serre, C. *Chem. Commun.* **2015**, *51*, 14458-14461.

(192) Lammert, M., Wharmby, M. T., Smolders, S., Bueken, B., Lieb, A., Lomachenko, K. A., Vos, D. D., Stock, N. *Chem. Commun.* **2015**, *51*, 12578-12581.

(193) Greenwood, N. N., Earnshaw, A. *Chemistry of the Elements*, Vol.; Elsevier Science, **2012**.

(194) Fu, Y., Sun, D., Chen, Y., Huang, R., Ding, Z., Fu, X., Li, Z. *Angew. Chem. Int. Ed.* **2012**, *51*, 3364-3367.

(195) a) Li, Y.-F., Xu, D., Oh, J. I., Shen, W., Li, X., Yu, Y. *ACS Catal.* **2012**, *2*, 391-398; b) Jaiban, P., Rachakom, A., Jiansirisomboon, S., Watcharapasorn, A. *Nanoscale Res. Lett.* **2012**, *7*, 1-5.

(196) a) Nguyen, H. G. T., Mao, L., Peters, A. W., Audu, C. O., Brown, Z. J., Farha, O. K., Hupp, J. T., Nguyen, S. T. *Catal. Sci. Technol.* **2015**, *5*, 4444-4451; b) Hayati, F., Chandren, S., Hamdan, H., Nur, H. *Bull. Chem. React. Eng. & Catal.* **2014**, *9*, 28-38; c) Xu, L., Huang, D.-D., Li, C.-G., Ji, X., Jin, S., Feng, Z., Xia, F., Li, X., Fan, F., Li, C., Wu, P. *Chem. Commun.* **2015**, *51*, 9010-9013.

(197) Wang, A., Zhou, Y., Wang, Z., Chen, M., Sun, L., Liu, X. *RSC. Adv.* **2016**, *6*, 3671-3679.

(198) Zhang, W., Huang, H., Liu, D., Yang, Q., Xiao, Y., Ma, Q., Zhong, C. *Microporous Mesoporous Mater.* **2013**, *171*, 118-124.

(199) Katada, N., Igi, H., Kim, J.-H. *The Journal of Physical Chemistry B* **1997**, *101*, 5969-5977.

(200) a) Kim, J., Kim, S.-N., Jang, H.-G., Seo, G., Ahn, W.-S. *Appl. Catal., A* **2013**, *453*, 175-180; b) Kajiwara, T., Higuchi, M., Watanabe, D., Higashimura, H., Yamada, T., Kitagawa, H. *Chem. Eur. J.* **2014**, *20*, 15611-15617.

(201) a) Mitsunobu, O. In *Comprehensive Organic Synthesis*, Vol., Pergamon, Oxford, **1991**, pp. 1-31; b) Lee, C., Matunas, R. In *Comprehensive Organometallic Chemistry III*, Vol., Elsevier, Oxford, **2007**, pp. 649-693.

(202) Bauer, K., Garbe, D., Surburg, H. *Common Fragrance and Flavor Materials: Preparation, Properties and Uses*, Vol.; Wiley, **2008**.

(203) Roca, F. F., De Mourgues, L., Trambouze, Y. *J. Catal.* **1969**, *14*, 107-113.

(204) Brandsma, L., Arens, J. F. In *The Ether Linkage (1967)*, Vol., John Wiley & Sons, Ltd. **2010**, pp. 553-615.

(205) Corma, A., Renz, M. *Angew. Chem. Int. Ed.* **2007**, *46*, 298-300.

(206) Corma, A., Llabrés i Xamena, F. X., Prestipino, C., Renz, M., Valencia, S. *J. Phys. Chem. C* **2009**, *113*, 11306-11315.

(207) Corma, A., Navarro, M. a. T., Renz, M. *J. Catal.* **2003**, *219*, 242-246.

(208) Boronat, M., Corma, A., Renz, M. In *Turning Points in Solid-State, Materials and Surface Science: A Book in Celebration of the Life and Work of Sir John Meurig Thomas*, Vol., The Royal Society of Chemistry **2008**, pp. 639-650.

(209) Heydrich, G., Gralla, G., Ebel, K., Friedrich, M.; Google Patents: 2011.

(210) a) Corma, A., Renz, M. *Chem. Commun.* **2004**, 550-551; b) Boronat, M., Concepcion, P., Corma, A., Navarro, M. T., Renz, M., Valencia, S. *Phys. Chem. Chem. Phys.* **2009**, *11*, 2876-2884.

(211) a) Alaerts, L., Séguin, E., Poelman, H., Thibault-Starzyk, F., Jacobs, P. A., De Vos, D. E. *Chem. Eur. J.* **2006**, *12*, 7353-7363; b) Vandichel, M., Vermoortele, F., Cottenie, S., De Vos, D. E., Waroquier, M., Van Speybroeck, V. *J. Catal.* **2013**, *305*, 118-129.

(212) Vermoortele, F., Bueken, B., Le Bars, G., Van de Voorde, B., Vandichel, M., Houthoofd, K., Vimont, A., Daturi, M., Waroquier, M., Van Speybroeck, V., Kirschhock, C., De Vos, D. E. *J. Am. Chem. Soc.* **2013**, *135*, 11465-11468.

(213) Jiang, J., Gándara, F., Zhang, Y.-B., Na, K., Yaghi, O. M., Klemperer, W. G. *J. Am. Chem. Soc.* **2014**, *136*, 12844-12847.

(214) Ramanathan, A., Castro Villalobos, M. C., Kwakernaak, C., Telalovic, S., Hanefeld, U. *Chem. Eur. J.* **2008**, *14*, 961-972.

(215) a) Corma, A., García, H. *Chem. Rev.* **2003**, *103*, 4307-4366; b) Kaminska, J., Schwegler, M. A., Hoefnagel, A. J., van Bekkum, H. *Rec. Trav. Chim. Pays-Bas* **1992**, *111*, 432-437; c) Wilson, K., Rénson, A., Clark, J. H. *Catal. Lett.* **1999**, *61*, 51-55; d) Kunkeler, P. J., van der Waal, J. C., Bremmer, J., Zuurdeeg, B. J., Downing, R. S., van Bekkum, H. *Catal. Lett.* **1998**, *53*, 135-138.

(216) Dhakshinamoorthy, A., Alvaro, M., Chevreau, H., Horcajada, P., Devic, T., Serre, C., Garcia, H. *Catal. Sci. Technol.* **2012**, *2*, 324-330.

(217) Xi, F.-G., Yang, Y., Liu, H., Yao, H.-F., Gao, E.-Q. *RSC. Adv.* **2015**, *5*, 79216-79223.

(218) a) Timofeeva, M. N., Panchenko, V. N., Abel, A. A., Khan, N. A., Ahmed, I., Ayupov, A. B., Volcho, K. P., Jhung, S. H. *J. Catal.* **2014**, *311*, 114-120; b) Vermoortele, F., Ameloot, R., Alaerts, L., Matthessen, R., Carlier, B., Fernandez, E. V. R., Gascon, J., Kapteijn, F., De Vos, D. E. *J. Mater. Chem.* **2012**, *22*, 10313-10321.

(219) Shimizu, K., Nishimura, M., Satsuma, A. *ChemCatChem* **2009**, *1*, 497-503.

(220) Likhar, P. R., Arundhathi, R., Kantam, M. L., Prathima, P. S. *Eur. J. Org. Chem.* **2009**, *2009*, 5383-5389.

(221) Jumde, V. R., Gonsalvi, L., Guerriero, A., Peruzzini, M., Taddei, M. *Eur. J. Org. Chem.* **2015**, *2015*, 1829-1833.

(222) Tamura, M., Tomishige, K. *Angew. Chem. Int. Ed.* **2015**, *54*, 864-867.

Publications

List of papers

This thesis is based on the following papers:

1. **Bifunctional iridium-(2-aminoterephthalate)–Zr-MOF chemoselective catalyst for the synthesis of secondary amines by one-pot three-step cascade reaction.**
   Mercedes Pintado-Sierra, Antonia M. Rasero-Almansa, Avelino Corma, Marta Iglesias, Félix Sánchez, Journal of Catalysis, **2013**, 299, 137–145.

2. **One-Pot Multifunctional Catalysis with NNN-Pincer Zr-MOF: Zr Base Catalyzed Condensation with Rh-Catalyzed Hydrogenation.**
   Antonia M. Rasero-Almansa, Prof. Avelino Corma, Prof. Marta Iglesias, Prof. Félix Sánchez, ChemCatChem., **2013**, 5, 3092-3100.

3. **Post-functionalized iridium-Zr-MOF as a promising recyclable catalyst for the hydrogenation of aromatics.**
   Antonia M. Rasero-Almansa, Prof. Avelino Corma, Prof. Marta Iglesias, Prof. Félix Sánchez, Green Chem., **2014**, 16, 3522.

4. **Design of a Bifunctional Ir-Zr Based Metal-Organic Framework Heterogeneous Catalyst for the N-Alkylation of Amines with Alcohols.**
   Antonia M. Rasero-Almansa, Prof. Avelino Corma, Prof. Marta Iglesias, Prof. Félix Sánchez, ChemCatChem., **2014**, 6, 1794-1800.

5. **Zr-Materials from Mixed Dicarboxylate Linkers. A study to Enhancing Stability for Catalytic Applications.**
   Antonia M. Rasero-Almansa, Prof. Avelino Corma, Prof. Marta Iglesias, Prof. Félix Sánchez. ChemCatChem., 2014, 6, 3426.

6. **Synthesis of bimetallic Zr-Ti MOFs and their as Lewis Acid Catalysis.**
   Antonia M. Rasero-Almansa, Marta Iglesias, Félix Sánchez. **Submitted** to Catalysis Science & Technology.